Design, development, analysis and comparison of human tissue-engineered skin substitute models

DOCTORAL THESIS

ÁLVARO SIERRA SÁNCHEZ

UNIVERSIDAD DE GRANADA

DOCTORAL PROGRAMME IN BIOMEDICINE

UNIVERSIDAD DE GRANADA

HOSPITAL UNIVERSITARIO VIRGEN DE LAS NIEVES

UNIDAD DE PRODUCCIÓN CELULAR E INGENIERÍA TISULAR

HOSPITAL UNIVERSITARIO VIRGEN DE LAS NIEVES

SUPERVISED BY

Salvador Antonio Arias Santiago, PhD

GRANADA, 2023

Editor: Universidad de Granada. Tesis Doctorales
Autor: Álvaro Sierra Sánchez
ISBN: 978-84-1195-504-1
URI: https://hdl.handle.net/10481/96720

“La mayor de las recompensas no merece la pena

si durante el camino para conseguirla no has disfrutado”

Á.S.S.

D. Salvador Antonio Arias Santiago, Profesor del Programa de Doctorado en Medicina Clínica y Salud Pública de la Universidad de Granada.

CERTIFICA que:

La Tesis Doctoral titulada "***Design, development, analysis and comparison of human tissue-engineered skin substitute models***" ha sido realizada por **D. Álvaro Sierra Sánchez**. El trabajo presentado ha sido realizado bajo mi dirección y demuestra la capacidad técnica e interpretativa de su autor en condiciones tan aventajadas que la hacen acreedora del título de Doctor, siempre que así lo considere el Tribunal designado para su juicio por la Comisión de Doctorado de la Universidad de Granada.

Granada, octubre de 2023.

Fdo: Dr. Salvador Arias Santiago

DOCTORATE FELLOWSHIP

The PhD candidate **Mr. Álvaro Sierra Sánchez** has done this Doctoral Thesis funded by a “Contrato Predoctoral de Formación en Investigación en Salud (PFIS)”, with the dossier number FI18/00269, awarded by the Instituto de Salud Carlos III (ISCIII) from the Spanish Government and co-funded by the European Union through the European Social Fund “*Investing in your future*”.

BECA PREDOCTORAL

El doctorando **D. Álvaro Sierra Sánchez** ha realizado esta Tesis Doctoral gracias a un “Contrato Predoctoral de Formación en Investigación en Salud (PFIS)”, con número de expediente FI18/00269, concedido por el Instituto de Salud Carlos III (ISCIII) perteneciente al Gobierno de España y cofinanciado por la Unión Europea a través del programa del Fondo Social Europeo “*Investing in your future*”.

INTERNATIONAL DOCTORATE MENTION

This Doctoral Thesis has been done in the context of an international cooperation so **"International Doctorate" Mention** is applied. The PhD candidate, **Mr. Álvaro Sierra Sánchez** has done a predoctoral internship supervised by Lucie Germain, PhD, full professor at the Department of Surgery of Université Laval and principal investigator of Centre de recherche en organogénèse expérimentale de l'Université Laval (LOEX) that belongs to the Centre Hospitalier Universitaire de Québec - Université Laval (Québec City, Canada). This PhD internship was done from the 28th of April of 2021 to the 24th of October of 2021 (6 months) and was funded by the Instituto de Salud Carlos III (ISCIII) from the Spanish Government and co-funded by the European Union thanks to the European Social Fund "*Investing in your future*", through the mobility aid "Ayudas para la Movilidad del Personal Investigador (M-AES)" with the dossier number MV20/00043.

MENCIÓN DOCTORADO INTERNACIONAL

La presente Tesis Doctoral se ha desarrollado en el marco de una colaboración internacional por lo que se opta al **Título de Doctor con Mención Internacional**. El doctorando, **D. Álvaro Sierra Sánchez** ha realizado una estancia predoctoral bajo la supervisión de la Dra. Lucie Germain, profesora del Departamento de Cirugía de la Université Laval e investigadora principal en el Centre de recherche en organogénèse expérimentale de l'Université Laval (LOEX) perteneciente al Centre Hospitalier Universitaire de Québec - Université Laval (Québec City, Canadá). Esta estancia se realizó en el período comprendido entre 28 de abril del 2021 y el 24 de octubre de 2021 (6 meses), financiada por el Instituto de Salud Carlos III (ISCIII) (Gobierno de España) y cofinanciado por la Unión Europea gracias al programa del Fondo Social Europeo "*Investing in your future*", a través de la ayuda de movilidad "Ayudas para la Movilidad del Personal Investigador (M-AES)" con número de expediente MV20/00043.

SCIENTIFIC PRODUCTION

SCIENTIFIC PRODUCTION

SCIENTIFIC PAPERS

1) **Sierra-Sánchez, Á.** et al. Hyaluronic acid biomaterial for human tissue-engineered skin substitutes: Preclinical comparative in vivo study of wound healing. Journal of the European Academy of Dermatology and Venereology 34, 2414–2427 (2020). **DOI:** 10.1111/jdv.16342 **(D1 – JCR (2019): 5.248 - Dermatology)**. **Corresponding Author:** Álvaro Sierra-Sánchez

2) **Sierra-Sánchez, Á.**, Montero-Vilchez, T., Quiñones-Vico, M. I., Sanchez-Diaz, M. & Arias-Santiago, S. Current Advanced Therapies Based on Human Mesenchymal Stem Cells for Skin Diseases. Front Cell Dev Biol 9, 515 (2021). **DOI:** 10.3389/fcell.2021.643125 **(Q1 – JCR (2020): 6.684 – Developmental Biology)**

3) **Sierra-Sánchez, Á.**, Kim, K. H., Blasco-Morente, G. & Arias-Santiago, S. Cellular human tissue-engineered skin substitutes investigated for deep and difficult to heal injuries. npj Regen Med 6, 1–23 (2021). **DOI:** 10.1038/s41536-021-00144-0 **(D1 – JCR (2020): 10.364 – Biomedical Engineering / Cell & Tissue Engineering)**. **Corresponding Author:** Álvaro Sierra-Sánchez

4) **Sierra-Sánchez, Á.** et al. Comparison of Two Human Skin Cell Isolation Protocols and Their Influence on Keratinocyte and Fibroblast Culture. Int J Mol Sci 24, 14712 (2023). **DOI:** 10.3390/ijms241914712 **(Q1 – JCR (2022): 5.6 – Biochemistry & Molecular Biology)**

5) **Sierra-Sánchez, Á.** et al. In vitro comparison of human plasma-based and self-assembled tissue-engineered skin substitutes: two different manufacturing processes for the treatment of deep and difficult to heal injuries. Burns Trauma 11, (2023). **DOI:** 10.1093/burnst/tkad043 **(D1 – JCR (2022): 5.3 – Surgery)**

ORAL PRESENTATIONS

1) **Authors:** Álvaro Sierra-Sánchez, Brice Magne, Etienne Savard, Christian Martel, Karel Ferland, Martin A. Barbier, Anabelle Demers, Danielle Larouche, Salvador Arias-Santiago, Lucie Germain. **Title:** *In vitro* comparison of self-assembled and plasma-based tissue-engineered skin substitutes: two different manufacturing processes for the treatment of severe burn patients. **Congress:** Tissue Engineering and Regenerative Medicine International Society (TERMIS) – EU Chapter 2022. **Place and date:** Krakow, 2022.

2) **Authors:** Álvaro Sierra-Sánchez (as Invited Speaker) **Title:** The role of tissue-engineered skin substitutes in surgical wounds. **Congress:** 31st European Academy of Dermatology and Venereology (EADV) Congress: Designing the future of Dermatology and Venereology. **Place and date:** Milano, 2022.

RESEARCH PROJECTS

1) **Title:** "Estudio y caracterización *in vitro* de sustitutos de piel artificial humana constituidos por diferentes biomateriales y tipos celulares". **Reference Number**: PPJIB2020.09 (Universidad de Granada) **Principal Investigator:** Sierra Sánchez, Álvaro. **Dates:** 1st January 2021 – 31st December 2021. **Amount:** 1,700 €.

SCIENTIFIC POSTERS

1) **Authors:** Álvaro Sierra-Sánchez, Antonio Lizana-Moreno, Ana Fernández-González, Olga Espinosa-Ibáñez, Antonio Martinez-Lopez, Jorge Guerrero-Calvo, Natividad Fernández-Porcel, Antonio Ruiz-García, Alexandra Ordóñez-Luque, Salvador Arias-Santiago. **Title:** Human tissue engineered skin substitutes (hTESSs) based on hyaluronic acid for wound healing: epidermal barrier study. **Congress:** Online 2020 78th AAD Annual Meeting. **Place and date:** Denver, 2020.

2) **Authors:** Álvaro Sierra-Sánchez, Alexandra Ordóñez-Luque, Olga Espinosa-Ibáñez, Antonio Lizana-Moreno, Jorge Guerrero-Calvo, Natividad Fernández-Porcel, Ana Fernández-González, Antonio Ruiz-García, Salvador Arias-Santiago. **Title:** *In vitro* study of different biomaterials combined with fibrin for the manufacture of human Tissue Engineered Skin Substitutes. **Congress:** Tissue Engineering and Regenerative Medicine International Society (TERMIS) – EU Chapter 2020. **Place and date:** Manchester, 2020.

3) **Authors:** Álvaro Sierra-Sánchez, Alexandra Ordóñez-Luque, Olga Espinosa-Ibáñez, Antonio Lizana-Moreno, Jorge Guerrero-Calvo, Natividad Fernández-Porcel, Ana Fernández-González, Antonio Ruiz-García, María Isabel Quiñones-Vico, Salvador Arias-Santiago. **Title:** *In vitro* characterization of different fibrin-based human tissue-engineered skin substitutes: preliminary evaluation of biomaterial and cell composition. **Congress:** IV National Congress for Young Researchers in Biomedicine. **Place and date:** Granada, 2020.

4) **Authors:** Álvaro Sierra-Sánchez, Brice Magne, Etienne Savard, Christian Martel, Salvador Arias-Santiago, Lucie Germain. **Title:** *In vitro* comparison of biomaterial-free and biomaterial-based human bilayer tissue-engineered skin substitutes. **Congress:** Skin Research Group Canada 8th Annual Conference. **Place and date:** Montreal, 2021.

5) **Authors:** **Álvaro Sierra-Sánchez,** Sandra Igual-Roger, Jorge Cabañas-Penagos, Luis Martínez-Heredia, Olga Espinosa-Ibáñez, Antonio Lizana-Moreno, María I. Quiñones-Vico, Ana Ubago-Rodríguez, Jorge Guerrero-Calvo, Natividad Fernández-Porcel, Ana Fernández-González, Salvador Arias-Santiago. **Title:** *In vitro* characterization of different human tissue-engineered skin substitutes composed of human plasma as main biomaterial and their manufacturing process: in search of personalized therapies for dermatological diseases. **Congress:** Tissue Engineering and Regenerative Medicine International Society (TERMIS) – EU Chapter 2023. **Place and date:** Manchester, 2023.

PRÓLOGO

PRÓLOGO

Este documento representa de una manera metafórica el diario de casi cinco años de mi vida y aunque probablemente sea el único texto de este tipo que jamás vuelva a escribir, estoy seguro de que será muy representativo de lo que está por venir.

Esta tesis doctoral representa, sobre todo, conocimientos científicos al margen, responsabilidad y decisiones. Solamente uno sabe por lo que ha pasado para llegar hasta este punto, con todo lo bueno, que ha sido mucho, pero también lo malo.

En ella se recogen, por un lado, aspectos positivos relacionados con la adquisición de conocimiento, de responsabilidad, de capacidad de toma de decisiones, de la llegada a tu vida de mucha gente enriquecedora, pero por otro, desvelan, no en pocas ocasiones, inseguridad, miedo, fracaso y decepción, e incluso el descubrimiento de la soledad; existencial, emocional y social.

Por todo ello, puedo decir que refleja un proceso de aprendizaje personal gracias al cual, poniendo algo de interés, se es capaz de aprender en un breve período de tiempo lo que es la vida: asumir la responsabilidad de tus decisiones, así como de tus actos, y aprender de aquellos en los que te equivocaste porque son los que te harán más fuerte, mejor científico y a la larga mejor persona.

Finalmente, no sé cuánta gente leerá este prólogo, pero lo importante es que, si el día de mañana yo lo vuelvo a leer, pueda reconocerme y decir que lo que aprendí gracias a esta tesis doctoral he sido capaz de aplicarlo el resto de mi vida, porque sólo entonces sabré que he tenido verdadero éxito como persona.

“Se es fruto de las acciones y decisiones del pasado, que en algún momento fue presente;

por ello ten siempre en cuenta qué quieres lograr y quién quieres ser”

Á.S.S.

AGRADECIMIENTOS

AGRADECIMIENTOS

Me gustaría remarcar que escribir una tesis doctoral no tendría que ser la excusa para agradecer, sino que, debería ser una más de todas esas muestras de apoyo y de cariño que en muchas ocasiones, al encontrarnos en la vorágine del día a día, se nos olvida dar a los que nos hacen la vida algo más fácil. Dicho esto, las palabras de agradecimiento que aquí se recogen nunca serán capaces de transmitir la totalidad de la gratitud por el apoyo recibido, directa o indirectamente, durante estos casi cinco años de tesis doctoral. Sólo espero que las personas aquí mencionadas vean devuelto, al menos, una parte de lo que ellas me han aportado en estos últimos años:

A mi director de tesis, **Salva**, gracias por la confianza depositada en mí desde el primer momento y permitirme ser parte de tu grupo y proyectos. Me has enseñado lo que es ser un buen líder, más que un jefe, dando ejemplo, guiándome desde la humildad y con el aprecio mutuo, que considero, nos tenemos, pero sin descuidar la alta exigencia que transmites cuando uno trabaja a tu lado. Ojalá a lo largo de mi carrera investigadora sea capaz de encontrar personas como tú, excelentes tanto a nivel profesional como personal.

A mis padres, **Jacin** y **Lumi**, gracias por el apoyo incondicional en todo momento. A pesar de que no seáis capaces de entender la mayoría de la investigación que aquí describo, esto no hubiera sido posible sin vosotros. A vosotros os debo ser la persona que soy hoy en día, habéis sido un ejemplo de esfuerzo, trabajo, disciplina, pero también de amor y cariño, aspectos fundamentales cuando lo que se persigue es la excelencia y dar lo mejor de uno mismo, a nivel profesional y personal. Gracias por no poner barreras a todo aquello que he querido hacer y por estar, sin pedir nada a cambio y a pesar de todo.

A mi hermano y cuñada, **David** y **Elena**, gracias por saber escuchar y querer comprender para así ser capaces de ayudarme. Gracias por la bonita familia que habéis formado junto a **Vega** y **Lucas**, mis sobrinos, a los que a pesar de no verlos todo lo a menudo que me gustaría espero que me quieran la mitad de lo que yo los quiero. En particular, gracias a ti **David**, porque la diferencia de edad ha hecho que quizás no seamos unos hermanos al uso, pero quiero que sepas que, precisamente por eso, siempre has sido ejemplo y referencia, sin el cual, quizás tampoco hubiera sido capaz de conseguir todo lo que he conseguido hasta ahora.

A **María José (MJ)**, gracias por escucharme en mis momentos de bajón y en los que no. Desde que acabamos la carrera sabía que siempre estarías ahí para cuando lo necesitase y no me equivocaba. Me alegro de que nuestra relación después de tantos años, y a pesar de la distancia, siga siendo tan estrecha y fuerte y, por supuesto, solo espero que perdure durante muchos años más, para intentar devolverte todo lo que me aportas.

A **Alexandra**, gracias por los momentos compartidos en el laboratorio y fuera de él. Quien iba a decir que aquella primera impresión distante se iba a convertir en una amistad que perdura desde Sevilla. A nivel laboral has sabido comprenderme porque somos bastante similares, y a nivel personal te has convertido en un apoyo en los momentos complicados y eres una de las personas que me llevo de Granada.

A **Mario**, **África** y **Javi**, a cada uno por distintos motivos, ya sea desde Madrid, Salamanca y Granada respectivamente, gracias por haberos convertido en apoyo en los momentos difíciles. A pesar de que haya habido épocas en las que nuestra relación no haya sido todo lo constante que nos hubiera gustado, siempre habéis estado ahí cuando ha hecho falta, ya sea para un consejo científico, apoyarme emocionalmente o simplemente tomar un café.

To my mates from Canada; **Lucie**, **Danielle**, **Amélie**, **Brice**, **Martin**, **Etienne**, **Karel**, **Anabelle**, **Christian**, **Emilie** and **Alex**, thanks to be my family there. Thank you, **Lucie**, for the opportunity to work in your laboratory, allow me to learn from you and help me to increase my scientific knowledge.

To **Brice**, mon ami, for helping me since the beginning and despite everything. As I told you on some occasion, you are one of the best scientists I've never met. Despite the years pass, I hope to continue hearing from you and be proud of all your achievements.

A **David**, **Andrés**, **Fer**, **Carlota**, **Sandra** y a todos los **Biotec Shore**, gracias porque en mayor o menor medida siempre habéis estado ahí. Llevo algo de todos vosotros dentro de mí, gracias a lo cual he conseguido ser la persona que soy hoy en día.

Al **resto de mis familiares**, gracias, porque a pesar de no comprender muy bien lo que hago, siempre habéis mostrado vuestro cariño, respeto y apoyo hacia mí.

A **Nacho**, **Paula, Olga** y **Luis**, gracias por escucharme y aconsejarme en esos días en los que uno tiraría la toalla y hacerme ver las cosas con otra perspectiva.

Al personal de la Unidad de Producción Celular e Ingeniería Tisular, del Servicio de Dermatología, del Servicio de Anatomía Patológica y del Servicio de Urología del Hospital Virgen de las Nieves, gracias por vuestra ayuda de una u otra manera en la consecución de esta tesis doctoral.

A todo aquel del que me haya podido olvidar y haya formado parte de este camino, por breve que fuese, gracias por haber compartido vuestro tiempo.

INDEX

INDEX

ABBREVIATIONS

ABBREVIATIONS

Ø	Diameter
3D	Three-dimensional
ABDO	Abdominal skin
AG	Agarose
ALI	Air/liquid interface culture methodology
AT-MSC	Adipose tissue-derived mesenchymal stem cell
AU	Arbitrary unit
bFGF	Basic fibroblast growth factor
BMZ	Basement membrane zone
CBMC	Cord blood mononuclear cell
CCL5	C-C motif chemokine 5
CDS	Cultured dermal substitute
CES	Cultured epithelial substitute
CFE	Colony-forming efficiency
Col	Collagen biomaterial
CSS	Composite skin substitute
DEHYD	Dehydrated condition
DEJ	Dermal-epidermal junction
DMEM	Dulbecco’s modified eagle’s medium
DPBS	Dulbecco’s phosphate buffered saline
DPSC	Dermal papilla stem cell
ECM	Extracellular matrix
EGF	Epidermal growth factor
ELISA	Enzyme-Linked Immunosorbent Assay

FGF	Fibroblast growth factor
Fib	Human plasma/fibrin biomaterial
Fn	Fibronectin biomaterial
FORE	Foreskin
FSC	Hair follicle stem cell
GMP	Good Manufacturing Practices
HA	Hyaluronic acid biomaterial
hAT-MSC	Human adipose tissue-derived mesenchymal stem cell
hBM-MSC	Human bone marrow-derived mesenchymal stem cell
hbTESSs	Human bilayer tissue-engineered skin substitute
HGF	Hepatocyte growth factor
hiPSCs	Human induced pluripotent stem cells
HLA	Human leukocyte antigen
hMSC	Human mesenchymal stem cell
HPSS	Human plasma plasma-based based skin substitute
HRP	Horseradish Peroxidase
hSSC	Human skin stem cell
hTESS	Human tissue-engineered skin substitute
hWJ-MSC	Human umbilical cord Wharton's jelly-derived mesenchymal stem cell
HYD	Hydrated condition
K	Keratin
Lam-1	Laminin conformation 1 biomaterial
Lam-2	Laminin conformation 2 biomaterial
LOEX	LOEX Tissue Engineering Laboratory
MSC	Mesenchymal stem cell
OD	Optical density

ON	Overnight
P	Passage
PDGF	Platelet derived growth factor
POSAS	Patient and observer scar assessment scale
S	Serine biomaterial
SASS	Self-assembled skin substitute
SD	Standard deviation
SEM	Standard error of the mean
SSC	Skin stem cell
SUB	Submerged culture methodology
TE	Tissue engineering
TEM	Transmission electron microscopy
TESS	Tissue-engineered skin substitute
TEWL	Transepidermal water loss
TGF-β	Transforming growth factor β
UPCIT	Unidad de Producción Celular e Ingeniería Tisular
UTS	Ultimate tensile strength
UV	Ultraviolet
VEGF	Vascular endothelial growth factor
VEGF-A	Vascular endothelial growth factor A

ABSTRACT

ABSTRACT

Tissue engineering is a multidisciplinary field which involves several areas such as cell biology, material science, engineering, or medicine. It appears as a necessity to solve the lack of organ donors or another efficient substitute for the tissue required. In the case of skin, tissue-engineered skin substitutes (TESSs) have been developed since more than forty years ago, however, due to the advances in technology, they have emerged as a promising therapeutic strategy in the last fifteen years. The main purpose in dermatology of these advanced therapies is to resemble as much as possible the native human skin and be an alternative to the gold standard treatment with autografts.

In the last years, many different TESSs have been developed, based on different characteristics such as cellular composition or biomaterials used as scaffold. Among the first, keratinocytes and fibroblasts have been the main cell types used, allowing the manufacture of cultured epithelial or dermal substitutes (monolayer), respectively, and composite skin substitutes (bilayer) where epidermis and dermis are resembled. However, trying to develop more complex skin substitutes, in the last years, more cell types have been incorporated and studied, such as melanocytes, adipocytes or mesenchymal stem cells. This fact has allowed to produce trilayer substitutes that are under research trying to improve the clinical TESSs already used. Regarding the biomaterial composition, collagen, hyaluronic acid or human plasma/fibrin are the most studied, alone or combined with others, however, in some cases, no biomaterial-based TESSs have been also developed. These can be constituted of an acellular dermal matrix where fibroblasts and keratinocytes are cultured or, even, the cultured fibroblasts, under specific conditions, are able to produce and secrete their own extracellular matrix that serves as scaffold.

In this context, the Unidad de Producción Celular e Ingeniería Tisular (UPCIT), the laboratory where this Doctoral Thesis has been developed, is able to produce a clinical human plasma-based skin substitute (HPSS) constituted of human plasma and agarose as secondary biomaterial and human primary keratinocytes and fibroblasts as cellular composition. However, agarose it is not naturally found in skin or human body and moreover, it is difficult to handle under Good Manufacturing Practices (GMP) conditions (all advanced therapy medicinal products must comply with this regulation to be used in patients). Moreover, the HPSS manufactured in the UPCIT it is a bilayer substitute constituted of keratinocytes and fibroblasts, however, the development of more complex or different HPSSs is an interesting approach for the treatment of different types of skin injuries or wounds.

Therefore, the objectives of this Doctoral Thesis are, I) to evaluate the skin cell isolation protocol used for the extraction of the human primary keratinocytes and fibroblasts used during the UPCIT's manufacturing process, II) to analyze several biological properties and culture methodologies of different versions of the HPSS model manufactured at UPCIT, combining, individually, six secondary

biomaterials (serine, fibronectin, collagen, laminin-1, laminin-2 and hyaluronic acid) with human plasma as scaffold (a seventh type without secondary biomaterial was also manufactured) and studying four cellular combinations [Trilayer (mesenchymal stem cells, fibroblasts and keratinocytes), Bilayer (fibroblasts and keratinocytes), Monolayer (keratinocytes) and Control (without cells) HPSSs], III) to determine the advantages and disadvantages of the HPSS model, by its comparison with another clinical TESS model where no biomaterials are used (self-assembled skin substitute – SASS) and IV) to determine the *in vivo* wound healing potential of a bilayer HPSS combined with hyaluronic acid as secondary biomaterial and compare the results with the gold standard treatment and secondary wound healing approaches.

Firstly, to evaluate the skin cell isolation protocol, the UPCIT's protocol, which is based on a one-step digestion strategy where the dermis and epidermis are firstly mechanically separated and subsequently digested, was compared with the two-step digestion protocol developed at LOEX laboratory (Canada) for the manufacture of the SASS clinical model. In this protocol, the dermis and epidermis are enzymatically separated by the effect of the enzyme thermolysin at the dermal-epidermal junction level and then, each tissue is individually digested. The results of this study revealed that the epithelial cell viability was higher using the LOEX-Protocol compared to the UPCIT-Protocol (93% vs. 85%) and the number of epithelial cells extracted per cm^2 of skin was also 3.4 times higher. However, when the dermal cells were isolated, no significant differences were reported. Moreover, once the keratinocytes and fibroblasts were cultured for several passages, no differences in terms of population doubling time, time of culture or percentage of expression of an epithelial stem cell marker (Keratin 19), were observed. These results proved the effectiveness of the UPCIT's protocol for its application into a clinical environment.

On the second study, several conditions of the HPSS model regarding the secondary biomaterial used, the skin cell tissue source or the cellular composition were evaluated by *in vitro* asssays such as cell viability, cell metabolic activity, protein secretion profile and histology. The results revealed that the *in vitro* properties of the HPSS model were dependent on the human plasma used more than the secondary biomaterial added and moreover, similar results were observed regardless of abdominal skin or foreskin cells were used. In addition, two culture methodologies were also compared, submerged (SUB) and air/liquid interface (ALI), demonstrating that better histological structure and higher secretion of useful wound healing proteins such as bFGF and, mainly, VEGF-A were reported when ALI was applied, although it was more time-consuming. Regarding cell composition, better results were reported when Trilayer and Bilayer HPSSs were developed, compared to Monolayer substitutes.

Once the *in vitro* biological properties of the several variations of the HPSS model manufactured at UPCIT were determined, the purpose was to compare them and also its mechanical properties, with

another clinical TESS model developed without the use of biomaterials (SASS). This is a bilayer model cultured under ALI methodology, and for this reason, bilayer HPSSs composed of human plasma and the most usually investigated secondary biomaterials (collagen and hyaluronic acid) were compared using the same skin cell populations for the manufacture of both models. A bilayer HPSS without secondary biomaterial was also included in this study. The results demonstrated that slight biological differences were observed between both models and between the HPSS subtypes, however, SASSs were more resistant to tensile forces (*p-value<0.01*), but HPSS manufacturing time was shorter (46-55 days for SASSs and 32-39 days for HPSSs), something to consider when a faster treatment is required.

Therefore, the previous studies demonstrated that the role of the secondary biomaterial used for the development of the HPSS model manufactured at UPCIT is not as important *in vitro*, however, their individual *in vivo* properties could determine better outcomes. To that purpose, a bilayer (because it is the type of cellular TESS most used in a clinical environment) HPSS constituted of hyaluronic acid as secondary biomaterial (for its *in vivo* properties, previously demonstrated in other studies) was manufactured and its wound healing potential was evaluated in a surgical excision skin wound model in mice for 8 weeks. The results reported by this HPSS were compared with the use of autografts, another bilayer HPSS constituted of agarose as secondary biomaterial (the oldest HPSS manufactured at UPCIT) and secondary, commercial or under research, wound healing approaches. Homeostasis analysis indicated similar values of transepidermal water loss and elasticity between the bilayer HPSS combined with hyaluronic acid (6.42±0.75 g/h/m^2, 0.42±0.08 AU), autografts (6.91±1.28 g/h/m^2, 0.40±0.08 AU) and healthy mouse skin (6.40±0.43 g/h/m^2, 0.35±0.03 AU). Moreover, histological results showed that bilayer HPSSs and autografts presented better skin structuration and higher expression of keratins.

On balance, the results of this Doctoral Thesis demonstrate that the design, development and manufacture of different subtypes of a HPSS model are a promising and useful strategy as advanced therapy. The possibility of using several secondary biomaterials and skin cell tissue sources without reporting significant differences in terms of their biological properties, the versatility of applying two culture methodologies depending on the needs (time vs. higher secretion of wound healing factors) and the ease of manufacturing different cellular compositions, together with the homogeneity of their *in vitro* results reported when compared with another clinical TESS model, determine that the HPSS model is robust and successful. This is particularly observed when hyaluronic acid was *in vivo* studied as secondary biomaterial, demonstrating a wound healing potential and a recovery of homeostasis parameters similar to those of autografts. Therefore, this research validates the translation of the HPSS model into a clinical environment and recommends its use as an alternative to autografts for the treatment of several skin injuries and wounds.

RESUMEN

RESUMEN

La ingeniería de tejidos es un campo multidisciplinar que involucra diversas áreas como la biología celular, la ciencia de materiales, la ingeniería o la medicina. Surge como necesidad para resolver los problemas relacionados con la falta de donantes de órganos o de la existencia de alternativas eficientes para el remplazo del tejido de interés. En el caso de la piel, los sustitutos de piel creados por ingeniería de tejidos (TESSs por sus siglas en inglés) surgieron hacen más de cuarenta años, sin embargo, debido al avance de las tecnologías, ha sido en los últimos quince años cuando se han erigido como una estrategia terapéutica prometedora. El principal objetivo de estas terapias avanzadas es tratar de asemejarse lo máximo posible a la piel humana nativa y ser una alternativa al tratamiento de referencia con autoinjertos.

En los últimos años, numerosos TESSs se han desarrollado, basados en distintos aspectos como la composición celular o los biomateriales utilizados como soporte. Entre los primeros, los queratinocitos y los fibroblastos han sido los principales tipos celulares utilizados, permitiendo la fabricación de sustitutos epiteliales o dérmicos (monocapa), respectivamente, y sustitutos bilaminares o bicapa, cuando se combinan ambos tipos celulares para imitar la epidermis y la dermis. Sin embargo, en los últimos años, en un intento por desarrollar sustitutos de piel más complejos, otros tipos celulares como melanocitos, adipocitos o células madre mesenquimales se han estudiado, dando lugar a sustitutos trilaminares con el objetivo de mejorar los modelos clínicos ya existentes. Atendiendo a los biomateriales, el colágeno, el ácido hialurónico o el plasma humano/fibrina son los más estudiados, tanto en solitario como en combinación con otros, sin embargo, en algunos casos se han desarrollado TESSs sin biomateriales donde una matriz dérmica acelular sirve como superficie de cultivo para fibroblastos y queratinocitos, o incluso, se ha promovido que los propios fibroblastos en cultivo sean capaces de producir y secretar, bajo condiciones específicas, su matriz extracelular que sirve como soporte.

En este contexto, la Unidad de Producción Celular e Ingeniería Tisular (UPCIT), el laboratorio donde se ha desarrollado esta Tesis Doctoral, es capaz de producir un sustituto de piel clínico basado en el plasma humano (HPSS por sus siglas en inglés), combinado con agarosa como biomaterial secundario y constituido por queratinocitos y fibroblastos primarios humanos. Sin embargo, la agarosa no se encuentra de manera natural en la piel o el cuerpo humano y es difícil de manipular bajo condiciones de Good Manufacturing Practices (GMP), unas normas que todo medicamento de terapias avanzadas debe cumplir cuando el objetivo es el tratamiento de pacientes. Además, el modelo piel fabricado en la UPCIT es bilaminar (queratinocitos y fibroblastos), por lo que el desarrollo y estudio de HPSSs diferentes y más complejos sería de interés para el tratamiento de diferentes tipos de lesiones y heridas cutáneas.

Por tanto, los objetivos de esta Tesis Doctoral son, I) evaluar el protocolo de aislamiento celular utilizado en la UPCIT para la obtención de queratinocitos y fibroblastos humanos primarios utilizados en el ámbito clínico, II) analizar varias propiedades biológicas y metodologías de cultivo de diferentes versiones del modelo de HPSS fabricado en la UPCIT, combinando el plasma humano con seis biomateriales secundarios (serina, fibronectina, colágeno, laminina-1, laminina-2 y ácido hialurónico) y sin combinar con ningún biomaterial secundario, y estudiando cuatro combinaciones celulares diferentes [HPSS Trilaminares (células madre mesenquimales, fibroblastos y queratinocitos), HPSS Bilaminares (fibroblastos y queratinocitos), HPSS Monocapa (queratinocitos) y Controles (sin células)], III) determinar las ventajas y los inconvenientes del modelo HPSS, mediante su comparación con otro modelo clínico en el que no se utilizan biomateriales (SASS por sus siglas en inglés) y IV) determinar *in vivo* el potencial para curar heridas de un HPSS bilaminar combinado con ácido hialurónico como biomaterial secundario y comparar los resultados con el tratamiento estándar y estrategias secundarias de curación de heridas.

En primer lugar, para evaluar el protocolo de aislamiento celular de la UPCIT, que se basa en una única digestión enzimática donde la dermis y la epidermis se separan mecánicamente para posteriormente ser digeridas, se comparó con el protocolo de aislamiento basado en dos digestiones que se aplica en el laboratorio LOEX (Canadá) durante el proceso de fabricación del modelo clínico SASS. En este, la dermis y la epidermis se separan por el efecto de la enzima termolisina que actúa a nivel de la unión dermoepidérmica y después cada tejido es digerido por separado. Los resultados de este estudio determinaron que la viabilidad de las células epiteliales aisladas fue mayor aplicando el protocolo LOEX que el de la UPCIT (93% vs. 85%), y además el número de células epiteliales extradías por superficie de piel fue también 3,4 veces mayor. Sin embargo, no se observaron diferencias en el aislamiento de las células dérmicas. Además, cuando los queratinocitos y los fibroblastos fueron cultivados durante varios pases, tampoco se observaron diferencias en aspectos como el tiempo de duplicación, el tiempo de cultivo o el porcentaje de expresión de marcadores de células madre epiteliales (Queratina 19). Estos resultados demostraron la eficacia del protocolo de aislamiento celular de la UPCIT para su aplicación en el ámbito clínico.

En el segundo estudio, varias condiciones del modelo HPSS, atendiendo al biomaterial secundario utilizado, la región anatómica de donde las células de la piel fueron extraídas o la composición celular fueron evaluadas *in vitro*, a través de ensayos de viabilidad celular, actividad metabólica celular, secreción de proteínas e histología. Los resultados demostraron que las propiedades biológicas de los HPSSs dependen del plasma humano utilizado durante el proceso de fabricación más que del biomaterial secundario incorporado y, además, se obtuvieron resultados similares independientemente del origen celular utilizado (piel abdominal o de prepucio). Aparte, también se compararon dos metodologías de cultivo, sumergido (SUB) y en interfase air/líquido (ALI por sus siglas en inglés), demostrando que esta segunda técnica permitió la obtención de sustitutos de piel

con mejor estructura y que secretaban una mayor cantidad de proteínas de interés para el proceso de curación de heridas, como bFGF y, principalmente, VEGF-A, sin embargo, requería mucho más tiempo de producción. En relación con la composición celular, en general se obtuvieron mejores resultados para los sustitutos Trilaminares y Bilaminares, en comparación con los Monocapa.

Una vez que las propiedades biológicas de varios subtipos del modelo HPSS fabricado en la UPCIT fueron determinadas *in vitro*, el objetivo fue compararlos, así como sus propiedades mecánicas, con otro modelo clínico de sustituto de piel creado por ingeniería de tejidos en el cual no se utilizan biomateriales durante el proceso de fabricación (SASS). Este es un modelo bilaminar cultivado mediante la técnica ALI, y por esa razón, se comparó con varios HPSSs bilaminares constituidos por plasma humano y los biomateriales secundarios más investigados (colágeno y ácido hialurónico). Ambos modelos de piel fueron fabricados utilizando las mismas poblaciones celulares y, en el caso del modelo HPSS también se fabricaron sustitutos de piel sin incluir un biomaterial secundario. Los resultados demostraron que existían mínimas diferencias biológicas entre ambos modelos y entre los distintos subtipos de HPSS estudiados, sin embargo, los SASSs eran más resistentes a las fuerzas tensoras (*p-valor<0,01*), aunque el tiempo de producción fue menor en el caso del modelo HPSSs (32-39 días frente a los 46-55 días del modelo SASS), algo a tener en cuenta cuando se necesita un rápido tratamiento.

Por tanto, los estudios previos demostraron que el rol del biomaterial secundario en el modelo HPSS producido en la UPCIT no es tan importante *in vitro*, sin embargo, sus propiedades individuales *in vivo* podrían ser determinantes a la hora de obtener mejores resultados. Por ello, un HPSS bilaminar (puesto que es el tipo de TESS celular más utilizados en clínica) combinado con ácido hialurónico como biomaterial secundario (por las propiedades previamente demostradas *in vivo* en otros estudios) fue fabricado y su potencial en la curación de heridas fue estudiado en un modelo de herida por escisión quirúrgica en ratones durante 8 semanas. Los resultados de este HPSS se compararon con los del uso de autoinjertos, los de otro HPSS bilaminar fabricado con agarosa como biomaterial secundario (el HPSS más antiguo fabricado en la UPCIT) y estrategias secundarias de curación de heridas, comerciales o en investigación. El análisis de homeostasis determinó que los valores de pérdida transepidérmica de agua y elasticidad eran similares entre los HPSS bilaminares constituidos de ácido hialurónico (6,42±0,75 g/h/m^2, 0,42±0,08 UA), los autoinjertos (6,91±1,28 g/h/m^2, 0,40±0,08 UA) y la piel sana de los ratones (6,40±0,43 g/h/m^2, 0,35±0,03 UA). Además, a nivel histológico los grupos tratados con los HPSSs bilaminares y los autoinjertos presentaron una mejor estructura y mayor expresión de queratinas.

En definitiva, los resultados de esta Tesis Doctoral demuestran que el diseño, desarrollo y fabricación de diferentes subtipos de un modelo HPSS son una estrategia prometedora y útil como terapia avanzada. La posibilidad de usar varios biomateriales secundarios y células de diferentes tejidos de

origen sin albergar diferencias significativas en sus propiedades biológicas, la versatilidad de usar dos metodologías de cultivo diferentes dependiendo de las necesidades (tiempo vs. mayor secreción de factores útiles para el proceso de curación de heridas) y la facilidad para fabricar diversas composiciones celulares, junto con la homogeneidad de los resultados obtenidos *in vitro* cuando se comparó con otro modelo clínico de sustituto de piel creado por ingeniería de tejidos, determinan que el modelo HPSS es robusto y exitoso. Esto se observa especialmente cuando el ácido hialurónico se utiliza como biomaterial secundario *in vivo*, demostrando un potencial de curación de heridas y una recuperación de los parámetros de homeostasis similar al uso de autoinjertos. Por tanto, esta investigación valida la traslación del modelo HPSS al ámbito clínico y sugiere que su uso puede ser una alternativa al tratamiento con autoinjertos para diferentes tipos de lesiones y heridas cutáneas.

I. INTRODUCTION

INTRODUCTION

1. HUMAN SKIN

Skin is the largest organ of the human body, constitutes 15% of the total weight and covers an area of 1.5-2 square meters[1]. Moreover, it is a vital organ with multitude of functions, one of which is to serve as a barrier to protect against external agents that can cause serious harm. Its relevance becomes apparent with extensive loss of skin due to deep injuries or burns, which affect many parts of human body (limbs, back and trunk). In these situations, the lack of donor tissue[2] (for autologous grafts) and delayed intervention can lead to hypothermia, fluid and electrolyte imbalance, sepsis, chronic wounds and even death[3].

Human skin thickness varies from 0.5 mm (eyelids) to 4.0 mm (palms)[4], but abdominal skin thickness is considered as reference due its similarity with other skin regions (2.4 mm)[5,6]. However, its histological structure through the human body is the same, composed of three layers (**Fig. 1**): the epidermis, from ectodermal origin, and the dermis and the hypodermis or subcutaneous tissue, both from mesodermal origin.

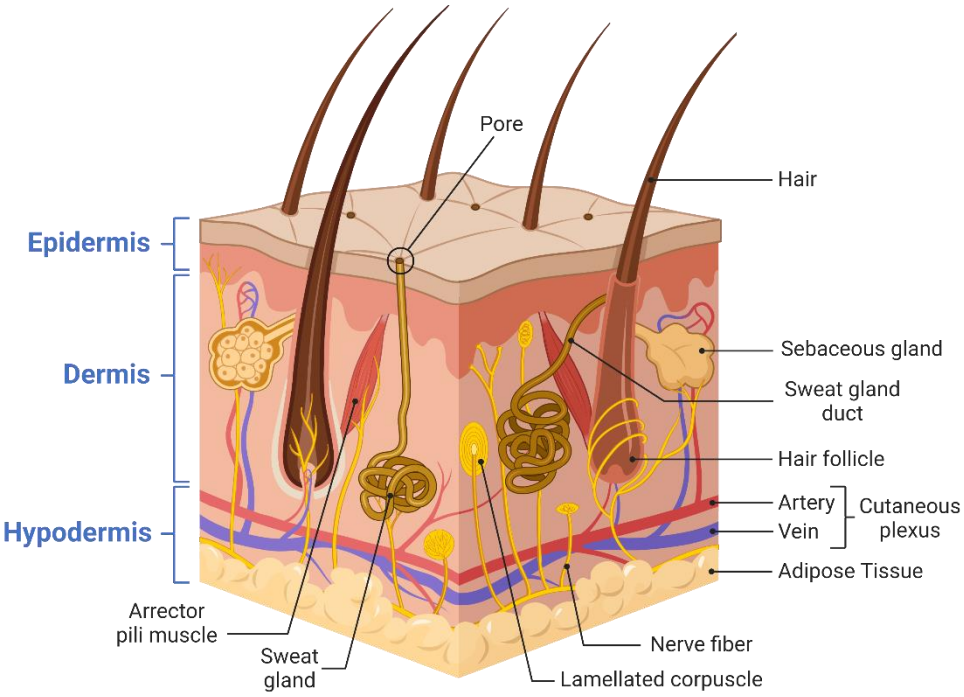

Fig. 1. ***Anatomy of the human skin.*** *Adapted from "Anatomy of the Skin", by BioRender.com (2023). Retrieved from https://app.biorender.com/biorender-templates.*

1.1. EPIDERMIS

The **epidermis** is the outer and nonvascular epithelial layer of the skin. Although it is composed of several cell types, keratinocytes are the majority type (95% of the cell mass of epidermis) and their main function is to synthesize keratin, required to maintain the structural integrity of skin[7]. Apart from keratinocytes, other specialized cells such as melanocytes; responsible for skin pigmentation and protection from ultraviolet (UV) light[8], Langerhans cells; that act as antigen-presenting cells helping to drive protective immune responses[9] and Merkel cells; which stablish synaptic contacts with somatosensory afferents and play a crucial role in sensory discernment[10], are also found along the epidermis.

Therefore, epidermis is a complex structure that constitutes a stratified squamous keratinized epithelium where keratinocytes are the main cellular component. These keratinocytes suffer a terminal differentiation process and consequently, five epidermal layers are observed (**Fig. 2**):

I) The **stratum basale** is the deepest layer of the epidermis attached to the basement membrane by hemidesmosomes[11]. It is a single cell-layer[1] where keratinocyte precursors are located, allowing the epidermis to constantly replenish itself[12]. Melanocytes, Langerhans cells and Merkel cells are also located in this layer. Moreover, in deep epidermal rete ridges of glabrous skin, skin stem cells (SSCs) that express Keratin 19 ($K19^+$) are located at this stratum. These cells are characterized by a higher proliferation rate than other keratinocytes[13].

II) The **stratum spinosum** is comprised of eight to ten layers of keratinocytes[14] that synthetize cytokeratin and produce intermediate tonofilaments that form the basis of tonofibrils[11]. These conform the characteristic spiny intercellular connections that also connect with the fibrous part of the desmosomes[15]. The alignment of these filaments causes the transition from the cuboidal and polyhedral keratinocytes to the flattened cells of upper layers[11]. Most of the Langerhans cells are located at this layer[14].

III) The **stratum granulosum** is constituted of three or five layers of flattened keratinocytes[15] constituted of keratohyalin granules that contain keratin precursors[14]. They also secrete lamellar bodies containing lipid granules responsible for the major permeability barrier function of the epidermis[11]. It is the most superficial layer of the epidermis containing living cells[1].

IV) The **stratum lucidum** is only observed in areas of thick skin such as palms and soles[11]. It is a thin stratum (two or three cell layers) constituted of eleidin a transformation product of keratohyalin[14] that will be converted to keratin in the stratum corneum.

V) The **stratum corneum** is the uppermost layer of epidermis and marks the final stage of keratinocyte maturation and development. It is comprised of twenty to thirty terminally differentiated,

enucleated skin cells known as horny cells or corneocytes[11,14]. These cells are characterized by retain only keratin filaments embedded in a filaggrin matrix. Cornified lipid envelopes replace the plasma membranes of the previous keratinocytes, and the cells flatten, connecting to one another with desmosomes and stacking as layers[16]. The presence of these corneocytes together with an extracellular lipid matrix serves as the body's first barrier from the external environment, providing mechanical reinforcement and regulating permeability among other homeostatic functions[16].

Apart from these strata, epidermis is also constituted by **epidermal appendages**, including eccrine and apocrine glands, ducts, and pilosebaceous units originated as down-growths from the epidermis during development. These structures are capable of re-epithelialize after an injury due to the migration of keratinocytes from adnexal epithelium to the surface of the epidermis[1].

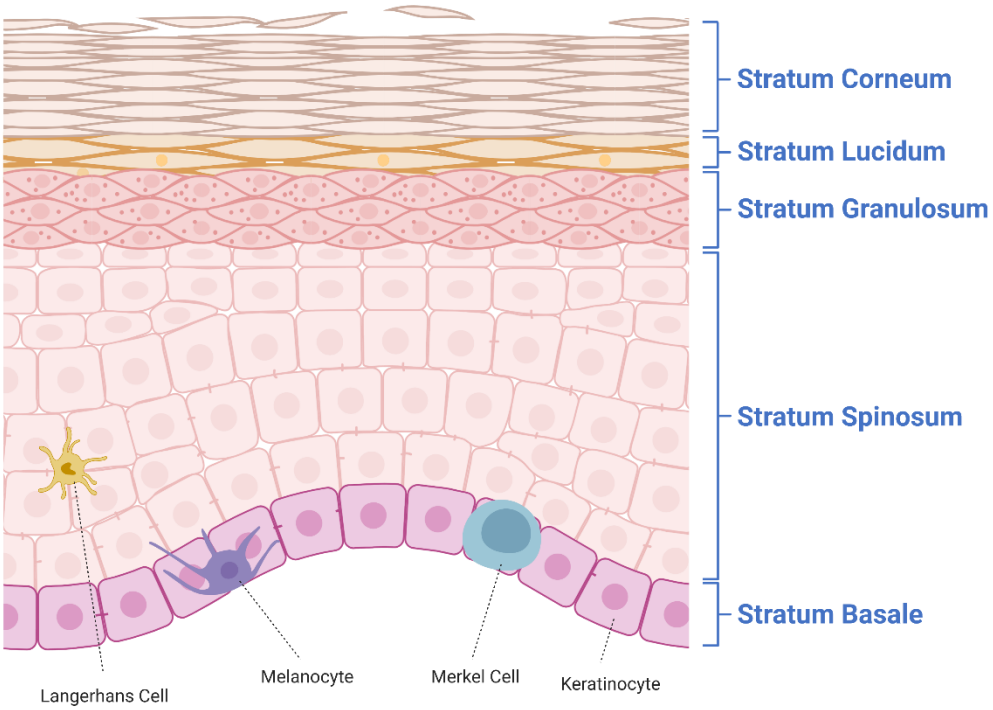

*Fig. 2. **Human skin epidermal layers.** Adapted from "Desmosomal Protein Distribution in the Epidermis", by BioRender.com (2023). Retrieved from https://app.biorender.com/biorender-templates.*

1.2. DERMIS

The **dermis** is a connective tissue layer of mesodermal origin between the epidermis and subcutaneous tissue. It is constituted of cells and an extracellular matrix (ECM) composed of collagen and elastin fibers, but also glycosaminoglycans, such as hyaluronic acid, proteoglycans, and glycoproteins[17]. It comprises the bulk of the skin and provides its pliability, elasticity, and tensile strength, apart from being involved in thermal regulation of the body due to the presence of vasoactive dermal vessels[1,17].

Several cell types such as fibroblasts, dendritic cells and mast cells are found in the dermis[11]. Fibroblasts are the main cell type and synthesize a great number of collagen (mainly type I collagen), reticular, and elastic fibers which interweave to increase dermal resilience and optimize its protection of the epidermis[11,18,19].

The dermis is also subdivided into two layers: the superficial or **papillary dermis**, and the deep or **reticular dermis**[11]. The papillary dermis is composed of loose connective tissue due to the weaker alignment of the collagen fibers and higher content of proteoglycans. Moreover, the number of fibroblasts (papillary fibroblasts) is higher than in the reticular dermis (reticular fibroblasts) and they are metabolically more active and proliferative[17,19,20]. In contrast, reticular dermis is a thick layer of dense connective tissue, where collagen fibers and elastin strands are ordered[17,19]. Regarding their interaction with other structures, papillary dermis interlock with the rete ridges of the epidermis for greater protection against shear forces. Furthermore, this superficial dermis also exchanges oxygen and waste products with the avascular epidermis due to the presence of loop capillaries. Meanwhile, the reticular dermis contains the encapsulated bodies of mechanoreceptors such as Ruffini and Pacinian corpuscles[11].

1.3. THE DERMAL-EPIDERMAL JUNCTION

Epidermis and dermis are two independent layers the human skin, however they interact due the **dermal-epidermal junction (DEJ)**. The DEJ, although without being considered as a skin layer, is a cell surface-associated ECM[21] necessary to achieve a proper structure and function development of human skin.

One of the characteristics structures that are in the DEJ are the rete ridges. As previously described, rete ridges are undulating down-growth microstructures of the epidermis within the papillary dermis that enhance the skin's mechanical strength and maintaining skin homeostasis[11,21–23]. Moreover, rete ridges increase the surface area of capillary-epidermal interface to improve nutrient supply to the avascular epidermis[24].

However, although rete ridges are important, the most characteristic structure of the DEJ is the basement membrane zone (BMZ). The BMZ is a porous area that allows cell interaction and the exchange of fluids between the basal keratinocytes and dermal fibroblasts[1]. Ultrastructure of BMZ is composed of four regions: basal cell plasma membrane with its hemidesmosomes, the lamina lucida, lamina densa and the sub-basal lamina fibrous elements[25].

Regarding the composition, the BMZ is comprised of laminin, which initiates BMZ assembly, but type IV collagen, responsible for tensile strength of the skin, is the majority component[1,21]. Moreover, several proteins such as nidogens, perlecan, fibulins and different types of laminins and collagen also constitute the BMZ[21]. Among them, type VII collagen, mainly produced by basal keratinocytes, is

essential for the proper development of the BMZ, because it is one of the components of anchoring fibrils[26–28]. Anchoring fibrils are fibrillar structures originated at the lamina densa and extended into the dermis that loop into the upper regions of the papillary dermis and reinsert into the lamina densa[21].

In addition, to improve the strength of the DEJ and the mechanical properties of skin, there are highly specialized integrin-mediated epithelial attachment structures called hemidesmosomes[21,29]. Hemidesmosomes make cells firmly adhere to the ECM by establishing a link between the underlying BMZ and the internal mechanical stress-resilient keratin intermediate filament network of basal keratinocytes[29].

1.4. HYPODERMIS

Finally, the **hypodermis** or subcutaneous adipose layer is underneath the dermis, and serves to connect the skin to the underlying fascia[4,30]. It is mainly constituted of adipocytes, vasculature, nerves, adipose tissue-derived mesenchymal stem cells (AT-MSCs) and sweat glands[30]. This layer maintains the mechanical and thermoregulatory properties of the human skin, but also, plays an important role in the regulation of epidermis and dermis, supporting keratinocyte and fibroblast proliferation[30].

Moreover, the adipose tissue has metabolic functions such as the production of vitamin D and triglycerides[4]. Interestingly, adipocyte precursor cells (considered as a pool of AT-MSCs[31]) are involved in skin wound healing through the repopulation of skin wound following inflammation and participating in fibroblast recruitment and final dermal reconstruction[32]. These cells also regulate follicular stem cell activation[33].

On balance, skin is a complex organ composed of several cell types and structures which their integrity and functions are required. Therefore, maintain skin homeostasis is essential for human life.

2. SKIN WOUND HEALING

Skin wound healing is a complex but well-orchestrated process divided in four overlapping phases (hemostasis, inflammation, proliferation, and remodeling; **Fig. 3**). It is a native biological response of the human body that plays a crucial role after a cutaneous injury, restoring function and appearance of damaged skin with minimal scarring[34]. This process requires the involvement and coordination of many cell types and signaling pathways[35].

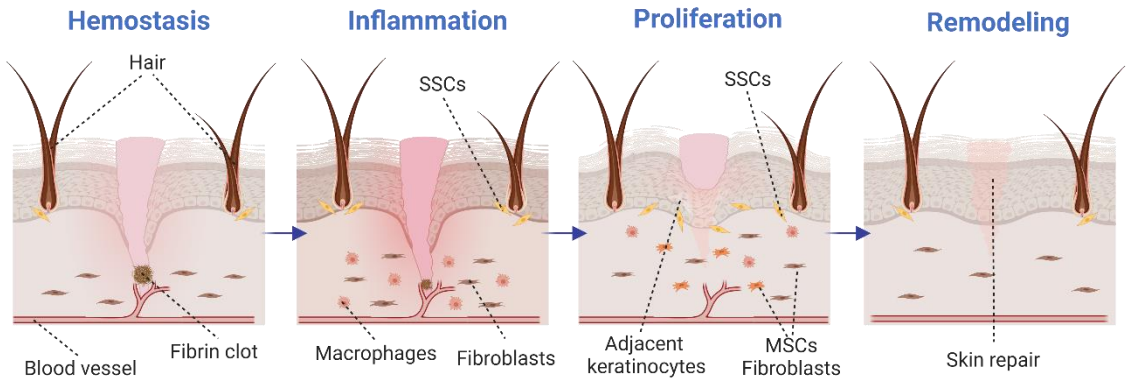

Fig. 3. ***Phases of skin wound healing process.*** *Hemostasis: activation of fibrin is responsible of clot formation and bleeding is stopped. Inflammation: damaged cells are phagocyted and factors are released to provoke cell migration and proliferation. Proliferation: cells such as dermal fibroblasts, mesenchymal stem cells (MSCs) and skin stem cells (SSCs) achieve wound's site and form a provisional extracellular matrix. Remodeling: collagen fibers are realigned, and residues are removed. Created with BioRender.com.*

2.1. HEMOSTASIS

Firstly, on **hemostasis**, vasoconstriction is achieved due to endothelin and factors released by injured cells, such as epinephrine and catecholamines, and moreover, platelets produce platelet-derived growth factor (PDGF) which activates mesenchymal stem cells (MSCs) from smooth muscles in the vessel walls causing contraction[35,36]. To conclude hemostasis, platelets, through G protein-coupled receptor, bind to thrombogenic subendothelial matrix[37], activating integrins (αIIbβ3 or α2β1) and glycoproteins (Ib-IX-V and VI) which increase the attachment to fibrinogen, fibronectin and von Willebrand factor and between platelets (platelets plugs)[38,39]. Finally, platelets within the plug releases many growth factors (PDGF, transforming growth factor β -TGF-β- or epidermal growth factor -EGF-), required for the next stages and moreover, provide a surface for assembly and activation of coagulation complexes lead by Factor X, and where, after Factor XIII crosslinks fibrin, thrombus is formed serving as provisional wound matrix[35,40].

2.1. INFLAMMATORY PHASE

In **inflammatory** phase, transcription-independent pathways (Ca^{2+} waves, reactive oxygen species gradients, and pyrogenic molecules) and damaged associated factors such as H_2O_2 are responsible of inflammatory cells recruitment, activating keratinocytes regeneration and promoting new vessel formation[35,41]. Neutrophils secrete antimicrobial agents, phagocyte bacteria and cell debris, and release cytokines such as C-C motif chemokine 5 (CCL5) that recruits macrophages to the wound[35,42,43]. Meanwhile, macrophages have a microbicidal and pro-inflammatory effect at the beginning, but then, develop an anti-inflammatory role which accelerate wound healing through the formation of new vessel ($Tie2^+$) and the release of vascular endothelial growth factor (VEGF)[35,42]. Moreover, they participate in proliferation phase; inducing the transition of dermal fibroblasts into myofibroblasts and depositing collagen and other ECM components, and also in re-epithelization and

remodeling; releasing proteases and phagocytizing excessive cells and matrix no required[35,40,42]. Mast cells are also important for wound contraction because synthesized enzymes chymase and tryptase as well as histamines and VEGF which stimulates keratinocyte proliferation and re-epithelialization and enhances fibroblast proliferation and collagen synthesis[35,44].

2.3. PROLIFERATION PHASE

Proliferation phase is also triggered by many different cell types[45]. The most important are endothelial cells which are responsible of angiogenesis in response to factors such as VEGF, PDGF, TGF-β and fibroblast growth factor (FGF). This is regulated by Notch pathways through VEGF-A produced by subcutaneous adipose stromal cells[35,46]. In addition, fibroblasts synthesize ECM and express genes which are responsible of their proliferation and migration, and myofibroblasts, transient cells derived from local fibroblasts and other cells such as mesenchymal stem cells and epithelial cells, also deposit ECM and exhibit contractile characteristics; processes that are fundamental for wound healing[35].

2.4. REGENERATION OR REMODELING PHASE

Finally, **regeneration** of the dermis is favorable due to their fibrous nature, allowing for migration and proliferation of macrophages and fibroblasts necessary for remodeling and promoting connective tissue formation[35,42]. In the case of epidermal layer, re-epithelialization is a complicated process where keratinocytes located in the wound edge loss their adhesions and express integrins which leads to increased Erk-MAPK signaling and inflammatory cytokine synthesis, causing hyperproliferation of keratinocytes and immune cell activation[35,47]. In addition, human skin stem cells (hSSCs) migrate from their niches in order to replace the lost keratinocytes[40,45,48] and also express higher levels of integrins (α2β1, α3β1, α6β4), that binds collagen or laminin[35], and release growth factors which participate in generation of epithelial cells like keratinocytes, promoting re-epithelization of injured skin[45,49–51].

On balance, wound healing is a coordinated and complex process where many factors such as, burns, inflammatory skin diseases, deep injuries, large sized or chronic wounds can provoke a deregulation due to an altered immune response and the lack of local adult skin cells and hSSCs available for migration, which causes problems to achieve a correct homeostatic restoration[48,52,53].

When these critical cells are lacking due to deep and difficult to heal wounds, human mesenchymal stem cells (hMSCs) can also contribute to re-epithelization[54] by stimulating collagen production and reducing fibrosis and scar formation by releasing many growth factors such as EGF or basic fibroblast growth factor (bFGF)[45].

Hence, much of the efforts have been dedicated to understanding the mechanisms of wound healing and to develop clinically viable therapies based on tissue engineering, to help patients restore function of damaged skin.

3. SKIN TISSUE ENGINEERING

3.1. TISSUE ENGINEERING: TOWARDS PERSONALIZED MEDICINE

Tissue engineering (TE) is an interesting and growing multidisciplinary field which involves several areas such as cell biology, material science, engineering, or medicine. It appears as a necessity to solve the lack of organ donors or another efficient substitute for the tissue required. For this reason, TE tries to manufacture artificial organs and tissues under controlled conditions to be transplanted *in vivo* in those cases where own patient's regenerative or reparative capacities are not achieved[55].

The study of TE strategies requires to evaluate many aspects such as cell sources, cell nature, material science, incorporation or not of growth factors and disease models required (injuries and animals). Regarding cell biology, selection of an appropriate cell type will depend on the target tissue but the main challenge for clinical use will be to select among allogeneic (stem cells included) or autologous source due to the advantages and disadvantages associated to each one[55–57]. The other important aspect in TE is material science; first approaches were based on the use of synthetic biomaterials which provided structural support and replaced organs but without functionality[56]. However, research of ECM has provoked the development of new biomaterials capable of resembling biological and mechanical aspects such as three-dimensional (3D) structures (scaffolds) which enable nutrient's transport and vascularization[55–57]. Considering their nature, biomaterials could be synthetic, naturally derived or acellular tissue matrices and they must be biocompatible, biodegradable and bioresorbable to be replaced by native tissue without rejection[56].

3.2. TISSUE-ENGINEERED SKIN SUBSTITUTES

In the case of skin, a **tissue-engineered skin substitute (TESS)** is any safe product, constituted of human cells and bio-scaffolds, capable of replacing damaged human skin and resembling its structural and functional characteristics such as flexibility, protective barrier or transepidermal water loss[58,59].

As described above, two are the main factors that may be regarded for TESS manufacture: cell composition and scaffold's biomaterial. Regarding **cell composition**, TESSs can be classified into: **Monolayer TESSs** that only resemble one of the layers of the skin, usually epidermis or dermis; **Bilayer TESSs**, those which resemble two layers of the skin, mainly epidermis and dermis, and more recently, **Trilayer TESSs** composed of epidermis, dermis and hypodermis. Taking this into

consideration, most of the TESSs are comprised of human adult keratinocytes and fibroblasts as part of epidermal and dermal layers, respectively[53]. However, due to the many advantageous properties[40,60] of human stem cells (hSCs) and the specific role of hSSCs and hMSCs in restoring homeostatic conditions[45,48], new approaches in the field of skin engineering are focusing on the incorporation of these cell types to TESSs[54] (**Table 1**).

***Table 1**. Different cell types used for tissue-engineered skin substitutes (TESSs) development.*

	Human Cell Type	Differentiation Capacity	Clinical/Ethical Issues
Human Adult Skin Cells	Keratinocytes	No	Autologous use: No Allogeneic use: Yes
	Fibroblasts	No	
	Melanocytes	No	
	Langerhans cells and Merkel cells	No	
Human Stem Cells	Skin Stem Cells	Yes (*in vitro* and *in vivo*)	Proliferative capacity of stem cells
	Induced Pluripotent Stem Cells	Yes (*in vitro* and *in vivo*)	Proliferative capacity of stem cells Genetic manipulation
	Mesenchymal Stem Cells*	Yes (*in vitro* and *in vivo*)	Proliferative capacity of stem cells *However, already used from autologous or allogeneic sources, for other diseases

Apart from cell composition, the selection of a suitable scaffold as dermal matrix is essential to support cell growth. Many **different biomaterials or strategies** have been investigated; from xenogeneic scaffolds such as porcine acellular matrix[61], natural polymers like silk-fibroin[62], agarose[63,64] or chitosan[65–67] to substances that resemble in better way the native dermal components of skin: collagen[68–87], plasma/fibrin[63,64,88–94], hyaluronic acid[63,70–75,95,96], elastin[69,97], amniotic membrane[98,99] or extracellular matrix derived from fibroblasts[2,100–102]. On balance, they differ in their internal structure: porous, fibrous, hydrogel or ECM nature which provide advantageous and drawbacks depending on therapeutic purposes[103].

For clinical purposes, the main biomaterials used have been collagen alone or combined with glycosaminoglycan, hyaluronic acid, plasma/fibrin, amniotic membranes and extracellular matrix derived from fibroblasts (**Table 2**).

Table 2. Main biomaterials used for tissue-engineered skin substitutes (TESSs) manufacture.

	Advantages	Drawbacks	References
Collagen	Most abundant animal protein High tensile strength and stability	Lack of intrinsic angiogenic properties	69–75,77,80,83–85,87,104,105
Collagen-Glycosaminoglycan	Glycosaminoglycan increases mechanical properties and fibril formation of collagen	Requires cross-linking	76,78,79,81,82,86,106
Hyaluronic Acid	Ease to handle Biosafety corroborated by its use in cosmetic field Angiogenic properties	Less mechanical properties in comparison with collagen	70–75,95,104,107
Plasma/Fibrin	Composed of proteins which participate in wound healing Enhances cell proliferation	Combination with other biomaterials is required to increase mechanical properties	88–94,108
Amniotic Membrane	High tensile strength Releases several growth factors for angiogenesis and cell proliferation	Difficult to obtain	98,99
Extracellular Dermal Matrix	Human skin-like ECM components Minimizes the host response	Specific training and more time are required to obtain it	2,101,102,109–111

4. CELLULAR TESSs FOR CLINICAL PURPOSES

As previously described, many cell types and biomaterials have been or are under research for the development of TESSs. The choice of the biomaterial plays a crucial role in cell growth and differentiation and TESS properties. However, the use of one, two or more combinations of several cell types determines the complexity of the TESS and may improve the success of treatment. The search and optimization of new strategies, tries to replace or, at least, complement the **gold standard treatment with autografts**.

4.1. CELL ISOLATION AND CULTURE

Immortalized or commercial cell lines are widely used in research due to their cell growth potential and well-known characteristics[112]. However, primary human cells are valuable in biomedical sciences for evaluating or characterizing different drugs, substances or molecules, for example[113]. Moreover, as advanced therapies are developing, human cells are used alone or combined with biomaterials and/or devices for the treatment of patients[114]. For this clinical purpose, the control of experimental and manufacturing conditions for primary cell cultures from the tissue biopsy is a key step[113].

To establish a primary cell culture, different aspects such as cell isolation protocol, cell attachment to plastic surfaces and culture media must be considered[112]. To initiate a primary culture from a biopsy, tissue explants can be seeded on culture flasks allowing cells to migrate out and proliferate. Alternatively, cells can be isolated by disaggregating the tissue mechanically and/or enzymatically to

produce a suspension of cells[115] that will be seeded on flasks and cultured using the appropriate growth medium.

Manufacturing autologous TESSs for clinical purposes requires the use of primary skin cells, commonly keratinocytes and fibroblasts, the main cell types of the epidermis/appendages and the dermis, respectively[116]. For this reason, and the limited size of the donor skin that is usually available for cell extraction, it is important to have an effective isolation protocol to be able to culture and expand those cells without affecting their properties. Despite the similarities between most skin cell isolation procedures, different protocols exist depending on the number and type of enzymatic digestions or the addition of mechanical disaggregation or not[117].

Therefore, it is important to optimize and use a successful isolation protocol that preserves the properties and characteristics of the different native human cell types as much as possible. Moreover, these methods should be robust, standardized and report a good cell yield to be able to reduce the manufacturing time in the case where the cell/tissue grafts are required to treat patients[118,119].

4.2. MAIN ADULT SKIN CELL TYPES USED FOR TESS MANUFACTURE AND THEIR LAYERED STRUCTURE

Most of the non-commercial skin substitutes studied are constituted by epidermal, dermal or both layers, where keratinocytes and fibroblasts are the most used cell types; however, some researchers explored the use of other cell types with the purpose of fabricating TESSs that better resemble native skin (**Fig. 4**).

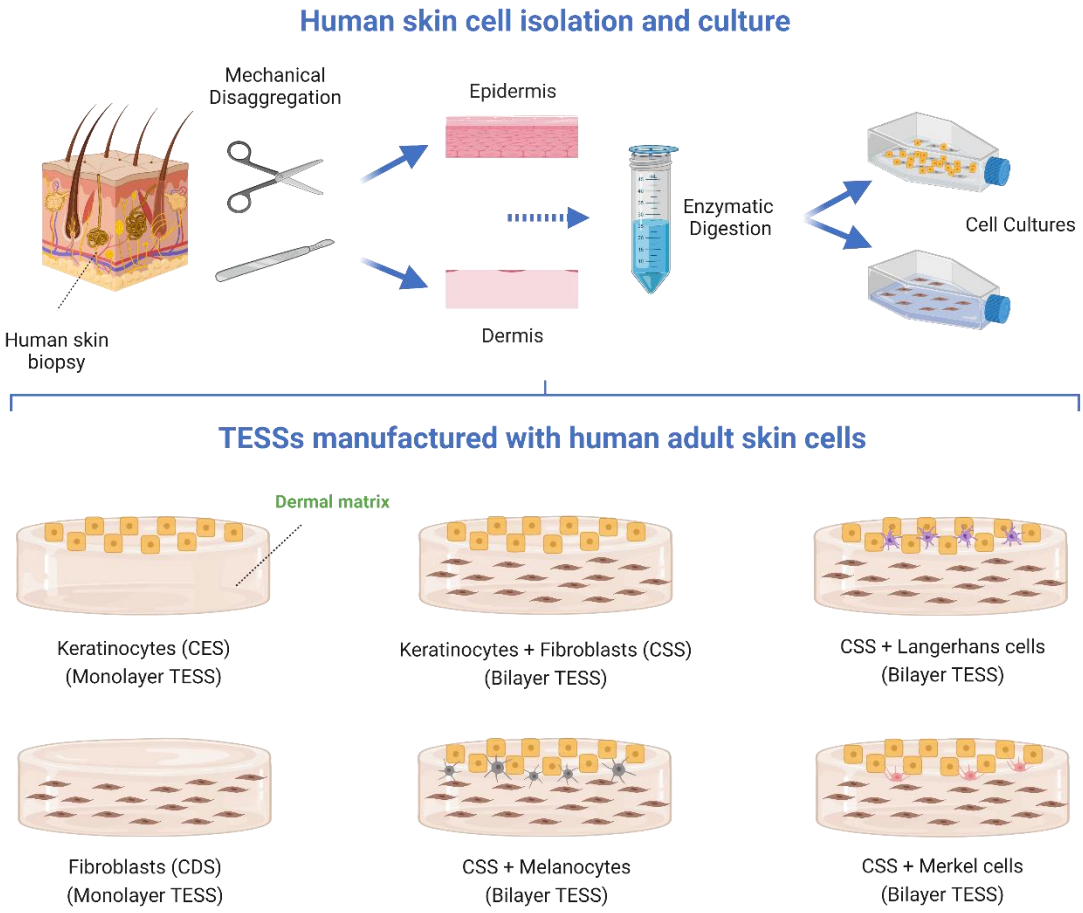

Fig. 4*. Tissue-engineered skin substitutes (TESSs) manufactured with human adult skin cells and their layered structure.** *After a deep, severe or chronic injury where, normal phases of wound healing are disrupted, fabrication of TESSs from cells of a human skin biopsy is the most usual advanced therapy. Keratinocytes, fibroblasts and the rest of epithelial cells are isolated, expanded and used in combination with a biological matrix to produce* ***monolayer TESSs *such as cultured epithelial substitutes (****CESs****) or cultured dermal substitutes (****CDSs****) and* ***bilayer TESSs*** *referred as composite skin substitutes (****CSSs****). Created with BioRender.com.*

4.2.1. HUMAN KERATINOCYTES (MONOLAYER TESSs)

Keratinocytes were the first skin cell type isolated and explored[120], and for this reason the former models of TESSs were based on these cells only. The development of these monolayer TESSs, referred as **cultured epithelial substitutes (CESs)**, mainly for burn patients, has been one of the main objectives, which has led to many extensively studied commercial devices[121,122].

Due to the important role of epidermis as a protective barrier, CESs with keratinocytes were the first monolayer TESSs explored in patients (**Table 3**). Since 1981, many clinical studies have analyzed the role of CESs in skin regeneration[69,88,89,107,109,123–133], mainly for the treatment of burns, although treatment of surgical wounds is also reported.

Regarding culture and manufacturing process of autologous CESs, in most of former studies keratinocytes were expanded and isolated by enzymatic detachment from culture flasks and directly engrafted onto patients[123–133]. In these cases, results differed depending on: parameters analyzed,

endpoint of follow-up or pretreatment strategy, but, in general, studies which only applied this type of CES reported worse results in terms of graft take, due probably to the effect of digestive enzymes on epithelial cells.

For this reason, some authors concluded that their use could be interested as temporary biological dressing[133] or combined with meshed split-thickness skin grafting[124,125,130]. In other cases, the previous engraftment of artificial[132] or allogeneic split-thickness skin grafts[125,128] improved the take of these conventional CESs and accelerate wound healing[132] due to the increase of capillarity density[125].

However, due to the risk associated to these strategies, researches have investigated the fabrication of more complex CESs where epithelial cells and biomaterials are cultured *in vitro* before engraftment[69,88,89,107,109]. Two studies evaluated the use of fibrin and in both cases take of grafts was higher, improving the relation cost-efficiency[88] and demonstrating that fibrin facilitated the formation of dermo-epidermal junction because ECM proteins secreted by autologous keratinocytes were retained[89].

However, other biomaterials have been applied for the development of clinical CESs. For example, the use of acellular dermis or membranes[107,109], reported similar values of Vancouver Scar Scores (VSSs) as autografts, 12 months after treatment[109] and higher percentage of reduction of skin wound dimensions (91.5%)[107]. Moreover, collagen and elastin have been also combined with autologous keratinocytes to be engrafted before the gold standard treatment is applied[69]. This strategy demonstrated an increased epithelialization against those areas where only autografts were applied (71% vs. 67%) and after 12 months of follow-up, Patient and Observer Scar Assessment Scale (POSAS) also reported better results (14.2±7.2 vs. 18.4±10.2) (NCT00832156)[69].

On balance, studies using CESs have evolved from the first reported, including new culture techniques and strategies, however it does not seem to be the best alternative when deep wounds or difficult to heal wounds needs to be treated.

Table 3. Clinical use of human cultured epithelial substitutes (CESs).

Reference	Cells	Type of Clinical Study	N (Male / Female)	Indication	[a]Outcomes
123	Autologous epidermal cells	Case Report	2 (2/0)	Burns	6 months after grafting the new epidermis could not be distinguished from native skin
124	Autologous keratinocytes	Case Report	17 (11/6)	Burns	In some cases, 80% of epithelialized skin was achieved after 6 weeks Hypertrophic scar formation was lower compared to areas treated with meshed skin grafts
125	Autologous keratinocytes	Case Report	26	Burns	Limited success
126	Autologous keratinocytes	Case Report	30	Burns (26) Giant congenital nevus (4)	Keratinocyte culture take was significantly lower compared to split thickness skin grafts
127	Autologous keratinocytes	Case Report	16	Burns	No impact on the definitive closure of massive burn wounds
128	Autologous keratinocytes	Case Report	5 (4/1)	Burns	Only two patients required any additional grafts to cover open wounds
129	Autologus epithelial cells	Case Report	28	Burns	After 5 years, CES engraftment was unpredictable and inconsistent Suggested to be used as a biologic dressing or experimental adjuvant
130	Autologous keratinocytes	Observational Study	37	Burns (29) Scald wounds (8)	Good cosmetic appearance when compared with meshed split-thickness skin grafting
88	Autologous keratinocytes	Case Report	7 (4/3)	Burns	After 1 month, epidermal regeneration and differentiation was achieved
b131	Autologous keratinocytes	Non-randomized trial	8	Burns	After follow-up, scars had a significantly smoother surface and less pigmentation than traditional meshed autografts
89	Autologous keratinocytes	Non-randomized controlled trial	7	Burns	An undulated DEJ was present underneath the grafted epithelia
132	Autologous epidermal cell sheets	Non-randomized controlled trial	14	Palmoplantar wounds	Expression of K9 was continuously observed after the transplantation
109	Autologous keratinocytes	Non-randomized controlled trial	7	Burns Reconstructive releases	After 14 days, successful vascularization was observed in 45.7±14.2% of the wounds
133	Autologous epithelial cells	Case Report	2 (2/0)	Burns	Poor graft take, so suggested to be used as temporary biological dressing
107	Allogeneic keratinocytes	Retrospective Observational Study	13 (7/6)	Chronic skin ulcers	There was an overall reduction of 91.5% of wound size in comparison with initial value
69 (NCT00832156)	Autologous epidermal cells	Randomized Controlled Trial (Parallel Assignment)	40 (25/15)	Burns	Epithelialization was increased in the wounds after 5-7 days (71.2±24.8%)

[a]Expression of measures: mean +/- standard deviation (range).
[b]Reconstructive procedures were required in the first 2 years for functional problems.
Treatment-related adverse events were only reported in one study[131].

4.2.2. HUMAN FIBROBLASTS (MONOLAYER TESSs)

The development of new culture techniques and the ability to isolate dermal fibroblasts have provoked that the number of clinical studies evaluating the use of another type of monolayer TESSs, called **cultured dermal substitutes (CDSs)**, for the treatment of chronic skin ulcers mainly, but also, surgical wounds and burns, have increased (**Table 4**)[70–75,98,107,110,134]. The findings from these studies

highlight that the use of this monolayer substitutes increases the release of cytokines and/or growth factors which activate many pathways for skin regeneration[70,73].

In most of the cases, CDSs were fabricated using allogeneic fibroblasts[70–75,98,107], cultured over different scaffolds and placed cell-seeded side down onto the wound surface. Some of these studies have compared different treatment demonstrating that, for example, cryopreserved fibroblasts used for CDS manufacture are capable of releasing cytokines and promoting re-epithelialization at the same level as fresh cells[73]. Moreover, the application of these advanced therapies improved wound healing compared to the conventional treatment with Vaseline gauze[98].

The use of an appropriate scaffold for the culture of these fibroblasts is also important. The combination of these cells with hyaluronic acid and collagen have been used for the treatment of several types of wounds[70–75], demonstrating that their application is interesting as biological wound dressing to produce granulation tissue and secrete VEGF, bFGF and ECM proteins useful for mesh-auto skin grafts.

Interestingly, the use of autologous fibroblasts for the CDS manufacture has been limited[110,134]. In these cases, the period between the recruitment of the patient and the treatment was increased, due to the necessity of cell isolation and expansion (more than 10 days)[110,134]. However, the time required for complete healing of diabetic ulcers have been lower in those cases where CDSs were applied compared with the control group (non-adherent foam dressings)[134].

On balance, the use of allogeneic fibroblasts is preferred against autologous fibroblasts, which could be explained by the use of the CDSs as temporary dressings to prepare the wound´s bed for future therapies or the small size of wounds treated (small ulcers), when a short-term biological recovery dictates the long-term outcomes[135].

Table 4. Clinical use of human cultured dermal substitutes (CDSs).

References	Cells	Type of Clinical Study	N (Male / Female)	Treatment-Related Adverse Events	Indication	Outcomes
70	Allogeneic fibroblasts	Case Report	6 (4/2)	In one patient, infection after 14 days was observed but resolved	Burns (5) Necrotizing fasciitis (1)	Permanent cover was not achieved, but released cell growth factors which improved wound healing
71	Allogeneic fibroblasts	Case Report	3 (2/1)	None	Skin ulcers prior to autologous skin grafting	A greater amount of healthy granulation tissue was produced and suitable for autologous skin grafting
72	Allogeneic fibroblasts	Case Report	13 (3/10)	One case presented local infection	Chronic and consecutive leg ulcers	Effective not only for producing tissue granulation and epithelialization, but also for removing necrotic tissue
73	Allogeneic cryopreserved or fresh fibroblasts	Case Report	7 (5/2)	None	Surgical wounds	Cryopreserved TESSs were able to release several cytokines and promote re-epithelialization in a similar way as fresh TESSs
74	Allogeneic fibroblasts	Case Report	5 (0/5)	None	Skin ulcers	Capable of promoting wound healing in intractable skin ulcers
75	Allogeneic fibroblasts	Case Report	8 (3/5)	One case presented local infection	Intractable skin ulcers	Healthy granulation tissue and epithelization were developed rapidly in many cases
134	Autologous fibroblasts	Randomized, Controlled, Multicenter Clinical Trial	31 (21/10)	None	Diabetic ulcers	Time required for complete healing was lower in the TESS group compared to the control group
110	Autologous fibroblasts	Prospective, Open-Labelled Clinical Trial	5 (5/0)	30 adverse events, two directly related to the treatment but resolved	Diabetic ulcers	Side effects were not serious Three patients were completely healed within 12 weeks after application
107	Allogeneic fibroblasts	Retrospective Observational Study	17 (11/6)	None	Chronic skin ulcers	There was an overall reduction of 73% in comparison with the initial wound size
98	Allogeneic fetal fibroblasts	Randomized, Double-Blind, Phase I Clinical Trial	10 (9/1)	None	Surgical wounds	Re-epithelialization was faster than in control groups

4.2.3. HUMAN KERATINOCYTES AND FIBROBLASTS (BILAYER TESSs)

In recent years, the combination of human keratinocytes and fibroblasts in bilayer TESSs, called **composite skin substitutes (CSSs)**, has been explored.

CSSs resemble normal skin by containing an epidermal layer of autologous or allogeneic keratinocytes and a dermal layer of fibroblasts incorporated into a stromal scaffold. They do not only provide structural dermo-epidermal support, but also deliver growth factors (EGF, PDGF, VEGF) and extracellular matrix that increase the rates of recovery and healing[136,137].

Therefore, although clinical benefits of CESs and CDSs have been realized in many patients; the most studied clinical TESSs have been CSSs composed of human keratinocytes and fibroblasts. These bilayer TESSs have been used for the treatment of several dermatological pathologies since 1989 (**Table 5**)[2,76–87,90–95,101,102].

Most of the studies evaluated the use of CSSs for the treatment of burns, however, experimental designs differed from cell populations used (autologous[2,76–79,81,82,84–87,90–95,101,102] or allogeneic[80,83]), biomaterials selected, randomization or not, comparison or not with other treatments or pretreatment required.

In those cases where different treatments were compared, engraftment of autografts was used as reference for each patient[2,78,80,82–87,93]. The use of allogeneic cells reported no graft take and the use of the gold standard treatment was required[83]. This demonstrates that the use of autologous cells is essential to provide a proper treatment. It has been proved that positive results were reported compared to autografts: the percentage of total body surface area closed was considerable (20.5%-29.9% for CSSs vs. 47.0%-52.1% for autografts, 28 days post-treatment[84,86]), time of healing was similar (7.4±0.9 days for CSSs vs. 7.9±1.5 days for autografts[80]), the total wound area closed was almost 100% (95.4% for CSSs vs. 99% for autografts after 28 days[82]) and less scar formation was observed[79]. Moreover, higher percentage of epithelialization has been reported after 21 of engraftment (63.5±35%)[87].

Therefore, the beneficial role of using CSSs alone[79,91,92,94,101,102] or combined with autografts[76,77,81,85,90,95] could improve patient's health, however, some authors have remarked the importance, as in the case of CESs, of a pretreatment with auto-dermis or allo-dermis to increase the clinical benefits[76,81,87,90,92].

Regarding the biomaterials used, different types of collagens[77,80,83–85,87] or combined with glycosaminoglycan[76,78,79,81,82,86] were the preferred sources, although different formulations of plasma/fibrin have been also reported[90–94]. Finally, the application of hyaluronic acid[95] or acellular dermal matrices derived from human fibroblasts[2,101,102] could be considered.

Table 5. Clinical use of human composite skin substitutes (CSSs).

References	Cells	Type of Clinical Study	N (Male / Female)	Treatment-Related Adverse Events	Indication	Outcomes
76	Autologous keratinocytes and fibroblasts	Case Report	4 (3/1)	None	Burns	Improved quality of healed skin
77	Autologous keratinocytes and fibroblasts	Case Report	2 (2/0)	None	Burns (1) Excised wounds (1)	Mature epidermis and well-differentiated papillary and reticular dermis were formed
78	Autologous keratinocytes and fibroblasts	Prospective Randomized Clinical Study	17	Increased incidence of exudates	Burns	Pigmentation was greater, scar was less raised, but regrafting was more frequent than when autografts were applied
79	Autologous keratinocytes and fibroblasts	Case Report	5 (4/1)	None	Burns	Connection between epidermis and connective tissue was observed
80	Allogeneic keratinocytes and fibroblasts	Prospective Randomized Compared Clinical Study	11	None	Surgical wounds	Rapid healing and reduction of the pain
81	Autologous keratinocytes and fibroblasts	Case Report	3 (3/0)	None	Burns	Stable epithelium covered a layer of newly formed fibrovascular tissue Smooth, pliable, and hypopigmented skin
82	Autologous keratinocytes and fibroblasts	Prospective, Randomized, Non-blinded Clinical Study	45 (34/11)	None	Burns	Healed skin was soft, smooth and strong with irregular pigmentation
83	Allogeneic keratinocytes and fibroblasts	Case Report	3 (2/1)	Local inflammation	Burns	A few islands of keratinocytes remained after 1 week on an inflamed bed
90	Autologous keratinocytes and fibroblasts	Case Report	2 (2/0)	None	Burns	Epidermal regeneration was stable, with good cosmetic outcome
84	Autologous keratinocytes and fibroblasts	Randomized Controlled Trial	40	None	Burns	Vancouver Scale Scores were not different for erythema, pliability, or scar height, but pigmentation remained deficient against autograft treatment
91	Autologous keratinocytes and fibroblasts	Case Series	20	None	Burns (13) Giant nevus (5) Graft-versus-host disease (1) Neurofibromatosis (1)	Permanent epithelization
95	Autologous keratinocytes, melanocytes and fibroblasts	Single Group Assignment Open Label Clinical Trial	11 (3/8)	None	Giant nevus (5) Tumors (2) Scars (3) Trauma (1)	Loss of the epithelial layer varied markedly (from 5 to 70%) while fibroblast cellular component growth prevailed
92	Autologous keratinocytes and fibroblasts	Multicenter Retrospective Observational Cohort Study	25 (23/2)	Thirteen patients presented wound infection (*P. aeruginosa* mainly)	Burns	Characteristic scarring of mesh interstices was avoided Epithelialization was observed
101	Autologous keratinocytes and fibroblasts	Prospective Uncontrolled Case Study	5 (1/4)	None	Skin ulcers	Effective treatment of long-standing hard-to-heal venous or mixed ulcers
102	Autologous keratinocytes and fibroblasts	Case Report	4 (1/3)	None	Burns	Dermal part had a well-vascularized dermal matrix and the bilayer structure was conserved
85	Autologous keratinocytes and fibroblasts	Case Report	1 (1/0)	None	Burns	CSS completely covered the wound area and smoothly adapted to the wound bed
93	Autologous keratinocytes and fibroblasts	Case Report	2	None	Burns	Appearance of the skin did not differ significantly from the areas treated with autografts
94	Autologous keratinocytes and fibroblasts	Case Report	1 (0/1)	None	Burns	Patient was discharged with a complete skin coverage and functionality

86	Autologous keratinocytes and fibroblasts	Prospective Randomized Open-Label Paired-Site Comparison Clinical Trial	16 (14/2)	None	Burns	Vascularization of the dermal component was achieved, barrier function was stabilized and basement membrane was restored
2	Autologous keratinocytes and fibroblasts	Case Series	14 (12/2)	None	Burns	No loss of the epithelium was observed during the first-year post-intervention or reported subsequently
87	Autologous keratinocytes and fibroblasts	Phase I Two-armed, Open-Label Prospective Clinical Trial	10 (6/4)	Four cases of hematoma	Burns (1) Reconstructive surgery for burn scars (9)	After 3 months, there was a multilayered, well-stratified epidermis and a dermal compartment comparable to native skin

4.2.4. HUMAN MELANOCYTES, MERKEL CELLS AND LANGERHANS CELLS

In order to develop TESSs that most resemble native human skin, apart from keratinocytes and fibroblasts, the incorporation of other cell types of the epidermal layer, such as melanocytes, Merkel and Langerhans cells, has been evaluated. However due to different aspects such as the difficulty of isolation and culture (Merkel and Langerhans cells) or the risk of uncontrolled proliferation (melanocytes), only preclinical studies are already published.

In the case of **melanocytes**, their role in wound healing has been evaluated in combination with keratinocytes and fibroblasts. Interestingly, most of these TESSs have been manufactured in combination with collagen as biomaterial[138–143] although, the use of extracellular dermal matrix derived from fibroblasts has been also reported[144].

These studies revealed, *in vitro* and *in vivo*, a proper integration, morphology and successful repair of skin defects in animals, at different time point after grafting[138–143]. Some of these *in vivo* studies evaluated the use of cryopreserved melanocytes to reduce the TESS manufacturing time, demonstrating a proper localization of these cells in the basal layer of the epidermis[142]. Moreover, cutaneous pigmentation and ultraviolet photoprotection have been proved to be restored[142,144], regardless of whether light or dark pigmentation phototype melanocytes are used[143].

In contrast, the use of **Merkel** and **Langerhans cells** in TESSs is limited due to the difficulty of isolation and culture. For this reason, only *in vitro* studies have reported the use of Langherhans cells derived from monocytes or myeloid leukemia cell lines for bilayer TESS manufacture (keratinocytes and fibroblasts), demonstrating their proper localization, after culturing process, in the suprabasal layers of the epidermis[145,146].

However, rest of the studies focused on these cell types only used human keratinocytes and fibroblast for TESS manufacture but the presence of Langerhans ($CD1a^+$ and human leukocyte antigen - HLA^+)[147–150] or Merkel cells ($K20^+$ - and HLA^+)[151] was reported. This indicates that keratinocyte cultures, isolated from human skin samples, are likely to contain a small proportion of these cells.

4.3. THE ROLE OF HUMAN STEM CELLS IN TESSs

Human stem cells such as skin stem cells (hSSCs), induced pluripotent stem cells (hiPSCs) and mesenchymal stem cells (hMSCs) have been investigated for therapeutic use to enhance wound healing[54,60,152]. This has led to the fabrication of more complex models of TESSs (**Fig. 5**), which could stimulate more rapid and complete healing; furthermore, drive expression of additional phenotypes to correct anatomic deficiencies through activation of biological signaling pathways[60]. However, only the use of hMSCs has been considered for clinical purposes[54], while hSSCs and hiPSCs have been only evaluated at preclinical level.

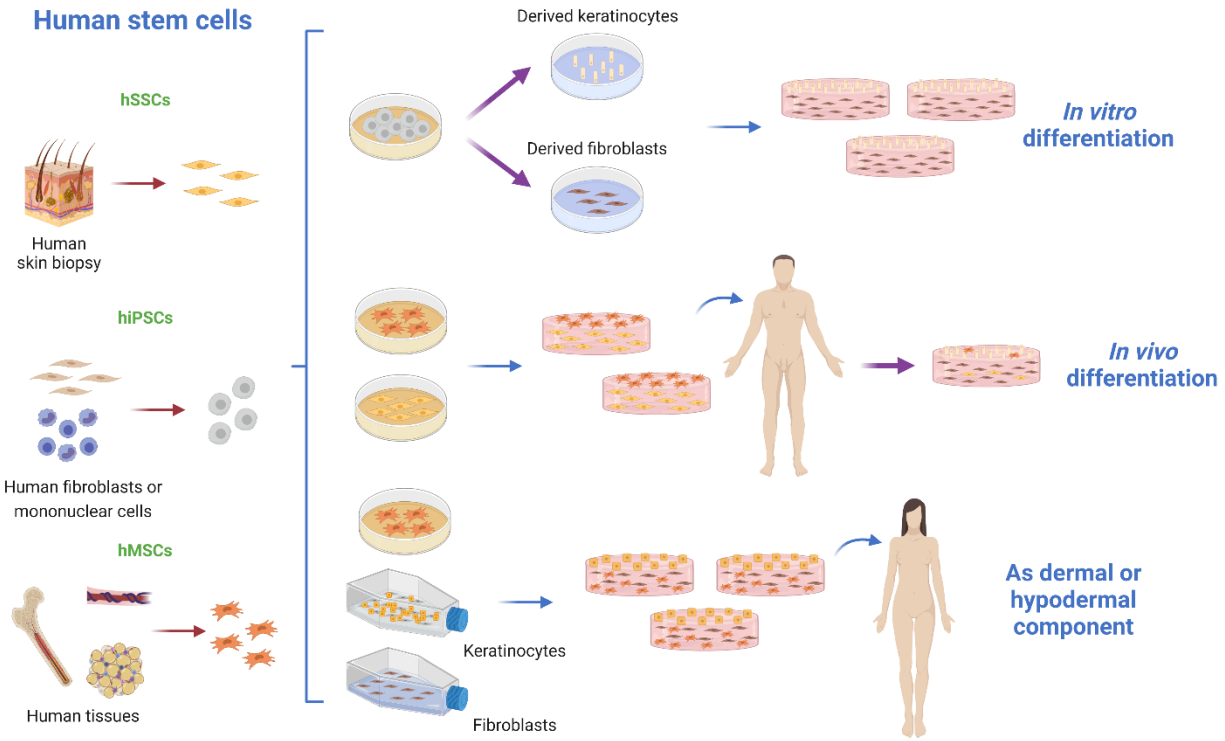

***Fig. 5*. Human stem cell strategies for tissue-engineered skin substitutes (TESSs).** *Different sources of stem cells could be **i)** differentiated in vitro to the main cutaneous lineages and then, uses to fabricate artificial skin; **ii)** embedded directly into dermal matrixes and engrafted to achieve an in vivo differentiation; or **iii)** combined with human keratinocytes and fibroblasts to benefit from their own angiogenic and immunomodulatory properties (**trilayer TESS**). hSSCs: human skin stem cell; hiPSCs: human induced pluripotent stem cells; hMSCs: human mesenchymal stem cells. Created with BioRender.com.*

4.3.1. HUMAN SKIN STEM CELLS

The skin is an attractive source of stem cells because of their abundant supply, easy accessibility, ease of harvesting, and possibly providing immune-privileged cells[153]. **Human skin stem cells (hSSCs)**, characterized by their quiescence state ($CD71^-$, $EGF\text{-}R^{low}$) and their strong adhesion capacity (high expression of integrin markers)[154], have been isolated from different parts of skin such as dermal papilla or hair follicles, among others[45,153,155,156]. In particular, dermal papilla stem cells (DPSCs), also called dermal hMSCs, have similar characteristics and differentiation capacity as

hMSCs from other tissues[156], and for this reason they are the hSSCs most studied for skin regeneration and wound repair.

The use of **hSSCs** for TESSs manufacture provides a wide range of possibilities. Several *in vitro* and *in vivo* studies have reported that the combination of DPSCs or hair follicle stem cells (FSCs) with different biomaterials or scaffolds are able to produce fibronectin deposits[66] or replace interfollicular fibroblasts in TESSs[157]. Interestingly, DPSCs as cellular component of the dermis improves basement membrane formation compared to interfollicular fibroblasts, together with an increased type IV collagen and VEGF expression[157]. Moreover, the *in vivo* comparison of bilayer TESSs composed of keratinocytes and different types of hSSCs as dermal component has demonstrated their capacity to support epidermal differentiation and stratification[158]. However, an enhanced expression of tropoelastin (a soluble precursor of elastic fibers) were only observed in skin grafts containing DPSCs, in a similar level to those composed of hAT-MSCs, demonstrating their potential to accelerate wound healing[158,159].

In addition to being embedded as dermal component, the use of hSSCs allows to add them as epidermal layer [61,67]. The combination of DPSCs with an acellular matrix as dermal compartment and the culture of FSCs as epidermal layer (bilayer TESS), has *in vivo* demonstrated a correct stratification, differentiation and well-ordered epithelia formation, successful integration (less contraction) and improved vascularization (higher expression of VEGF)[61].

4.3.2. HUMAN INDUCED PLURIPOTENT STEM CELLS

Human induced pluripotent stem cells (hiPSCs) are stem cells generated from individual somatic cells by exogenous expression of several transcription factors to initiate the reprogramming process[160]. In skin regeneration and for TESSs, hiPSCs have been successfully obtained from fibroblasts[161–163] or cord blood mononuclear cells (CBMCs)[164], and differentiated *in vitro* into fibroblasts and keratinocytes [161–164].

The application of these differentiated cells has been demonstrated to be useful for the development of TESS models for preclinical research. These hiPSCs-derived fibroblasts are capable of producing and secreting mature type VII collagen in addition to expressing other types of collagen (I, III and IV)[161]. Moreover, the manufacture of bilayer TESSs using these cells has demonstrated their capacity to support functional and terminal differentiation of human primary keratinocytes (K1 and loricrin expression)[161].

Apart from being differentiated into fibroblasts, the use of hiPSCs-derived keratinocytes has been also reported. Their combination to produce bilayer TESSs has been demonstrated to resemble histological structure of nature human skin[161]. Moreover, the manufacture of monolayer TESSs composed of hiPSCs-derived keratinocytes expressing K14 and p63, has shown their capacity to form

the same structure as the human epidermis and, develop endoplasmic reticulum Ca^{2+} store, essential for normal keratinocyte signaling and differentiation[163].

To improve the survival of skin grafts and avoid immune rejection, CBMCs have emerged as a potential cell source for regenerative medicine and hiPSCs. One advantage of CBMCs as a source is the mandatory HLA typing during the CBMC banking process, making available valuable HLA-matched research materials that can be obtained easily[164]. The differentiation of hiPSCs from CBMCs into fibroblasts and keratinocytes has allowed to produce 3D skin organoids; and after being engrafted in mice, they have resembled native human skin structure. Moreover, similar expression of CD73 and CD105 as primary fibroblasts; and upregulation of involucrin and loricrin (epidermal differentiation markers), supported this result[164].

In addition to fibroblasts and keratinocytes, hiPSCs have been differentiated into other cell types such as melanocytes[162], sensory neurons and Schwann cells[165]. They have been generated *in vitro* and successfully incorporated into TESSs with the purpose of fabricating more complex, functional and complete skin substitutes, although exhaustive *in vivo* analysis is still required.

4.3.3. HUMAN MESENCHYMAL STEM CELLS

Human mesenchymal stem cells (hMSCs) are non-hematopoietic multipotent adult progenitor cells that are found in various tissues including, mainly, bone marrow, umbilical cord and adipose tissue. They can be easily harvested and expanded from the different tissues of adult donors[166], avoiding any potential ethical issues associated with using embryonic stem cells or with genetic manipulations when using hiPSCs.

Moreover, their hypo-immunogenic property allows its immediate use as prepared allogeneic cells without significant host reaction[167–170], although recent studies have indicated that the immune compatibility between donor and recipient is also important because hMSCs are immune evasive rather than immune privileged[135,171,172]. This is an important fact because immunogenicity of allogeneic hMSCs have been proven[173], but no acute adverse events have been reported when were applied as therapy in several pathologies[172]. To avoid this concern, immunosuppression treatment could be effective for the use of allogeneic cells in many clinical conditions, however, this poses a risk for long-term therapies where other pathologies could be developed due to a continuous suppression of immune system and moreover, in the case of skin or TESS transplants, is either less or/not effective[174]. On balance, although immune rejection of allogeneic hMSCs occurs more slowly than other cell types[171,173], they are immune evasive rather than immune privileged and for this reason, it could be interesting to use haplo-identical hMSCs[135,171] to increase the potential benefits of allogeneic TESSs when autologous approach is not possible.

Despite this concern, the use of hMSCs for dermatological diseases and TESS manufacture seems to be interesting due to their anti-inflammatory capacity[175], that can be also useful in dampening the inflammatory milieu of chronic non-healing wounds and aid in the healing process, and their possibility to differentiate into both mesenchymal and non-mesenchymal lineages such as ectodermal keratinocyte-like cells[176], dermal cells[177], endothelial cells, and different skin appendages[176,178]. In addition, together with adult skin cells and hSSCs, hMSCs contribute to re-epithelization in normal wound healing process by stimulating collagen production and reducing fibrosis and scar formation by releasing many growth factors such as EGF, TGF-β, VEGF and bFGF[45]. Therefore, the development and research of hMSC based strategies in dermatology have increased in recent years[54].

4.3.3.1. Human bone marrow-derived MSCs (hBM-MSCs) in TESSs

hBM-MSCs are the most studied at preclinical level and the major source of hMSCs. In the skin, hBM-MSCs' regenerative potential and their ability to differentiate into non-mesenchymal lineages including endothelial cells, keratinocyte-like cells, and skin appendages[179], have been demonstrated to be useful for wound healing.

These cells have good *in vitro* differentiation capacity, mainly, into dermal cells, but also into epidermal cells[177]. However, the existing preclinical studies evaluating their use for TESSs manufacture, have focused on their differentiation potential *in vivo*[177,179,180]. hBM-MSCs embedded into[177,180] or cultured over[177,179] different dermal matrixes such as collagen[177] or fibrin[179], have led a complete wound healing *in vivo*[177,179]. Moreover, these engrafted TESSs (monolayer[179] or bilayer[177]) have been able to generate a differentiated epidermis[177,179] and dermis[177].

In addition, the combination of hBM-MSCs and keratinocytes, to produce bilayer TESSs, has showed that this model is able to support keratinocytes' growth and differentiation *in vitro*[180]. Interestingly, the comparison of hMSCs from different sources (hBM-MSCs, umbilical cord Wharton's jelly (hWJ-MSCs) and hAT-MSCs) cultured as the epidermal layer in monolayer TESSs has demonstrated a proper *in vitro* and *in vivo* differentiation into an epithelial-like layer ($K5^+$ expression), mainly for hAT-MSCs-based TESSs[179].

Regarding clinical studies, the use of hBM-MSCs for TESSs manufacture, as the other hMSCs, has been limited[104,105,111] (**Table 6**). Autologous hBM-MSCs have been used in combination with fibroblasts on a collagen and hyaluronan membrane for the treatment of ulcers, demonstrating an increased vascularization of the dermis due to the differentiation potential of hMSCs into endothelial progenitor cells which produced VEGF and bFGF[104]. Moreover, monolayer TESSs constituted of autologous hBM-MSCs into collagen[105] or decellularized dermal matrixes[111] have been also reported for the treatment of different dermatological pathologies, showing better outcomes than comparator

groups[105,111], improving subcutaneous and vascular endothelia formation (by an increased infiltration of CD34+ cells)[105].

4.3.3.2. Human umbilical cord Wharton's jelly-derived MSCs (hWJ-MSCs) in TESSs

Perinatal stem cells such as **hWJ-MSCs** have been shown to have excellent proliferation and differentiation capabilities to be applied in regenerative medicine[181].

The use of hWJ-MSCs for TESS manufacture of preclinical model have focused on their addition into or culture over different biomaterials as monolayer TESSs[62,182,183] or to constitute the epithelial layer of bilayer TESS composed of fibrin/agarose and fibroblasts as dermal stroma[64].

Preliminary results have demonstrated their *in vivo* potential to differentiate and stratify into typical epithelial layers[64]. Moreover, the use of hWJ-MSCs as stromal component of TESSs for *in vivo* grafting in mice has induced a faster healing and a higher number of blood vessels in the wound when compared to comparator groups[182] and showed multi-direction differentiation into newly formed skin and its appendages such as sebaceous glands, hair follicles and sweat glands[183].

Interestingly, a hWJ-MSC suspension has been used as adjuvant therapy together with a monolayer TESS constituted of an upper layer of hWJ-MSCs[62]. It seems to be that the injection of this cell suspension, at the edge of the wounds in mice, improves collagen dermis organization and diminishes both innate and adaptive immune infiltrates compared to the single treatment with TESSs[62].

For clinical purposes, only one study has evaluated the use of allogeneic hWJ-MSCs in combination with amniotic membranes for the treatment of chronic ulcers[99] (**Table 6**). The application of these TESSs decreased patients' pain and a high wound healing rate was reported after 9 days of engraftment (96.7%)[99].

4.3.3.3. Human adipose tissue-derived MSCs (hAT-MSCs) in TESSs

hAT-MSCs are an attractive source for manufacturing hMSCs-based TESSs for their ease of harvesting and expansion in culture and versatile differentiation potential[176,184,185]. Moreover, compared to MSCs from other sources such as the bone marrow, the procurement of hAT-MSCs is associated with lower morbidity and higher yield of cells[181].

The main use of hAT-MSCs for the development of TESSs has been as dermal component, alone or combined with other cell types. For example, it has been proven that the *in vitro* manufacture of bilayer TESSs comprised of hAT-MSCs as dermal layer enhances keratinocytes proliferation and increases type IV collagen expression at the DEJ[186,187]. Moreover, the *in vivo* evaluation of these bilayer TESSs in several animal skin wound models has reported faster wound regeneration and less inflammatory

cell infiltration than control groups[188], in addition to an increase of wound healing rates[189] by promoting angiogenesis and re-epithelization[190,191].

Furthermore, favorable outcomes have been also observed when hAT-MSCs are combined with other cells to constitute the dermal stroma. The manufacture of trilayer TESSs composed of hAT-MSCs co-cultured with human endothelial cells in the dermal layer, combined with human keratinocytes as epithelial layer have been able to form capillary structures *in vitro*[192]. Interestingly, the addition of hAT-MSCs to pigmented TESSs constituted of keratinocytes and melanocytes as epidermal layer and collagen, fibroblasts and hAT-MSCs as dermal and hypodermal layers, generated less dark TESSs than those manufactured with fibroblasts only[193]. This means that the cytokines released by hAT-MSCs maintain melanocytes in an immature state where melanin synthesis is decreased[193].

Regarding clinical TESSs incorporating hAT-MSCs (**Table 6**), autologous[106,108] and allogeneic[194] sources have been evaluated. Collagen-glycosaminoglycan[106] and plasma[108] have been the biomaterials used as scaffolds to culture the autologous hAT-MSCs (monolayer TESSs); demonstrating their usefulness as a complementary treatment to autografts when dealing with highly complex burns patients with contractures[106] or to achieve a total re-epithelialization in chronic ulcers[108].

Allogeneic hAT-MSCs have been also studied (NCT02619877) embedded into a hydrogel (monolayer TESS) for the treatment of chronic ulcers. Results have demonstrated no clinical rejection after 12 weeks and a higher efficiency, determined by a Kaplan-Meier median time to complete wound healing of 28.5 days for the treatment group compared to 63.0 days for the control group (Mepitel®)[194].

Table 6. Clinical use of human mesenchymal stem cells in tissue-engineered skin substitutes (TESSs).

References	Cells	Type of Clinical Study	N (Male / Female)	Indication	Outcomes
104	Autologous hBM-MSCs	Case Report	1	Diabetic wounds	Wound size decreased and vascularity of the dermis increased after 29 days
105	Autologous hBM-MSCs	Case Series	20 (9/11)	Severe burns (2) Decubitus ulcer (11) Skin ulcers (7)	High tissue regenerative ability was observed and the healing mechanism was activated
111	Autologous hBM-MSCs	Case Report	1 (1/0)	Burns – Scar excision wounds	Contraction of skin was significantly less at the hBM-MSC transplantation site than at the control site
99	Allogeneic hWJ-MSCs	Randomized Clinical Trial	5	Chronic diabetic wounds	After treatment, some patients reported even a decline in pain
106	Autologous hAT-MSCs	Case Report	2 (0/2)	Surgical wounds – Burns	This technique was not recommended routinely, but should be considered for burns patients with contractures affecting cosmetically or functionally challenging areas
194 (NCT02619877)	Allogeneic hAT-MSCs	Phase II Multicenter Randomized Clinical Trial (Parallel Assignment-Single Blind)	22 (14/8) 17 (13/4) – Control Group	Chronic diabetic ulcers	Complete wound closure was achieved for 82% of patients in the treatment group and 53% in the control group at week 12
108	Autologous hAT-MSCs	Prospective clinical analysis	6 (3/3)	Chronic diabetic ulcers	There was granulation tissue formation, 7 days after topical application After 90 days, a healed and re-epithelialized tissue was observed
No treatment-related adverse events were reported.					

On balance, the use of hMSCs-based TESSs for the treatment of dermatological pathologies could increase patient's health and quality of life in a significant way. Apart from generating more complex substitutes (trilayer TESSs), the use of these cells helps to increase the regenerative capacity of the own patient's hMSCs due to their role in wound healing and, on the other hand, the immunomodulatory capacities associated to them, are important to regulate the immunological response. However, despite of the fact that many promising advanced therapies based on the use of hMSCs have been developed and evaluated, there is a necessity of increasing the investigation at preclinical level that would allow to accomplish more clinical research to evaluate their safety and effectiveness.

5. BIOMATERIALS AS THE SKELETON OF TESSs

As previously described, the design of TESSs therapies requires the development of a proper dermal matrix to provide appropriate mechanical stability and biological properties. A 3D structure is required for guiding tissue formation into the desired shape and providing adequate transport of nutrients and growth factors to promote tissue growth[195]. For this reason, the use of biomaterials is widespread for TESSs development. Biomaterials may be of different nature, including solid, liquid, and gel substances. This broad characterization has been specified through the years due to the technology used and their intended application, and it might change in the upcoming years due to the breakthrough of new applications or devices in medicine that will require biomaterials[196].

First definition of biomaterial was reported by Williams in 1987[197], who identified this term as "nonviable material used in a medical device, intended to interact with biological systems". However, this definition has evolved to include the wide range of applications where different materials interact with biology[195]. Nowadays, biomaterials are defined as any substance (other than drugs) or combination of substances synthetic or natural in origin which can be used for any period, as a whole or as a part of a system, which treats, augments, or replaces any tissue organ or function of the body[198]. In addition, they must be biocompatible to avoid host rejection in a specific application[197].

For these reasons, scaffolds for TESS manufacture must resemble and mimic the function of the natural extracellular dermal matrix[199–201], considering the properties of the materials and the relation with the biological environment[196]. Moreover, they must support keratinocytes and provide a correct environment for fibroblasts growth, apart from promoting recruiting/seeding, adhesion, proliferation, differentiation and neo-tissue genesis[200,201].

To that purpose, three main types of biomaterials including natural, synthetic and composite (the combination of natural and synthetic) have been analyzed[201]. All of them should be characterized topologically and biochemically for maintain cell viability, adhesion and differentiation[202,203], in an attempt to demonstrate that they are capable of eliciting specific cellular responses and directing new tissue formation mediated by specific interactions[204]. Among these, natural materials such as collagen, hyaluronic acid or plasma/fibrin (**Table 2**), have been more studied because they contain protein motifs that facilitate cell adhesion, and demonstrate better compatibility and degradation *in vivo*, particularly when incorporating biomolecules which conform skin ECM[205]. A brief description of them and the rest of the main biomaterials used for the development of clinical TESS is detailed below:

Collagen is the most abundant of animal proteins, localized in soft and hard connective tissues where its fibrils, with high tensile strength and stability via cross-linking, comprise the majority of ECM and form a highly organized 3D scaffold that surrounds the cells. Moreover, it is a dynamic and flexible biomaterial (used as sponge, gel or membrane) with high biocompatibility and intrinsic

biodegradability ideal for biomedical applications[206]. **Glycosaminoglycan** is a negatively charged polysaccharide and one of the most prevalent cross-links of collagen, that affects their mechanical properties and fibril formation[207]. The main aspect to consider the incorporation into TESSs is the presence of negatively charged carboxyl and sulfate groups that are responsible of maintaining water in tissues[208], and therefore, skin barrier.

Hyaluronic acid is also an important component of human skin[209,210] and its use for TESSs is recommended. It is easy to handle, their biosafety has been corroborated by its use as injectable dermal fillers[211], and its effectiveness have been demonstrated for skin restoration in terms of hydration and transepidermal water loss[212], mainly when the water regulation and neoangiogenic boost are relevant issues[213]. Moreover, biodegraded hyaluronic acid, enhances angiogenic pathways and the migration and proliferation of cells[214].

In the case of **plasma/fibrin-based matrices**, their use for TESSs have reported positive results due to the presence of many natural components responsible of coagulation and involved in the first stages of wound healing. It has been demonstrated that enhances cell proliferation (keratinocytes mainly), due to the presence of basement membrane proteins such as laminin, collagen or Perlecan[215].

Finally, amniotic membrane and extracellular dermal matrix are the less common biomaterials or strategies used for TESSs, however, they also provide structural support and secrete important proteins or factors required for wound healing. **Amniotic membrane** has high tensile strength due to a structure comprised of an epithelial monolayer, a thick basement membrane and avascular stroma. In addition, it releases several growth factors for angiogenesis, downregulates TGF-β expression, promotes fibroblast differentiation and keratinocytes proliferation, and reduces levels of pain and discomfort experienced by the patients[216]. The use of **extracellular dermal matrix** derived from fibroblast is an interested strategy because the use of natural ECM shares many properties with native human skin and minimizes the host response after transplantation[217], but specific training is required to carry out it successfully.

5.1. THE USE OF HUMAN PLASMA/FIBRIN AS BIOMATERIAL FOR TESS MANUFACTURE

Human plasma is a light-yellow liquid that carries the blood components throughout the body. Moreover, it is the acellular component of the blood but contains water (90%), proteins, carbohydrates, lipids, salts, enzymes, nutrients or waste products from the blood cells, among others (**Fig. 6**). Therefore, it is constituted of the most complex human-derived proteome and for this reason, it is used for preparation of many therapeutic products[218]. However, due to its nature and variability between donors, the characterization of its protein profile and the identification of protein biomarkers

has been limited[218,219]. Although it is known that human plasma contains a high proportion of albumin (~55% of the total protein composition), there is also a wide dynamic range in abundance of other proteins and a tremendous heterogeneity of its predominant glycoproteins[218].

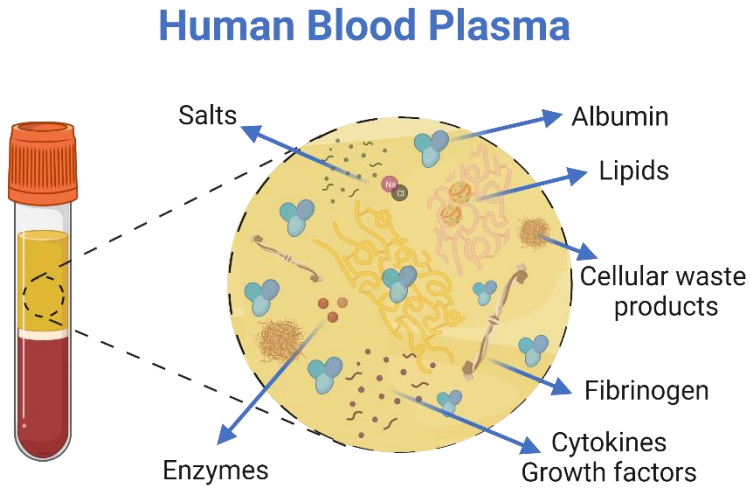

Fig. 6. ***Schematic representation of the human blood plasma composition.*** *Created with BioRender.com.*

The usefulness of human plasma as biomaterial for TESSs lies in the fact that it is an acellular component derived from human donors, so immune rejection is avoided[220]. Moreover, the presence of the clotting proteins fibrinogen and thrombin, allows to generate a provisional matrix or hydrogel that closely mimics ECM[221] after a process referred as "coagulation cascade" (**Fig. 7**). This process can be triggered *in vitro* by several procedures such as crosslinking via enzymes or UV radiation[222,223] or adding different Ca^{2+} concentrations[224,225]. Moreover, these gelation processes determine the mechanical properties of the hydrogels[221].

The coagulation cascade is a series of proteolytic events, physiologically triggered when there is an injury[226]. Moreover, several elements such as different type of cells, proteins or enzymes are involved in this complex process[226]. However, for TESS manufacture the use of human plasma and other reagents can *in vitro* resemble this process to be able to generate dermal matrixes for **human plasma-based skin substitutes (HPSSs)**[63]. Briefly, the principle of this process is that human plasma contains prothrombin (Factor II) which interacts with the added calcium chloride (Ca^{2+})[63] to catalyze the enzymatic reaction with thromboplastin. The product of this enzymatic reaction is thrombin (Factor IIa) which acts to convert fibrinogen (Factor I) to fibrin (Factor Ia), responsible for hemostatic clot. Therefore, **fibrin** is the protein of interest when human plasma-based hydrogels want to be produced. However, to assure that this clot or hydrogel is stable *in vitro* for TESS manufacture, tranexamic acid should be added[63], known to inhibit fibrinolysis by its attachment to the plasminogen/plasmin system.

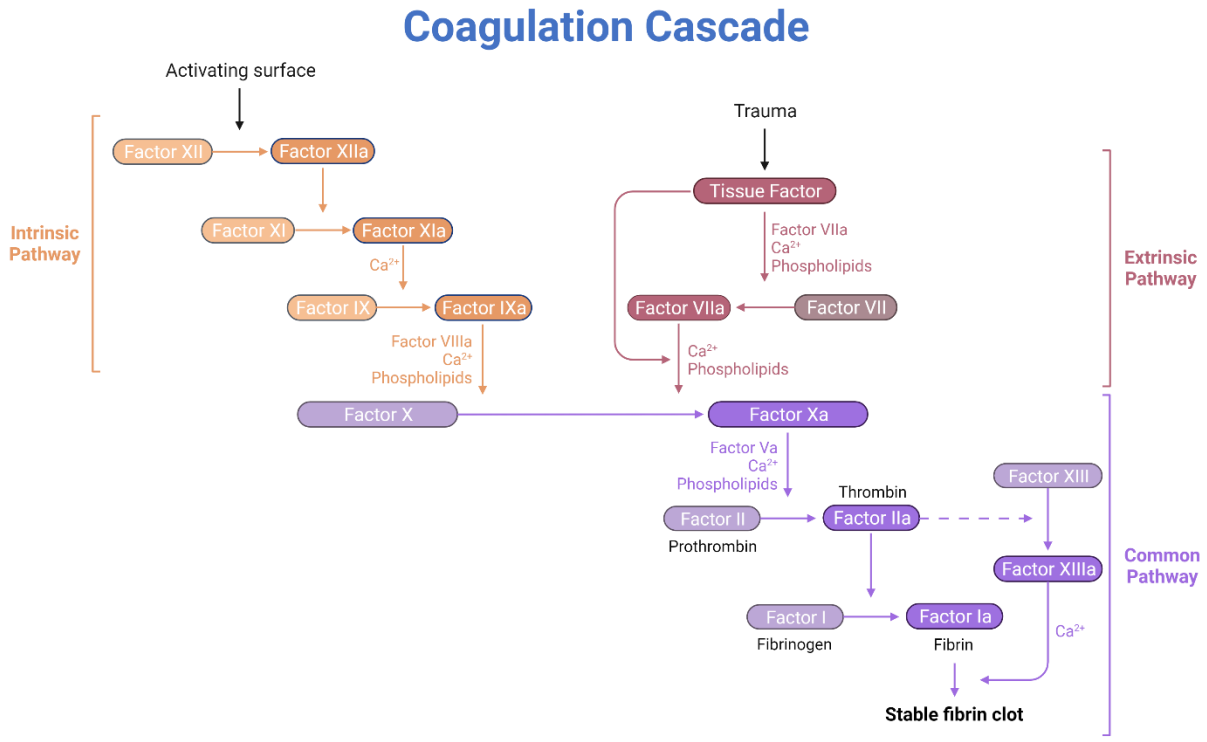

Fig. 7. ***Schematic representation of the coagulation cascade physiological process.*** *Adapted from "Coagulation Cascade", by BioRender.com (2023). Retrieved from https://app.biorender.com/biorender-templates.*

5.1.1. FIBRIN: USEFUL STRUCTURE AND PROPERTIES FOR TESSs

Fibrinogen is a large, complex, fibrous glycoprotein with three pairs of polypeptide chains (Aα, Bβ and γ). The action of the enzyme thrombin cleaves the small peptides A and B from α and β chains respectively, yielding as result a fibrin monomer[227,228]. Then, several nonenzymatic reactions result in an orderly sequence of macromolecular assembly steps, where protofibrils aggregate and branch, generating a 3D clot network together with other plasma proteins[227,229]. Finally, the clot is stabilized by covalent ligand or crosslinking of specific amino acids by a transglutaminase (Factor XIIIa)[227].

Therefore, this enzymatic reaction provokes that a soluble protein changes to a (hydro)gel phase upon formation of a three-dimensional filamentous network[230]. Interestingly, hydrogel formation takes place when only 15-20% of the fibrinogen is converted to fibrin[231]. Several parameters can be described regarding fibrin structure, such as thickness of the fibers, porosity or permeability, however these aspects vary depending on the polymerization conditions (fibrinogen and thrombin concentrations, pH, temperature and the presence of other plasma proteins)[232]. Unfortunately, for tissue engineering applications some of these variables can be controlled (pH, temperature), however, when human plasma from different donors is used, protein composition will undoubtedly vary.

Regarding **biological characteristics of the fibrin matrix**, apart from providing a temporary scaffold for tissue healing and remodeling, also allows to bind several proteins and growth factors located into and around the wound. Among them, fibronectin, FGF and VEGF enable this matrix to play an active

role in wound healing through specific interactions with cells[232]. Moreover, the addition of nature components to this ECM, such as collagen, fibronectin, hyaluronic acid or keratins can impart cell instructions cues not found in a fibrin gel alone[229].

In addition to their regenerative capacities alone or combined with other molecules, **mechanical properties of the fibrin matrix** are also interesting. In a physiological environment, fibrin clot must stop bleeding but allows cell penetration, which means that it owns specific elastic and plastic deformation and embolization characteristics[227]. Therefore, fibrin has a viscoelastic behavior[227,232] which means that this polymer presents both elastic and viscous properties. The elastic properties are determined by the stiffness or storage modulus, while the inelastic properties are measured by the creep compliance or loss modulus/loss tangent[227]. Unfortunately, there are not standard values or a universal characterization of the mechanical properties of the fibrin matrix derived from human blood plasma samples, due to the different nature, composition and the inter-variability between donors. Despite of this, it is well-known how different forces, strains and the modulation of the concentration of the different components of the human plasma affect to the fibrin matrix structure and properties[227,229,232].

The mechanical characterization by creep experiments has reported an irreversible deformation of the fibrin network but the stiffness is completely recovered when the stress is removed, which means that there are not net changes of its structure[233]. Moreover, the application of external compression demonstrates that fibrin exhibits a nonlinear mechanical behavior: firstly, a viscoelastic response to compression is observed, where more of the fibrin fibers are straight, followed by a stress plateau where more and more fibers buckle and collapse, to finish with a network densification with a stress–strain response that is markedly nonlinear and dominated by bending of fibers after buckling and inter-fiber contact[234]. In addition, the application of a downward force on the top surface of the clot or hydrogel has demonstrated that the top layers are compressed earlier and stronger that the bottom regions[235]. Interestingly, it has been reported that when low strains are applied, stress is directly proportional to strain so that the stiffness of the fibrin matrix is constant, but at large strains the stiffness of the clot increases 20-fold[236], which may be important biologically.

Despite of this overall characterization of the fibrin mechanical properties, the composition of the human plasma also has a great impact on fibrin hydrogels behavior. For example, clots ligated with Factor XIIIa tend to have a higher stiffness and a lower inelastic component of deformation[227,236]. In contrast, an increased calcium concentration results in the formation of more dense gels with increased fiber size but lower rigidity[229]. Moreover, the hydrogel stiffness is affected to a greater degree by fibrinogen concentration rather than thrombin concentration[237]. Finally, incorporation of cells such as fibroblasts into fibrin hydrogels also influences their stiffness resulting in a small increase[237].

Apart from this intrinsic characterization, **controlling fibrin fiber alignment** is an addition design parameter than can be utilized to impart anisotropic mechanical properties to fibrin gels and has been shown to affect cellular responses[229]. Cell-mediated gel contraction technique has demonstrated that the culture of human dermal fibroblasts in asymmetric cruciform geometries increases collagen deposition[238]. Moreover, the application of a magnetic field[239] or a controlled parallel flow during polymerization[240] increases mechanical anisotropy[239] and oriented alignment is achieved as flow rate increases[240], respectively. Finally, the use of electrospinning techniques during gel formation provides less soft and extensible gels than when natural polymerization takes place[241]. Interestingly, these methodologies are considered during polymerization process however, the application of plastic compression once gels are formed has been demonstrated to be useful to enhance biomechanical properties of fibrin, generating denser hydrogels due to the reduction of their water content[242].

Regarding the **degradation of fibrin gels**, these are highly susceptible by proteolytic cleavage mediated by plasmin and matrix metalloproteinases present in the human plasma[229]. Therefore, this process must be controlled to achieve the desire effect for tissue regeneration. Several inhibitors have been added to fibrin hydrogels to slow proteolysis, including tranexamic acid[63], aprotinin and pharmacological metalloproteinases inhibitors[229]. However, for TESS manufacture, the degradation of fibrin is useful because it releases products which have been shown to stimulate vascular smooth muscle cell proliferation as well as collagen and elastin deposition[243], important for skin wound healing.

Therefore, human plasma/fibrin is a useful natural polymer for skin wound healing. Apart from being used as hydrogel for TESS manufacture (detailed information will be included in subsequent sections), this biopolymer has been studied as a glue or to generate microbeads (from 50 µm to 250 µm of diameter)[228]. Fibrin glue, also referred as fibrin sealant or fibrin tissue adhesive, has been widely used as a helper tool to improve skin grafts success, especially in difficult grafting sites[228], due to its hemostasis and antibacterial properties, its capacity to serve as delivery system for growth factors and as a template for cell migration, improving graft adherence and take[244]. Finally, the application of fibroblasts encapsulated into fibrin microbeads has reported high fibroblast proliferation and an increased angiogenesis and granulation tissue formation in pig excisional wounds[245].

5.2. PRECLINICAL USE OF HUMAN PLASMA/FIBRIN FOR TESS MANUFACTURE

As previously indicated the use of human plasma/fibrin for tissue engineering applications has been widely studied. Several preclinical investigations have evaluated its use for TESS manufacture for more than 30 years. Moreover, *in vitro* and *in vivo* research has been published in a similar amount, which indicates its translational potential into a clinical environment.

Although the use of human plasma or fibrin is the preferred strategy, at preclinical level, investigation of other animal sources such as bovine[246–263], porcine[264,265], ovine[266,267], canine[268,269] or plasma/fibrin from rats[270–275] have been also studied.

Regarding the role of human plasma/fibrin for TESS manufacture it has been demonstrated its versatility as scaffold with or without cells. Its use without being combined with cells, as a **sealant** to replace or reduce the use of sutures for skin grafts, reducing scar formation[276], reported an increased formation of blood vessels and capillaries[277] and a higher production of VEGF[278] in excisional wounds generated on mice and rats, respectively. Moreover, **wound dressing** approach, also without cells have been also developed and studied as temporary or permanent treatment for wounds. Results in a full-thickness wound mouse model demonstrated its potential for dermal repair and vascularization[279]. In addition, the combination of these wound dressings with other components such as laminin heparin binding domains[280] or acellular dermal matrixes[281] increased its regenerative potential and promoted wound healing *in vivo* by improving the retention of growth factors and their subsequent release in chronic wound on mice[280] or improving revascularization, re-epithelialization and well-differentiated epidermis formation in excisional full-thickness wounds on mice[281].

However, when these wound dressings are compared with the use of human plasma/fibrin combined with cells, better results have been reported in terms of wound closure, re-epithelialization and neovascularization[282]. For this reason, monolayer, bilayer and trilayer TESSs have been also studied.

Human plasma/fibrin-based monolayer TESSs are widely studied at preclinical level. For this reason, several approaches have been reported depending on the cell type and how biomaterial and cells are combined. For example, human keratinocytes have been embedded into plasma hydrogels[283,284] although the most usual is to culture them on top[285–287]. On balance the use of fibrin as scaffold for keratinocytes growth has shown proper adhesiveness and survival rates especially when the content of fibrinogen is lower (15%)[288]. Regarding their wound healing potential, the engraftment of this monolayer TESSs on mice with full-thickness skin defects reported good take percentage after 2-3 weeks and expression of type IV collagen at the basement membrane was confirmed[285].

On the other hand, when fibroblasts are used for monolayer TESS manufacture, they are usually embedded into the hydrogel, although some mechanical studies explored their use cultured on top[220]. Fibroblasts encapsulated into these scaffolds have shown good proliferation rates either clinical fibrin or plasminogen-depleted fibrin were used[283] and good elastic properties[289]. Moreover, the use of this substitutes for regenerative purposes have been proved on diabetic rats with surgical skin defects, demonstrating higher re-epithelialization and collagenization rates compared to controls without cells[290].

Apart from human keratinocytes and fibroblasts, other cell types such as hMSCs[282,291–296] and perivascular[297] or endothelial cells[298] have been studied embedded into[282,291,293,295,297] or cultured over[294,296,298] human fibrin hydrogels. Interestingly, most of the studies reporting the use of hMSCs have applied hAT-MSCs[291,293–296] although cells from bone marrow[292] and umbilical cord[282] have been also evaluated.

Regarding their application for wound healing purposes, most of the *in vivo* studies have been focused on the angiogenic properties of these TESSs, demonstrating in full-thickness wounds on mice or rats that neovascularization was achieved[282]. This was accomplished by promoting angiogenesis and vascular regeneration[296] faster than control treatments without cells[295], which also improved re-epithelialization[297].

Despite the successful results observed with monolayer TESSs, the incorporation and combination of different cell types to develop more complex skin substitutes have provoked the study of **human plasma/fibrin-based bilayer TESSs**.

Together with monolayer TESSs, the bilayer model constituted of human plasma/fibrin is the most studied and defined. Most of the substitutes evaluated are constituted of human fibroblasts embedded into a hydrogel as dermal component and then human keratinocytes are seeded and cultured on top. However, other cell combinations have been also reported, such as human endothelial cells and fibroblasts embedded into a pegylated fibrin matrix and injected subcutaneously in mice[299] or hWJ-MSCs cultured as epidermal layer over a dermal layer of plasma/agarose and human fibroblasts, demonstrating their capacity to *in vivo* differentiate into epithelial cells[64].

In any case, the combination of human fibroblasts and keratinocytes is preferred, either for in *vitro*[289,300–312] or *in vivo*[63,313–318] studies. Regarding *in vitro* studies, the first demonstrated the feasibility of developing and culturing this type of skin substitutes where a differentiated epidermis was observed[300,301]. However, trying to achieve a complete characterization, their optical properties have been also studied with similar results in terms of absorption and scattering to the native human skin[307]. Moreover, the concentration of fibrin and the contraction of the hydrogels have been also determined, concluding that a higher concentration of fibrin is able to reduce contraction[309], although a height's hydrogel reduction of 30% is unavoidable during the first 24 hours likely due to the intrinsic fibrin matrix properties[310]. In addition, the possibility of storing these bilayer TESSs at 4ºC in basal medium for 3 days has been corroborated[303]. Finally, the combination of human plasma/fibrin with other biomaterials such as hyaluronic acid[308] or elastin[311], or even the development of innervated models of skin[312] have been also studied.

In the case of *in vivo* studies evaluating the use of human plasma/fibrin-based bilayer TESSs, all of them were studied in full-thickness or surgical skin wounds generated on mice. Applying this strategy, stratified and keratinized epithelium was observed[313], basement membrane formation was

corroborated by a correct expression of laminin at the dermal-epidermal junction[315] and a proper development of the dermis was also reported[319], resembling native human skin structure. Interestingly, this bilayer TESS has been also used for the development of skin substitutes constituted of transduced keratinocytes with type VII collagen for the treatment of recessive dystrophic epidermolysis bullosa, demonstrating the generation of a cohesive and orderly stratified epithelium with all the characteristics of normal human epidermis, including rapid formation of anchoring fibrils[314].

Despite the successful results reported using monolayer and bilayer TESSs, in recent years the development of **human plasma/fibrin-based trilayer TESSs** has increased, mainly for *in vitro* studies. As in the case of the bilayer substitutes, human fibroblasts and keratinocytes are preferred for dermis and epidermis formation, however for the hypodermis-like layer, hMSCs from different sources[192,320,321], adipocytes[321] or human endothelial cells[192,322] have been studied.

Among hMSCs, most of the studies evaluated the use of hAT-MSCs, demonstrating their capacity to promote the production of extracellular matrix that stimulated cellular growth, proliferation and keratinocyte differentiation[192,320,321]. Moreover, after culturing process, these cells were able to differentiate into adipocytes, when cultured together with mature adipocytes[321], or endothelial cells, when co-cultured with human endothelial cells, due to the release of VEGF or hepatocyte growth factor (HGF) by themselves to promote angiogenesis and skin repair and regeneration[192]. Interestingly, one study used hAT-MSCs to be differentiated into epithelial cells, fibroblasts and adipocytes when mixed with the appropriate scaffolds (pegylated fibrin, collagen) and inducers, demonstrating their suitability for the development of trilayer TESSs utilized for immediate wound coverage[323].

In addition, the use of human endothelial cells alone into the hypodermal layer also induced the formation of capillary-like structures within the dermis[322] and the application of hBM-MSCs has been also reported as subcutaneous layer, contributing to the epidermal differentiation program, with more proliferating basal cells depositing basal membrane proteins and differentiating into mature keratinocytes that were able to generate a pluristratified epithelium[320].

On the other hand, few *in vivo* studies on rats have reported the use of plasma/fibrin-based trilayer TESSs but using bovine fibrin to develop the hydrogel[251,252]. Results demonstrated that the addition of hAT-MSCs as hypodermal layer anastomosed to the recipient's vasculature within only four days and the neo-epidermis efficiently established tissue homeostasis, without contraction of the dermis[252]. Despite the positive outcomes observed using Trilayer TESSs, the lack of *in vivo* studies demonstrates the necessity of further research.

To conclude, although most of the preclinical studies used human plasma/fibrin as single scaffold, other biomaterials have been combined to improve its mechanical or wound healing properties. Among them, collagen[248,293,323–325], polyethylene glycol[291,293,295,299,326] or hyaluronic acid[63,289,308,327,328] are the most studied.

5.3. CLINICAL USE OF HUMAN PLASMA/FIBRIN FOR TESS MANUFACTURE

Several studies have evaluated the use of human plasma/fibrin at preclinical level for the development of TESS, however, translation into a clinical environment is a difficult step due to the safety, effectiveness, quality and economical necessities required. For these reasons the number of clinical studies is reduced: 12 case series or reports[90,91,93,329–337], 3 clinical trials[338–340], 1 observational study[92] and 1 pre-post pilot study[108]. Among them, one study is a protocol description[338] and other two have already recruited patients, but no results have been posted yet[334,339] (**Table 7**).

Regarding tissue source, autologous[108,331,333,335–338] or allogeneic[90–93,329,330,332,334,340] human plasma/fibrin have been researched indistinctly for clinical purposes. Wound dressings without cells[329,330,333,335–338] and bilayer TESSs[90–93,332,334,340] have been the preferred strategies to study, followed by monolayer[108,331,339] and trilayer TESSs[340]. Interestingly, hMSCs from allogeneic[331,339] or autologous[108] sources (umbilical cord blood[331] or adipose tissue[108,339]) were the only type of cells used for monolayer TESSs manufacture, while for bilayer and trilayer TESSs, autologous cells such as keratinocytes, fibroblasts[90–93,332,334,340] and hAT-MSCs[340] for epidermal, dermal and hypodermal layers respectively, were used.

Moreover, three studies used this tissue engineering approach as a temporary cover before skin grafts were applied[330,333,339]. In addition, several types of wounds have been treated such as periorbital skin defects[329], chronic wounds[330,336], ulcers[108,333,338,340] or traumas[331,337], however burns have been the most studied in terms of number of studies and patients[90–93,334,339].

To conclude, the use of human plasma/fibrin alone has been the preferred strategy[90–93,108,329,331–333,336,337,339], but other biomaterials or scaffolds such as Integra®[330], gelatin or hydrocolloids dressings[338], agarose[334], human collagen[340] or human amnion[335] have been combined to improve its mechanical and regenerative properties.

Table 7. Clinical use of human plasma/fibrin in tissue-engineered skin substitutes (TESSs).

References / Year	Plasma/Fibrin Source	Type of Clinical Study	Type of TESS / Cells	N (Male / Female)	Indication	[a]Outcomes
329 / 1977	Allogeneic	Case Report	Wound dressing / ---	40 (32/8)	Surgically created periorbital skin defects	Grafts were gradually replaced by new epithelial tissue growing in from the periphery of the wound edge
330 / 2004	Allogeneic (Combined with Integra®)	Case Report	As a glue combined with Integra® for temporary wound dressing before skin transplantation (Evaluation of the effect of negative pressure therapy) / ---	12 (7/5)	Acute and chronic wounds	The mean period from Integra coverage to skin transplantation was 24±3 days in the conventional treatment group but only 10±1 days in the fibrin/negative-pressure therapy group
90 / 2004	Allogeneic	Case Report	Bilayer TESSs / Autologous fibroblasts and keratinocytes	2 (2/0)	Burns	Epidermal regeneration analyzed 2 months after grafting was complete (100% of the grafted area)
331 / 2004	Autologous	Case Report	Monolayer TESSs / Allogeneic *hUCB-MSCs (**HLA compatible)	2 (1/1)	Trauma and radiation injuries	The level of improvement, scored arbitrarily from 0 to 4, was 3 and 4
91 / 2006	Allogeneic	Case Series	Bilayer TESSs / Autologous fibroblasts and keratinocytes	20	13 – Burns 5 – Giant nevus 1 – Graft versus host disease 1 – Neurofibromatosis	The engineered skin took in all patients. The epithelization obtained was permanent in all cases
92 / 2011	Allogeneic	Multicenter retrospective observational cohort study	Bilayer TESSs / Autologous fibroblasts and keratinocytes	25 (23/2)	Burns	Characteristic scarring of mesh interstices was avoided. Epithelialization was observed
338 / 2015	Autologous (Combined with gelatin or hydrocolloid dressings)	Open-label, Non-Randomized, Controlled Clinical Trial	Wound dressing / ---	Estimation:30	Difficult to heal chronic skin ulcers	Protocol Description
332 / 2015	Allogeneic	Case Series	Bilayer TESSs / Autologous fibroblasts and keratinocytes	8 (3/5)	Hypertrophic scars due to full-thickness burns	After 8 weeks re-epithelialization and reduction of hypertrophic scars was achieved in 2 patients Decreased pain rate
333 / 2016	Autologous	Case Report	As temporary wound dressing before skin graft / ---	1 (1/0)	Refractory skin ulcer	Process of re-epithelialization was completed after 4 months
93 / 2016	Allogeneic	Case Report	Bilayer TESSs / Autologous fibroblasts and keratinocytes	2 pediatric patients	Burns	Appearance of the skin did not differ significantly from the areas treated with autografts
339 NCT03113747 / 2017	No tissue source indicated	Randomized Clinical Trial Parallel Assignment	Monolayer TESSs / Allogeneic hAT-MSCs	Estimation: 20	Burns	No results posted yet

		(Open Label) Phases 1 and 2	(Followed by autografts)			
334 / 2019	Allogeneic (Combined with agarose)	Case Series	Bilayer TESSs / Autologous fibroblasts and keratinocytes	9 adult patients (7/2) 3 pediatric patients (1/2)	Burns	No results posted yet
340 IRCT2015110224834N1 / 2020	Allogeneic (Combined with human collagen)	Clinical Trial	Trilayer TESSs and Bilayer TESSs / Autologous hAT-MSCs, fibroblasts and keratinocytes	5 Trilayer (4/1) 5 Bilayer (4/1)	Diabetic foot ulcers	Increased skin thickness and density in the vascular beds of the hypodermis of Trilayer treated patients
335 / 2020	Autologous (Combined with allogeneic human amnion)	Case Report	Wound Dressing / ---	1 (1/0)	Toxic epidermal necrolysis	Significant acceleration of wound healing (6 days)
108 / 2020	Autologous	Prospective clinical analysis (Pre-post pilot study)	Monolayer TESSs / Autologous hAT-MSCs	6 (3/3)	Chronic diabetic ulcers	There was granulation tissue formation starting from 7 days after topical application. After 90 days, a healed and re‐epithelialized tissue was observed
336 / 2021	Autologous	Case Series	Wound Dressing / ---	1 (1/0)	Non-healing wounds	After 7 days no maceration and oozing were observed After 3 injections wound was completely healed
337 / 2021	Autologous	Case Report	Wound Dressing / ---	1 (0/1)	Reconstruction of exposed skull in a complex craniovertebral polytrauma	Application of plasma facilitated wound regeneration
[a]Expression of measures: mean +/- standard deviation (range). No treatment-related adverse events were reported.						
***hUCB-MSCs:** human umbilical cord blood mesenchymal stem cells. ****HLA:** human leukocyte antigen.						

II. JUSTIFICATION AND HYPOTHESIS

JUSTIFICATION

In recent years, the design, development, optimization, study and use of human tissue-engineered skin substitutes (hTESSs) has increased due to their clinical potential. Several pathologies such as burns, chronic wounds and ulcers and surgical injuries because of a tumor extirpation are, have been or would be benefited of these approaches. In some cases, for example severely burned patients, the lack of donor tissue for autografts is the main limitation, while for the rest of the dermatological conditions, previously described, the possibility of developing an autologous skin substitute from a small biopsy is a promising strategy instead of applying a full-thickness skin autograft.

Even though several clinical studies have already evaluated the safety and effectiveness of several hTESS models, these are still not able to totally resemble the native human skin. Moreover, different hTESS models have been developed and it is difficult to compare them only by published data. The most interesting would be to do a side-by-side comparison using the same skin cell population, after applying similar cell isolation and expansion protocols, and using specific material and methods for each manufacturing process. This would lead to know more about the specific benefits of each model and if they would be more suitable for one or other dermatological pathology, however, this has not been accomplished yet due to economical, material or expertise requirements.

For this reason, this Doctoral Thesis aims at, on the one hand, evaluating two skin cell isolation protocols already used for the development of clinical hTESSs, and moreover, comparing side-by-side two clinical hTESSs models to determine their similarities and differences. The clinical models studied, which comply with Good Manufacturing Practices (GMP) regulations, are the human plasma-based skin substitute (HPSS), manufactured at Unidad de Producción Celular e Ingeniería Tisular (UPCIT) located at Hospital Virgen de las Nieves, Granada, Spain, and the bilayer self-assembled skin substitute (SASS) developed by LOEX Tissue Engineering Laboratory from Centre de recherche du CHU de Québec-Université Laval, Canada. On the other hand, this Doctoral Thesis also seeks to increase the knowledge of the clinical hTESS model manufactured at UPCIT, evaluating the incorporation of other biomaterials and cell types and compare them in a preclinical environment to determine their strengths and weaknesses.

HYPOTHESIS

The design, development and study of several subtypes, in terms of biomaterial and/or cellular composition, of the clinical human tissue-engineered skin substitute model already manufactured at Unidad Producción Celular e Ingeniería Tisular (Hospital Virgen de las Nieves, Granada, Spain) will increase our knowledge about it and will provide useful preclinical information to improve its quality. Moreover, the side-by-side comparison with another clinical model will allow us to be aware of its benefits and limitations, to enhance its strengths and improve its weaknesses. Finally, the *in vivo* evaluation of some of the subtypes previously studied will give insight into the wound healing process which would benefit patients' health.

III. OBJECTIVES

OBJECTIVES

GENERAL OBJECTIVE

To design, develop, optimize, characterize and manufacture by tissue engineering, at preclinical level, several human plasma-based skin substitutes (HPSSs). The purpose will be their prospective translation into a clinical environment as advanced therapy for the treatment of different dermatological pathologies.

SPECIFIC OBJECTIVES

1) To evaluate a skin cell isolation and expansion protocol currently used, by comparison with another protocol already applied for clinical tissue-engineered skin substitute (TESS) manufacture.

2) To study and compare, *in vitro*, several versions of the human plasma-based skin substitute model regarding aspects such as:

    2.1) Secondary biomaterial's composition.

    2.2) Cell viability after partial dehydration process.

    2.3) Skin cell tissue source.

    2.4) Culture methodology.

    2.5) Cellular structure.

3) To compare, *in vitro*, the most usually investigated secondary biomaterials for the manufacture of bilayer HPSSs with another clinical TESS already applied for the treatment of patients.

4) To evaluate, *in vivo*, the wound healing potential and homeostasis parameters of some of the HPSSs previously studied and compare the results with the gold standard treatment (autografts) and secondary wound healing approaches.

IV. METHODOLOGY

METHODOLOGY

CHAPTER 1: COMPARISON OF TWO HUMAN SKIN CELL ISOLATION PROTOCOLS AND THEIR IMPORTANCE IN TRANSLATIONAL RESEARCH

The standard skin cell isolation protocol applied at Unidad de Producción Celular e Ingeniería Tisular (UPCIT) from Hospital Virgen de las Nieves, Granada (Spain), the laboratory where this Doctoral Thesis was developed, was compared with the one developed at LOEX Tissue Engineering Laboratory from Centre de recherche du CHU de Québec-Université Laval, Quebec City (Canada). Both have been already applied for clinical purposes.

1.1. SKIN CELL ISOLATION AND CULTURE

Human keratinocytes and fibroblasts were extracted from three human adult skin biopsies (abdomen (n=2) and face (n=1)) from healthy patients (49, 49 and 60 years old; N=3). Main differences between both skin cell isolation protocols were the number of enzymatic digestions applied and enzymes used. Before starting to apply both isolation protocols, adipose tissue and/or blood traces were removed.

1.1.1. TWO-STEP DIGESTION PROTOCOL (**LOEX-PROTOCOL**)

Human skin samples were washed in 30 mL of a solution constituted of PBS 1X, 100 U/mL penicillin (Sigma-Aldrich, Saint Louis, MO, USA), 25 µg/mL gentamicin (Gemini Bio, West Sacramento, CA, USA) and 0.5 µg/mL fungizone (Bristol-Myers Squibb, New York City, NY, USA), by shaking for 2 minutes at room temperature (10 times). Then, human skin biopsies were transferred to a 60×15 mm Petri dish (Fisherbrand®, Waltham, MA, USA) with the epidermis facing up and cut into several pieces 1-2 mm wide. Tissues were digested for 16 hours at 4ºC in 10 mL of a solution composed of 0.5 mg/mL thermolysin (Sigma-Aldrich) dissolved in HEPES 1X (MP Biomedicals, Santa Ana, CA, USA) and 1 mM $CaCl_2$ (Sigma-Aldrich) (pH 7.45). Next day, the epidermis and dermis were separated using tweezers, kept in washing solution and prepared for the second enzymatic digestion[341,342].

1.1.1.1. Epithelial cell isolation

Fragments of the epithelium were incubated for 25 minutes at 37ºC in 20 mL of a 0.05% Trypsin (Gibco™, Waltham, MA, USA) /0.01% EDTA stirring solution (J.T. Baker, Phillipsburg, NJ, USA). Then, cell suspension was neutralized, filtered using a Cell Strainer of 100 µm (Fisherbrand®) and centrifuged (10 min / 24ºC / 300 x g). Finally, epithelial cells were counted, seeded at 4×10^4 cells/cm^2 on a feeder layer of irradiated human fibroblasts (8×10^3 cells/cm^2) and cultured in keratinocyte medium [Dulbecco-Vogt modified Eagle medium (Gibco™): Ham's F12 (Gibco™), ratio 3:1, supplemented with 24.25 µg/mL adenine (Sigma-Aldrich), 5 µg/mL insulin (Sigma-Aldrich), 0.4 µg/mL hydrocortisone (Galenova, Saint-Hyacinthe, QC, Canada), 0.212 µg/mL isoproterenol hydrochloride

(Sigma-Aldrich), 5% bovine HyClone FetalClone II serum (GE Healthcare, Chicago, IL, USA), 10 ng/mL human epidermal growth factor (Austral Biologicals, San Ramon, CA, USA), 100 U/mL penicillin (Sigma-Aldrich) and 25 µg/mL gentamicin (Gemini Bio)][341,342]. This primary culture was named passage 0 (P0).

1.1.1.2. Dermal cell isolation

Dermal tissue was digested for 3 hours at 37ºC by stirring in 20 mL of a solution constituted of 0.125 U/mL Type H collagenase (Roche, Basilea, Switzerland) diluted in fibroblast medium [Dulbecco-Vogt modified Eagle medium (Gibco™) supplemented with 10% Avantor Seradigm FB Essence (Avantor®, Radnor, PA, USA), 100 U/mL penicillin (Sigma-Aldrich) and 25 µg/mL gentamicin (Gemini Bio)]. After incubation, cell suspension was filtered using a Cell Strainer of 100 µm (Fisherbrand®), separated into four 50 mL tubes (5 mL/tube) and digestion was neutralized with 45 mL/tube of fibroblast medium. After centrifugation of the cell suspensions (10 min / 24ºC / 450 x g), the supernatant was discarded until 10 mL were left in each tube, pellets were resuspended and combined to have two tubes with 20 mL in each. These were centrifuged (10 min / 24ºC / 450 x g) and previous steps were repeated once to obtain one tube with 20 mL of cell suspension. Finally, this tube was centrifuged (10 min / 24ºC / 450 x g). Dermal cells were counted and seeded at 4×10^4 cells/cm^2 in fibroblast medium[341,342]. This primary culture was named passage 0 (P0).

1.1.2. ONE-STEP DIGESTION PROTOCOL (**UPCIT-PROTOCOL**)

Firstly, human skin biopsies were washed for 30 minutes, submerged in a solution constituted of PBS 1X, 100 U/mL penicillin (Sigma-Aldrich), 25 µg/mL gentamicin (Gemini Bio) and 0.5 µg/mL fungizone (Bristol-Myers Squibb) at room temperature. Then, the samples were transferred to a 60×15 mm Petri dish (Fisherbrand®) with the epidermis facing down. Most of the dermis was mechanically detached using scissors and a scalpel and kept for fibroblast isolation.

1.1.2.1. Epithelial cell isolation

Epidermis was mechanically fragmented into small pieces using scissors and incubated for 15 minutes in a stirring 5 mL of TrypLE Select Enzyme 10X (Gibco™) at 37ºC (8 cycles). After each cycle, digested solution containing the cells and pieces of tissue was filtered using a Cell Strainer of 100 µm (Fisherbrand®). The filtered cell suspension was neutralized using 10 mL of keratinocyte medium and kept, while remaining tissue was digested again. After the 8th cycle, the cell suspension was centrifuged (10 min / 24ºC / 300 x g). Cells were counted and seeded at 1.3×10^5 cells/cm^2 on a *feeder* layer of irradiated human fibroblasts (8×10^3 cells/cm^2) and cultured in keratinocyte medium. This primary culture was named passage 0 (P0).

1.1.2.2. Dermal cell isolation

Dermis was fragmented using scissors and digested using a stirring solution of 2 mg/mL of Type I collagenase (Gibco™) in Dulbecco-Vogt modified Eagle medium (Gibco™) for 20 hours at 37ºC. The digested tissue was filtered using a Cell Strainer of 100 µm (Fisherbrand®), neutralized using fibroblast medium and centrifuged (20 min / 24ºC / 450 x g). Finally, dermal cells were counted and seeded at 1.15×10^5 cells/cm^2 in fibroblast medium. This primary culture was named passage 0 (P0).

1.1.3. CULTURE MAINTENANCE AND PASSAGES

The culture medium of keratinocytes and fibroblasts was changed every two days until cells reached 90-95% confluence; then cells were trypsinized and cultured again until they reached P4. From P1 to P4, cell seeding density in both protocols was the same for keratinocytes (6.5×10^3 cells/cm^2) and fibroblasts (8×10^3 cells/cm^2).

1.2. EVALUATION OF CELL CHARACTERISTICS

1.2.1. CELL SIZE, VIABILITY AND YIELD

The number of human epithelial and dermal cells and their diameter (Ø) were measured using a Z2 Coulter® Particle Count and Size Analyzer (Beckman Coulter™, Brea, CA, USA). Cell size was evaluated just after isolation (Fresh Cells) and at the end of each passage from P0 to P4. Setting parameters were stablished between 7 µm and 21 µm for fresh cells and between 8 µm and 24 µm for cells cultured from P0 to P4. The mean size value was used for statistical analysis.

Cell viability was determined by trypan blue staining (Gibco™). The viable cell yield per cm^2 was calculated using the total number of cells and the area of each human skin sample for fresh cells, and the surface area of the culture flasks for cells recovered from P0 to P4.

1.2.2. CULTURE AND POPULATION DOUBLING TIME

For each passage, the population doubling time was calculated by dividing the number of doublings (n) by the number of days (culture time). The number of doublings (n) over the culture period was calculated using the following mathematical equation where the total number of cells at the end of the culture process (Ne) and the initial number of cells seeded (Ni) were considered:

$$n = \frac{\log Ne - \log Ni}{\log 2}$$

1.3. CLONOGENICITY OF EPITHELIAL CELL CULTURES

The size (diameter, Ø) and the number of colonies were evaluated for epithelial cells seeded at P0 and P1. For a given biopsy, passage and isolation protocol, 5 culture flasks (T25 cm^2) were seeded with 10^3 epithelial cells (keratinocytes)/flask and cultured for the same number of days for both protocols. Keratinocyte medium was not changed during the first 5 days of culture and then, medium was changed every two days until colonies started to join with each other.

Colonies were washed 3 times with 4 mL of PBS 1X at 37ºC and fixed with 4 mL of filtered formaldehyde (3.7%) (Chaptec, Montréal-Est, QC, Canada) for 30 minutes at room temperature. Then, colonies were stained with 1.5 mL of Rhodamine 1% (Thermo Fisher Scientific, Waltham, MA, USA) for 15-20 minutes at room temperature, rinsed with distilled water and dried.

Colonies were manually counted and classified by their diameter size, measured using ImageJ software (NIH, Bethesda, MD, USA), into I) holoclones: Ø ≥ 4.5 mm; formed by stem cells that rapidly grow, II) paraclones: Ø ≤ 1.5 mm; constituted by cells programmed for limited growth, which consequently form uniformly small, terminal colonies; and III) meroclones: 4.5 mm > Ø > 1.5 mm; containing cells with different proliferative capacities[343].

Using this data, colony-forming efficiency (CFE)[344] and the percentage of each type of colony, considering the total number of colonies, were calculated:

$$CFE = \frac{Number\ of\ holoclones}{Initial\ number\ of\ keratinocytes\ seeded\ (10^3)} \times 100$$

$$\%\ of\ Total\ Colonies = \frac{Number\ of\ colonies\ (for\ each\ type)}{Total\ number\ of\ colonies} \times 100$$

1.4. KERATIN 19 (K19) ANALYSIS BY FLOW CYTOMETRY

The number of K19 positive keratinocytes after P0 and P1 was evaluated by flow cytometry. Cells were recovered after trypsinization, washed in PBS 1X (3 times) and fixed in filtered formaldehyde 3.7% (pH=7) (Chaptec) for 30 minutes at 4ºC (1 mL of formaldehyde /10^6 cells). Then cells were washed again with cold PBS 1X (3 times) and kept at 4ºC in 1 mL of PBS 1X/10^6 cells until flow cytometry analysis.

For each protocol and passage, two samples of at least 4×10^5 cells were immunolabeled. Cells were centrifuged at 450 x g for 5 minutes at 15ºC. The supernatant was discarded, and keratinocytes were washed with 500 µL of 10% BD Perm/Wash Buffer (BD Biosciences, Franklin Lakes, NJ, USA) diluted in MilliQ water. Then cells were immunolabeled for 45 minutes at room temperature in darkness with

mouse IgG2a anti-human K19 primary antibody (clone A53-B/A244, gift from U. Karsten, Institute of Biological Sciences, University of Rostock, Germany; 1:200). For negative controls, keratinocytes were incubated with mouse IgG2a antibody (DAKO, Glostrup, Denmark; 1:20). After 3 washes, samples were immunolabeled with PE-conjugated goat anti-mouse IgG2a secondary antibody (Invitrogen, Waltham, MA, USA; 1:200) and incubated for 45-60 minutes at room temperature in darkness. After 3 washes, each sample was resuspended in 200 uL of PBS FACS solution [PBS 1X, 0.5 mM EDTA (Sigma-Aldrich) and 2% Serum] and analyzed using BD FACSMelody™ Cell Sorter (BD Biosciences).

1.5. STATISTICAL ANALYSIS

Microsoft Excel software was used for primary analysis of raw data, and GraphPad Prism 8 (San Diego, CA, USA) and FlowJo™ v10 (BD Biosciences) were used for statistical analysis and graphs. Normal distribution of the data was corroborated by Shapiro-Wilk test. Then, depending on the comparison, One-way ANOVA and Tukey's multiple comparisons tests or Multiple t-test and Holm-Sidak's method were used to analyze the results. All values were presented as mean value ± standard deviation (SD). The significance threshold was set at 0.05.

1.6. ETHICS

This study was conducted according to the Declaration of Helsinki and was approved by the research ethics committee for human subjects of the CHU de Quebec-Université Laval. All tissue donors provided informed written consent.

1.7. GRAPHICAL ABSTRACT OF CHAPTER 1

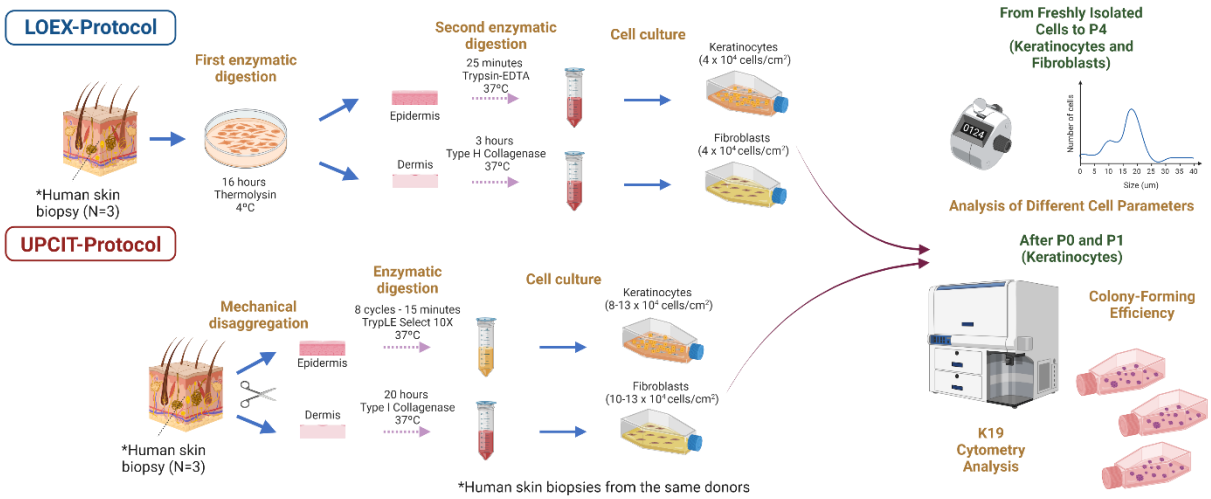

Fig. 8. ***Study design of Chapter 1.*** *Created with BioRender.com.*

CHAPTER 2: IN VITRO ANALYSIS OF DIFFERENT HUMAN PLASMA-BASED SKIN SUBSTITUTES (HPSSs)

2.1. SKIN CELL ISOLATION AND CULTURE

Human keratinocytes and fibroblasts were extracted from eleven human skin biopsies (abdomen (n=3) and foreskin (n=8)) from healthy patients. Adipose tissue and/or blood traces were removed before starting the one-step digestion protocol (UPCIT-Protocol with slight modifications) applied for skin cell isolation.

Firstly, human skin biopsies were washed for 30 minutes, submerged in a solution constituted of Dulbecco's Phosphate Buffered Saline (DPBS; Sigma-Aldrich, St Louis, USA), 160 µg/mL gentamicin (Laboratorios Normon, Madrid, Spain), 100 µg/mL cefotaxime (Medochemie, Limassol, Cyprus), 100 µg/mL vancomycin (Reig Jofre, Barcelona, Spain) and 1.25 µg/mL amphotericin b (Sigma-Aldrich). Then, the samples were transferred to a 60×15 mm Petri dish (Fisherbrand®, Waltham, MA, USA) with the epidermis facing down. Most of the dermis was mechanically detached using scissors and a scalpel and kept for fibroblast isolation.

2.1.1. EPITHELIAL CELL ISOLATION

Epidermis was mechanically fragmented into small pieces using scissors and incubated for 15 minutes in a stirring 5 mL of TrypLE Select Enzyme 10X (Gibco™, Waltham, MA, USA) at 37ºC (8 cycles). After each cycle, digested solution containing the cells and pieces of tissue were filtered using a Cell Strainer of 100 µm (Fisherbrand®). The filtered cell suspension was neutralized using 10 mL of keratinocyte medium [Dulbecco's Modified Eagle's Medium (DMEM) (Sigma-Aldrich): Ham's F12 (Sigma-Aldrich), ratio 2:1, supplemented with 584 µg/mL L-glutamine (Sigma-Aldrich), 96 µg/mL gentamicin (Laboratorios Normon), 24 µg/mL adenine hydrochloride hydrate (Sigma-Aldrich), 5.25 µg/mL human insulin solution (Sigma-Aldrich), 1.25 µg/mL amphotericin b (Sigma-Aldrich), 400 ng/mL hydrocortisone (Sigma-Aldrich), 25 ng/mL human epidermal growth factor (Sigma-Aldrich), 1.4 ng/mL triiodo-L-thyronine sodium salt (Sigma-Aldrich) and 10% fetal bovine serum (Gibco™)] and kept, while remaining tissue was digested again. After the 8th cycle, the cell suspension was centrifuged (10 min / 24ºC / 1,500 rpm). Cells were counted and seeded at 1.3×10^5 cells/cm^2 on a *feeder* layer of irradiated mouse embryonic fibroblasts (4×10^4 cells/cm^2) and cultured in keratinocyte medium. This primary culture was named passage 0 (P0).

2.1.2. DERMAL CELL ISOLATION

Dermis was fragmented using scissors and digested using a stirring solution of 2 mg/mL of Type I collagenase (Gibco™) in Dulbecco's Modified Eagle's Medium (DMEM) (Sigma-Aldrich) for 20 hours at 37ºC. The digested tissue was filtered using a Steriflip-GP Sterile Centrifuge Tube Top Filter Unit

of 0.22 µm (Merck Millipore, Burlington, MA, USA), neutralized using fibroblast medium [Dulbecco's Modified Eagle's Medium (DMEM) (Sigma-Aldrich) supplemented with 584 µg/mL L-glutamine (Sigma-Aldrich), 96 µg/mL gentamicin (Laboratorios Normon) and 10% fetal bovine serum (Gibco™)] and centrifuged (10 min / 24ºC / 1,500 rpm). Finally, dermal cells were counted and seeded at 1.15×10^5 cells/cm^2 in fibroblast medium. This primary culture was named passage 0 (P0).

2.1.3. CULTURE MAINTENANCE AND PASSAGES

The culture medium of keratinocytes and fibroblasts was changed every two or three days until cells reached 90-95% confluence; then cells were trypsinized and cultured again until reached the enough number of cells for HPSS manufacturing. From P1 cell seeding density for keratinocytes was 7.5×10^3 cells/cm^2 on a *feeder* layer of irradiated mouse embryonic fibroblasts (10^4 cells/cm^2) and for fibroblasts was 3.5×10^3 cells/cm^2.

2.2. HUMAN ADIPOSE TISSUE MSC ISOLATION AND CULTURE

Human mesenchymal stem cells were extracted, as previously described[345], from subcutaneous adipose tissue sample from one donor (n=1). Before starting the isolation protocol, blood traces were removed.

Firstly, subcutaneous fat was washed for 30 minutes with a solution constituted of Dulbecco's Phosphate Buffered Saline (DPBS; Sigma-Aldrich, St Louis, USA), 160 µg/mL gentamicin (Laboratorios Normon, Madrid, Spain), 100 µg/mL cefotaxime (Medochemie, Limassol, Cyprus) and 100 µg/mL vancomycin (Reig Jofre, Barcelona, Spain). Then, the sample was transferred to a glass try and mechanically detached using scissors.

After that, a second mechanical separation was applied using a mincer and the grinding tissue was enzymatically digested in a stirring solution of 1 mg/mL of Type A collagenase (Hoffmann-La Roche, Basel, Switzerland) at 37ºC for 2 hours. Then, the result of the digestion was neutralized with MSC medium [Dulbecco's Modified Eagle's Medium (DMEM) (Sigma-Aldrich) supplemented with 869 µg/mL alanine-glutamine (Sigma-Aldrich), 96 µg/mL gentamicin (Laboratorios Normon), 50 µg/mL vancomycin (Reig Jofre) and 10% fetal bovine serum (Gibco™)] and after several filtration and centrifugation processes, hAT-MSCs were counted and cultured at 1.5×10^4 cells/cm^2 in MSC medium This primary culture was named passage 0 (P0).

The culture medium of hAT-MSCs was changed every three days until cells reached 90-95% confluence; then cells were trypsinized, seeded at 3.5×10^3 cells/cm^2 and expanded until reached the end P1 or P2. Then, hAT-MSCs were cryopreserved in a solution constituted of Fetal Bovine Serum (Gibco™) and 10% dimethyl sulfoxide (Sigma-Aldrich). Finally, when required, hAT-MSCs were thawed and expanded until reached the enough number of cells for HPSS manufacturing.

2.3. HPSS MANUFACTURE

The eleven human skin cell populations (keratinocytes and fibroblasts) were used for manufacturing all type of cellular HPSSs that will be described in subsequent sections. The future application of hAT-MSCs in this clinical TESS model is supposed to be allogeneic, for this reason the same cell population (previously aliquoted and frozen) was used for manufacturing the HPSSs in those cases where a hypodermal layer was included.

2.3.1. BIOMATERIAL COMPOSITION

This TESS model is based on the use of human plasma/fibrin (**Fib**) as main biomaterial to produce a hydrogel that will support cell growth and differentiation. Therefore, frozen human blood plasma from healthy donors was collected from the Centro Regional de Transfusión Sanguínea of Granada. Human plasma from different donors were mixed to generate a pool which was aliquoted, frozen at -20ºC and used for all experiments to avoid inter-variability between samples.

However, as previously described, human plasma for HPSS manufacture has been also combined with other biomaterials to improve their properties. For this reason, **six secondary biomaterials** were evaluated, in combination with human plasma, to determine their biological properties (**Table 8**). The final concentration of each secondary biomaterial into the hydrogel was stablished after preliminary studies where clinical handling was evaluated (data not shown).

***Table 8**. Information about secondary biomaterials used for HPSS manufacture.*

Biomaterial	Company	Final Concentration	Abbreviation
Serine (S)	Biogelx™, Lanarkshire, UK	670 µg/mL	S
Fibronectin (RGD)	Biogelx™, Lanarkshire, UK	740 µg/mL	Fn
Collagen (GFOGER)	Biogelx™, Lanarkshire, UK	780 µg/mL	Col
Laminin (IKVAV)	Biogelx™, Lanarkshire, UK	790 µg/mL	Lam-1
Laminin (YIGSR)	Biogelx™, Lanarkshire, UK	910 µg/mL	Lam-2
Hyaluronic Acid	Fidia Farmaceutici S.p.A., Abano Terme, Italy	750 µg/mL	HA

Information between brackets indicates the combination of amino acids used for biomaterial production and that resembles the physiological motif structure of the different peptides described.

Amino acid abbreviations: **A:** Alanine, **D:** Aspartic acid, **E:** Glutamic acid, **F:** Phenylalanine, **G:** Glycine, **I:** Isoleucine, **K:** Lysine, **O:** Hydroxyproline, **R:** Arginine, **S:** Serine, **V:** Valine, **Y:** Tyrosine.

HPSSs without any secondary biomaterial (only human plasma) were also manufactured to compare the results.

2.3.2. CELL LAYER COMPOSITION

Regarding cell structure, four types of HPSSs were produced for each biomaterial combination and human skin cell population: **Trilayer HPSSs**; constituted of a hypodermal layer of 6×10^4 hAT-MSCs/mL, a dermal layer of 6×10^4 human fibroblasts/mL and an epidermal layer constituted of 1.77×10^5 keratinocytes/cm^2, **Bilayer HPSSs;** comprised of a dermal layer of 6×10^4 human fibroblasts/mL and an epidermal layer constituted of 1.77×10^5 keratinocytes/cm^2, **Monolayer HPSSs**; which resembled an epidermal layer of 1.77×10^5 keratinocytes/cm^2, and **Control HPSSs**; as wound dressings without cells.

All TESSs were manufactured in 6 insert well plates with 0.4 µm pore polyester membrane (Corning® Transwell®, Sigma-Aldrich). The final volume was 5 mL/hydrogel and different steps were carried out depending on the cell composition (**Tables 9 and 10**).

Table 9. Reagents and volume for Trilayer HPSS manufacture.

	Reagents for hypodermal layer	Volume	Reagents for dermal layer	Volume
Solution 1	Calcium Chloride 100 mg/mL ($CaCl_2$) (BBraun, Melsungen, Germany)	0.060 mL	Calcium Chloride 100 mg/mL ($CaCl_2$) (BBraun, Melsungen, Germany)	0.060 mL
	Water for injection (Fresenius Kabi, Bad Homburg, Germany)	0.0335 mL	Water for injection (Fresenius Kabi, Bad Homburg, Germany)	0.0335 mL
Solution 2	Human Plasma	2.075 mL	Human Plasma	2.075 mL
	MSC medium + hAT-MSCs	0.156 mL	Fibroblast medium + human fibroblasts	0.156 mL
	Secondary Biomaterial*	0.125 mL	Secondary Biomaterial*	0.125 mL
	Tranexamic Acid 100 mg/mL (MEDA Pharma, Bad Homburg, Germany)	0.0505 mL	Tranexamic Acid 100 mg/mL (MEDA Pharma, Bad Homburg, Germany)	0.0505 mL
Hypodermal layer was manufactured 3-4 hours before dermal layer to allow a partial hydrogel formation to clearly differentiated both layers but allowing their integration. *In the case of the HPSSs manufactured without any secondary biomaterial, the same extra volume of human plasma was added.				

Table 10. Reagents and volume for Bilayer, Monolayer and Control HPSS manufacture.

	Reagent for dermal layer	Volume
Solution 1	Calcium Chloride 100 mg/mL ($CaCl_2$) (BBraun, Melsungen, Germany)	0.120 mL
	Water for injection (Fresenius Kabi, Bad Homburg, Germany)	0.067 mL
Solution 2	Human Plasma	4.150 mL
	Fibroblast medium + human fibroblasts (Bilayer TESS) or no cells (Monolayer and Control HPSSs)	0.312 mL
	Secondary Biomaterial*	0.250 mL
	Tranexamic Acid 100 mg/mL (MEDA Pharma, Bad Homburg, Germany)	0.101 mL
For Bilayer HPSSs addition of human fibroblasts was required for dermal layer, however for Monolayer and Control HPSSs only fibroblast medium was required. *In the case of the HPSSs manufactured without any secondary biomaterial, the same extra volume of human plasma was added.		

Briefly, all reagents were previously warmed at 37ºC and then both solutions were prepared in independent tubes. For Solution 2, secondary biomaterial and tranexamic acid were the last reagents to be added. Then, Solution 2 were mixed with Solution 1 and after shaking three times, the mixed solution was carefully pipetted into the 6 insert well plates. After 2-3 hours at 37ºC hydrogel was formed and culture fibroblast medium was added and incubate overnight (ON) at 37ºC (for Trilayer TESSs, this process took place once dermal layer was manufactured).

The following day, keratinocytes were added on top of the corresponding hydrogels in a 500 µL of keratinocyte medium. They were allowed to adhere to the surface for 1-2 hours and then fibroblast medium was replaced by keratinocyte medium to fully cover the HPSSs.

2.3.3. HPSS CULTURE AND PARTIAL DEHYDRATION PROCESS

Two culture methodologies were applied for the development of the HPSSs: submerged or air/liquid interface culture. At the end of both strategies, HPSSs were subjected to a partial dehydration process[242] using a sandwich system where absorbent papers and meshes of different pore sizes were used together with a glass disc to apply a pressure of 460 Pa for 2 minutes that improved their mechanical properties and handling[242].

2.3.3.1. Submerged culture (SUB)

Seven batches were produced and cultured applying the submerged approach (**SUB**): three human skin cell populations from abdominal skin (N=3; **ABDO**) and four from foreskin (N=4; **FORE**) were used for manufacturing Trilayer, Bilayer, Monolayer and Control TESSs as previously described.

Keratinocyte medium was changed every two days for 7-10 days from keratinocyte's addition. This strategy is the one applied at UPCIT for clinical TESS manufacture and consists in fully covering the hydrogel to promote cell proliferation and growth.

2.3.3.2. Air/Liquid Interface culture (ALI)

Five batches, all of them from different human skin cell populations from foreskin (N=5), were manufactured using the air/liquid interface approach (**ALI**). Trilayer, Bilayer, Monolayer and Control TESSs for each skin cell population and secondary biomaterial were also produced but after culturing them for 7-10 days in submerged conditions, then air/liquid interface strategy was applied for 10-13 more days, changing the culture medium every two days. This is based on exposing the epidermal layer to the air while the stromal layers are fully covered with keratinocyte medium exempt of human epidermal growth factor. The purpose is to induce the terminal differentiation of the epithelium but promoting the proliferation and growth of the rest of the layers.

2.4. CELL VIABILITY

Cell viability after manufacturing process of HPSSs was evaluated using LIVE/DEAD™ Viability/Cytotoxicity Kit (Invitrogen™, Waltham, MA, USA); a two-color assay to determine viability of cells based on their esterase activity and plasma membrane integrity. A sample of 8 mm of diameter was taken from each HPPS manufactured, washed 3 times with DPBS (Sigma-Aldrich) and incubated for 45 minutes at room temperature in a solution constituted of DPBS and two fluorophores: calcein-AM (1:2000) which emits green fluorescence (517 nm) due to the intracellular esterase activity of viable cells and ethidium homodimer-1 (1:500) that emits red fluorescence (617 nm) when binds to DNA due to the loss of plasma membrane integrity of dead cells.

Then, after washing with DPBS (3 times), at least three digital images of each HPSS were taken using a Leica DM2000 microscope coupled with a Leica Mercury Burner 100W Hg Lamp and a Leica DMC2900 camera (Leica, Wetzlar, Germany). Images were processed using Leica Application Suite (LAS) 4.12 software (Leica).

These digital images were used to count live and dead cells and determine the mean cell viability of each HPSS. In the case of submerged HPSSs, cell viability was determined before (**HYD**) and after dehydration (**DEHYD**) process to evaluate the effect of this process. Therefore, several conditions were compared as detailed in **Table 11**:

***Table 11**. Conditions analyzed and compared for cell viability of HPSSs.*

Conditions compared	Culture methodology	Regardless of	Total number of replicas considered for each condition compared (n)	Number of human skin cell population used (N)
Secondary biomaterial used for each type of cellular HPSS and dehydration process Fib/S vs. Fib/Fn vs. Fib/Col vs. Fib/Lam-1 vs. Fib/Lam-2 vs Fib/HA vs. Fib Hydrated (HYD) vs. Dehydrated (DEHYD) Trilayer vs. Bilayer vs. Monolayer	Submerged	Skin cell tissue source	7	7
Secondary biomaterial used for each type of cellular HPSS and culture methodology Fib/S vs. Fib/Fn vs. Fib/Col vs. Fib/Lam-1 vs. Fib/Lam-2 vs Fib/HA vs. Fib Submerged culture (SUB) vs. Air/Liquid Interface culture (ALI) Trilayer vs. Bilayer vs. Monolayer	Both (Dehydrated)	Skin cell tissue source	7-SUB 5-ALI	7-SUB 5-ALI
Partial dehydration process for each type of cellular HPSS Hydrated (HYD) vs. Dehydrated (DEHYD) Trilayer vs. Bilayer vs. Monolayer	Submerged	Secondary biomaterial and skin cell tissue source	49	7
Skin cell tissue source for each type of cellular HPSS Abdominal skin (ABDO) vs. Foreskin (FORE) Trilayer vs. Bilayer vs. Monolayer	Submerged (Hydrated and dehydrated)	Secondary biomaterial	21-ABDO 28-FORE	3-ABDO 4-FORE
Culture methodology for each type of cellular HPSS Submerged culture (SUB) vs. Air/Liquid Interface culture (ALI) Trilayer vs. Bilayer vs. Monolayer	Both (Dehydrated)	Secondary biomaterial and skin cell tissue source	49-SUB 35-ALI	7-SUB 5-ALI

2.5. CELL METABOLIC ACTIVITY

Cell metabolic activity of HPSSs was evaluated using PrestoBlue™ (Invitrogen™); a colorimetric assay which allows to measure resazurin reduction level (absorbance at 570 and 600 nm) by living cells. To that purpose, two samples of 5 mm of diameter was taken from each HPSS and incubated at 37ºC in a PrestoBlue™-phosphate buffered saline (1/10) solution for 20 hours. Then the supernatant was collected, and absorbance was measured using a Multi-mode Reader Synergy™ HTX (BioTek, Winooski, VT, USA). The percentage of reduction was calculated using the following equation:

$$\%\ Reduction = \frac{(O2\ x\ A1) - (O1\ x\ A2)}{(R1\ x\ C2) - (R2\ x\ C1)}\ x\ 100$$

- $O1$: molar extinction coefficient (E) of oxidized PrestoBlue™ (Blue) at 570 nm => 80586
- $O2$: E of oxidized PrestoBlue™ (Blue) at 600 nm => 117216
- $R1$: E of reduced PrestoBlue™ (Red) at 570 nm => 155677
- $R2$: E of reduced PrestoBlue™ (Red) at 600 nm => 14652
- $A1$: absorbance of test HPSS at 570 nm
- $A2$: absorbance of test HPSS at 600 nm
- $C1$: absorbance of Control HPSS at 570 nm
- $C2$: absorbance of Control HPSS at 600 nm

The mean value of the two samples taken from each HPSS was used for statistical analysis. These data allowed to compare several conditions (**Table 12**):

***Table 12**. Conditions analyzed and compared for cell metabolic activity of HPSSs.*

Conditions compared	Culture methodology	Regardless of	Total number of replicas considered for each condition compared (n)	Number of human skin cell population used (N)
Secondary biomaterial used for each type of cellular HPSS and culture methodology Fib/S vs. Fib/Fn vs. Fib/Col vs. Fib/Lam-1 vs. Fib/Lam-2 vs Fib/HA vs. Fib Submerged culture (SUB) vs. Air/Liquid Interface culture (ALI)	Both	Skin cell tissue source	7-SUB 5-ALI	7-SUB 5-ALI
Skin cell tissue source for each type of cellular HPSS Abdominal skin (ABDO) vs. Foreskin (FORE) Trilayer vs. Bilayer vs. Monolayer	Submerged	Secondary biomaterial	21-ABDO 28-FORE	3-ABDO 4-FORE
Culture methodology for each type of cellular HPSS Submerged culture (SUB) vs. Air/Liquid Interface culture (ALI) Trilayer vs. Bilayer vs. Monolayer	Both	Secondary biomaterial and skin cell tissue source	49-SUB 35-ALI	7-SUB 5-ALI

2.6. PROTEIN SECRETION PROFILE ANALYSIS

For protein secretion profile analysis, the culture medium surrounding the HPSSs was collected and stored at -80ºC at the end of the manufacturing process for further analysis. Three human growth factors (bFGF, EGF and VEGF) and one cytokine (CCL5), involved in wound healing process, were measured and quantified using commercial kits based on Sandwich-ELISA (Enzyme-Linked Immunosorbent Assay) principle (Elabscience®, Houston, TX, USA).

Briefly, for each protein analyzed, culture medium was incubated in wells precoated with the specific antibody, then a secondary biotinylated detection antibody specific for the protein of interest and Avidin-Horseradish Peroxidase (HRP) conjugated were added successively to each micro plate well and incubated. After several washes, the substrate solution was added to each well and enzyme-substrate reaction was terminated by the addition of stop solution. Those wells containing the protein of interested showed a yellow color. The optical density (OD) was measured spectrophotometrically at a wavelength of 450±2 nm using a Multi-mode Reader Synergy™ HTX (BioTek). The concentration was determined by comparing the OD of the samples to the standard curve, using the GainData® software (Arigo, Hsinchu City, Taiwan).

Several comparisons were analyzed (**Table 13**), however in the case where submerged and air/liquid interface culture methodologies were directly compared, the culture medium collected and analyzed from submerged samples was the one surrounding the same HPSSs that were subsequently cultured by the air/liquid interface strategy.

***Table 13**. Conditions analyzed and compared for each protein analyzed by ELISA.*

Conditions compared	Culture methodology	Regardless of	Total number of replicas considered for each condition compared (n)	Number of human skin cell population used (N)
Secondary biomaterial used for each type of cellular HPSS and culture methodology Fib/S vs. Fib/Fn vs. Fib/Col vs. Fib/Lam-1 vs. Fib/Lam-2 vs Fib/HA vs. Fib Submerged culture (SUB) vs. Air/Liquid Interface culture (ALI)	Both	Skin cell tissue source	7-SUB 5-ALI	7-SUB 5-ALI
Skin cell tissue source for each type of cellular HPSS Abdominal skin (ABDO) vs. Foreskin (FORE) Trilayer vs. Bilayer vs. Monolayer	Submerged	Secondary biomaterial	21-ABDO 28-FORE	3-ABDO 4-FORE
Culture methodology for each type of cellular HPSS Submerged culture (SUB) vs. Air/Liquid Interface culture (ALI) Trilayer vs. Bilayer vs. Monolayer	Both	Secondary biomaterial and skin cell tissue source	35-SUB 35-ALI	5-SUB 5-ALI
To normalize the results of ELISA analysis, the corresponding Control HPSS values were subtracted to the values of the rest of cellular HPSSs manufactured. This normalization is important because Control HPSSs are constituted of the same human plasma (as the rest of cellular HPSSs), which is also a source of different factors and cytokines, some of which are the ones included in this study.				

2.7. HISTOLOGICAL ANALYSIS

For histological analysis, only dehydrated samples were fixed in formaldehyde 4% (pH=7) (Casa Álvarez, Madrid, Spain) and embedded in paraffin (Thermo Fisher Scientific, Waltham, MA, USA). Five-micrometer thick sections were stained with Hematoxylin / Eosin (Casa Álvarez). Digital images were acquired using a Leica DM2000 microscope coupled with Leica DMC2900 (brightfield) camera (Leica). Images were processed using Leica Application Suite (LAS) 4.12 software (Leica).

2.8. STATISTICAL ANALYSIS

Microsoft Excel and Adobe Photoshop 2020 software were used for primary analysis of raw data, and GraphPad Prism 8 (San Diego, CA, USA) was used for statistical analysis and graphs. Normal distribution of the data was evaluated by Shapiro-Wilk test. For biomaterial comparison if normal distribution was confirmed, the results were analyzed by One-way ANOVA and Tukey's multiple comparisons tests, however if no normal distribution was corroborated, Friedman and Dunn's multiple comparisons tests were performed. To compare different conditions of the same biomaterial, Multiple t-test and Holm-Sidak's method were used to analyze the results. For the rest of conditions and groups compared, when normal distribution was corroborated, Welch's t-test was performed. However, when no normal distribution was confirmed, Mann-Whitney test was used for analysis of the results.

All values were presented as mean value ± standard deviation (SD). The significance threshold was set at 0.05.

2.9. ETHICS

This study was conducted according to the Declaration of Helsinki and was approved by the Provincial Ethics Committees of Granada for human subjects. All tissue donors provided informed written consent.

2.10. GRAPHICAL ABSTRACT OF CHAPTER 2

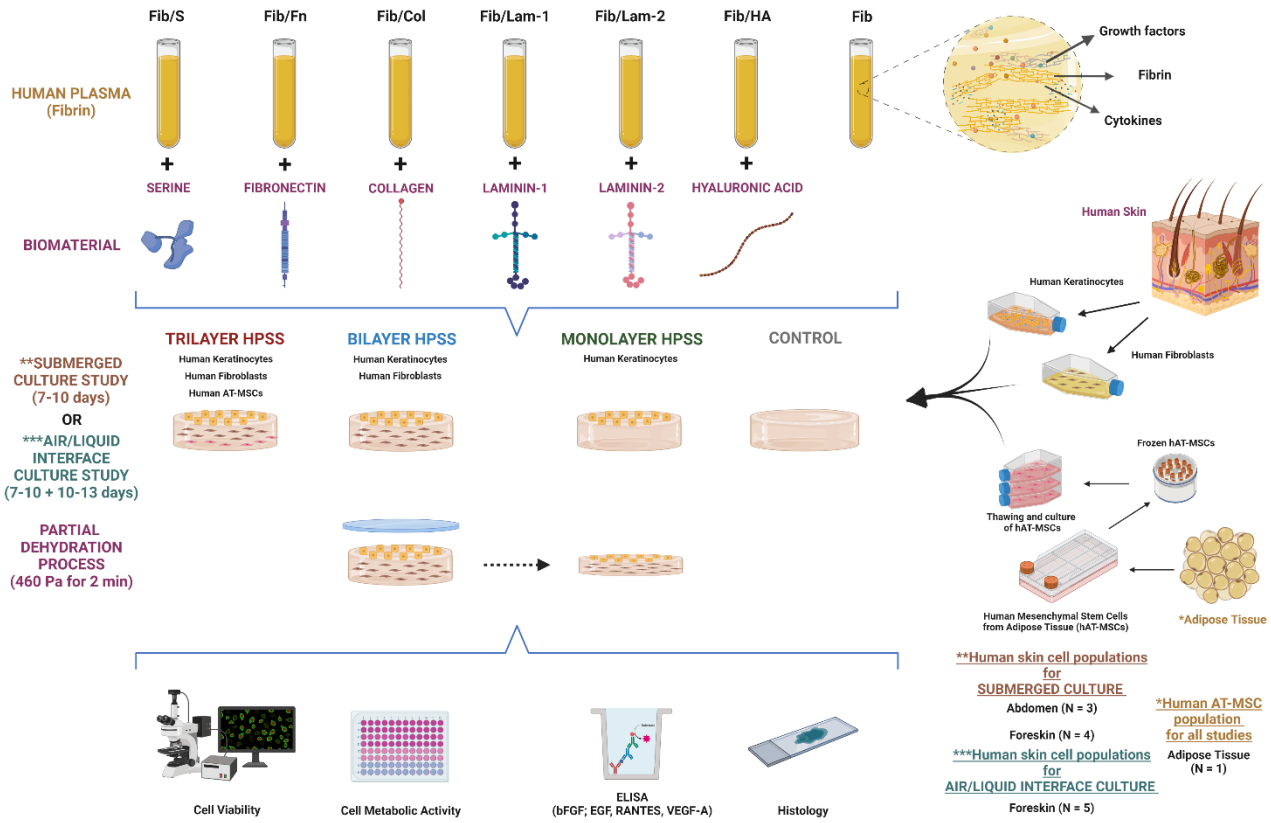

Fig. 9. ***Study design of Chapter 2.*** *Created with BioRender.com.*

CHAPTER 3: COMPARISON OF TWO CLINICAL HUMAN BILAYER TISSUE-ENGINEERED SKIN SUBSTITUTES (hbTESSs)

3.1. SKIN CELL ISOLATION AND CULTURE

Human keratinocytes and fibroblasts were isolated, as previously described[341,346,347] from different anatomical regions (chest (n=2) and abdomen (n=1)) of three human adult skin biopsies from healthy patients (22, 49 and 55 years old; N=3). Dermal fibroblasts were cultured in fibroblast medium [Dulbecco-Vogt modified Eagle medium (Gibco™, Waltham, MA, USA) supplemented with 10% Avantor Seradigm FB Essence serum (Avantor®, Radnor, PA, USA), 100 U/mL penicillin (Sigma-Aldrich, St. Louis, MO, USA) and 25 µg/mL gentamicin (Gemini Bio, West Sacramento, CA, USA)]. Keratinocytes were grown on a feeder layer of irradiated human fibroblasts and cultured in keratinocyte medium [Dulbecco-Vogt modified Eagle medium (Gibco™): Ham's F12 (Gibco™), ratio 3:1, 24.25 µg/mL adenine (Sigma-Aldrich), 5 µg/mL insulin (Sigma-Aldrich), 0.4 µg/mL hydrocortisone (Galenova, Saint-Hyacinthe, Canada), 0.212 µg/mL isoproterenol hydrochloride (Sigma-Aldrich), 5% bovine HyClone FetalClone II serum (GE Healthcare, Chicago, IL, USA), 10 ng/mL human epidermal growth factor (Austral Biologicals, San Ramon, CA, USA), 100 U/mL penicillin (Sigma-Aldrich) and 25 µg/mL gentamicin (Gemini Bio)]. For hbTESS production, cells were used at passage one to three for fibroblasts and three to four for keratinocytes. Each skin cell population (keratinocytes and fibroblasts from the same donor) was used to produce several replicas of both hbTESS models (4 replicas for the self-assembled skin substitute (**SASS**) model and 3 replicas for each biomaterial combination of the human plasma-based skin substitute (**HPSS**) model).

3.2. HUMAN BILAYER TISSUE ENGINEERED-SKIN SUBSTITUTE PRODUCTION

3.2.1. SELF-ASSEMBLED SKIN SUBSTITUTES (SASSs)

SASSs were manufactured as previously described[217,341,348]. To produce one fibroblast-derived tissue sheet (three sheets were required for each SASS), fibroblasts were seeded at 8×10^3 cells/cm^2 on 60×15 mm Tissue Culture Dishes (Falcon – BD, Franklin Lakes, NJ, USA) and cultured in fibroblast medium supplemented with 50 µg/mL ascorbic acid (Sigma-Aldrich) for 18-20 days. Then, keratinocytes were seeded over one of the three fibroblast-derived sheets at 10^5 cells/cm^2 (for each SASS) and cultured for 4 days in keratinocyte medium containing 50 µg/mL ascorbic acid. Next, two fibroblast-derived sheets and one with keratinocytes on top (for each SASS) were stacked and cultured at the air-liquid interface. The resulting constructs were cultured for 10 days in keratinocyte medium exempt of epidermal growth factor and supplemented with 50 µg/mL ascorbic acid. Finally, SASSs were collected for analysis. For each skin cell population (keratinocytes and fibroblasts isolated from the same donor), 4 SASSs were manufactured (n=12 [3 skin cell populations x 4 replicas]).

3.2.2. HUMAN PLASMA-BASED SKIN SUBSTITUTES (HPSSs)

HPSSs were manufactured in 60×15 mm Petri dishes (Fisherbrand™, Waltham, MA, USA). Three different human plasma-based hydrogels (final volume: 10 mL) were prepared: plasma as unique biomaterial (**Fib**), combined with 750 µg/mL hyaluronic acid (**Fib/HA**) (Sigma-Aldrich) or with 780 µg/mL collagen peptides (**Fib/Col**) (Biogelx™, Lanarkshire, UK). Fibroblasts at 1.405×10^5 cells/mL were embedded into hydrogels and cultured for 1 day in fibroblast medium supplemented with 50 µg/mL ascorbic acid. Next day, 1.77×10^5 keratinocytes/cm^2 were seeded on top and cultured for 7 days in keratinocyte medium containing 50 µg/mL ascorbic acid. Then, HPSSs were cultured at the air-liquid interface for 10 days in keratinocyte medium exempt of epidermal growth factor and supplemented with 50 µg/mL ascorbic acid. Before analyzing, to enhance the biomechanical properties[242], hbTESSs were partially dehydrated by pressure using a glass disc (460 Pa, for 1 minute). For each skin cell population (keratinocytes and fibroblasts isolated from the same donor) and biomaterial used, 3 HPSSs were manufactured (n=27 [3 skin cell populations x 3 biomaterials x 3 replicas]).

3.3. MECHANICAL TEST ANALYSIS

3.3.1. ADHESIVE STRENGTH OF THE DERMAL-EPIDERMAL JUNCTION (PEEL TEST)

To assess the adhesive strength of the dermal-epidermal junction of skin substitutes, a peel test was performed as previously described by Larose, A. *et al*.[349]. Briefly, a 10 mm width strip was cut out of each sample. The dermis and the epidermis were then manually separated on a small part of the strip and were fixed in the grips of an Instron ElectroPuls E1000 (Instron Corporation, Norwood, MA, USA) mechanical tester with a Dynacell® 10 Newton (N) load cell (accuracy of ± 0.0005 N). The dermis was then pulled apart from the epidermis at a constant rate of 0.7 mm/s by the mechanical tester, while the loadcell recorded the force required to do so. Force-displacement data were plotted using MATLAB script (MathWorks, Natick, MA, USA). Average adhesive strength was calculated using the data in the permanent regime section of the curve and normalized by the width of the strip. To confirm that peeling occurred at the dermal-epidermal junction, the test was interrupted before the complete separation of the two layers and a biopsy of the separation line was fixed and embedded for histology analysis by Masson's Trichrome staining.

3.3.2. TENSILE STRENGTH AND ELASTICITY

A dog-bone shaped specimen was cut out from each sample using a homemade metallic punch. Each sample was then mounted into an Instron ElectroPuls E1000 mechanical tester (Instron Corporation) with a Dynacell® 10 Newton (N) load cell (accuracy of ± 0.0005 N) and stretched at a constant 0.2 mm/s rate until complete failure. The distance between the two grips was considered as the gauge length, and the cross-section area was determined by multiplying the width of the punch (3 mm) and

the thickness of the sample measured on the histological slides. The stress-strain curves were plotted using a MATLAB script (MathWorks) according to the recorded force-displacement data, sample cross-section area and gauge length. The elastic modulus (slope of the linear region) and ultimate tensile stress (highest stress value recorded before failure) were then determined using the plotted curve. The ultimate tensile strength (UTS) represents the maximal amount of stress that the hbTESS can support before failure. The elastic modulus represents the ability of the hbTESS to be stretched and to return to its original shape after unloading. A high elastic modulus represents a stiffer behavior.

3.4. HISTOLOGICAL ANALYSIS

For histological analysis, samples were fixed in formaldehyde 3.7% (pH=7) and embedded in paraffin. Five-micrometer thick sections were stained with Hematoxylin / Eosin and Masson's Trichrome (Weigert's hematoxylin, fuchsin-ponceau and aniline blue). Digital images were acquired using an Axio Imager.Z2 microscope coupled with AxioCam ICc1 (brightfield) camera (Carl Zeiss Canada Ltd., North York, Canada). These samples were used for thickness measurements.

3.5. CELL METABOLIC ACTIVITY

Cell metabolic activity of hbTESSs was evaluated using PrestoBlue™ (Invitrogen™, Waltham, MA, USA); a colorimetric assay which allows to measure resazurin reduction level (absorbance at 570 and 600 nm) by living cells. To that purpose, a sample of 10 mm of diameter was taken from each hbTESSs and incubated at 37ºC in a PrestoBlue™-phosphate buffered saline (1/10) solution for 20 hours. Then the supernatant was collected, and absorbance was measured using a Thermo Scientific Varioskan® Flash (Thermo Fisher Scientific, Waltham, MA, USA). The percentage of reduction was calculated using the following equation:

$$\%\ Reduction = \frac{(O2\ x\ A1) - (O1\ x\ A2)}{(R1\ x\ C2) - (R2\ x\ C1)}\ x\ 100$$

- $O1$: molar extinction coefficient (E) of oxidized PrestoBlue™ (Blue) at 570 nm => 80586
- $O2$: E of oxidized PrestoBlue™ (Blue) at 600 nm => 117216
- $R1$: E of reduced PrestoBlue™ (Red) at 570 nm => 155677
- $R2$: E of reduced PrestoBlue™ (Red) at 600 nm => 14652
- $A1$: absorbance of test hbTESS at 570 nm
- $A2$: absorbance of test hbTESS at 600 nm
- $C1$: absorbance of control well (media plus PrestoBlue™ but no cells) at 570 nm
- $C2$: absorbance of control well (media plus PrestoBlue™ but no cells) at 600 nm

3.6. DNA QUANTIFICATION ASSAY

The Kit DNeasy Blood & Tissue (Qiagen, Hilden, Germany) was used to extract DNA from frozen samples of each previously weighted hbTESS and Quant-iT Picogreen dsDNA Assay Kit (Invitrogen™) was used for DNA quantification by fluorescence (485 nm/520 nm) and measured using a Thermo Scientific Varioskan® Flash (Thermo Fisher Scientific).

3.7. IMMUNOFLUORESCENCE ANALYSIS

For immunofluorescence analysis, the protocol was previously described[350]. Briefly, samples were embedded in Tissue-Tek OCT compound (Sakura Finetek Inc., Torrance, CA, USA) and frozen in liquid nitrogen. Indirect immunofluorescence assays were performed on 5 µm-thick cryosections permeabilized with acetone (10 min at −20 °C). The antibodies used were: mouse monoclonal anti-human keratin (K) 10 (Abcam, Cambridge, UK; 1:500), rabbit polyclonal anti-human type IV collagen (Novus Biologicals, Toronto, Canada; 1:500), anti-human Ki67 (Abcam; 1:400), anti-human Loricrin (Biolegend, San Diego, CA, USA; 1:1000), guinea polyclonal anti-human K15 (ARP, Waltham, MA, USA; 1:1000). Negative controls consisted in the omission of primary antibodies during the labeling reaction were included and normal human skin was used as positive control. As secondary antibodies Alexa-488-conjugated donkey anti-rabbit (Life technologies, Waltham, MA, USA; 1:1600), Alexa-594-conjugated donkey anti-mouse (Life technologies; 1:1600) and Alexa-594-conjugated goat anti-guinea pig (Life technologies; 1:200) were used. For K19 analysis, direct immunofluorescence assay was performed using mouse anti-human keratin 19-Cyanine 3 (clone A53-B/A244, gift from U. Karsten, Institute of Biological Sciences, University of Rostock, Germany; 1:200). Cell nuclei were counterstained with Hoechst reagent 33258 (Sigma-Aldrich).

Immunofluorescence sections were observed under a Zeiss Axio Imager.Z2 microscope (Carl Zeiss Canada Ltd.) and photographed with Axiocam HRm Monochrome digital camera. Images were processed using AxioVision 4.8.2 software (Carl Zeiss Canada Ltd.).

3.7.1. PERCENTAGE OF POSITIVE BASAL EPIDERMAL CELLS ANALYSIS

ImageJ software (NIH, Bethesda, MD, USA) was used to process immunofluorescence pictures. For each intra-replicate, three different pictures of the marked protein of interest and the same three pictures of Hoechst were chosen. After erasing dermal cells counterstained with Hoechst, positive basal epidermal cells for the protein of interest and all epidermal cells in Hoechst were counted. Finally, the percentage of positive basal epidermal cells by total number of epidermal cells was calculated for each picture and the mean value for each intra-replicate was calculated and used for statistical analysis.

3.8. WESTERN BLOT ANALYSIS

After the culture process, small samples of hbTESSs were collected and directly frozen in liquid nitrogen. The samples were then grinded using CryoMill (Retsch, Haan, Germany) with two steel beads (Ø=5 mm) per sample and six shaking cycles of 1 minute at 24 Hz. Cell lysis was achieved using a PBS 1X solution containing 1% NP40 (Bio Basic, Amherst, NY, USA), 1% Triton-X-100 (Bio-Rad, Hercules, CA, USA), 0.5% Sodium Deoxycholate (Fisher Chemical, Waltham, MA, USA) 0.1% SDS (Bio-Rad) and 1% Protease/Phosphatase inhibitor (Cell Signaling, Danvers, MA, USA). Supernatants were collected after centrifugation at 13,000 x g for 10 minutes at 4ºC. The total protein content was evaluated with Micro BCA™ Protein Assay Kit (Thermo Fisher Scientific).

For each sample, 20 µg of proteins were loaded on 10% SDS-acrylamide gels (Bio-Rad). After 3 hours of migration at 80V, proteins were electro-transferred for 1.5 hours at 4ºC on Nitrocellulose Blotting Membrane (Amersham™ Protran™, Sigma-Aldrich). Membranes were blocked for 30 minutes at room temperature (RT) in TBS 1X containing 5% skimmed milk (Bio Basic) and 0.5% Tween 20 (Sigma-Aldrich), and then incubated ON at 4ºC with primary antibodies: rabbit polyclonal anti-human type I and IV collagen (Novus Biologicals; 1:1500 and 1:4000, respectively) and mouse monoclonal anti-human β-Actin (Sigma-Aldrich; 1:5000-10000) as control. Membranes were washed eight times and incubated over agitation for 1 hour at RT with horseradish peroxidase-conjugated goat anti-rabbit and anti-mouse (Invitrogen™; 1:5000). To reveal antibody-binding sites, SuperSignal™ West Dura (Thermo Fisher Scientific) was used. The signal was detected using a Fusion Fx7 (Vilber Lourmat, Collégien, France) and analyzed with ImageJ software (NIH, Bethesda, MD, USA).

3.9. TRANSMISSION ELECTRON MICROSCOPY (TEM)

Skin substitutes were fixed with 2.5% glutaraldehyde (Electron Microscopy Sciences, Hatfield, PA, USA) in 0.1M cacodylate buffer (Mecalab, Montreal, Canada) at 4ºC ON. The next day, the fixative was removed and samples were washed 4 times with cacodylate buffer at 4ºC for 15 minutes. Finally, samples were kept in cacodylate solution and sent to Microscopy Service of Université Laval for inclusion and staining with uranyl acetate and lead citrate. Images were taken with a LIBRA 120 PLUS Transmission Electron Microscope (Carl Zeiss SMT, Oberkochen, Germany) at Scientific Instrumentation Center of Universidad de Granada.

3.10. STATISTICAL ANALYSIS

Microsoft Excel software was used for primary analysis of raw data, and GraphPad Prism 8 (San Diego, CA, USA) was used for statistical analysis and graphs. Data for each group of analysis and parameter obeyed a normal distribution, corroborated by Shapiro-Wilk test. Then, One-way ANOVA

and Tukey's multiple comparisons tests were used to analyze the results of each assay. All values are presented as mean value ± standard deviation (SD). The significance threshold was set at 0.05.

3.11. ETHICS

This study was conducted according to the Declaration of Helsinki and was approved by the research ethics committee for human subjects of the CHU de Quebec-Université Laval. All tissue donors provided informed written consent.

3.12. GRAPHICAL ABSTRACT OF CHAPTER 3

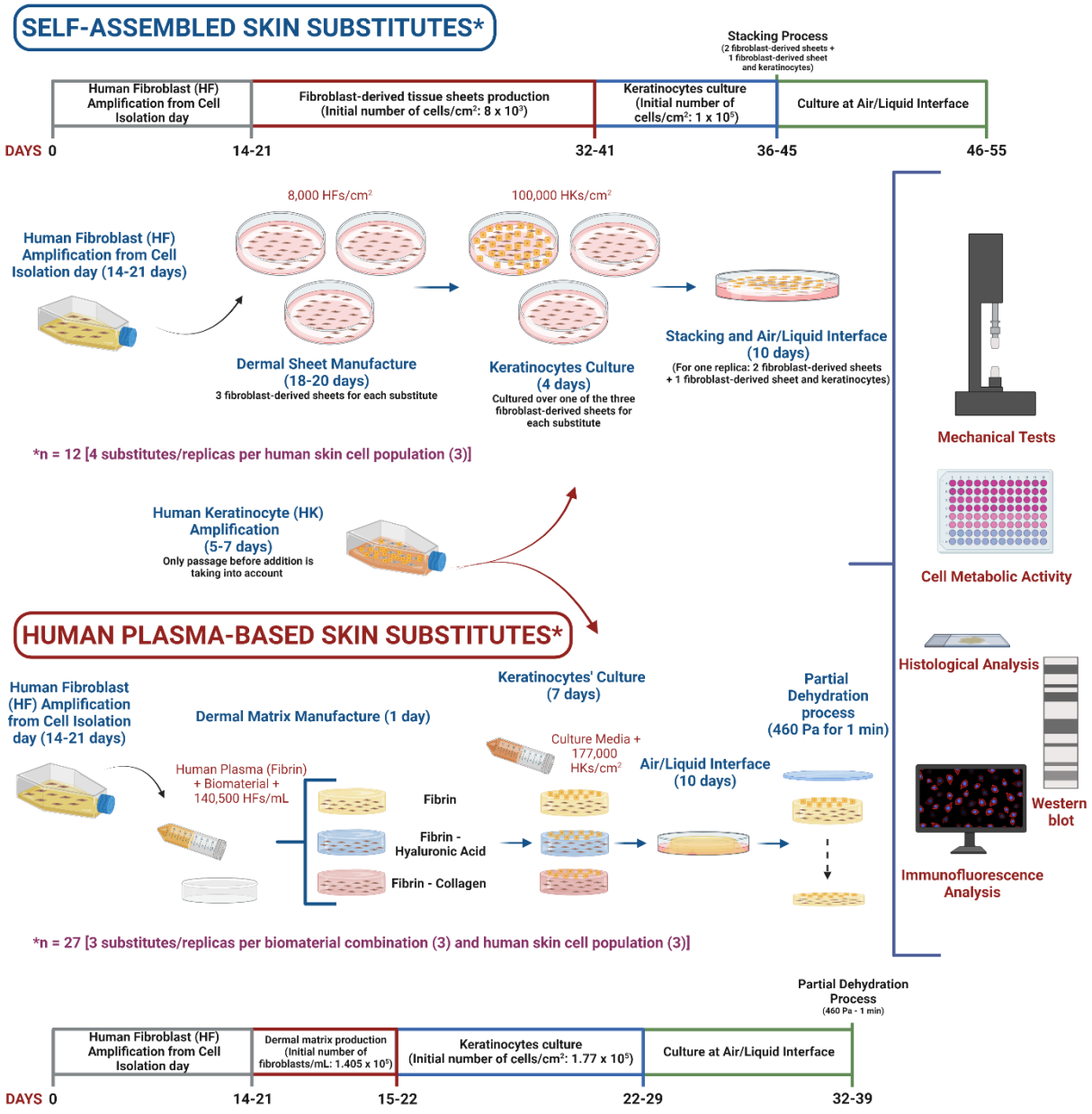

Fig. 10. ***Study design of Chapter 3.*** *Created with BioRender.com.*

CHAPTER 4: IN VIVO COMPARISON OF THE WOUND HEALING POTENTIAL OF BILAYER HUMAN PLASMA-BASED SKIN SUBSITUTES (HPSSs), SECONDARY WOUND HEALING APPROACHES AND THE GOLD STANDARD TREATMENT

4.1. SKIN CELL ISOLATION AND CULTURE

Human keratinocytes and fibroblasts were extracted from a human skin biopsy from abdomen from a healthy patient. Adipose tissue and/or blood traces were removed before starting the one-step digestion protocol (UPCIT-Protocol with slight modifications) applied for skin cell isolation.

Firstly, human skin biopsy was washed for 30 minutes, submerged in a solution constituted of Dulbecco's Phosphate Buffered Saline (DPBS; Sigma-Aldrich, St Louis, USA), 160 µg/mL gentamicin (Laboratorios Normon, Madrid, Spain), 100 µg/mL cefotaxime (Medochemie, Limassol, Cyprus), 100 µg/mL vancomycin (Reig Jofre, Barcelona, Spain) and 1.25 µg/mL amphotericin b (Sigma-Aldrich). Then, the sample was transferred to a 60×15 mm Petri dish (Fisherbrand®, Waltham, MA, USA) with the epidermis facing down. Most of the dermis was mechanically detached using scissors and a scalpel and kept for fibroblast isolation.

4.1.1. EPITHELIAL CELL ISOLATION

Epidermis was mechanically fragmented into small pieces using scissors and incubated for 15 minutes in a stirring 5 mL of TrypLE Select Enzyme 10X (Gibco™, Waltham, MA, USA) at 37ºC (8 cycles). After each cycle, digested solution containing the cells and pieces of tissue were filtered using a Cell Strainer of 100 µm (Fisherbrand®). The filtered cell suspension was neutralized using 10 mL of keratinocyte medium [Dulbecco's Modified Eagle's Medium (DMEM) (Sigma-Aldrich): Ham's F12 (Sigma-Aldrich), ratio 2:1, supplemented with 584 µg/mL L-glutamine (Sigma-Aldrich), 96 µg/mL gentamicin (Laboratorios Normon), 24 µg/mL adenine hydrochloride hydrate (Sigma-Aldrich), 5.25 µg/mL human insulin solution (Sigma-Aldrich), 1.25 µg/mL amphotericin b (Sigma-Aldrich), 400 ng/mL hydrocortisone (Sigma-Aldrich), 25 ng/mL human epidermal growth factor (Sigma-Aldrich), 1.4 ng/mL triiodo-L-thyronine sodium salt (Sigma-Aldrich) and 10% fetal bovine serum (Gibco™)] and kept, while remaining tissue was digested again. After the 8th cycle, the cell suspension was centrifuged (10 min / 24ºC / 1,500 rpm). Cells were counted and seeded at 1.3×10^5 cells/cm^2 on a *feeder* layer of irradiated layer of irradiated human fibroblasts (10^4 cells/cm^2) and cultured in keratinocyte medium. This primary culture was named passage 0 (P0).

4.1.2. DERMAL CELL ISOLATION

Dermis was fragmented using scissors and digested using a stirring solution of 2 mg/mL of Type I collagenase (Gibco™) in Dulbecco's Modified Eagle's Medium (DMEM) (Sigma-Aldrich) for 20 hours at 37ºC. The digested tissue was filtered using a Steriflip-GP Sterile Centrifuge Tube Top Filter Unit of 0.22 µm (Merck Millipore, Burlington, MA, USA), neutralized using fibroblast medium [Dulbecco's Modified Eagle's Medium (DMEM) (Sigma-Aldrich) supplemented with 584 µg/mL L-glutamine (Sigma-Aldrich), 96 µg/mL gentamicin (Laboratorios Normon) and 10% fetal bovine serum (Gibco™)] and centrifuged (10 min / 24ºC / 1,500 rpm). Finally, dermal cells were counted and seeded at 1.15×10^5 cells/cm^2 in fibroblast medium. This primary culture was named passage 0 (P0).

4.1.3. CULTURE MAINTENANCE AND PASSAGES

The culture medium of keratinocytes and fibroblasts was changed every two or three days until cells reached 90-95% confluence; then cells were trypsinized and cultured again until reached the enough number of cells for HPSS manufacturing. From P1 cell seeding density for keratinocytes was 7.5×10^3 cells/cm^2 on a *feeder* layer of irradiated human fibroblasts (10^4 cells/cm^2) and for fibroblasts was 3.5×10^3 cells/cm^2.

4.2. HPSS MANUFACTURE

The same human keratinocytes and fibroblasts isolated and cultured were used for manufacturing two types of bilayer HPSSs depending on the secondary biomaterial used [hyaluronic acid (HA) (Fidia Farmaceutici S.p.A., Abano Terme, Italy) or agarose (AG) (Sigma-Aldrich)]. The results of previous chapters demonstrated that no significant differences were observed *in vitro* regarding secondary biomaterial used, for this reason, the *in vivo* study of HA and AG was based on the clinical experience of both biomaterials for cosmetical purposes and/or wound healing[94,211,212,351,352].

The frozen human blood plasma from healthy donors was collected from the Centro Regional de Transfusión Sanguínea of Granada. Human plasma from different donors were mixed to generate a pool which was aliquoted, frozen at -20ºC and used for all experiments to avoid inter-variability between samples.

Regarding cell structure, two types of HPSSs were produced for each biomaterial combination: **Bilayer HPSSs;** constituted of a dermal layer of 3×10^4 human fibroblasts/mL and an epidermal layer constituted of 6.7×10^4 keratinocytes/cm^2 and **Control HPSSs**; as secondary wound healing approaches without cells (acellular substitutes).

All TESSs were manufactured in 6 insert well plates with 0.4 µm pore polyester membrane (Corning® Transwell®, Sigma-Aldrich). Several reagents were mixed and the final volume was 5 mL/hydrogel (**Table 14**).

Table 14. Reagents and volume for Bilayer and Control HPSS manufacture.

	Reagent for dermal layer	Volume
Solution 1	Calcium Chloride 100 mg/mL ($CaCl_2$) (BBraun, Melsungen, Germany)	0.120 mL
	Water for injection (Fresenius Kabi, Bad Homburg, Germany)	0.067 mL
Solution 2	Human Plasma	4.150 mL
	Fibroblast medium + human fibroblasts (Bilayer TESS) or no cells (Control HPSSs)	0.312 mL
	Secondary Biomaterial (HA or AG)	0.250 mL
	Tranexamic Acid 100 mg/mL (MEDA Pharma, Bad Homburg, Germany)	0.101 mL
For Bilayer HPSSs addition of human fibroblasts was required for dermal layer, however for Control HPSSs only fibroblast medium was required. Final concentration of HA into the hydrogel: 750 µg/mL Final concentration of AG into the hydrogel: 1100 µg/mL		

Briefly, all reagents were previously warmed at 37ºC and then both solutions were prepared in independent tubes. For Solution 2, secondary biomaterial and tranexamic acid were the last reagents to be added. Then, Solution 2 were mixed with Solution 1 and after shaking three times, the mixed solution was carefully pipetted into the 6 insert well plates. After 2-3 hours at 37ºC, hydrogel was formed and culture fibroblast medium was added and incubated ON at 37ºC.

The following day, keratinocytes were added on top of the corresponding hydrogels in a 500 µL of keratinocyte medium. They were allowed to adhere to the surface for 1-2 hours and then fibroblast medium was replaced by keratinocyte medium to fully cover the HPSSs.

Keratinocyte medium was changed every two days for 7-10 days from keratinocyte's addition. The submerged strategy, the standard culture methodology of the UPCIT that consists in fully covering the hydrogel to promote cell proliferation and growth, was applied in this study. At the end of the culture process, HPSSs were subjected to a partial dehydration process[242] using a sandwich system where absorbent papers and meshes of different pore sizes were used together with a glass disc to apply a pressure of 460 Pa for 2 minutes that improved their mechanical properties and handling[242].

4.3. ANIMAL PROCEDURES AND EXPERIMENTAL GROUPS

44 BALB/cAnNRj-*Foxn1*^{nu} male, immunodeficient, athymic, nude and albino mice, of four weeks of life were studied (Janvier Labs, Le Genest-Saint-Isle, France).

Firstly, a surgery to remove a skin area of 2 cm^2 from upper dorsal, in longitudinal position to the spine of mouse, was performed using a surgical knife. To that purpose mice were anesthetized by intraperitoneal injection (ketamine (150 mg/kg) and xylazine (10 mg/kg)). Then, a human TESS, a collagen wound dressing (Biobrane®, Smith & Nephew, London, UK), a dermal matrix scaffold without cells or a skin autograft were grafted in the damaged area as a reconstructive surgery.

8 mice were transplanted with a bilayer HPSS constituted of human fibroblasts and keratinocytes and a fibrin/hyaluronic acid scaffold (**Fib/HA**), other 8 mice were treated with a bilayer HPSS composed of human fibroblasts and keratinocytes and a fibrin/agarose scaffold (**Fib/AG**), 16 mice (8 and 8) were grafted with both combinations of biomaterials without cells (**Control-Fib/HA** and **Control-Fib/AG**), 6 mice were treated with Biobrane® (**Collagen-Dressing**) and finally, 6 mice were transplanted with a skin autograft from the hind leg (**Autograft**). Values of native mouse skin were also obtained, measuring a healthy area of skin from each mouse (**Healthy Mouse Skin**) included in the study (N=44).

For all groups, engraftments were affixed to the wound using five or six stitches. Moreover, to prevent their loss and improve the wound healing process, wounds were covered with Mepitel® (Mölnlycke Health Care, Gothenburg, Sweden), an antibiotic ointment (Mupirocin 20 mg/g, ISDIN, Barcelona, Spain) and a self-adhesive bandage which was removed one-week post-surgery. In addition, as postoperative treatment, an anti-inflammatory drug was subcutaneously injected (2 mg/kg – Metacam®, Boehringer Ingelheim, Ingelheim am Rhein, Germany).

In the case of autograft's group, the wound generated in the hind leg was closed using three clips (Ligaclip® MCA, Johnson & Johnson - Ethicon Endo-Surgery, Inc., Cincinnati, OH, USA) and covered in the same way as engrafted areas.

4.4. SKIN REPAIR MONITORING

An exhaustive clinical follow-up was performed for 8 weeks, evaluating the macroscopic integration of the engraftments, how the surgical defects healed and measuring the wound/scar area. Moreover, after the last endpoint (week 8) an evaluation of the scars was made using an adaptation of the Patient and Observer Scar Assessment Scale (POSAS)[353,354].

Every 2 weeks, mice were anesthetized to avoid unnecessary stress and homeostasis skin analysis was performed using the probe system Microcaya (Microcaya S.L., Bilbao, Spain) which allowed to measure different homeostasis parameters in grafts and healthy mouse skin (Healthy Mouse Skin): Thermometer® allowed to measure infrared temperature in ºC; Skin pH-meter® determined pH of skin using a glass rod with all elements required to measure it; Tewameter® measured transepidermal water loss (TEWL) or water evaporation in g/h/m^2, based on the principle of diffusion in an open chamber; Cutometer® applied suction (450 mbar of negative pressure – 2 seconds) to evaluate the elasticity in arbitrary units (AU); and Corneometer® determined moisturization through the capacitance of a dielectric medium (in AU). Erythema and pigmentation were also measured (in AU) using Mexameter® that obtained indirect information about skin vascularization (hemoglobin levels) and pigmentation (melanin) based on the light absorption/reflection of three specific wavelengths. In all cases where appropriate, a higher value in AU means a greater presence of the studied parameter.

4.5. HISTOLOGICAL AND IMMUNOHISTOCHEMICAL ANALYSIS

Half of the mice were sacrificed after 4 weeks, whereas the remaining mice were sacrificed after 8 weeks, by injection of an overdose of anesthetic drug. Skin biopsies from grafts were collected, fixed in formaldehyde 4% (pH=7) (Casa Álvarez, Madrid, Spain) and embedded in paraffin (Thermo Fisher Scientific, Waltham, MA, USA). Four-micrometer thick sections were stained with Hematoxylin / Eosin (Merck, Darmstadt, Germany) at Pathology Department of Virgen de las Nieves University Hospital Granada (Spain) to study the histological structure.

To determine the protein expression of the epithelial layer and to confirm the presence of human cells in both, the HPSSs manufactured and the regenerated skin, immunohistochemical analysis of keratins [Mouse anti-human Keratin AE1-AE3 Cocktail Antibody (Clone AE1/AE3) (Master Diagnostica, Granada, Spain)] and human leukocyte antigen E (HLA-E) [(Mouse anti-human HLA-E Monoclonal Antibody (MEM-E/02), (Invitrogen™, Waltham, MA, USA)] were carried out, respectively. The sections were dewaxed, hydrated, and heat-treated in 1 mM EDTA (pH=8) (Vitro SA, Sevilla, Spain) for antigenic retrieval using a PT module (Thermo Fisher Scientific) at 95°C for 20 minutes. Then, they were incubated for 10-20 min at room temperature with the diluted antibodies (1:100). An appropriate isotype for each antibody was used as negative control. The immunohistochemical staining was conducted in an automatic immunostainer (Autostainer 480, Lab Vision™, Thermo Fisher Scientific) using the micropolymer-peroxidase-based method (Ultravision Quanto, Master Diagnostica).

Digital images were acquired using a Leica DM2000 microscope coupled with Leica DMC2900 (brightfield) camera (Leica, Wetzlar, Germany). Images were processed using Leica Application Suite (LAS) 4.12 software (Leica).

4.6. STATISTICAL ANALYSIS

Microsoft Excel software was used for primary analysis of raw data, and GraphPad Prism 8 (San Diego, CA, USA) was used for statistical analysis and graphs. Two-way ANOVA and Tukey's multiple comparisons tests were performed to determine significant differences between wound/scar areas through the time. In the case of the homeostasis, erythema and pigmentation analysis, mean and standard error of the mean (SEM) values per week (2, 4, 6 and 8) were represented for each parameter and study group, comparing the results with healthy mouse skin values (Healthy Mouse Skin). In addition, Two-way ANOVA test, considering time and type of engraftment was used to analyze each parameter and subsequently, Tukey's multiple comparisons test, considering all treatments, was conducted to determine significance throughout the time and with the values of Healthy Mouse Skin group. The significance threshold was set at 0.05.

4.7. ETHICS

This study was conducted according to the Declaration of Helsinki and was approved by the Provincial Ethics Committees of Granada for human subjects. All tissue donors provided informed written consent.

All animal handling procedures complied with national and European Union legislation (Spanish RD 53/2013 and EU Directive 2010/63) for the welfare of animals used for scientific purposes and accordance with the Ethical Principles and Guidelines for the Use of Animals approved by Provincial Ethics Committees of Granada.

4.8. GRAPHICAL ABSTRACT OF CHAPTER 4

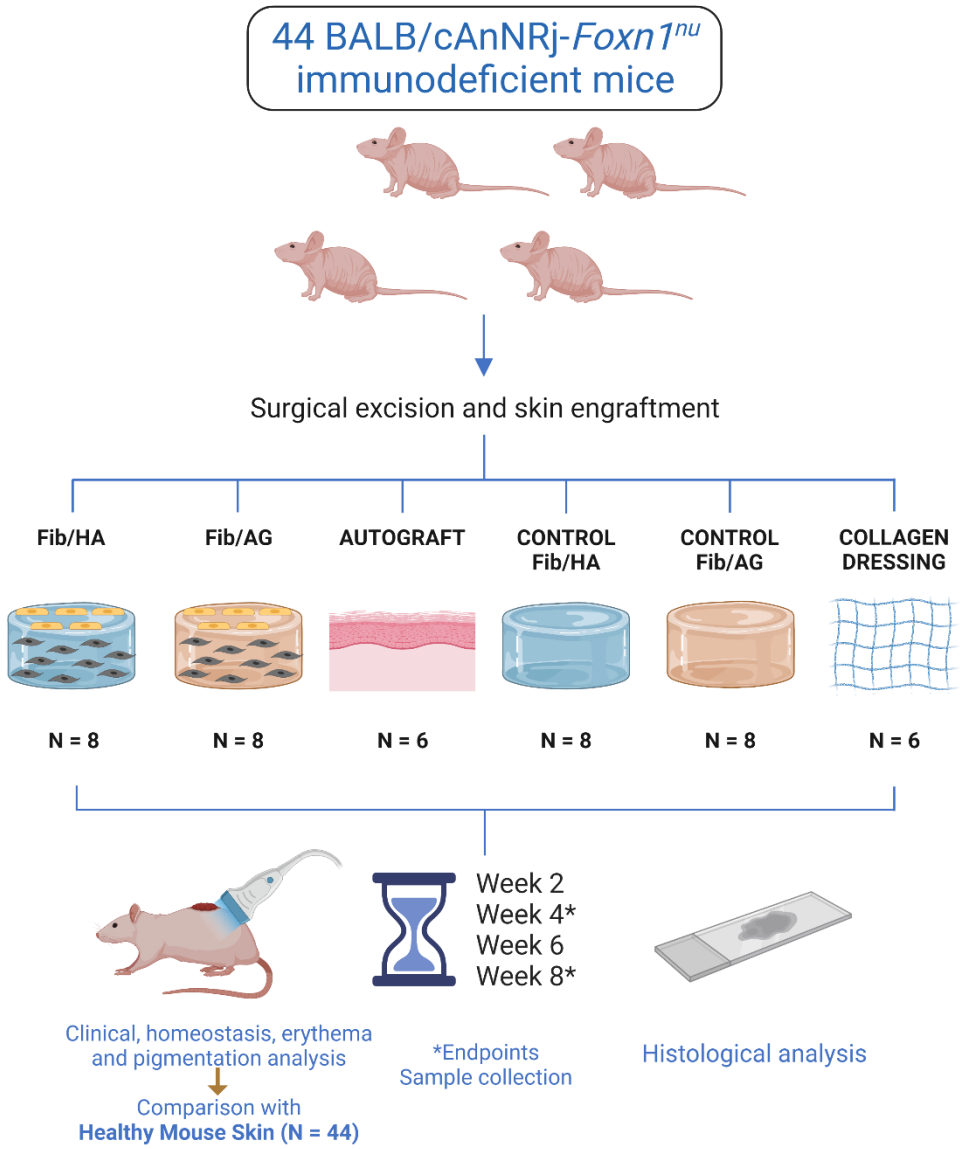

Fig. 11. ***Study design of Chapter 4.*** *Created with BioRender.com.*

V. RESULTS

DOI: 10.3390/ijms241914712
Journal: IJMS
1st Quartile: Biochemistry & Molecular Biology
(IF: 5.6 => JCR – 2022)

RESULTS

CHAPTER 1: COMPARISON OF TWO HUMAN SKIN CELL ISOLATION PROTOCOLS AND THEIR IMPORTANCE IN TRANSLATIONAL RESEARCH

1.1. EVALUATION OF CELL CHARACTERISTICS

1.1.1. CELL SIZE, VIABILITY AND YIELD

1.1.1.1. Epithelial cells

The size (diameter, Ø) of the epithelial cells isolated with both the LOEX- and UPCIT-Protocols was similar at each time point (freshly isolated and at each passage). For both methods, the freshly isolated cells were significantly (*p-value<0.001*) smaller than the cultured keratinocytes (P0 to P4) (**Fig. 12A**).

The evaluation of cell viability indicated that the viability of freshly isolated epithelial cells was higher when the LOEX-Protocol was used compared to the UPCIT-Protocol (93±2 % vs. 85±1%, respectively; *p-value<0.01*). However, after cell culture over several passages no significant differences were observed. The cell viability varied between 89% and 95% for the cultured keratinocytes (P0 to P4) for both protocols (**Fig. 12B** and **12C**).

The cell yield after isolation from the skin biopsy was significantly higher (*p-value<0.05*) with the LOEX-Protocol ($3.28\times10^{6}\pm0.92\times10^{6}$ cells/cm^2 biopsy) than with the UPCIT-Protocol ($9.52\times10^{5}\pm4.81\times10^{5}$ cells/cm^2 biopsy) (**Fig. 12D**). No significant differences were observed between the protocols in the number of keratinocytes recovered per cm^2 for a given passage between P0 and P4 (**Fig. 12E**).

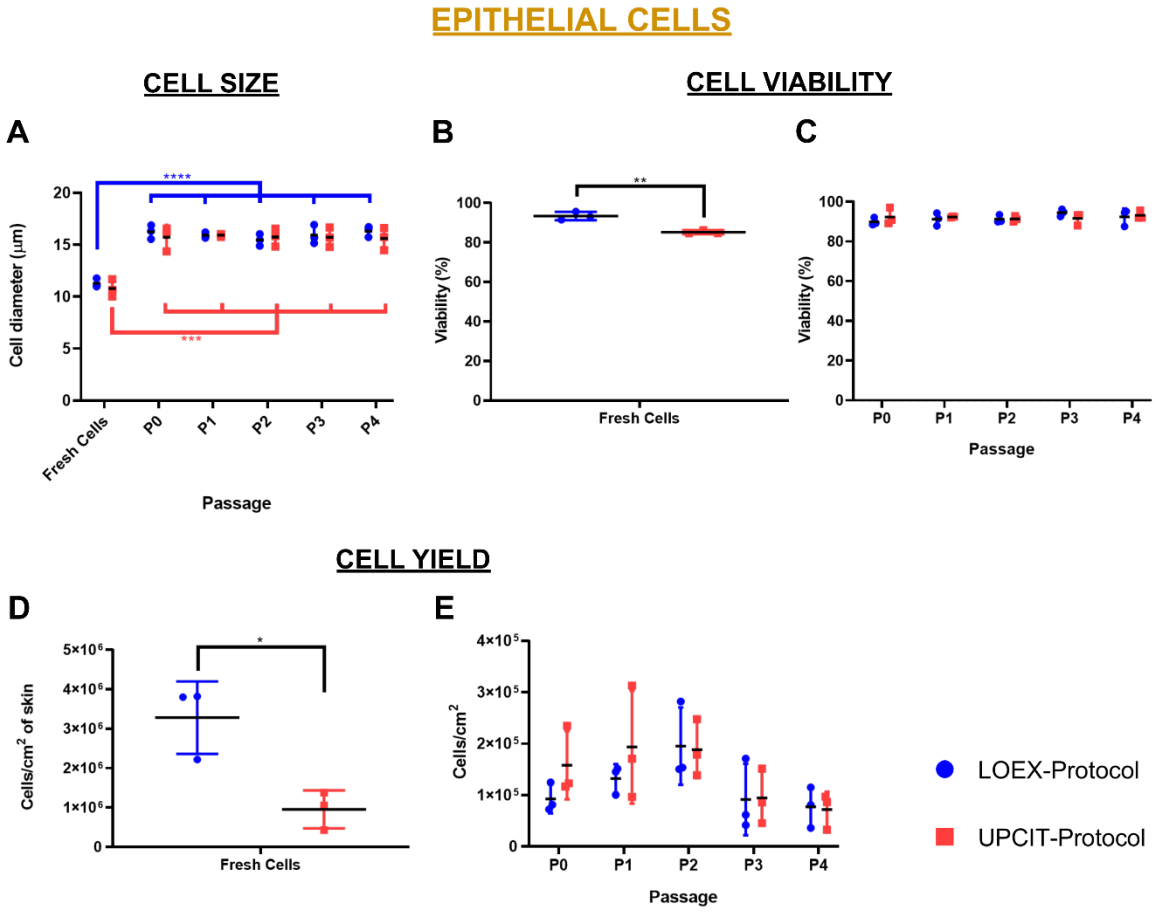

Fig. 12. ***Comparison of cell size, viability and yield of epithelial cells/keratinocytes.*** *A Cell size (Ø); B Cell viability after cell isolation from the biopsy (Fresh Cells); C Cell viability after each passage (P0-P4); D Number of cells isolated per cm² of skin; E Number of cells recovered after each passage per cm² (P0-P4). Statistical significance: *p-value<0.5; **p-value<0.01; ***p-value<0.001; ****p-value<0.0001, One-way ANOVA and Tukey's multiple comparisons tests for comparison between passages for each protocol and Multiple t-tests and Holm-Sidak method for comparison between protocols for each passage. Data is shown as mean value (horizontal black line) ± SD (N=3 for each protocol). LOEX-Protocol: Two-step digestion protocol; UPCIT-Protocol: One-step digestion protocol. P: Passage; P0: Primary culture.*

1.1.1.2. Dermal cells

As for the epithelial cells, the size of the dermal cells was significantly lower just after isolation compared to the cultured cells (P0 to P4) for the LOEX- and UPCIT-Protocols (*p-value<0.001* and *p-value<0.0001*). No significant difference was observed between the protocols at each time point (fresh cells, P0 to P4) (**Fig. 13A**).

The cell viability of the freshly isolated cells (**Fig. 13B**) and cultured cells was over 90% using both protocols although small differences were observed after P0 (*p-value<0.05*) (**Fig. 13C**).

Regarding cell yield, although a higher number of freshly isolated dermal cells was obtained using the LOEX-Protocol compared to the UPCIT-Protocol, no significant difference was reported (**Fig. 13D**). Although more fibroblasts were recovered after P0 with the UPCIT-Protocol compared to the LOEX-Protocol (2.4-fold higher, *p-value<0.05*) (**Fig. 13E**), it must be stated that the initial number of freshly isolated dermal cells seeded by culture surface area was also higher (2.8 times).

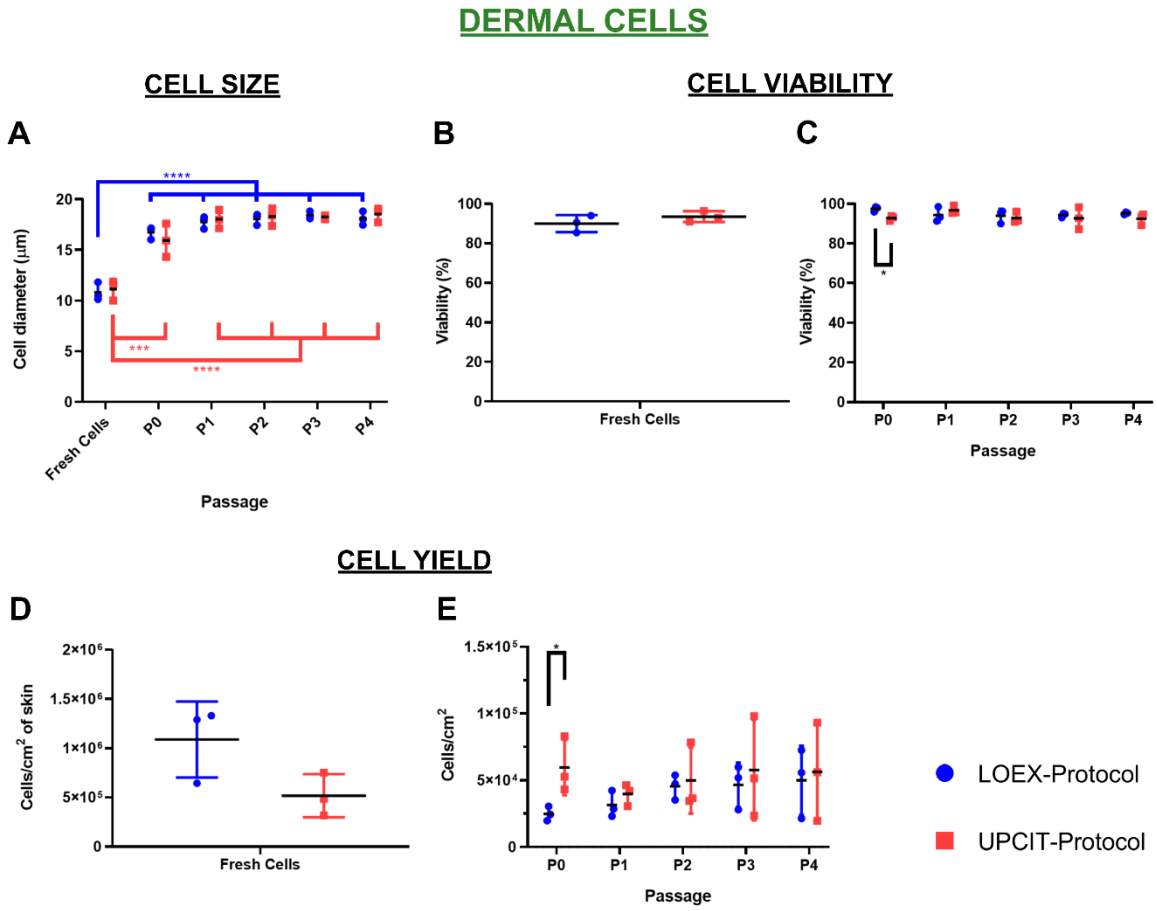

Fig. 13. ***Comparison of cell size, viability and yield of dermal cells/fibroblasts.*** *A Cell size (Ø); B Cell viability after cell isolation from the biopsy (Fresh Cells); C Cell viability after each passage (P0-P4); D Number of cells isolated per cm² of skin; E Number of cells recovered after each passage per cm² (P0-P4). Statistical significance: *p-value<0.5; ***p-value<0.001; ****p-value<0.0001, One-way ANOVA and Tukey's multiple comparisons tests for comparison between passages for each protocol and Multiple t-tests and Holm-Sidak method for comparison between protocols for each passage. Data is shown as mean value (horizontal black line) ± SD (N=3 for each protocol). **LOEX-Protocol**: Two-step digestion protocol; **UPCIT-Protocol**: One-step digestion protocol. **P**: Passage; **P0**: Primary culture.*

1.1.2. CULTURE AND POPULATION DOUBLING TIME

1.1.2.1. Epithelial cells

For keratinocyte cultures, the time necessary to reach confluence was similar for both protocols at each passage (**Fig. 14A**). Moreover, a similar population doubling time was observed for both protocols at passages P1 to P4. A significant difference between the keratinocytes isolated by the two protocols was only observed in the primary culture (P0) (*p-value<0.01*) (**Fig. 14B**). The negative value for the UPCIT-Protocol (-27±32 days) indicated that the initial number of epithelial cells seeded was higher than the number of keratinocytes recovered at the end of the culture period, although a high variability between skin biopsies was noticed (**Fig. 14B**). For cells isolated with the LOEX-Protocol, the comparison of the population doubling time revealed significant differences between P0 and the other passages (*p-value<0.001* for P1 and P2; *p-value<0.01* for P3 and P4) (**Fig. 14B**). Representative pictures of the keratinocytes cultured at P0 at various times are included in **Fig. 14C**.

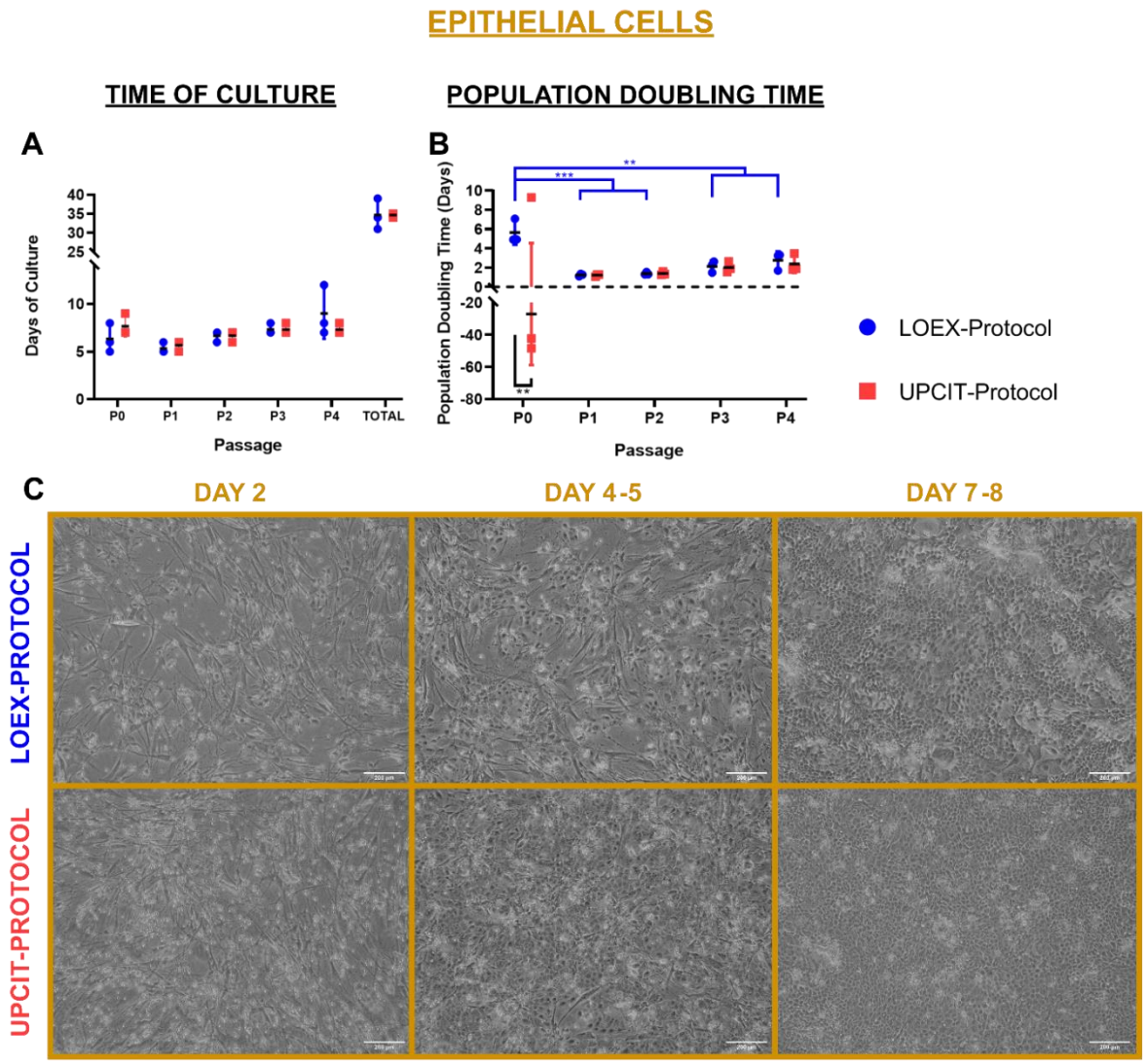

Fig. 14. Comparison of culture time and population doubling time of epithelial cells/keratinocytes. *A Time to reach confluence for different passages; B Population doubling time; C Representative pictures of keratinocytes' culture after 2, 4-5, 7-8 days of primary culture. Scale bar: 200 µm. Statistical significance: **p-value<0.01; ***p-value<0.001, One-way ANOVA and Tukey's multiple comparisons tests for comparison between passages for each protocol and Multiple t-tests and Holm-Sidak method for comparison between protocols for each passage. Data is shown as mean value (horizontal black line) ± SD (N=3 for each protocol). LOEX-Protocol: Two-step digestion protocol; UPCIT-Protocol: One-step digestion protocol. P: Passage; P0: Primary culture.*

1.1.2.2. Dermal cells

Fibroblasts isolated with the two protocols proliferated in culture and reached confluence at the same speed (**Fig. 15A**), and their population doubling time was comparable (**Fig. 15B**). However, for each method, a significant difference in the population doubling time between the primary culture (P0) and passages (P1 to P4) was observed (*p-value<0.01* for the LOEX-Protocol and *p-value<0.05* for the UPCIT-Protocol) (**Fig. 15B**). The phenotype of the fibroblasts was similar (**Fig. 15C**).

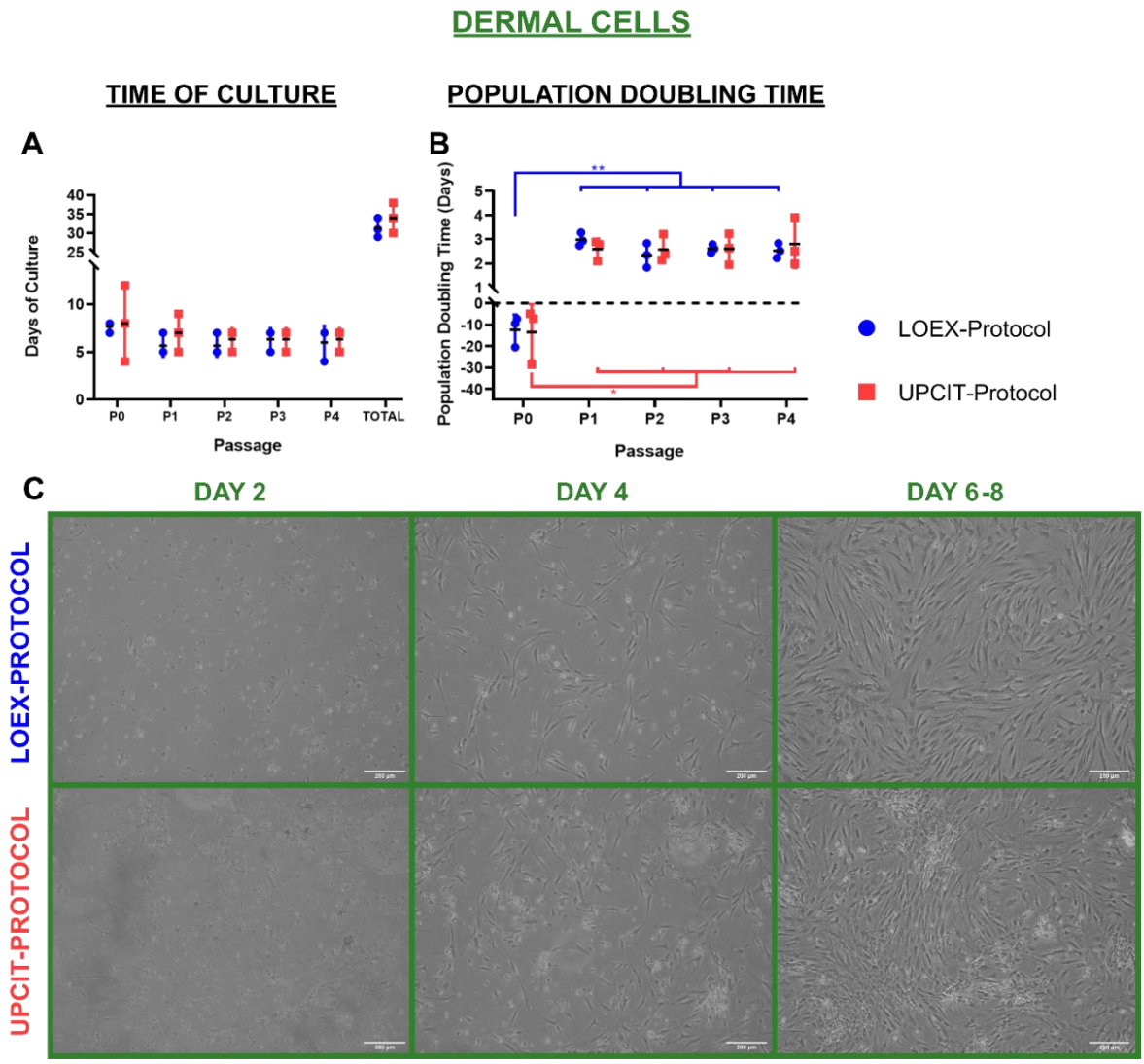

Fig. 15. ***Comparison of culture and population doubling time of dermal cells/fibroblasts.*** *A Time to reach confluence for different passages; B Population doubling time; C Representative pictures of fibroblasts' culture after 2, 4, 6-8 days of primary culture. Scale bar: 200 µm. Statistical significance: *p-value<0.05; **p-value<0.01, One-way ANOVA and Tukey's multiple comparisons tests for comparison between passages for each protocol and Multiple t-tests and Holm-Sidak method for comparison between protocols for each passage. Data is shown as mean value (horizontal black line) ± SD (N=3 for each protocol). LOEX-Protocol: Two-step digestion protocol; UPCIT-Protocol: One-step digestion protocol. P: Passage; P0: Primary culture.*

1.2. CLONOGENICITY OF EPITHELIAL CELL CULTURES

Epithelial stem cells are known to be clonogenic. To evaluate the clonogenicity of epithelial cells isolated from both protocols, the size and number of colonies formed by keratinocytes was monitored.

Since the size of a colony reveals the proliferation potential of the epithelial cell that generated it, the diameter (Ø) of the colonies was measured to determine the percentage of holoclones (Ø ≥ 4.5 mm), meroclones (4.5 mm > Ø > 1.5 mm) and paraclones (Ø ≤ 1.5 mm). The proportion of holoclones, meroclones and paraclones, was similar regardless of the cell isolation protocol applied (**Fig. 16A** and **16B**). Between P0 and P1, the percentage of holoclones decreased whereas the proportion of meroclones and paraclones increased for both protocols.

A similar colony-forming efficiency (CFE) – defined as the percentage of holoclones from the initial number of epithelial cells seeded – was observed for both the LOEX- and UPCIT-Protocols but decreased from P0 to P1 (Fig. 16C). However, the total number of colonies was higher after P1 compared to P0 in both protocols (*p-value<0.05* for the LOEX-Protocol and *p-value<0.01* for the UPCIT-Protocol), although no significant difference was observed regarding the isolation protocol used (Fig. 16D). Representative pictures of CFE staining are included in Fig. 16E.

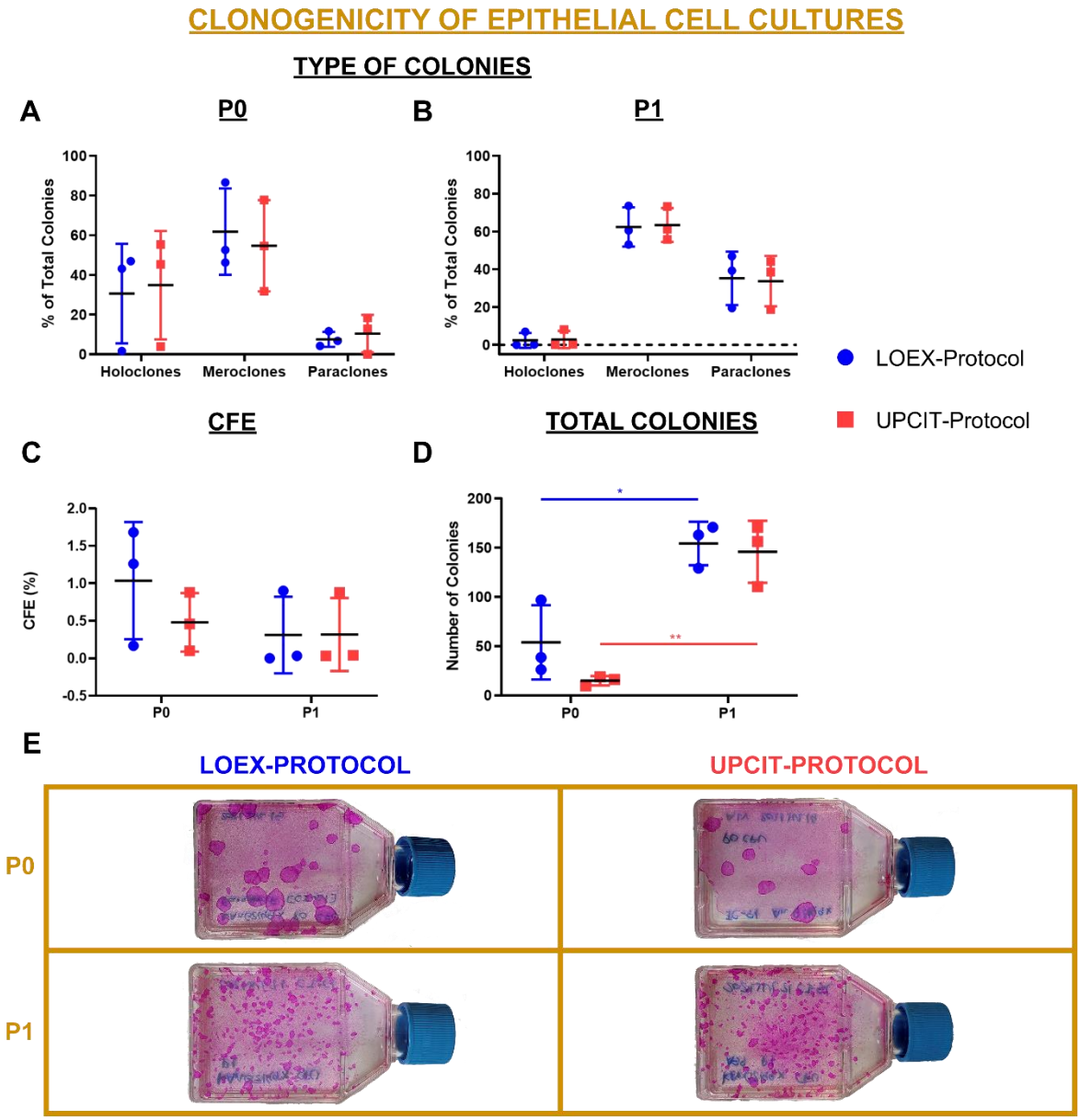

Fig. 16. ***Clonogenicity of epithelial cells.*** *A Comparison between protocols of the percentage of colonies that are holoclones, meroclones or paraclones after primary culture; B Comparison between protocols of the percentage of colonies that are holoclones, meroclones or paraclones after P1; C Colony-forming efficiency (CFE; the percentage of holoclones from the initial number of epithelial cells seeded); D Total number of colonies; E Macroscopic pictures of CFE assay after P0 and P1. Statistical significance: *p-value<0.05; **p-value<0.01; for type of colony analysis: Multiple t-tests and Holm-Sidak method for comparison between protocols for each type of colony and passage; for CFE and total colonies analysis: Multiple t-tests and Holm-Sidak method for comparison between passages for each protocol and for comparison between protocols for each passage. Data is shown as mean value (horizontal black line) ± SD (N=3 for each protocol). LOEX-Protocol: Two-step digestion protocol; UPCIT-Protocol: One-step digestion protocol. P: Passage; P0: Primary culture.*

1.3. KERATIN 19 (K19) ANALYSIS BY FLOW CYTOMETRY

K19 is a marker associated with skin epithelial stem cells[13]. The proportion of keratinocytes expressing K19, was measured by flow cytometry at P0 and P1. The results indicated that no significant differences were observed regardless of the cell isolation protocol or the cell passage (**Fig. 17A**). Representative pictures of the K19 cytometry analysis are included in **Fig. 17B**.

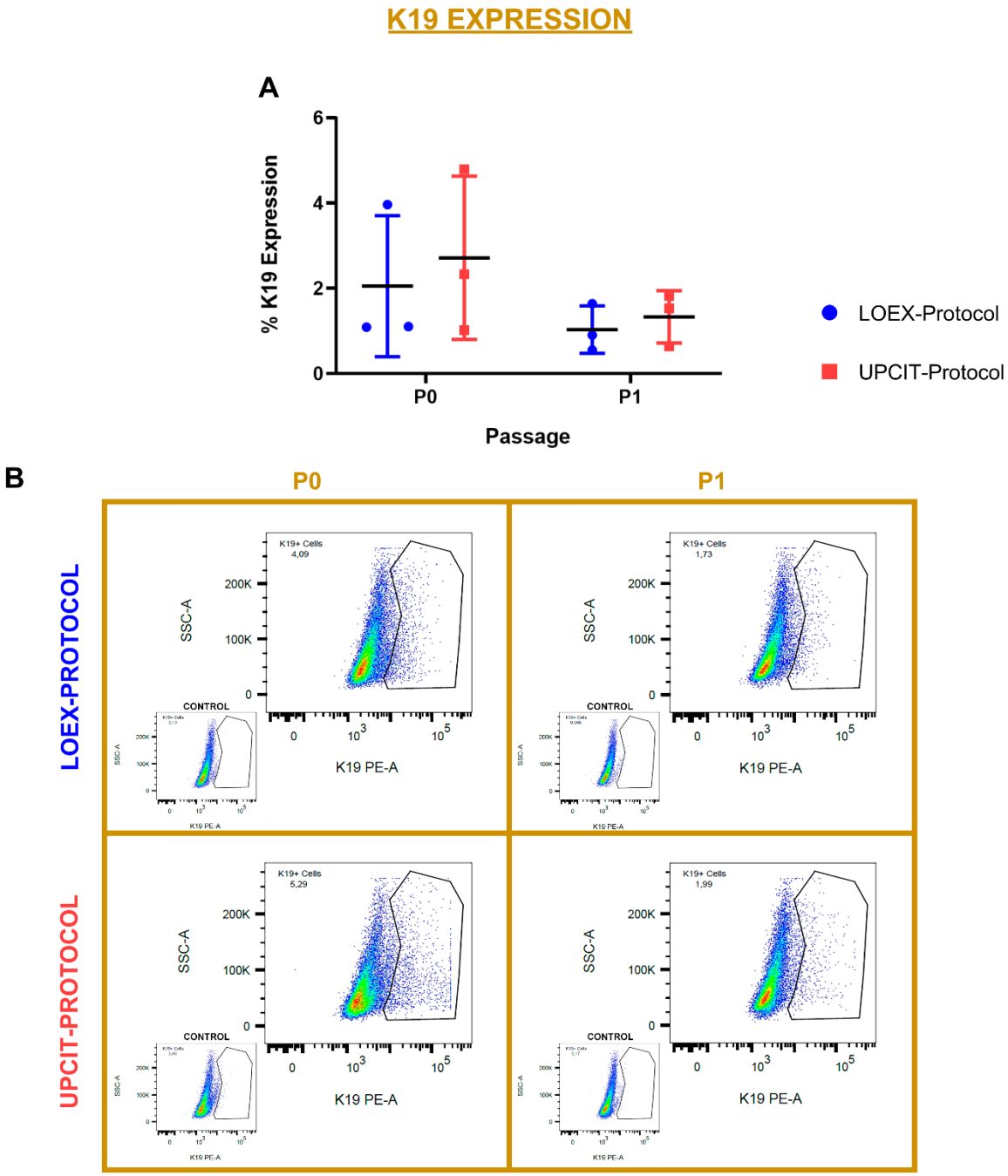

Fig. 17. ***Comparison of Keratin 19 (K19) expression by flow cytometry.*** ***A*** *Comparison between protocols of the percentage of K19⁺ epithelial cells after P0 and P1;* ***B*** *Representative graphs of cytometry assays, including their controls. Multiple t-tests and Holm-Sidak method for comparison between passages for each protocol and for comparison between protocols for each passage. Data is shown as mean value (horizontal black line) ± SD (N=3 for each protocol)* ***LOEX-Protocol****: Two-step digestion protocol;* ***UPCIT-Protocol****: One-step digestion protocol.* ***P****: Passage;* ***P0****: Primary culture.*

CHAPTER 2: IN VITRO ANALYSIS OF DIFFERENT HUMAN PLASMA-BASED SKIN SUBSITUTES

2.1. ANALYSIS OF SECONDARY BIOMATERIALS USED FOR HPSS MANUFACTURE

Six secondary biomaterials combined with human plasma/fibrin were used for manufacturing four types of cellular HPSSs (Trilayer, Bilayer, Monolayer and Control): **Fib/S**, **Fib/Fn**, **Fib/Col**, **Fib/Lam-1**, **Fib/Lam-2** and **Fib/HA**. Skin substitutes without secondary biomaterial were also manufactured (**Fib**).

2.1.1. CELL VIABILITY

2.1.1.1. Influence of partial dehydration process

Cell viability results revealed that no significant differences were observed between secondary biomaterials used, under hydrated (HYD) or dehydrated (DEHYD) conditions (**Fig. 18A**, **18B** and **18C**). Moreover, the effect of partial dehydration was similar regardless of secondary biomaterial used, reducing cell viability from ~82% to ~72% in Trilayer and Bilayer HPSSs (**Fig. 18A and 18B**) and from ~66% to ~60% in Monolayer HPSSs (**Fig. 18C**). However, this decrease was no significant except for Trilayer HPSSs manufactured with Fib/Lam-1 where a small statistical significance was reported (*p-value<0.05*) (**Fig. 18A**).

2.1.1.2. Influence of culture methodology

In this case cell viability was determined only after dehydration process and, as in the previous section, no significant differences were observed between secondary biomaterials used, under submerged (SUB) or air/liquid interface (ALI) strategy (**Fig. 18D**, **18E** and **18F**). Regarding the comparison between culture methodologies, for each type of secondary biomaterial used and type of cellular HPSS, no statistical significance was observed. However, ALI approach increased cell viability of Trilayer and Bilayer HPSSs [from ~72% to ~78% (**Fig. 18D and 18E**)], but a decrease was reported in Monolayer HPSSs [from ~60% to ~54% (**Fig. 18F**)].

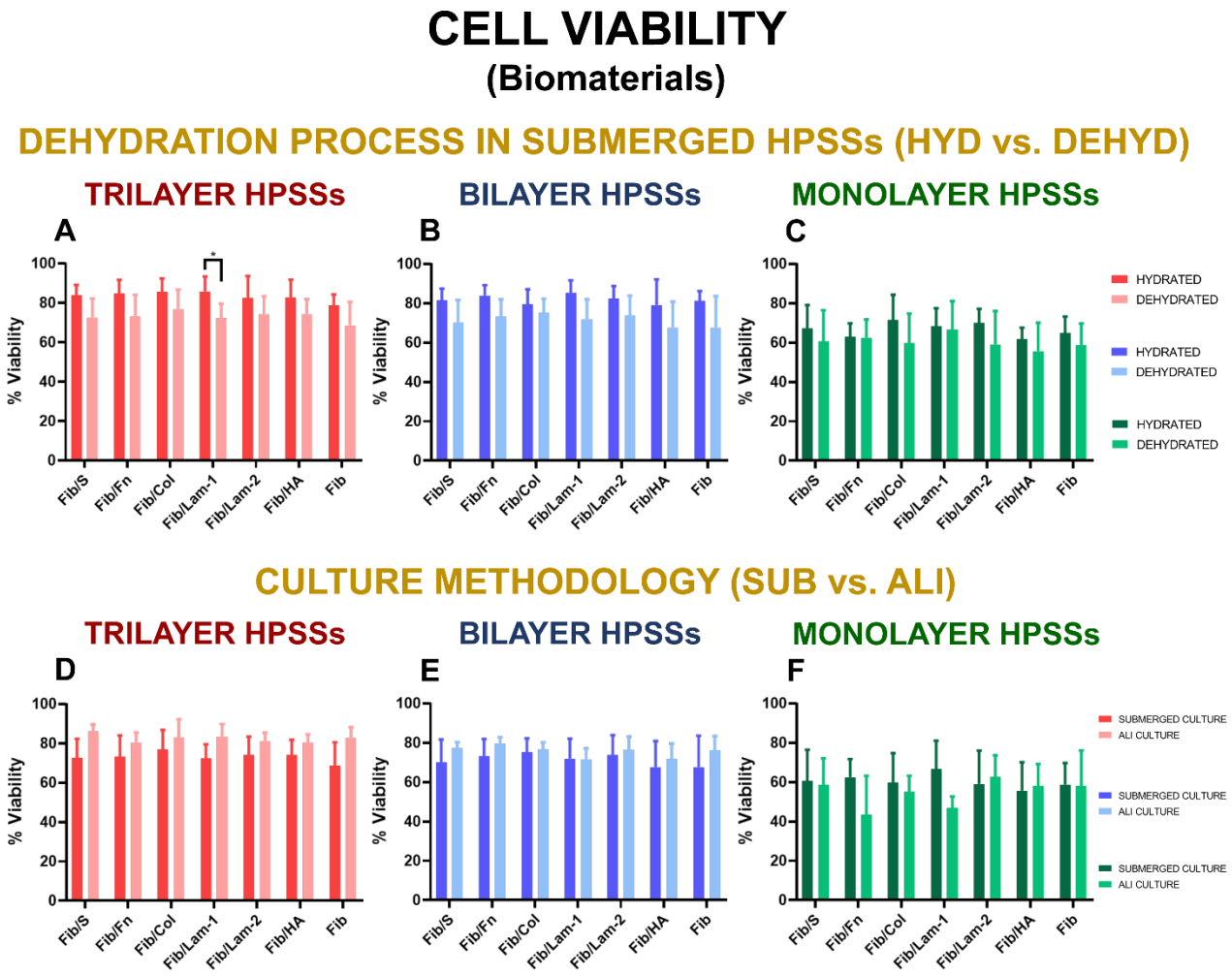

Fig. 18. ***Cell viability analysis of human plasma-based skin substitutes (HPSSs) manufactured with several secondary biomaterials.*** *A Cell viability of Trilayer HPSSs before and after dehydration process; B Cell viability of Bilayer HPSSs before and after dehydration process; C Cell viability of Monolayer HPSSs before and after dehydration process; D Cell viability of Trilayer HPSSs cultured under submerged and air/liquid interface methodologies; E Cell viability of Bilayer HPSSs cultured under submerged and air/liquid interface methodologies; F Cell viability of Monolayer HPSSs cultured under submerged and air/liquid interface methodologies. Statistical significance: *p-value<0.05; for comparison between biomaterials for each condition: One-way ANOVA and Tukey's multiple comparisons tests (if normal distribution) or Friedman and Dunn's multiple comparisons tests (if no normal distribution); for comparison between conditions for each biomaterial: Multiple t-test and Holm-Sidak's method. Data is shown as mean value ± SD; N=7 for hydrated (n=7) and dehydrated (n=7) conditions; N=7 for submerged condition (n=7) and N=5 for air/liquid interface condition (n=5). Fib/S: Fibrin/Serine; Fib/Fn: Fibrin/Fibronectin; Fib/Col: Fibrin/Collagen; Fib/Lam-1: Fibrin/Laminin-1; Fib/Lam-2: Fibrin/Laminin-2; Fib/HA: Fibrin/Hyaluronic Acid; Fib: Fibrin. HYD: hydrated; DEHYD: dehydrated. SUB: submerged; ALI: air/liquid interface.*

2.1.2. CELL METABOLIC ACTIVITY

The influence of the secondary biomaterial used in cell metabolic activity was evaluated for SUB and ALI culture methodologies and compared between them (**Fig. 19**). In the same way as cell viability results, no significant differences were observed between secondary biomaterials analyzed (**Fig. 19A**, **19B** and **19C**). Moreover, comparison of culture strategies revealed that ALI approach reduced cell metabolic activity in all cases (**Fig. 19A**, **19B** and **19C**), however only significant differences were reported in most of the Monolayer HPSSs (**Fig. 19C**), being higher when Fib/Col was applied (*p-value<0.0001*), followed by Fib/Fn, Fib/Lam-1 and Fib (*p-value<0.01*) and Fib/S and Fib/HA (*p-value<0.05*). Interestingly, no significant difference was reported in substitutes composed of Fib/Lam-2.

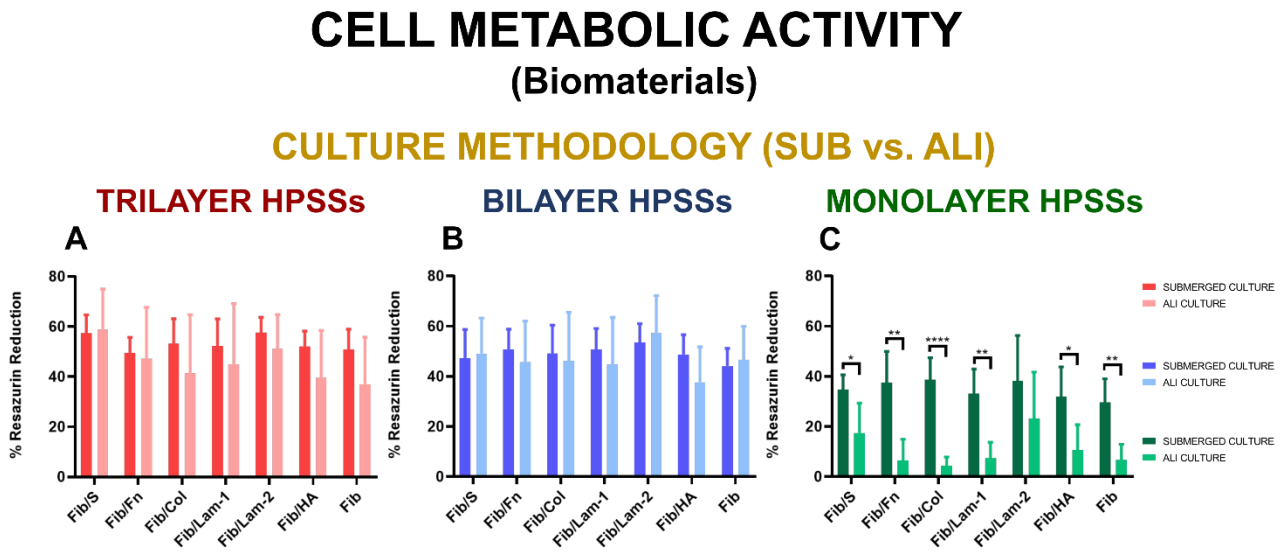

Fig. 19*. Cell metabolic activity of human plasma-based skin substitutes (HPSSs) manufactured with several secondary biomaterials.** ***A *Cell metabolic activity of Trilayer HPSSs cultured under submerged and air/liquid interface methodologies;* ***B*** *Cell metabolic activity of Bilayer HPSSs cultured under submerged and air/liquid interface methodologies;* ***C*** *Cell metabolic activity of Monolayer HPSSs cultured under submerged and air/liquid interface methodologies. Statistical significance: *p-value<0.05, **p-value<0.01, ****p-value<0.0001; for comparison between biomaterials for each condition: One-way ANOVA and Tukey's multiple comparisons tests (if normal distribution) or Friedman and Dunn's multiple comparisons tests (if no normal distribution); for comparison between conditions for each biomaterial: Multiple t-test and Holm-Sidak's method. Data is shown as mean value ± SD; N=7 for submerged condition (n=7) and N=5 for air/liquid interface condition (n=5).* ***Fib/S****: Fibrin/Serine;* ***Fib/Fn****: Fibrin/Fibronectin;* ***Fib/Col****: Fibrin/Collagen;* ***Fib/Lam-1****: Fibrin/Laminin-1;* ***Fib/Lam-2****: Fibrin/Laminin-2;* ***Fib/HA****: Fibrin/Hyaluronic Acid;* ***Fib****: Fibrin.* ***SUB****: submerged;* ***ALI****: air/liquid interface.*

2.1.3. PROTEIN SECRETION PROFILE ANALYSIS

Protein secretion profile (bFGF, EGF, VEGF-A and CCL5) for each type of secondary biomaterial used was determined by ELISA assays for SUB and ALI methodologies (**Fig. 20**). Overall, for any of the proteins, cellular HPSSs and culture strategy studied no significant differences were observed regarding secondary biomaterial used (**Fig. 20A - 20L**).

In the case of bFGF, secretion was higher when ALI methodology was applied for Trilayer, Bilayer and Monolayer HPSSs but no significant differences were reported compared to SUB strategy (**Fig. 20A**, **20B** and **20C**).

Regarding EGF, as results were normalized by subtracting the value of Control HPSSs without cells most of the results were negative (**Fig. 20D**, **20E** and **20F**), which means that more amount of this protein was recovered in Control groups, indicating that cells captured and used this growth factor for several purposes. Considering culture methodology, lower values were reported when ALI approach was applied and significant differences were observed compared with SUB strategy for all biomaterials [*p-value<0.0001* for Trilayer HPSSs (**Fig. 20D**); *p-value<0.0001* for Bilayer HPSSs (**Fig. 20E**); and *p-value<0.01* for Monolayer HPSSs (**Fig. 20F**)].

Secretion of VEGF-A was higher when ALI strategy was applied (**Fig. 20G, 20H** and **20I**) but only significant differences were observed in Bilayer HPSSs for all biomaterials (*p-value<0.05* and *p-value<0.01*) (**Fig. 20H**), compared with SUB methodology. Trilayer substitutes manufactured with Fib/HA and Fib and cultured under ALI conditions also secreted significant more amount of VEGF-A than their homologous HPSSs cultured using the SUB approach (*p-value<0.01*) (**Fig. 20G**).

Finally, analysis of CCL5 (**Fig. 20J**, **20K** and **20L**), a proinflammatory cytokine, revealed that although significant differences, release of this protein was higher for all biomaterials when ALI culture was applied in Trilayer and Bilayer HPSSs (**Fig. 20J** and **20K**). On the other hand, for Monolayer HPSSs, secretion of CCL5 decreased in all biomaterials when ALI was applied (**Fig. 20L**).

2.1.4. SECTION SUMMARY

On balance, the results of this section revealed that no significant differences were reported regarding the secondary biomaterials used for HPSS manufacture. This could mean that most of the *in vitro* biological properties associated to the biomaterial's composition are due to the human plasma used during the production process. For this reason, rest of the comparisons analyzed in this chapter are evaluated regardless of secondary biomaterial used.

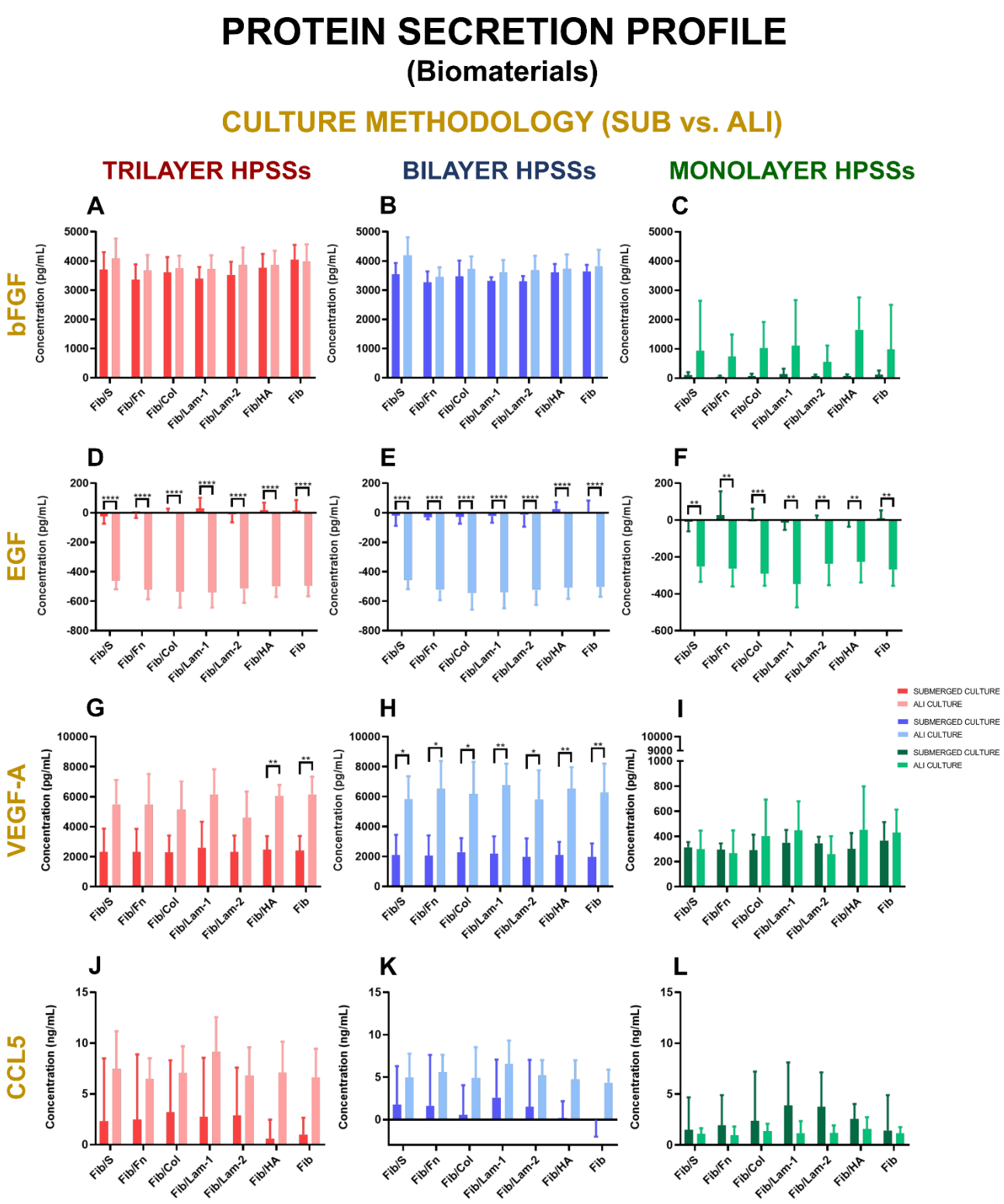

Fig. 20. ***Protein secretion profile of human plasma-based skin substitutes (HPSSs) manufactured with several secondary biomaterials. bFGF secretion:*** *A Trilayer HPSSs cultured under submerged and air/liquid interface methodologies; B Bilayer HPSSs cultured under submerged and air/liquid interface methodologies; C Monolayer HPSSs cultured under submerged and air/liquid interface methodologies.* ***EGF secretion:*** *D Trilayer HPSSs cultured under submerged and air/liquid interface methodologies; E Bilayer HPSSs cultured under submerged and air/liquid interface methodologies; F Monolayer HPSSs cultured under submerged and air/liquid interface methodologies.* ***VEGF-A secretion:*** *G Trilayer HPSSs cultured under submerged and air/liquid interface methodologies; H Bilayer HPSSs cultured under submerged and air/liquid interface methodologies; I Monolayer HPSSs cultured under submerged and air/liquid interface methodologies.* ***CCL5 secretion:*** *J Trilayer HPSSs cultured under submerged and air/liquid interface methodologies; K Bilayer HPSSs cultured under submerged and air/liquid interface methodologies; L Monolayer HPSSs cultured under submerged and air/liquid interface methodologies. Statistical significance: *p-value<0.05, **p-value<0.01, ***p-value<0.001, ****p-value<0.0001; for comparison between biomaterials for each condition: One-way ANOVA and Tukey's multiple comparisons tests (if normal distribution) or Friedman and Dunn's multiple comparisons tests (if no normal distribution); for comparison between conditions for each biomaterial: Multiple t-test and Holm-Sidak's method. Data is shown as mean value ± SD; N=5 for submerged (n=5) and air/liquid interface (n=5) conditions. Fib/S: Fibrin/Serine; Fib/Fn: Fibrin/Fibronectin; Fib/Col: Fibrin/Collagen; Fib/Lam-1: Fibrin/Laminin-1; Fib/Lam-2: Fibrin/Laminin-2; Fib/HA: Fibrin/Hyaluronic Acid; Fib: Fibrin. SUB: submerged; ALI: air/liquid interface.*

2.2. EFFECT OF PARTIAL DEHYDRATION PROCESS ON CELL VIABILITY

The effect of partial dehydration process applied after culturing the HPSSs was evaluated on cell viability. To that purpose, HPSSs manufactured with seven different skin cell populations (N=7) and cultured under submerged methodology were studied and compared before (**HYD**) and after (**DEHYD**) dehydration process was applied (**Fig. 21**).

The direct comparison of the different cellular HPSSs manufactured, revealed that partial dehydration process reduced cell viability in Trilayer, Bilayer and Monolayer HPSSs (**Fig. 21A**, **21B** and **21C**, respectively). This decrease was statistically significant in Trilayer and Bilayer HPSSs (*p-value<0.05*) (**Fig. 21A** and **21B**), while a slight reduction was reported in Monolayer HPSSs (from 66.7±5.9% to 60.3±8.3%) (**Fig. 21C**) but without a significant difference.

Moreover, an overall analysis and comparison of the different cellular HPSSs for each level of hydration revealed that viability was significantly greater for Trilayer and Bilayer substitutes compared with Monolayer HPSSs, in both conditions (**Fig. 21D**). These differences were higher in hydrated status (*p-value<0.0001* and *p-value<0.001* for Trilayer and Bilayer groups, respectively) than in dehydrated condition (*p-value<0.05* for both Trilayer and Bilayer HPSSs). Representative microscope pictures of LIVE/DEAD™ Viability/Cytotoxicity assay are included in **Fig. 21E**.

2.2.1. SECTION SUMMARY

On balance, the effect of the partial dehydration process applied after submerged culturing process decreased cell viability, mainly in Trilayer and Bilayer substitutes. On the other hand, this methodology did not affect as much to the Monolayer HPSSs, however, their viability was statistically lower than the others cellular groups and this was maintained, although to a lesser extent, when they were dehydrated.

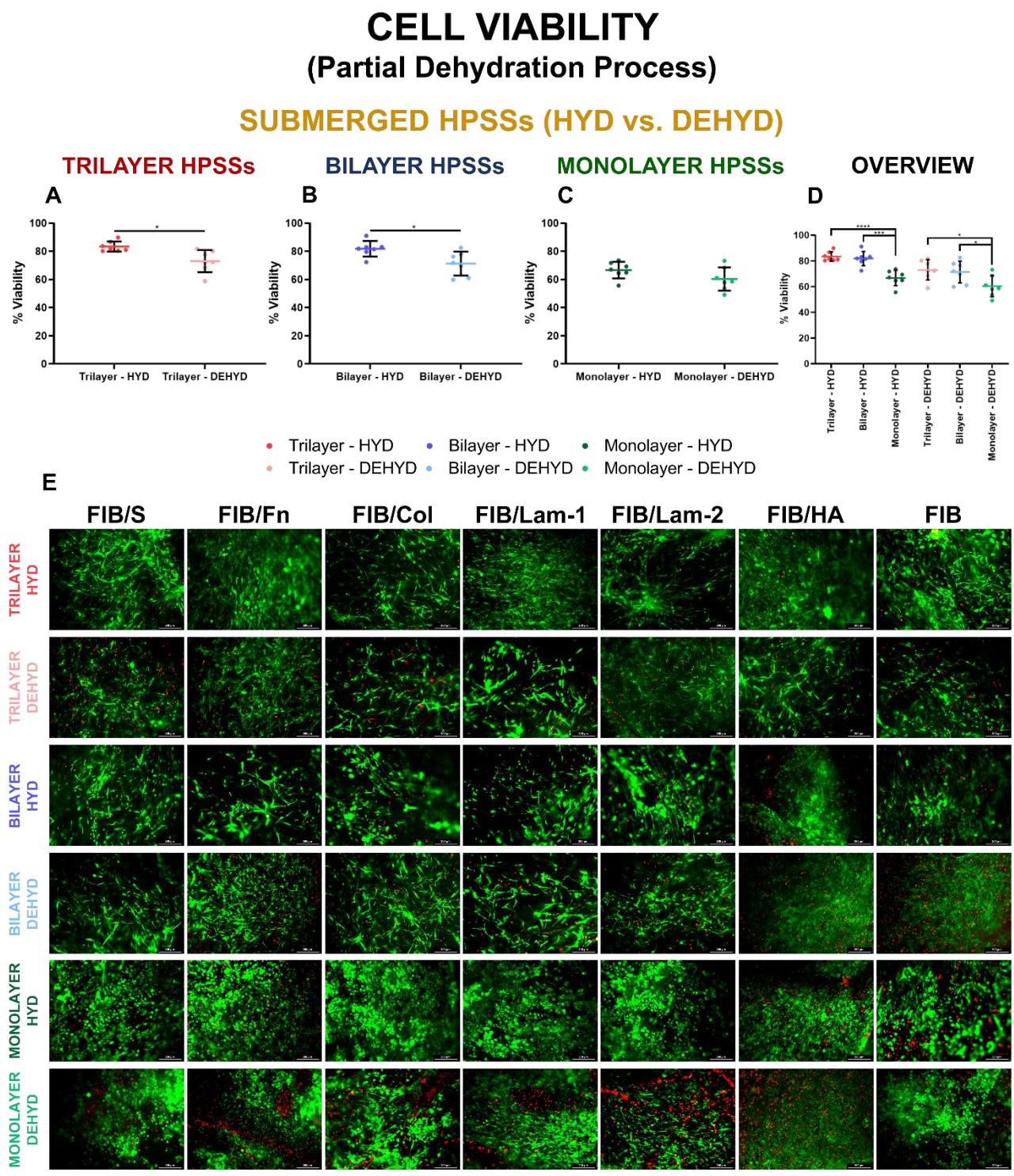

Fig. 21. ***Cell viability analysis of human plasma-based skin substitutes (HPSSs) before and after partial dehydration process.*** *A Cell viability of Trilayer HPSSs; B Cell viability of Bilayer HPSSs; C Cell viability of Monolayer HPSSs; D Overall analysis of the different cellular HPSSs and their hydration status; E Representative microscope pictures of LIVE/DEAD™ Viability/Cytotoxicity assay. Scale bar: 200 µm. Statistical significance: *p-value<0.05, ***p-value<0.001, ****p-value<0.0001, Welch's t-test. Data is shown as mean value ± SD; N=7 for hydrated (n=49) and dehydrated (n=49) conditions. HYD: hydrated; DEHYD: dehydrated. Fib/S: Fibrin/Serine; Fib/Fn: Fibrin/Fibronectin; Fib/Col: Fibrin/Collagen; Fib/Lam-1: Fibrin/Laminin-1; Fib/Lam-2: Fibrin/Laminin-2; Fib/HA: Fibrin/Hyaluronic Acid; Fib: Fibrin.*

2.3. ANALYSIS OF SKIN CELL TISSUE SOURCES USED FOR HPSS MANUFACTURE

Two human skin cell tissue sources were used for isolation and culture of keratinocytes and fibroblasts required for HPSS manufacture. These substitutes were cultured following the submerged methodology and compared regardless of the biomaterial used. The skin cells were procured from abdominal skin (**ABDO**; N=3) and foreskin (**FORE**; N=4) and an individual comparison according to their cell layer composition was provided for each condition evaluated. Moreover, an overview and analysis of the behavior of the different cellular HPSSs, depending on the skin cell tissue source, was also provided.

2.3.1. CELL VIABILITY

Cell viability was evaluated before (**Fig. 22**) and after (**Fig. 23**) dehydration process was applied.

2.3.1.1. Hydrated HPSSs

Cell viability of hydrated HPSSs manufactured using abdominal skin or foreskin cells was similar in all cases and no significant differences were observed between Trilayer (**Fig. 22A**), Bilayer (**Fig. 22B**) or Monolayer (**Fig. 22C**) HPSSs. However, viability seemed to be slightly higher in those substitutes composed of abdominal skin cells compared to foreskin cells [86.1±4.2% vs. 81.1±1.6% for Trilayer groups (**Fig. 22A**), 85.8±4.2% vs. 78.9±4.4% for Bilayer groups (**Fig. 22B**) and 67.8±3.7% vs. 65.9±7.7% for Monolayer groups (**Fig. 22C**)].

In addition, an overview of the different groups for each type of skin cell tissue source revealed that viability of Trilayer and Bilayer HPSSs was similar but significantly higher than in Monolayer HPSSs (*p-value<0.01* for ABDO and *p-value<0.05* for FORE) (**Fig. 22D**). Representative microscope pictures of LIVE/DEAD™ Viability/Cytotoxicity assay are included in **Fig. 22E**.

2.3.1.2. Dehydrated HPSSs

As in the case of hydrated HPSSs, no significant differences were reported between Trilayer (**Fig. 23A**), Bilayer (**Fig. 23B**) or Monolayer (**Fig. 23C**) HPSSs manufactured with abdominal skin or foreskin cells. Interestingly, unlike in the case of hydrated HPSSs, cell viability values were more similar and even slightly higher in those substitutes constituted of foreskin cells [74.1±6.8% (ABDO) vs. 72.3±9.6% (FORE) for Trilayer groups (**Fig. 23A**), 70.7±11.3% (ABDO) vs. 71.8±7.6% (FORE) for Bilayer groups (**Fig. 23B**) and 54.7±6.1% (ABDO) vs. 64.6±7.5% (FORE) for Monolayer groups (**Fig. 23C**)].

Moreover, an overall comparison of the different groups for each type of skin cell tissue source revealed that although viability was higher for Trilayer and Bilayer HPSSs, only a significant difference was reported when Trilayer and Monolayer HPSSs from ABDO group were analyzed (*p-value<0.05*) (**Fig. 23D**). Representative microscope pictures of LIVE/DEAD™ Viability/Cytotoxicity assay are included in **Fig. 23E**.

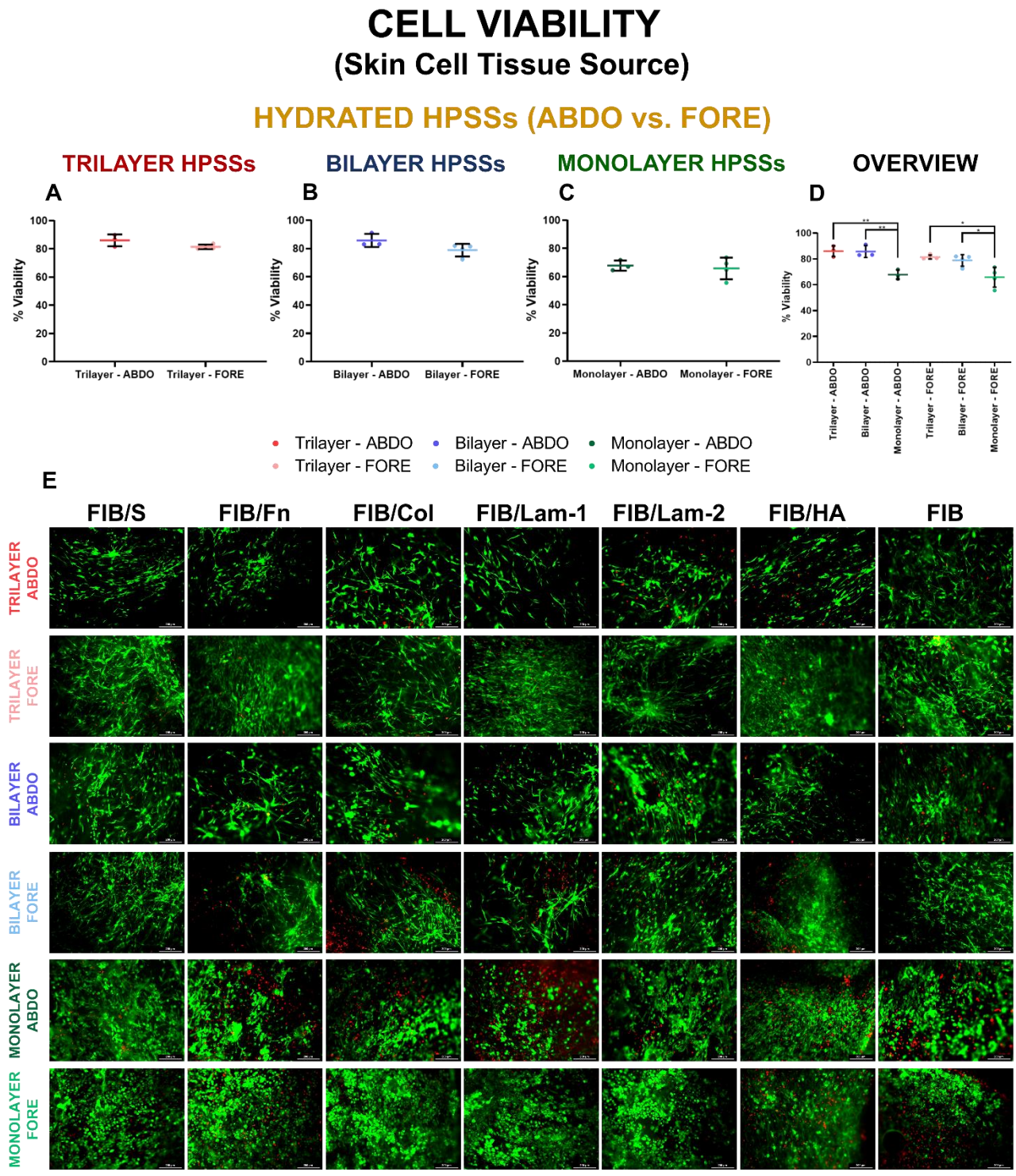

Fig. 22. ***Cell viability analysis of human plasma-based skin substitutes (HPSSs) manufactured with several skin cell tissue sources before partial dehydration process.*** *A Cell viability of Trilayer HPSSs; B Cell viability of Bilayer HPSSs; C Cell viability of Monolayer HPSSs; D Overall analysis of the different cellular HPSSs and their skin cell tissue source; E Representative microscope pictures of LIVE/DEAD™ Viability/Cytotoxicity assay. Scale bar: 200 µm. Statistical significance: *p-value<0.05, **p-value<0.01, Welch's t-test. Data is shown as mean value ± SD; N=3 for abdominal skin source (n=21) and N=4 for foreskin source (n=28). ABDO: abdominal skin source; FORE: foreskin source. Fib/S: Fibrin/Serine; Fib/Fn: Fibrin/Fibronectin; Fib/Col: Fibrin/Collagen; Fib/Lam-1: Fibrin/Laminin-1; Fib/Lam-2: Fibrin/Laminin-2; Fib/HA: Fibrin/Hyaluronic Acid; Fib: Fibrin.*

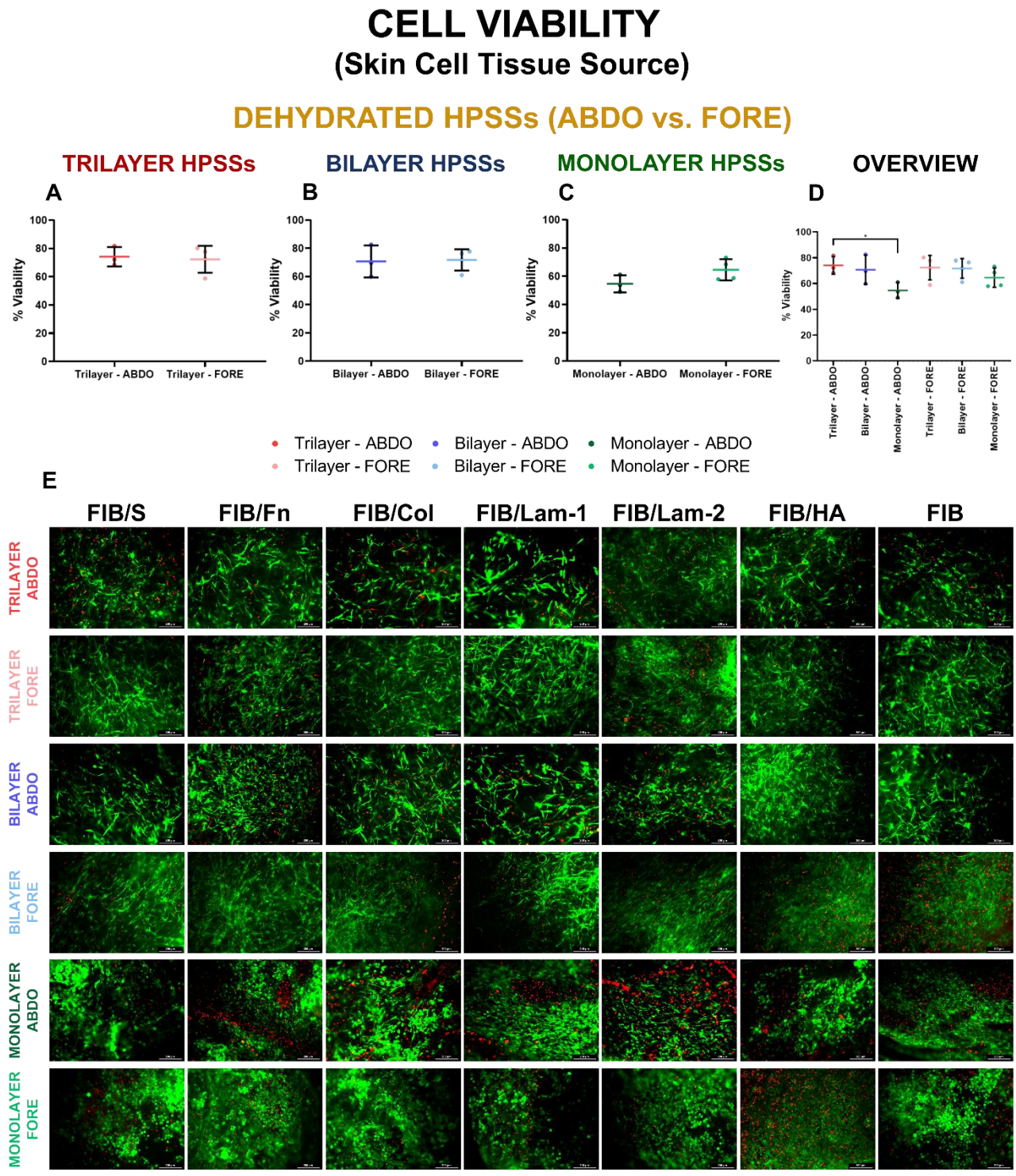

Fig. 23. ***Cell viability analysis of human plasma-based skin substitutes (HPSSs) manufactured with several skin cell tissue sources after partial dehydration process.*** *A Cell viability of Trilayer HPSSs; B Cell viability of Bilayer HPSSs; C Cell viability of Monolayer HPSSs; D Overall analysis of the different cellular HPSSs and their skin cell tissue source; E Representative microscope pictures of LIVE/DEAD™ Viability/Cytotoxicity assay. Scale bar: 200 µm. Statistical significance: *p-value<0.05, Welch's t-test. Data is shown as mean value ± SD; N=3 for abdominal skin source (n=21) and N=4 for foreskin source (n=28). ABDO: abdominal skin source; FORE: foreskin source. Fib/S: Fibrin/Serine; Fib/Fn: Fibrin/Fibronectin; Fib/Col: Fibrin/Collagen; Fib/Lam-1: Fibrin/Laminin-1; Fib/Lam-2: Fibrin/Laminin-2; Fib/HA: Fibrin/Hyaluronic Acid; Fib: Fibrin.*

2.3.2. CELL METABOLIC ACTIVITY

In the case of cell metabolic activity (**Fig. 24**), no significant differences were observed regarding cell tissue source between Trilayer (**Fig. 24A**), Bilayer (**Fig. 24B**) or Monolayer (**Fig. 24C**) substitutes. However, slightly higher values of the percentage of resazurin reduction were reported when foreskin cells were used in all cases; 50.0±3.0% (ABDO) vs. 55.7±5.6% (FORE) for Trilayer HPSSs (**Fig. 24A**), 46.3±4.6% (ABDO) vs. 51.3±8.2% (FORE) for Bilayer HPSSs (**Fig. 24B**) and 33.9±3.0% (ABDO) vs. 35.5±13.9% (FORE) for Monolayer HPSSs (**Fig. 24C**).

Overall analysis of the different tissue sources revealed that, as in the case of cell viability, Trilayer and Bilayer substitutes reported higher values for both abdominal and foreskin cells used. These results are consistent with the initial number of cells seeded on each type of hTESS. However, no significant differences were observed when foreskin cells were applied. On the other hand, when abdominal skin cells were used, significant differences were reported between Trialyer and Bilayer groups compared with Monolayer HPSSs (*p-value<0.01* and *p-value<0.05*, respectively) (**Fig. 24D**).

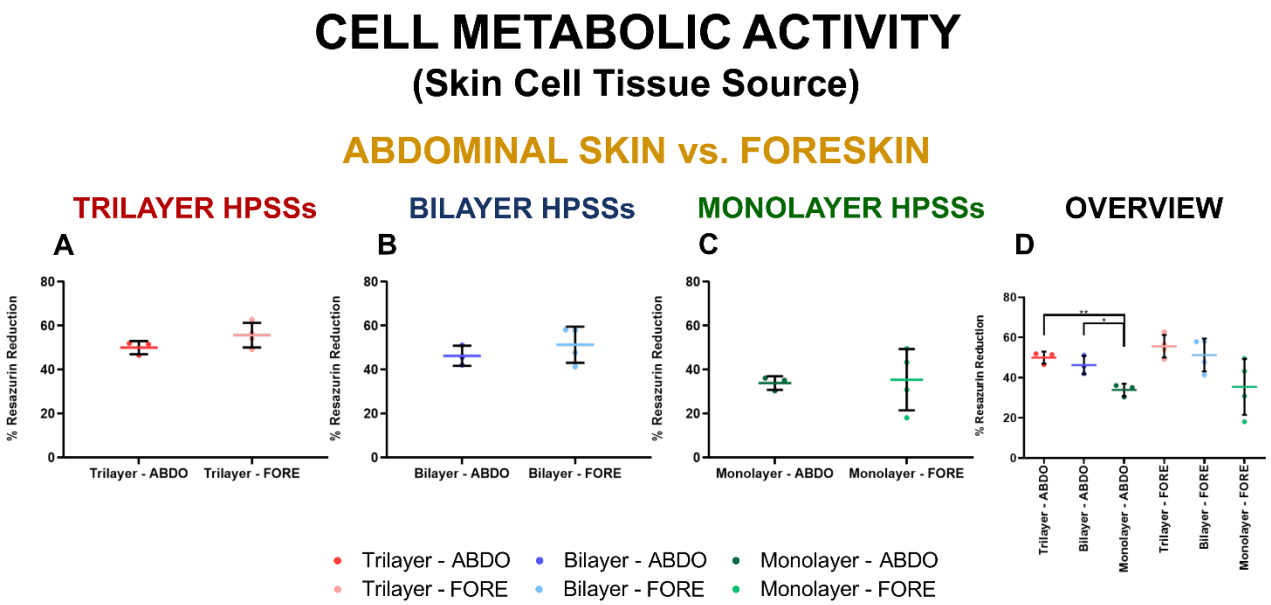

Fig. 24. ***Cell metabolic activity of human plasma-based skin substitutes (HPSSs) manufactured with several skin cell tissue sources.*** *A Cell metabolic activity of Trilayer HPSSs; B Cell metabolic activity of Bilayer HPSSs; C Cell metabolic activity of Monolayer HPSSs; D Overall analysis of the different cellular HPSSs and their skin cell tissue source. Statistical significance: *p-value<0.05, **p-value<0.01, Welch's t-test. Data is shown as mean value ± SD; N=3 for abdominal skin source (n=21) and N=4 for foreskin source (n=28). ABDO: abdominal skin source; FORE: foreskin source.*

2.3.3. PROTEIN SECRETION PROFILE ANALYSIS

Regarding the protein secretion profile (bFGF, EGF, VEGF-A and CCL5) when direct comparison of each type of skin cell tissue source was analyzed, no significant differences were reported for any of the cellular HPSSs studied (**Fig. 25**). Interestingly, the trend for each of the proteins analyzed differed depending on the tissue source used:

Those HPSSs constituted of foreskin cells secreted higher amount of bFGF and VEGF-A (**Fig. 25A**, **25B**, **25C**, **25I**, **25J** and **25K**). However, when EGF and CCL5 were studied, secretion was slightly higher when abdominal skin cells were applied (**Fig. 25E**, **25F**, **25G**, **25M**, **25N** and **25O**). Curiously, the concentration of these last proteins (after subtracting the Control HPSS values) was close to zero or negative when foreskin cells were used which could mean that these cells require to capture or use them for several purposes, in a greater degree than abdominal skin cells.

Finally, the overview of the different cellular HPSSs for each of the skin cell tissue source analyzed revealed that secretion of bFGF was significantly higher in Trilayer and Bilayer HPSSs compared with Monolayer group for both types of cells ($p\text{-}value<0.05$ in ABDO and $p\text{-}value<0.01$ in FORE) (**Fig. 25D**). In the case of VEGF-A the trend was the same, however only significant differences were reported when foreskin cells were applied ($p\text{-}value<0.05$) (**Fig. 25L**). For EGF and CCL5, no significant differences were observed between cellular groups neither abdominal nor foreskin cells were applied, but, interestingly, higher expression was reported in Monolayer HPSSs (**Fig. 25H** and **25P**).

2.3.4. HISTOLOGICAL APPEARANCE

Histological appearance of the several cellular HPSSs manufactured with each type of skin cell tissue source and secondary biomaterial revealed that no visual differences were reported (**Fig. 26**). A thin epidermis was observed in all cases, due probably to the submerged culture methodology applied. Moreover, a tendency to less thickness HPSSs was observed when fewer cellular layers were included (**Fig. 26**).

2.3.5. SECTION SUMMARY

On balance, although small differences were observed when abdominal skin or foreskin cells were used for HPSS manufacture, none of them were significant. This means that the use of one tissue or other another does not affect the biological properties of the human plasma-based skin substitute model studied.

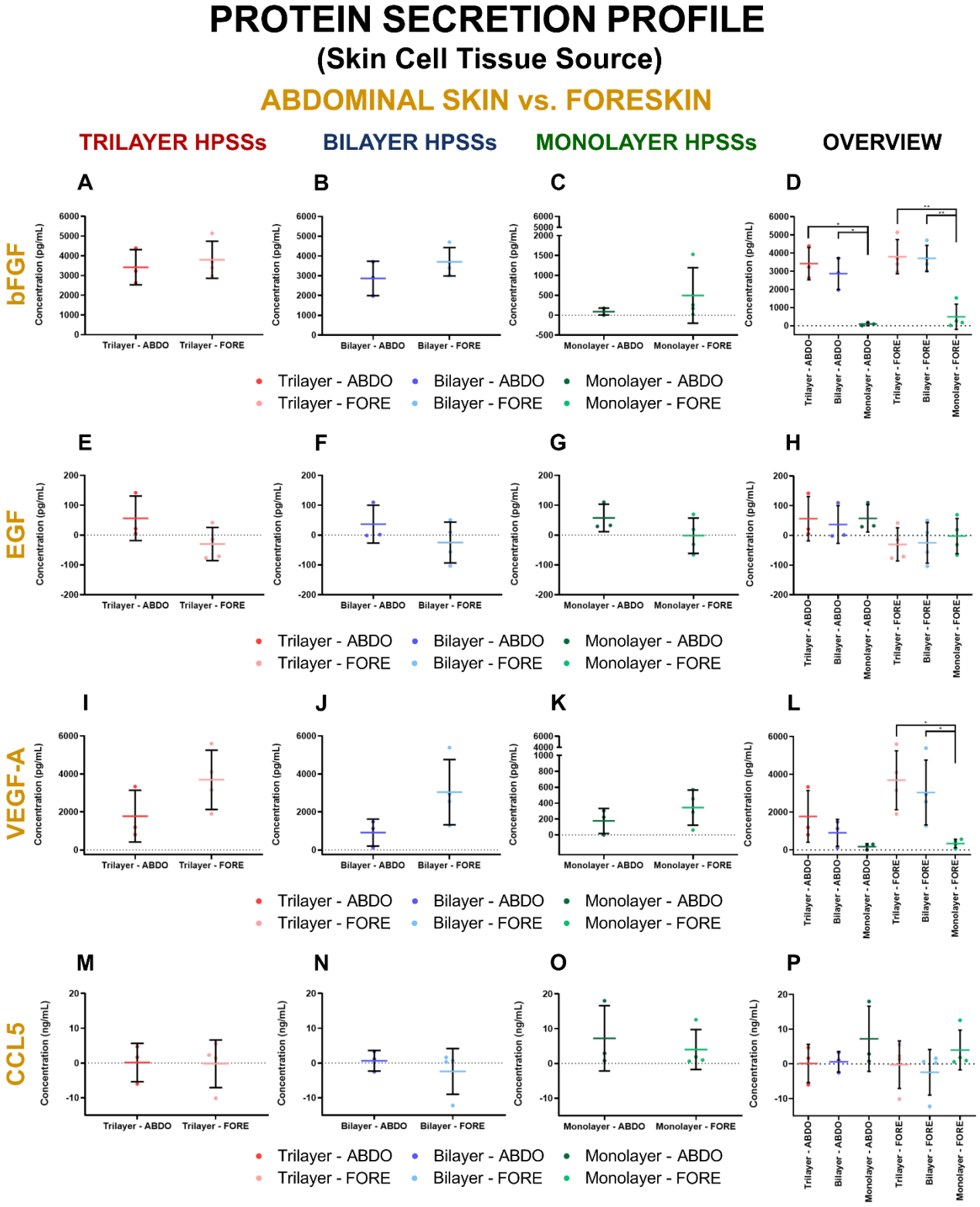

Fig. 25. ***Protein secretion profile of human plasma-based skin substitutes (HPSSs) manufactured with several skin cell tissue sources. bFGF secretion:*** *A Trilayer HPSSs; B Bilayer HPSSs; C Monolayer HPSSs; D Overall analysis of the different cellular HPSSs and their skin cell tissue source.* ***EGF secretion:*** *E Trilayer HPSSs; F Bilayer HPSSs; G Monolayer HPSSs; H Overall analysis of the different cellular HPSSs and their skin cell tissue source.* ***VEGF-A secretion:*** *I Trilayer HPSSs; J Bilayer HPSSs; K Monolayer HPSSs; L Overall analysis of the different cellular HPSSs and their skin cell tissue source.* ***CCL5 secretion:*** *M Trilayer HPSSs; N Bilayer HPSSs; O Monolayer HPSSs; P Overall analysis of the different cellular HPSSs and their skin cell tissue source. Statistical significance: *p-value<0.05, **p-value<0.01, Welch's t-test (if normal distribution) or Mann-Whitney test (if no normal distribution). Data is shown as mean value ± SD; N=3 for abdominal skin source (n=21) and N=4 for foreskin source (n=28).* ***ABDO****: abdominal skin source;* ***FORE****: foreskin source.*

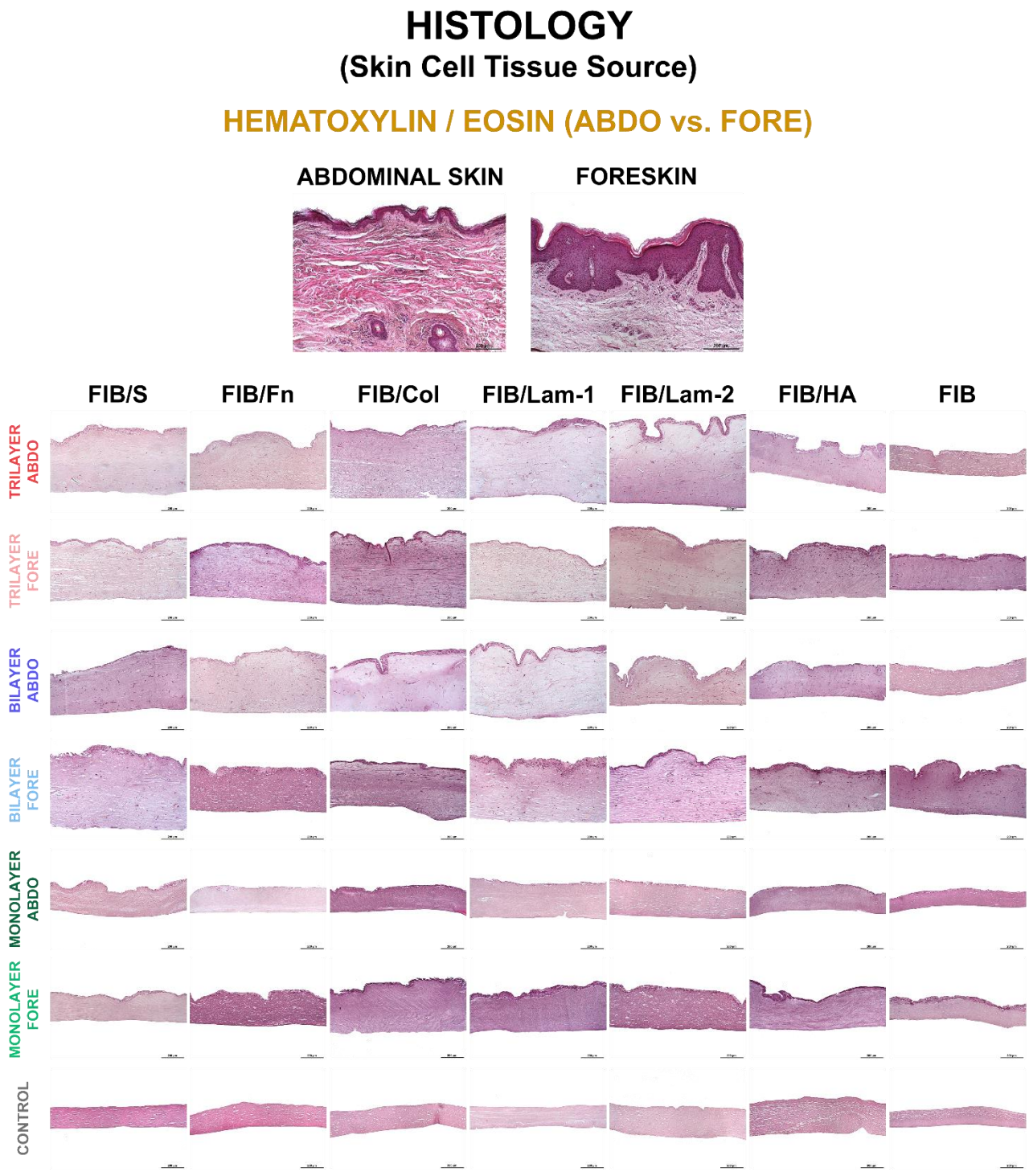

***Fig. 26*. Histological appearance (Hematoxylin / Eosin staining) of native human skin and human plasma-based skin substitutes (HPSSs) manufactured with several skin cell tissue sources.** ***ABDO**: abdominal skin source; **FORE**: foreskin source. **Fib/S**: Fibrin/Serine; **Fib/Fn**: Fibrin/Fibronectin; **Fib/Col**: Fibrin/Collagen; **Fib/Lam-1**: Fibrin/Laminin-1; **Fib/Lam-2**: Fibrin/Laminin-2; **Fib/HA**: Fibrin/Hyaluronic Acid; **Fib**: Fibrin. Scale bar: 200 µm.*

2.4. COMPARISON OF CULTURE METHODOLOGIES

Two culture methodologies used for manufacturing the cellular HPSSs were evaluated and compared. On the one hand, the submerged methodology, where keratinocyte medium fully covered the substitutes for 7-10 days to promote cell proliferation and growth. On the other hand, for air/liquid interface approach, after culturing the substitutes under submerged conditions, then keratinocyte medium exempt of human epidermal growth factor was removed from the epidermal layer for 10-13 days to induce the terminal differentiation. Seven different skin cell populations were cultured under submerged conditions (**SUB**; N=7) and five were evaluated by air/liquid interface methodology (**ALI**; N=5). In the case of the protein secretion profile analysis, culture medium was collected when HPSSs were changed from SUB to ALI culture, so number of biological samples was 5 for both methodologies in this study. Moreover, an overview and analysis of the behavior of the different cellular HPSSs, depending on the culture methodology, was also provided in this section.

2.4.1. CELL VIABILITY

Cell viability was evaluated after dehydration process of the HPSSs culture under submerged and air/liquid interface (**Fig. 27**). Comparison of both methodologies for each type of cellular HPSS revealed that cell viability of Trilayer (**Fig. 27A**) and Bilayer (**Fig. 27B**) was slightly higher when ALI culture was applied, although only a significant difference was observed in Trilayer group (*p-value<0.05*) (**Fig. 27A**). Interestingly, ALI culture decreased cell viability of Monolayer HPSSs but without statistical significance (from 60.3±8.3% to 54.7±6.8%) (**Fig. 27C**).

Moreover, the comparison of the different cellular HPSSs for each culture methodology revealed that viability was higher in Trilayer and Bilayer than in Monolayer HPSSs, although, this difference was higher in ALI culture (*p-value<0.001* for Trilayer group and *p-value<0.01* for Bilayer group vs. *p-value<0.05* for both types of substitutes in SUB) (**Fig. 27D**). In addition, a significant difference was also observed between Trilayer and Bilayer groups cultured and ALI conditions (*p-value<0.01*) (**Fig. 27D**). Representative microscope pictures of LIVE/DEAD™ Viability/Cytotoxicity assay are included in **Fig. 27E**.

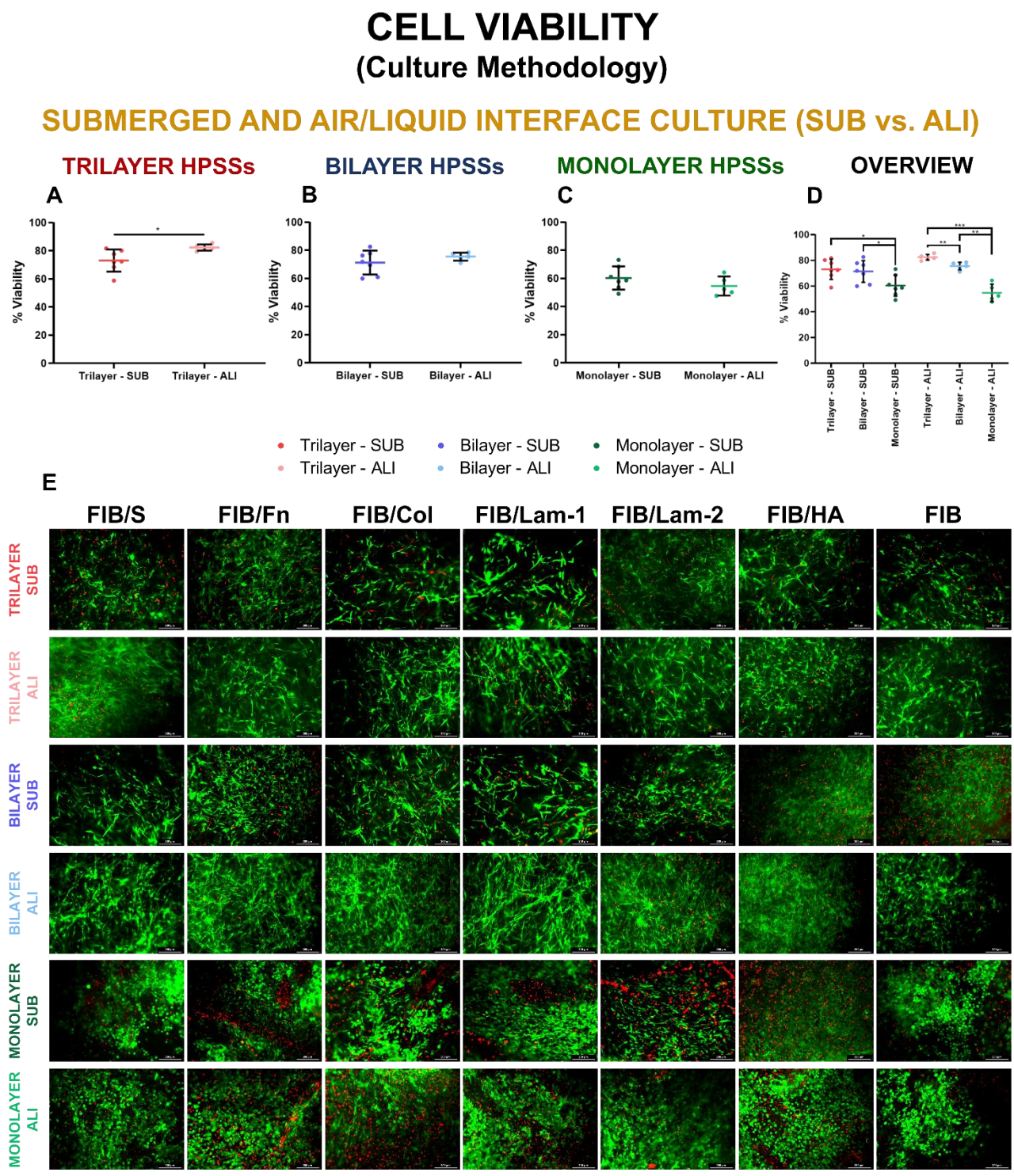

Fig. 27. ***Cell viability analysis of human plasma-based skin substitutes (HPSSs) cultured under submerged and air/liquid interface methodologies.*** *A Cell viability of Trilayer HPSSs; B Cell viability of Bilayer; C Cell viability of Monolayer HPSSs; D Overall analysis of the different cellular HPSSs and their culture methodology; E Representative microscope pictures of LIVE/DEAD™ Viability/Cytotoxicity assay. Scale bar: 200 µm. Statistical significance: *p-value<0.05, **p-value<0.01, ***p-value<0.001, Welch's t-test. Data is shown as mean value ± SD; N=7 for submerged condition (n=49) and N=5 for air/liquid interface condition (n=35). SUB: submerged culture; ALI: air/liquid interface culture. Fib/S: Fibrin/Serine; Fib/Fn: Fibrin/Fibronectin; Fib/Col: Fibrin/Collagen; Fib/Lam-1: Fibrin/Laminin-1; Fib/Lam-2: Fibrin/Laminin-2; Fib/HA: Fibrin/Hyaluronic Acid; Fib: Fibrin.*

2.4.2. CELL METABOLIC ACTIVITY

The comparison of both methodologies revealed that ALI culture decreased cell metabolic activity in all cellular groups [from 53.3±5.3% to 45.7±18.5% in Trilayer HPSSs (**Fig. 28A**), from 49.2±6.9% to 46.7±13.2% in Bilayer HPSSs (**Fig. 28B**), from 34.8±10.1% to 10.9±5.1% in Monolayer HPSSs (**Fig. 28C**)]. However, only significant differences were observed in Monolayer HPSSs (*p-value<0.001*) (**Fig. 28C**).

Analysis of the cellular HPSSs for each culture conditions indicated that viability of Trilayer and Bilayer HPSSs were similar between them for both, SUB and ALI methodologies (**Fig. 28D**). However, when these values were compared with Monolayer's viability, significant differences were observed (*p-value<0.05* and *p-value<0.01*) (**Fig. 28D**).

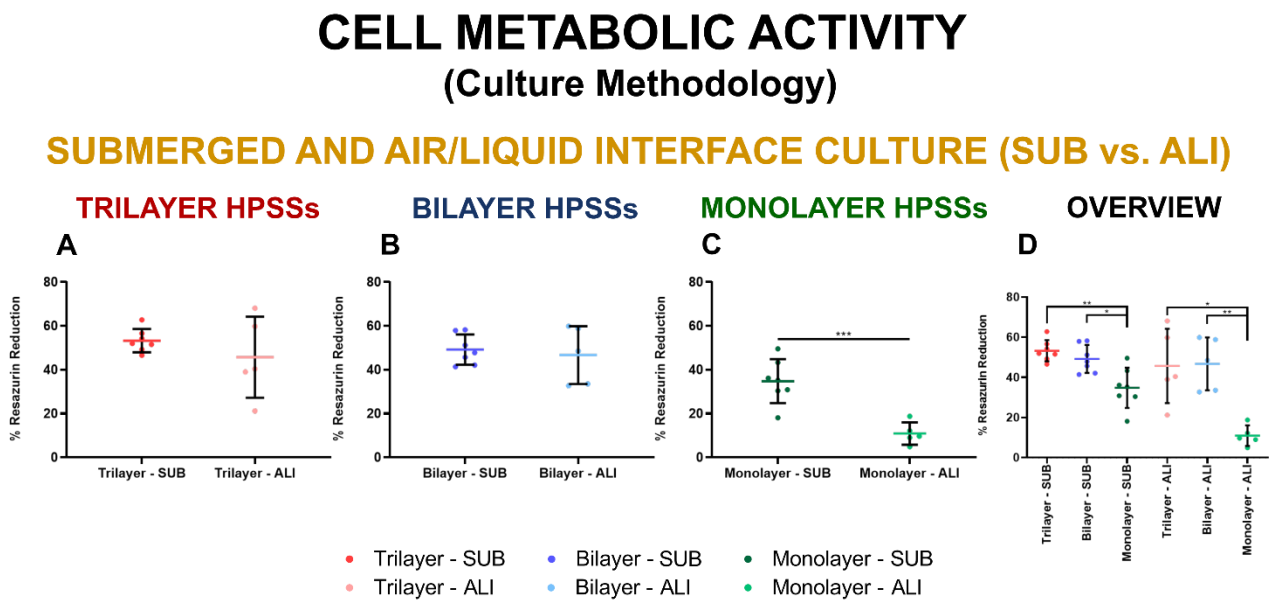

Fig. 28. ***Cell metabolic activity of human plasma-based skin substitutes (HPSSs) cultured under submerged and air/liquid interface methodologies.*** ***A*** *Cell metabolic activity of Trilayer HPSSs;* ***B*** *Cell metabolic activity of Bilayer;* ***C*** *Cell metabolic activity of Monolayer HPSSs;* ***D*** *Overall analysis of the different cellular HPSSs and their culture methodology. Statistical significance: *p-value<0.05, **p-value<0.01, ***p-value<0.001, Welch's t-test. Data is shown as mean value ± SD; N=7 for submerged condition (n=49) and N=5 for air/liquid interface condition (n=35).* ***SUB****: submerged culture;* ***ALI****: air/liquid interface culture.*

2.4.3. PROTEIN SECRETION PROFILE

The analysis of the protein secretion profile (bFGF, EGF, VEGF-A and CCL5) of both methodologies completes the analysis of the previous section where the different secondary biomaterials were individually studied for SUB and ALI cultures (**Fig. 20**). In this case, the condition of the secondary biomaterial was ignored and small differences were reported (**Fig. 29**).

The secretion of bFGF was higher when ALI methodology was applied in Trilayer (**Fig. 29A**), Bilayer (**Fig. 29B**) and Monolayer HPSSs (**Fig. 29C**). However, only significant differences were observed in Monolayer substitutes (*p-value<0.05*) (**Fig. 29C**). Moreover, comparison of the cellular HPSSs in each culture methodology revealed that Trilayer and Bilayer substitutes secreted significantly higher amount of bFGF than Monolayer groups (*p-value <0.0001*) (**Fig. 29D**).

In the case of EGF, values were close to zero for SUB condition and negative when ALI was applied for all groups (**Fig. 29E**, **29F** and **29G**). Significant differences were observed in all cases although the lower was reported in the case of Monolayer HPSSs (*p<0.001*) (**Fig. 29G**). An overview of the different groups for each culture methodology revealed that the values of the SUB culture were similar regardless of the cellular composition (**Fig. 29H**). On the other hand, in the case of ALI, negative values were reported in all groups although the highest value was observed in Monolayer group, reporting significant differences compared with both, Trilayer and Bilayer HPSSs (*p-value<0.001*) (**Fig. 29H**).

Regarding VEGF-A analysis, as in the case of bFGF, the secretion was higher when ALI methodology was applied and significant differences were reported in Trilayer (*p-value<0.01*) (**Fig. 29I**) and Bilayer (*p-value<0.01*) (**Fig. 29J**) HPSSs. Monolayer substitutes under ALI conditions also secreted higher amount of VEGF-A but without a statistically significant difference (**Fig. 29K**). Comparison of the cellular HPSSs, for each culture condition, revealed that Trilayer and Bilayer substitutes secreted similar amount of VEGF-A in both cases, and significantly higher than the secretion reported by Monolayer groups (*p-value<0.05* in SUB and *p-value<0.01* in ALI) (**Fig. 29L**).

Finally, secretion analysis of the cytokine CCL5 indicated the ALI culture increased the secretion of this protein, mainly in Trilayer (**Fig. 29M**) and Bilayer (**Fig. 29N**) groups, where significant differences were observed compared with SUB condition in both cases (*p-value<0.05*). Regarding the Monolayer groups, a slightly higher secretion of CCL5 was reported in SUB, although without a significant difference (**Fig. 29O**). The overview of the different cellular HPSSs for each culture methodology indicated that similar secretion was reported in the case of SUB groups (**Fig. 29P**). However, under ALI condition a significantly higher secretion was observed in Trilayer and Bilayer HPSSs compared with Monolayer substitutes (*p-value<0.01*) (**Fig. 29P**).

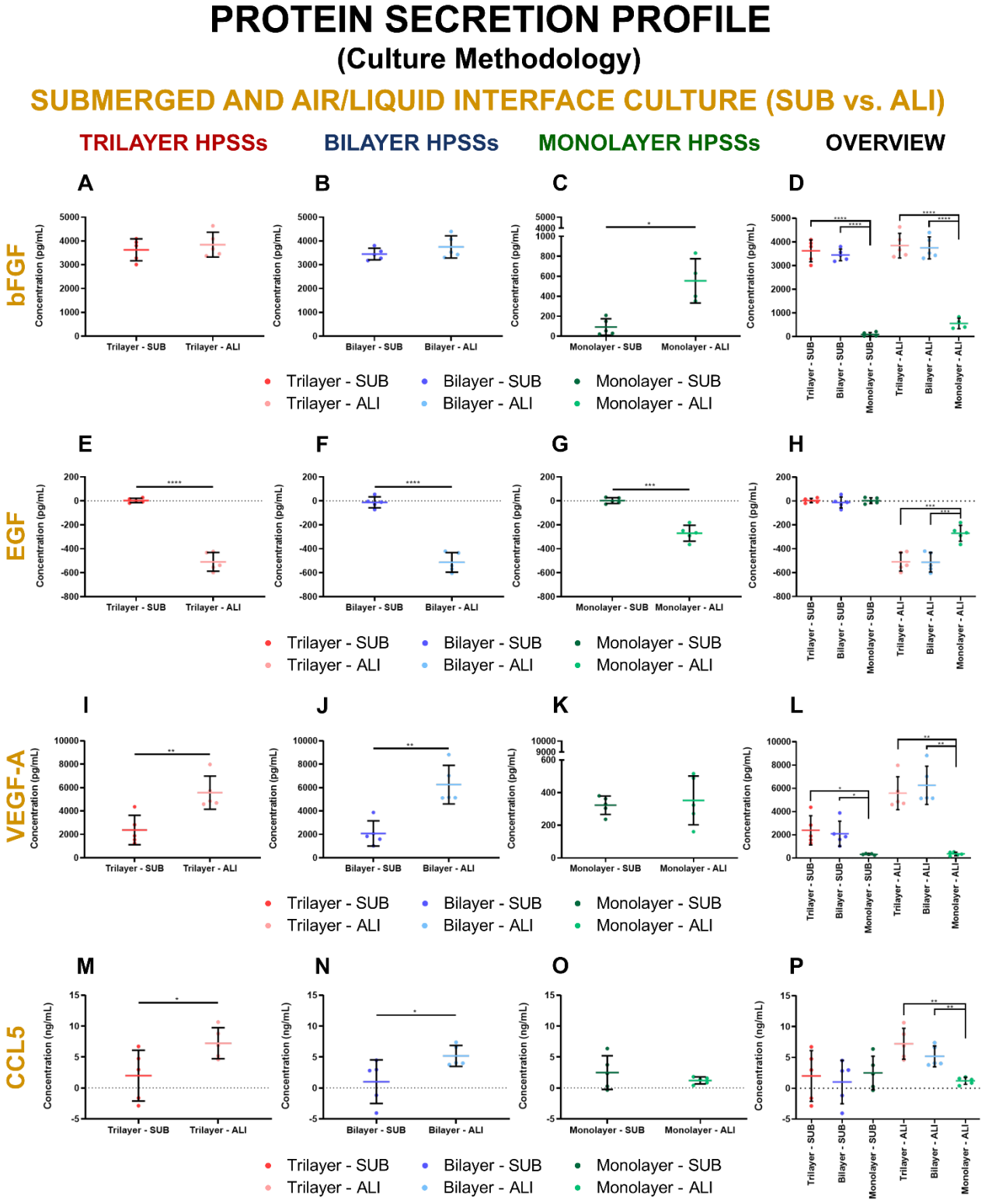

Fig. 29. ***Protein secretion profile of human plasma-based skin substitutes (HPSSs) cultured under submerged and air/liquid interface methodologies. bFGF secretion:*** *A Trilayer HPSSs; B Bilayer HPSSs; C Monolayer HPSSs; D Overall analysis of the different cellular HPSSs and culture methodology applied.* ***EGF secretion:*** *E Trilayer HPSSs; F Bilayer HPSSs; G Monolayer HPSSs; H Overall analysis of the different cellular HPSSs and culture methodology applied.* ***VEGF-A secretion:*** *I Trilayer HPSSs; J Bilayer HPSSs; K Monolayer HPSSs; L Overall analysis of the different cellular HPSSs and culture methodology applied.* ***CCL5 secretion:*** *M Trilayer HPSSs; N Bilayer HPSSs; O Monolayer HPSSs; P Overall analysis of the different cellular HPSSs and culture methodology applied. Statistical significance: *p-value<0.05, **p-value<0.01, ***p-value<0.001, ****p-value<0.0001, Welch's t-test. Data is shown as mean value ± SD; N=5 for submerged (n=35) and air/liquid interface (n=35) conditions. SUB: submerged culture; ALI: air/liquid interface culture.*

2.4.4. HISTOLOGICAL APPEARANCE

Histological appearance of the several cellular HPSSs manufactured under each type of culture methodology and secondary biomaterial revealed that a thicker epidermis was observed when ALI methodology was applied in all groups (Fig. 30).

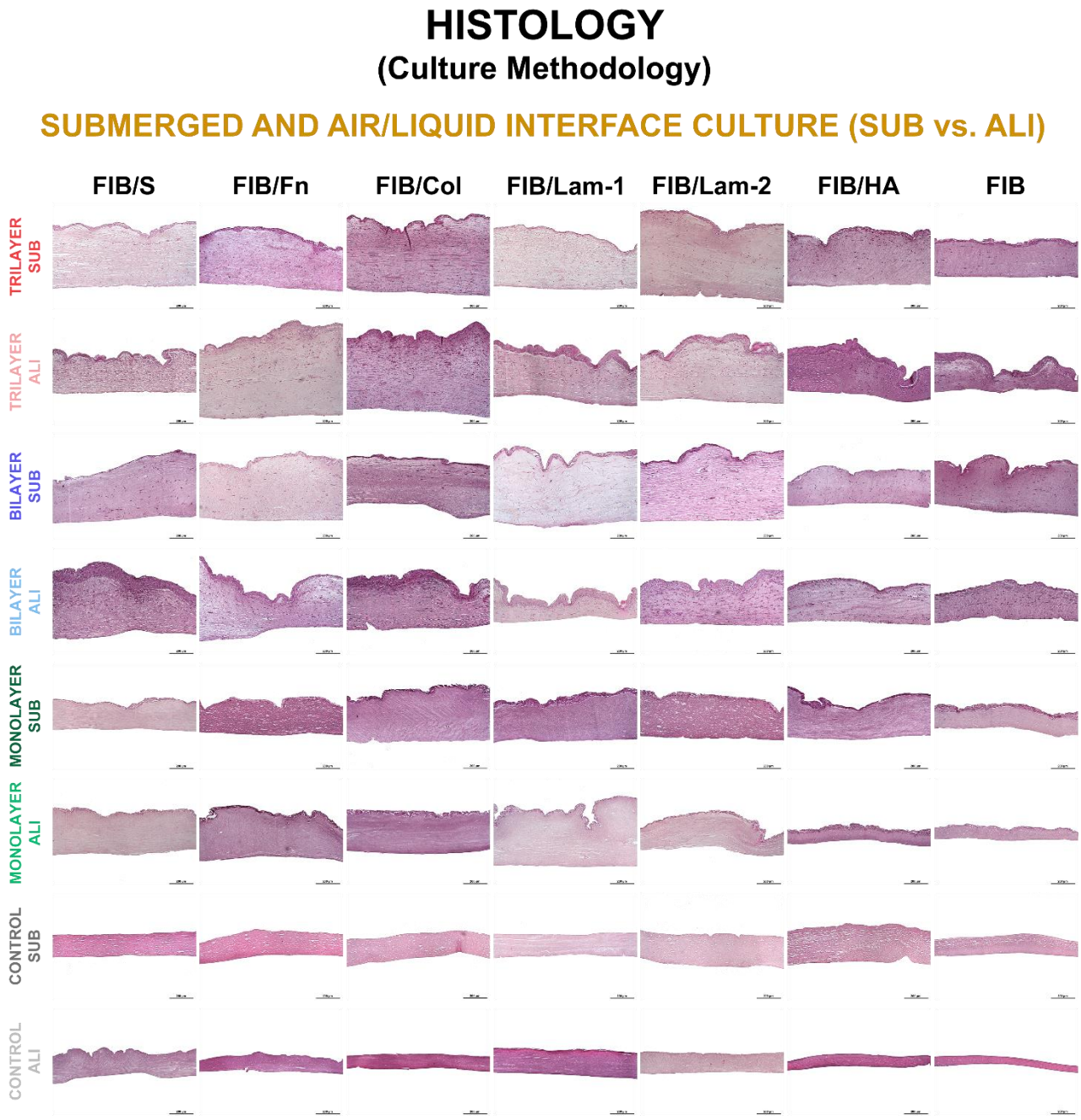

Fig. 30. ***Histological appearance (Hematoxylin / Eosin staining) of human plasma-based skin substitutes (HPSSs) cultured under submerged or air/liquid interface methodologies.*** ***SUB****: submerged culture;* ***ALI****: air/liquid interface culture.* ***Fib/S****: Fibrin/Serine;* ***Fib/Fn****: Fibrin/Fibronectin;* ***Fib/Col****: Fibrin/Collagen;* ***Fib/Lam-1****: Fibrin/Laminin-1;* ***Fib/Lam-2****: Fibrin/Laminin-2;* ***Fib/HA****: Fibrin/Hyaluronic Acid;* ***Fib****: Fibrin. Scale bar: 200 µm.*

2.4.5. SECTION SUMMARY

On balance, the application of ALI methodology demonstrated minor differences in terms of cell viability and metabolic activity compared to SUB condition. However, significant differences were reported with regard of the protein secretion profile and a thicker epidermis was observed when ALI was applied.

DOI: 10.1093/burnst/tkad043
Journal: Burns & Trauma
1st Decile: Surgery
(IF: 5.3 => JCR – 2022)

CHAPTER 3: COMPARISON OF TWO CLINICAL HUMAN BILAYER TISSUE-ENGINEERED SKIN SUBSTITUTES (hbTESSs)

3.1. HISTOLOGICAL APPEARANCE AND ADHESIVE STRENGTH OF THE DERMAL-EPIDERMAL JUNCTION OF hbTESSs

Human healthy skin has a complex structure and a large amount of collagen is found in the dermis (stained in blue by Masson's trichrome staining; **Fig. 31**).

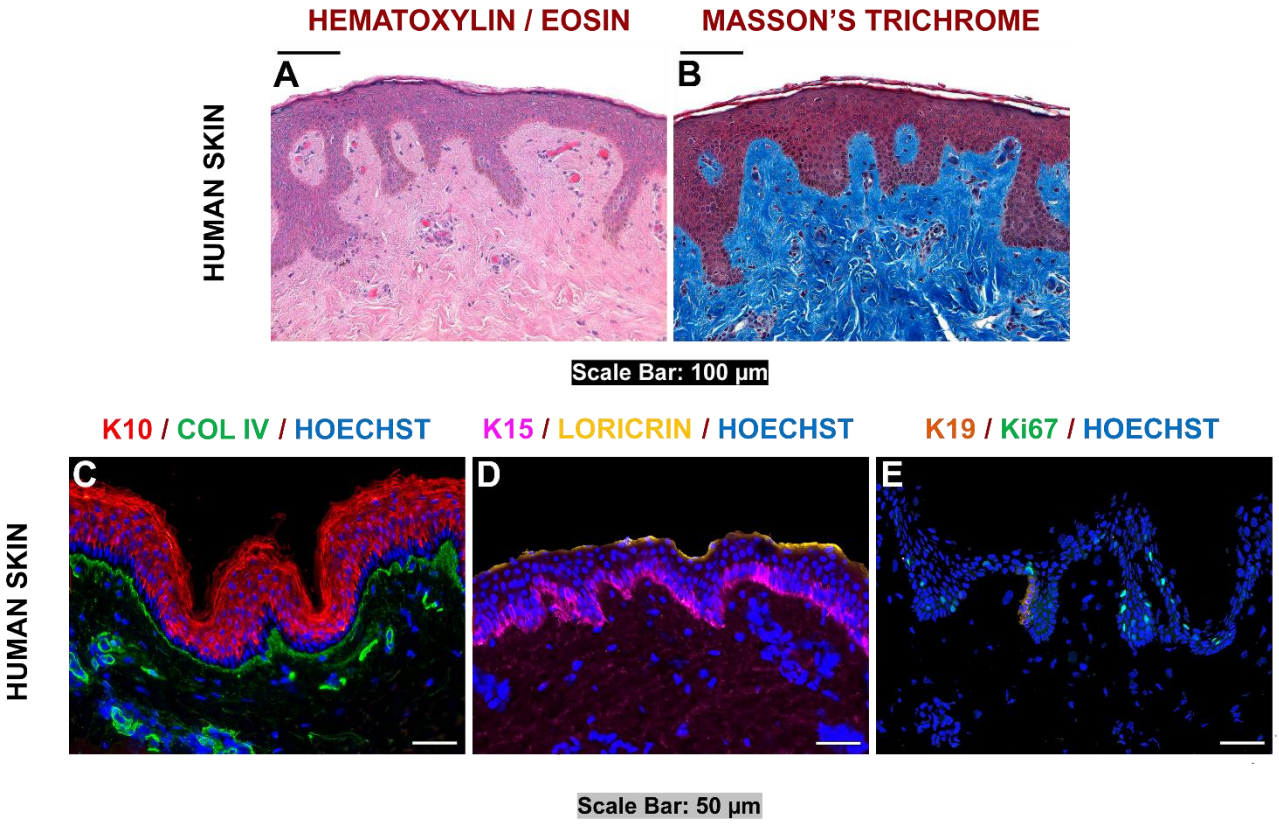

Fig. 31. ***Histological and immunofluorescence pictures of human healthy skin.*** *A Hematoxylin / Eosin staining; B Masson's Trichrome staining. Scale bar: 100 µm. C Keratin 10 (K10-red)/Type IV collagen (COL IV-green)/Hoechst nucleus (blue) staining; D Keratin 15 (K15-purple)/Loricrin (yellow)/Hoechst nucleus (blue) staining; E Keratin 19 (K19-orange)/Ki67 (green)/Hoechst nucleus (blue) staining. Scale bar: 50 µm.*

Regarding skin substitutes, despite differing manufacturing times (46-55 days for SASSs and 32-39 days for HPSSs (**Fig. 10**)), all hbTESSs developed a differentiated epidermis with a granular layer and a cornified envelop as shown by histology (**Fig. 32**). However, HPSSs exhibited more accumulation of stratum corneum (**Fig. 32D - 32L**) and were slightly thicker than SASSs (**Fig. 32M**). Moreover, Masson's trichrome staining (**Fig. 32B, 32E, 32H** and **32K**) indicated that collagen was more homogeneously distributed through the dermal layer in SASSs (**Fig. 32B**) compared with HPSSs. The staining of the ECM under the basement membrane was more blue in the SASSs, while it appeared purplish in the rest of the dermal layers (**Fig. 32E, 32H** and **32K**).

Therefore, histological observation of skin substitute models showed a proper bilayered structure without detachment or separation between dermis and epidermis (**Fig. 32**; Hematoxylin / Eosin and Masson's Trichrome staining). To characterize the adhesive strength of the dermal-epidermal junction (DEJ), peel tests[349] were performed. The adhesive strengths of the DEJ for the Fib, Fib/HA and Fib/Col skin substitutes were similar, with a mean adhesive strength of 1.47±0.47 mN/mm, which was 1.93 times lower compared to SASSs with a mean adhesive strength of 2.84±2.48 mN/mm (**Fig. 32N**). Although experiments were repeated, data collected for SASSs were more variable depending on the cell donor used for manufacturing (**Fig. 33**). Histology was used after peel testing to confirm that the detachment occurred at the DEJ (**Fig. 32C, 32F, 32I** and **32L**) indicating that the peel test measured the force anchoring the epidermis to the dermis.

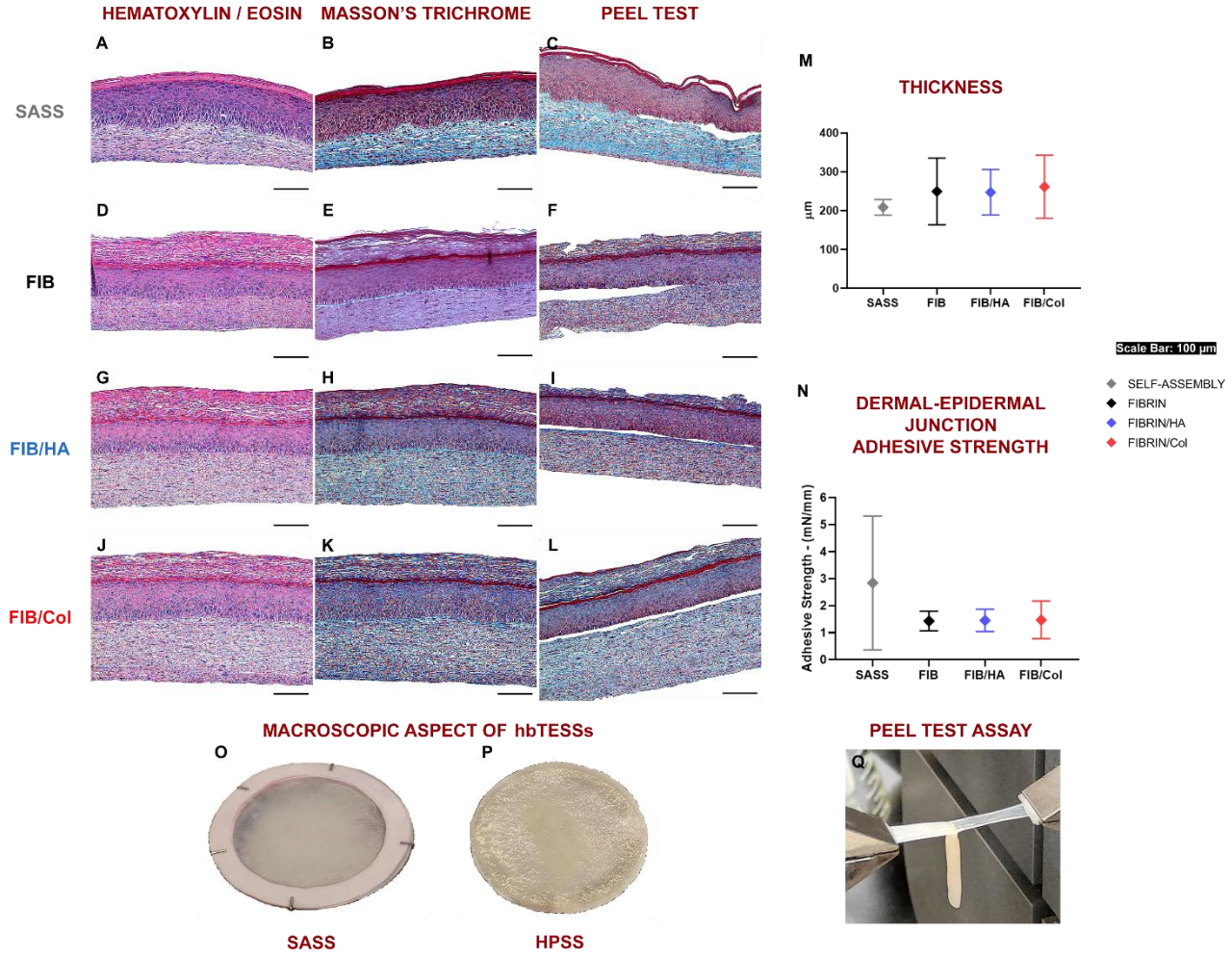

Fig. 32. ***Histological pictures, thickness measurement and dermal-epidermal junction adhesive strength of hbTESSs evaluated by the peel test.*** *From left to right in all groups: Hematoxylin / Eosin staining, Masson's Trichrome staining and confirmation that peeling occurred at the adequate localization, the dermal-epidermal junction. Self-assembled skin substitute (**SASS**): **A**, **B** and **C**; Human plasma-based (**Fib**) skin substitute: **D**, **E** and **F**; Human plasma-based and hyaluronic acid (**Fib/HA**) skin substitute: **G**, **H** and **I**; Human plasma-based and collagen (**Fib/Col**) skin substitute: **J**, **K** and **L**. **M** Measure of the hbTESS thickness using histological pictures (N=3; n = 12, 9, 9, 9 for each group, respectively). **N** Dermal-epidermal junction adhesive strength evaluation (N=3; n = 18, 10, 10, 9 for each group, respectively). Macroscopic aspect of **O** SASS and **P** human plasma-based skin substitute (HPSS). **Q** Representative picture of peel test assay. Scale bar: 100 µm. One-way ANOVA and Tukey's multiple comparisons tests. Data is shown as mean value ± SD.*

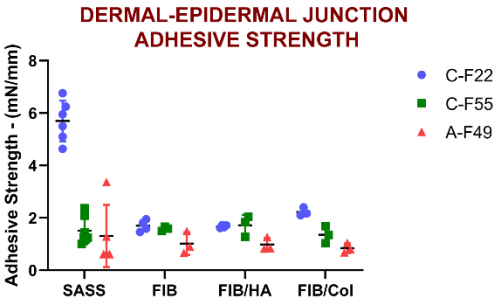

Fig. 33. ***Peel test results for each replica of hbTESS produced with the three human skin cell populations studied.*** *Variability between samples is observed. C: Chest; A: Abdomen; F: Female; 22, 55 and 49: Age.*

3.2. TENSILE STRENGTH AND ELASTICITY OF hbTESSs

Mechanical analysis was completed by the evaluation of tensile strength and elastic properties of hbTESSs (**Fig. 34**). SASSs presented higher ultimate tensile strength (UTS) values than HPSSs. Therefore, SASSs were more resistant to tensile forces (*p-value<0.01*). Surprisingly, considering the properties of native proteins used as biomaterials, Fib/Col was less resistant compared to SASSs (*p-value<0.001*) (**Fig. 34A**).

On the other hand, the elastic modulus indicated that no significant differences were observed between the three human plasma-based skin substitutes. However, SASSs were significantly stiffer than the other hbTESSs (*p-value<0.001*) (**Fig. 34B**).

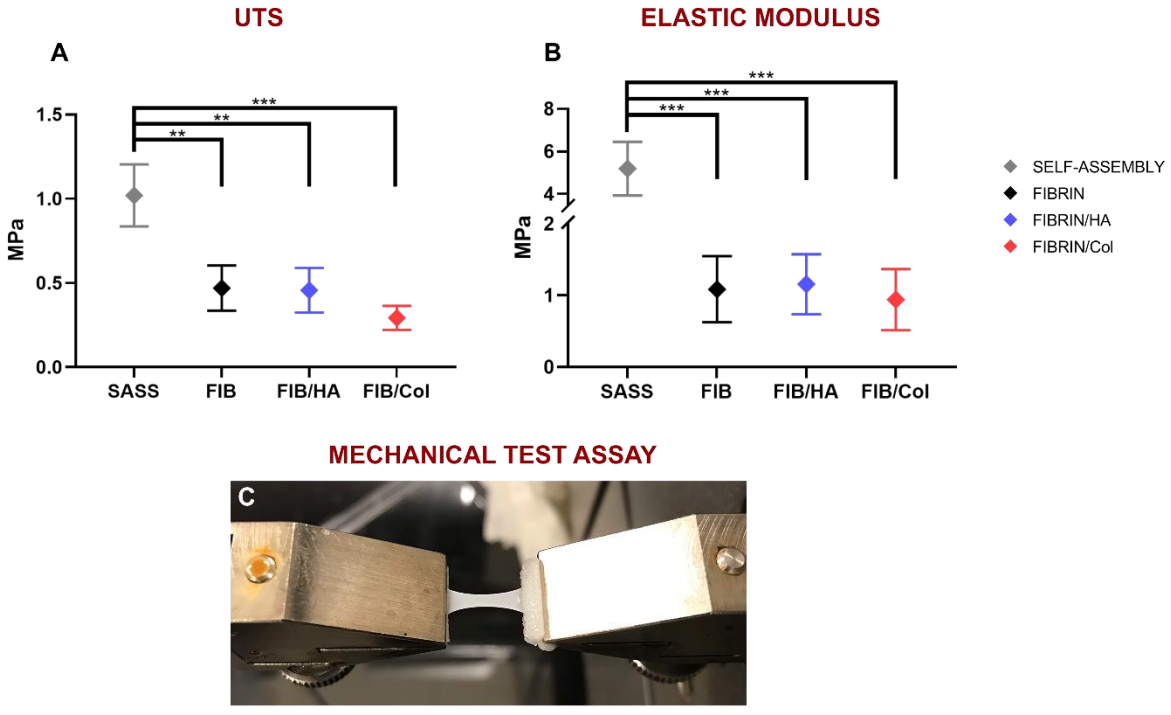

Fig. 34. ***Mechanical properties' analysis of the different hbTESSs*** *(self-assembled skin substitute (**SASS**), human plasma-based (**Fib**), human plasma-based and hyaluronic acid (**Fib/HA**) and human plasma-based and collagen (**Fib/Col**) skin substitutes). **A** Evaluation of ultimate tensile strength (UTS) (N=3; n = 12, 9, 9, 9 for each group, respectively); **B** Elastic modulus' results (N=3; n = 12, 9, 9, 9 for each group, respectively); **C** Representative picture of mechanical test assay. Statistical significance: **p-value<0.01; ***p-value<0.001, One-way ANOVA and Tukey's multiple comparisons tests. Data is shown as mean value ± SD.*

3.3. CELL METABOLIC ACTIVITY AND DNA QUANTIFICATION OF hbTESSs

At the end of the culture process, cell metabolic activity and amount of DNA per mg of sample were evaluated (**Fig. 35**). Considering the percentage of resazurin reduction, cell metabolic activity was slightly lower in SASSs although no significant differences were observed compared to HPSSs (**Fig. 35A**). In contrast, the amount of DNA per mg of sample was significantly higher in SASSs compared to HPSSs (*p-value<0.05*) (**Fig. 35B**), suggesting that the number of cells in human plasma-based skin substitutes was lower.

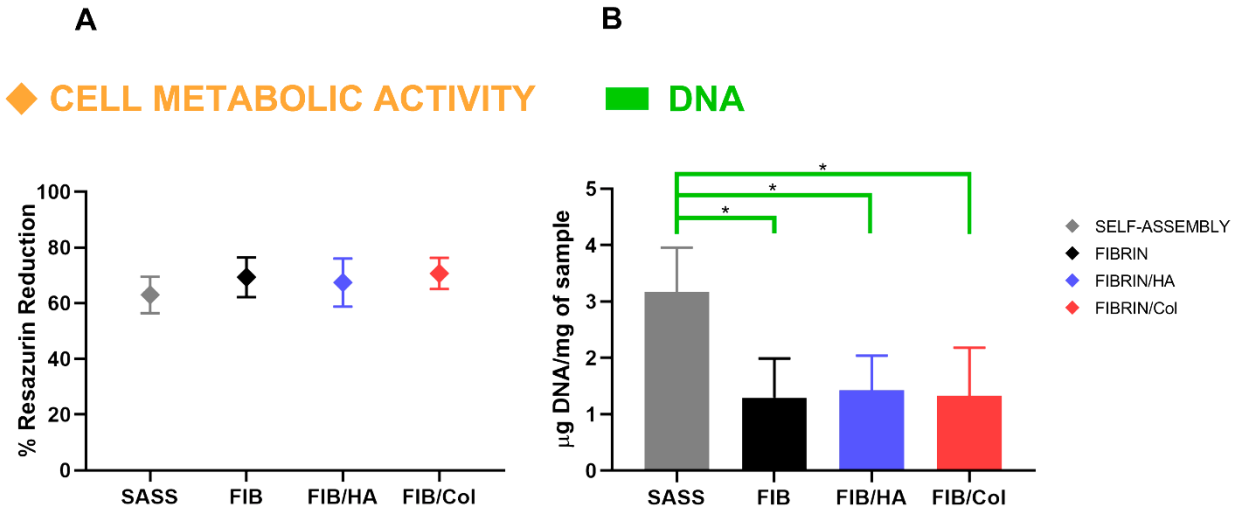

Fig. 35. ***Cell metabolic activity and amount of DNA in hbTESSs.*** ***A*** *Cell metabolic activity measured by Presto Blue™ assay and* ***B*** *DNA quantification by mg of tissue in self-assembled skin substitute (**SASS**), human plasma-based (**Fib**), human plasma-based and hyaluronic acid (**Fib/HA**) and human plasma-based and collagen (**Fib/Col**) skin substitutes (N=3; n = 18, 10, 10, 10 for each group, respectively). Statistical significance: *p-value<0.05, One-way ANOVA and Tukey's multiple comparisons tests. Data is shown as mean value ± SD.*

3.4. IMMUNOFLUORESCENCE ANALYSIS OF hbTESSs

To achieve the characterization of both hbTESS models, different skin associated markers were studied by double immunofluorescence labeling. For Keratin 19 (K19) and Ki67 markers, the percentage of positive basal epidermal cells by total number of epidermal cells was measured to provide quantitative results (**Fig. 36**).

3.4.1. KERATIN 10/TYPE IV COLLAGEN

K10 in healthy human skin is found across suprabasal layers (**Fig. 36**). Both hbTESS models expressed K10 through the keratinocytes of suprabasal epidermal layers (**Fig. 36A**, **36D**, **36G** and **36J**; **Red**). According to the histological results, HPSSs presented a less compact stratum corneum positive for K10 (**Fig. 36D**, **36G** and **36J**). Type IV collagen was expressed at the DEJ in all tested hbTESSs (**Fig. 36A**, **36D**, **36G** and **36J**; **Green**), like in native human skin control (**Fig. 31**), but a

diffuse expression was observed in the dermis of SASSs (**Fig. 36A**) whereas it was mainly located at the DEJ in HPSSs (**Fig. 36D**, **36G** and **36J**).

3.4.2. KERATIN 15/LORICRIN

K15 expression (**Fig. 36B**, **36E**, **36H** and **36K**; **Purple**) was not confined to the basal layer like in the native human skin (**Fig. 31**) but also to upper cell layers in all tested hbTESSs, and it was more pronounced in SASSs (**Fig. 36B**). Loricrin expression, like in the granular layer of the native human epidermis (**Fig. 31**), was similar between all tested hbTESS (**Fig. 36B**, **36E**, **36H** and **36K**; **Yellow**).

3.4.3. KERATIN 19/Ki67

K19 is a stem-cell-associated marker[13] and Ki67, a proliferative marker, present in a small proportion of epidermal cells (0.51±0.37% for K19 and 12.66±2.75% for Ki67) and expressed in cells of the basal layer that are in contact with the basement membrane (**Fig. 31**). $K19^+$ (**Orange**) and $Ki67^+$ (**Green**) cells were observed in the basal layer of epidermis of all tested hbTESSs (**Fig. 36C**, **36F**, **36I** and **36L**). Notably, a K19 non-specific staining was also visualized in the suprabasal layers but was not considered for analysis.

A tendency toward a slightly higher proportion of epidermal cells expressing K19 was observed in HPSSs compared to SASSs, although no significant differences were measured (**Fig. 36M**). In contrast, the percentage of epidermal cells expressing Ki67 was higher in SASSs, although a significant difference was only observed compared to Fib ($p\text{-value}<0.05$) (**Fig. 36N**).

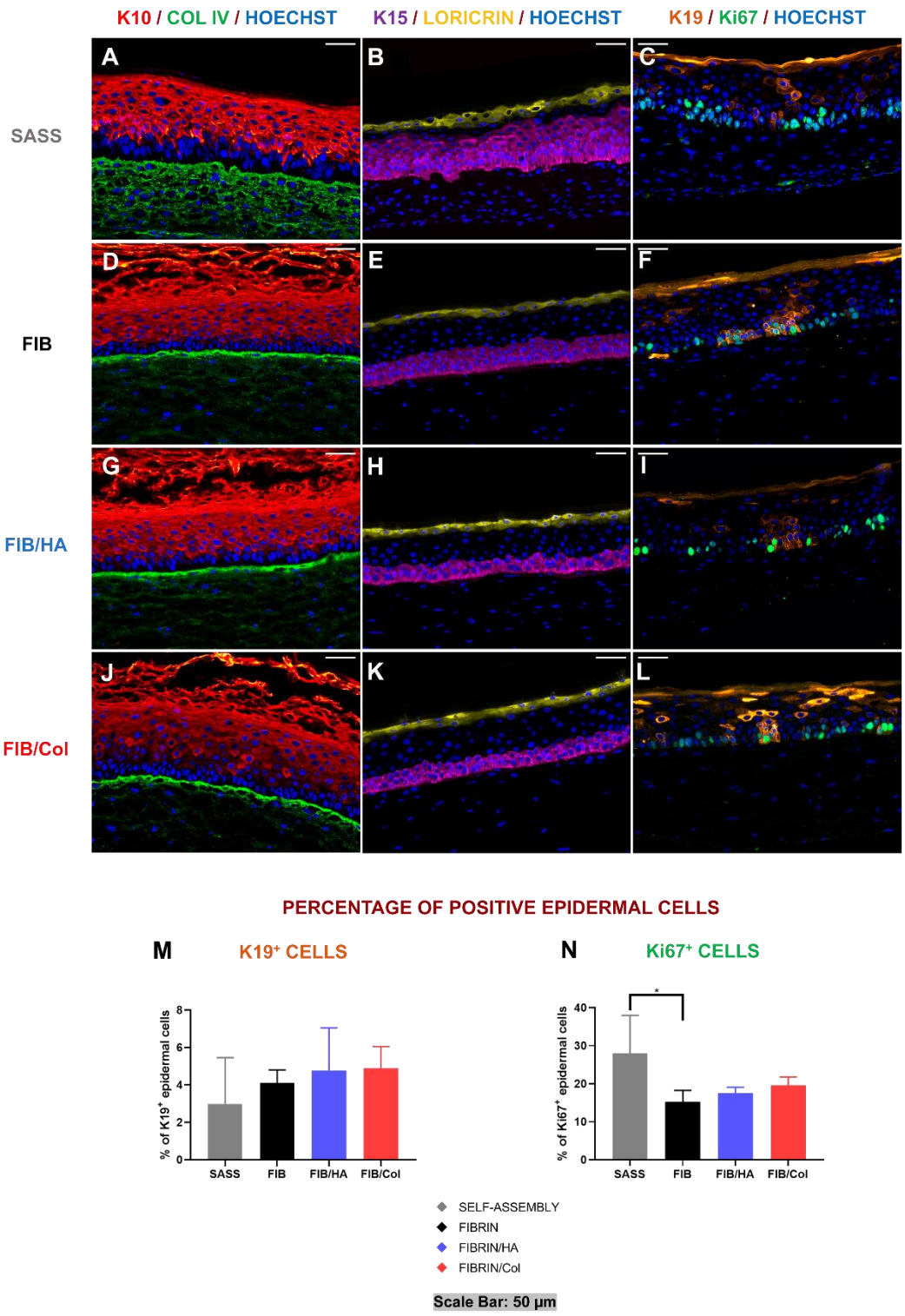

Fig. 36. ***Immunofluorescence pictures and analysis of hbTESSs.*** *From left to right in all groups: I) Keratin 10 (K10-red)/Type IV collagen (COL IV-green)/Hoechst nucleus (blue), II) Keratin 15 (K15-purple)/Loricrin (yellow)/Hoechst nucleus (blue) and III) Keratin 19 (K19-orange)/Ki67 (green)/Hoechst nucleus (blue) staining. Self-assembled skin substitute (**SASS**): **A**, **B** and **C**; Human plasma-based (**Fib**) skin substitute: **D**, **E** and **F**; Human plasma-based and hyaluronic acid (**Fib/HA**) skin substitute: **G**, **H** and **I**; Human plasma-based and collagen (**Fib/Col**) skin substitute: **J**, **K** and **L**. **M** Percentage of epidermal cells that are K19⁺ and localized in the basal layer (N=3; n = 16, 9, 9, 9 for each group, respectively). **N** Percentage of epidermal cells that are Ki67⁺ and localized in the basal layer (N=3; n = 16, 9, 9, 9 for each group, respectively). Scale bar: 50 µm. Statistical significance: *p-value<0.05, One-way ANOVA and Tukey's multiple comparisons tests. Data is shown as mean value ± SD.*

3.5. TYPE I AND TYPE IV COLLAGEN PROTEIN QUANTIFICATION IN hbTESSs

Western blot quantification revealed that type I collagen was 2.20 times higher in Fib/Col skin substitutes and 1.89 times higher in SASSs compared to Fib and Fib/HA skin substitutes although no significant differences were observed (**Fig. 37A** and **37C**).

Quantification of type IV collagen by Western blot revealed that, although without significance, more protein was present in SASS; 2.65 times higher than Fibrin, 5.3 times higher than Fib/HA and 11.1 times higher than Fib/Col skin substitutes (**Fig. 37B** and **37D**), a result consistent with the immunofluorescence tissue labeling.

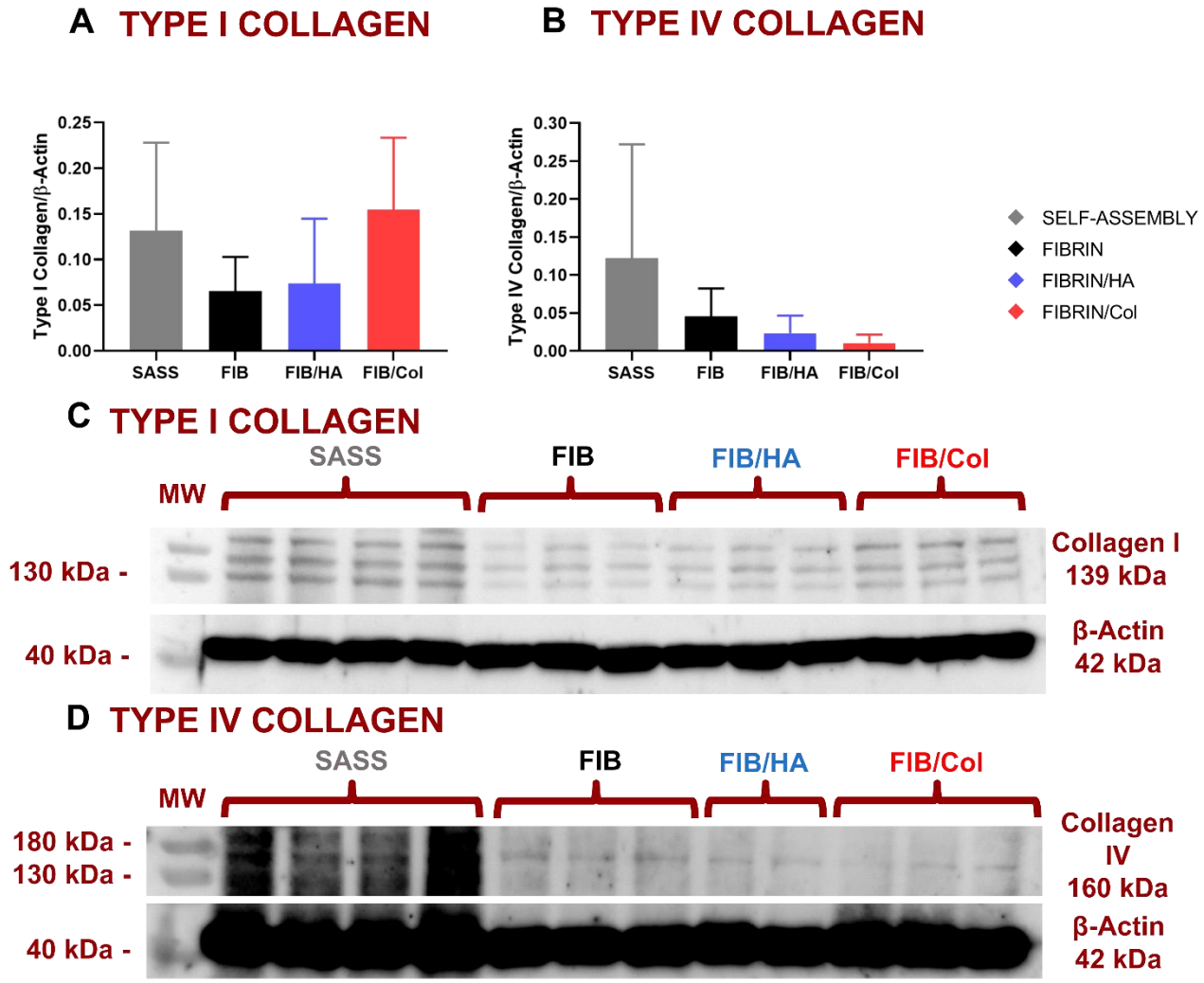

Fig. 37. ***Western blot analysis of type I and IV collagen of hbTESSs*** *(self-assembled skin substitute (SASS), human plasma-based (Fib), human plasma-based and hyaluronic acid (Fib/HA) and human plasma-based and collagen (Fib/Col) skin substitutes (N=3; n = 12, 9, 9, 9 for each group, respectively)). A Ratio of type I collagen on β-actin protein; B Ratio of type IV collagen on β-actin protein; C and D Representative pictures of a type I and a type IV collagen Western blot, respectively. One-way ANOVA and Tukey's multiple comparisons tests. Data is shown as mean value ± SD.*

3.6. ULTRASTRUCTURAL ASPECT OF HPSSs

The ultrastructure of SASSs has been previously characterized by Transmission Electron Microscopy (TEM), demonstrating the presence of a basement membrane, with numerous hemidesmosomes, as well as fibroblasts surrounded by the ECM they produced, comprising collagen fibers in the dermal layer after culturing at the air-liquid interface[2,217,349,355]. To define the ultrastructural aspect of human plasma-based skin substitutes, TEM analysis was conducted (**Fig. 38**). A discontinuous basement membrane without hemidesmosomes was visualized at the DEJ (**Fig. 38A**, **38B** and **38C**), indicating that the basement membrane assembly was initiated. Fibroblasts and ECM elements were also observed in all HPSSs (**Fig. 38D**, **38E** and **38F**), including collagen fibers (**Fig. 38G**, **38H** and **38I**), whose relative amounts were consistent with the type I collagen quantified by Western blot (**Fig. 37**).

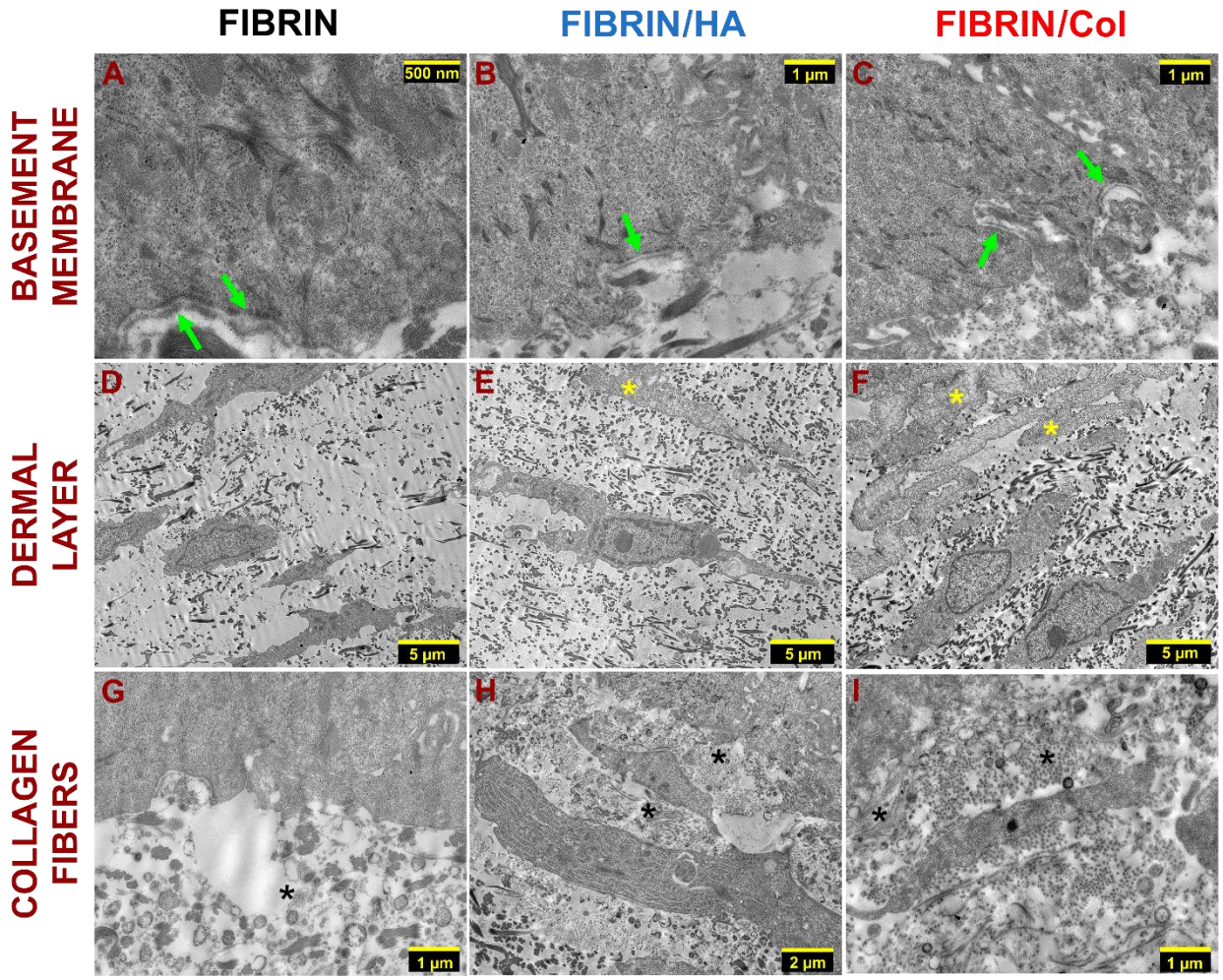

Fig. 38. ***Transmission electron microscopy (TEM) pictures of human plasma-based skin substitutes (HPSSs).*** *Basement membrane pictures (green arrows) of **A** Human plasma-based (**Fib**); **B** Human plasma-based and hyaluronic acid (**Fib/HA**); **C** Human plasma-based and collagen (**Fib/Col**) skin substitutes. Dermal layer ultrastructure of **D** Fibrin; **E** Fibrin/HA; **F** Fibrin/Col skin substitutes. Yellow asterisks indicate the presence of biomaterial deposits. Collagen fibers appearance of **G** Fibrin; **H** Fibrin/HA; **J** Fibrin/Col skin substitutes. Black asterisks indicate the presence and orientation of collagen fiber packages.*

DOI: 10.1111/jdv.16342
Journal: JEADV
1st Decile: Dermatology
(IF: 5.248 => JCR – 2019)

CHAPTER 4: IN VIVO COMPARISON OF THE WOUND HEALING POTENTIAL OF BILAYER HUMAN PLASMA-BASED SKIN SUBSITUTES (HPSSs), SECONDARY WOUND HEALING APPROACHES AND THE GOLD STANDARD TREATMENT

4.1. HISTOLOGICAL AND IMMUNOHISTOLOGICAL APPEARANCE OF HPSSs

Histological and immunohistochemical analysis of both types of HPSS (**Fig. 39A – 39F**), after one week of *in vitro* culture and prior to grafting, revealed correct cell integration and proliferation in Fib/HA and Fib/AG (**Fig. 39A** and **39D**) and expression of epithelial keratins was also observed (**Fig. 39B** and **39E**). Human origin of cells was demonstrated by moderate expression of HLA-E marker in both cases, and mainly in epithelial layers (**Fig. 39C** and **39F**). Constructs without cells were also analyzed; Control-Fib/HA (**Fig. 39G – 39I**) and Control-Fib/AG (**Fig. 39J – 39L**), revealing the structuration and organization of both biomaterials but without expression of any markers. These results were compared with healthy mouse skin used for autografts, where more structured cell layers were observed (**Fig. 39M** and **39N**) but without expression of human HLA-E marker (**Fig. 39O**).

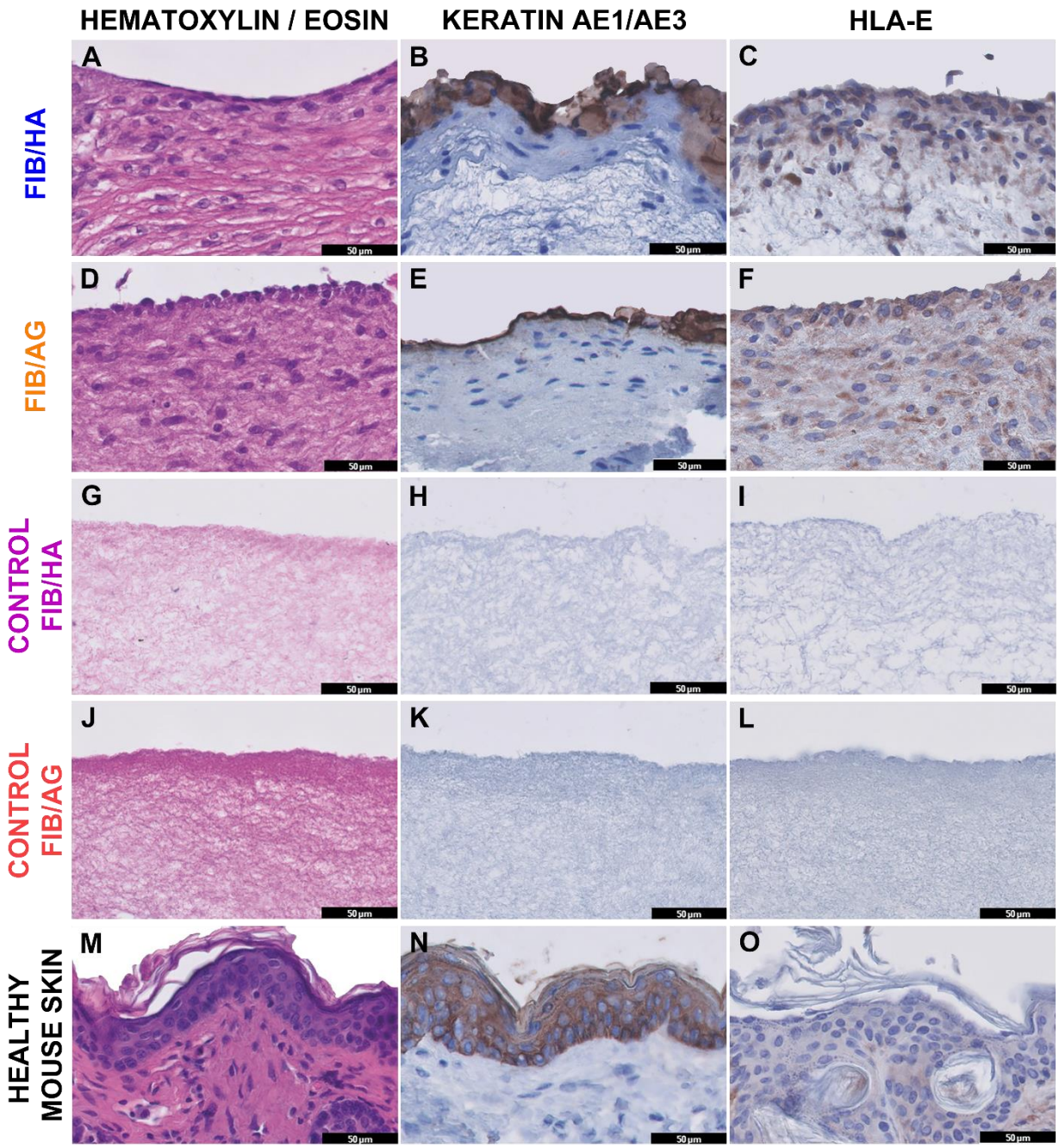

***Fig. 39*. Histological and immunohistochemical analysis of HPSSs constituted of HA an AG after one week of in vitro culture, and comparative with healthy mouse skin.** *Graphs from left to right, for each type of HPSS manufactured and healthy mouse skin, represent Hematoxylin / Eosin, Keratin AE1/AE3 and HLA-E staining. **Fib/HA**: **A**, **B** and **C**; **Fib/AG**: **D**, **E** and **F**; **Control-Fib/HA**: **G**, **H** and **I**; **Control-Fib/AG**: **J**, **K** and **L** and **Healthy Mouse Skin**: **M**, **N** and **O**. Scale bar: 50 µm.*

4.2. CLINICAL/WOUND HEALING EVALUATION

Appropriate biointegration was observed for all type of engraftments after 2 weeks, without complications (**Fig. 40**). Wound healing process and regeneration of skin were faster and more effective in the case of the groups of mice treated with Autograft and Fib/HA. In the case Fib/AG, total skin repair was observed after 8 weeks, however, Control-Fib/HA, Control-Fib/AG and Collagen-Dressing groups experienced slower improvement.

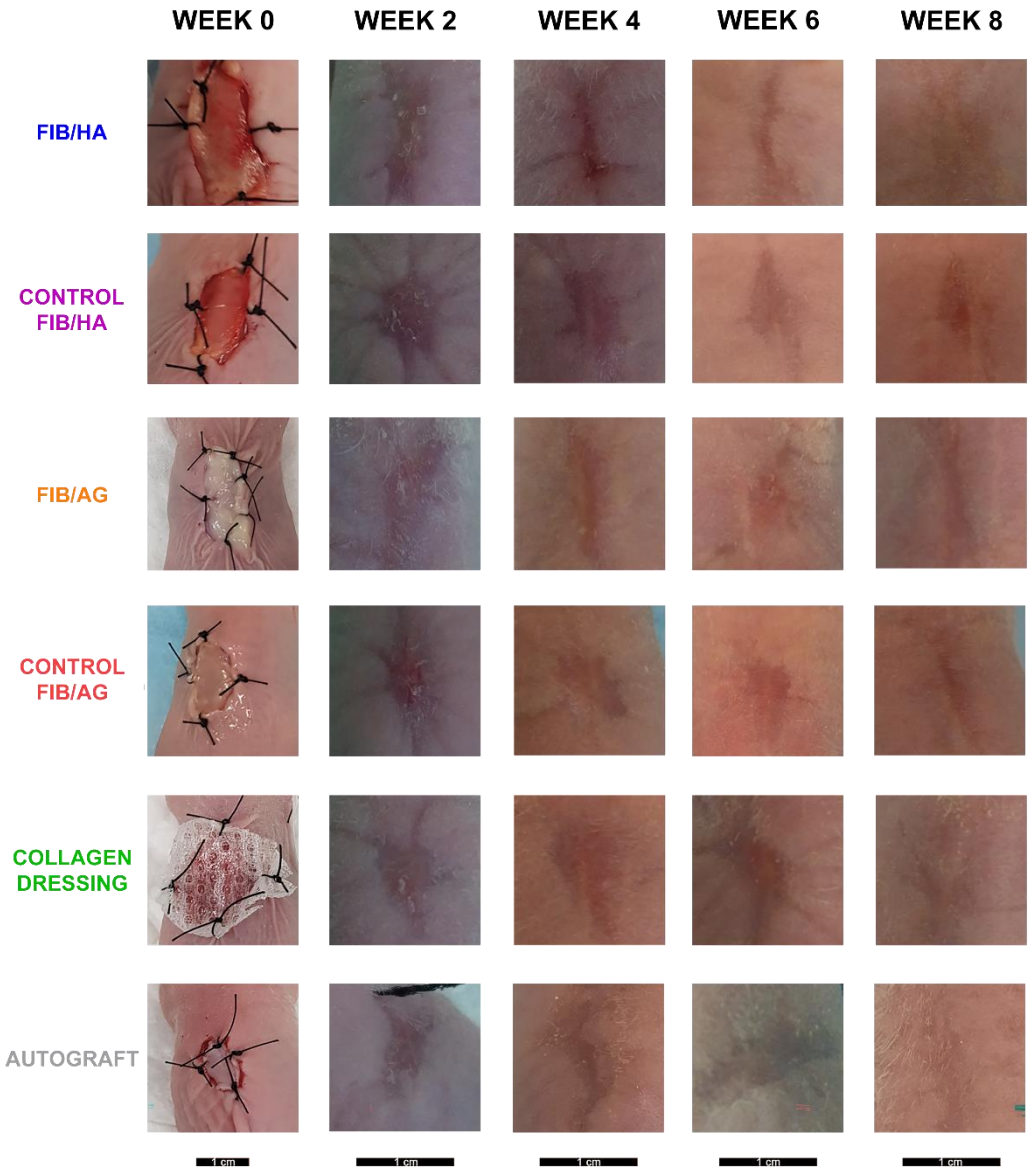

***Fig. 40*. Macroscopic images of wound healing process over time.** *Type of engraftment is indicated in each row, meanwhile, progression time (week 0, 2, 4, 6 or 8) is represented in each column. Scale bars of each column of images are represented at the bottom of the figure: 1 cm.*

Visual clinical evaluation (Fig. 40) correlated with quantitative analysis of wound/scar area (Fig. 41), where significant differences were observed between the day of the surgery (Week 0) and the rest of the weeks in all groups (*p-value<0.0001*). This indicated that after 2 weeks, the effect of all grafts on wound healing process was positive, but at the end of the study (Week 8), only in Fib/HA and Autograft groups, wound/scar area disappeared. Values of wound/scar area are included in Table 15.

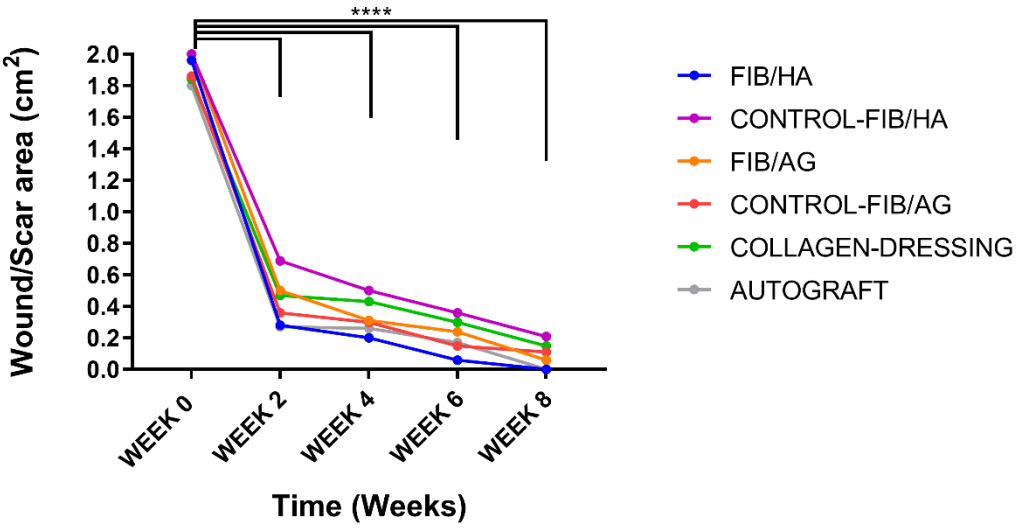

Fig. 41. Quantitative evaluation of wound/scar area through the time for each group of treatment. *Statistical significance: ****p-value<0.0001. Two-way ANOVA and Tukey's multiple comparisons tests. Data is shown as mean value ± SEM.*

Table 15. Results of wound/scar area through the time for each treatment.

Group of treatment	Week 0	Week 2	Week 4	Week 6	Week 8
Fib/HA	1.96 cm^2	0.28 cm^2	0.20 cm^2	0.06 cm^2	0.00 cm^2
Control-Fib/HA	2.00 cm^2	0.69 cm^2	0.50 cm^2	0.36 cm^2	0.21 cm^2
Fib/AG	2.00 cm^2	0.50 cm^2	0.31 cm^2	0.24 cm^2	0.06 cm^2
Control-Fib/AG	1.86 cm^2	0.36 cm^2	0.30 cm^2	0.15 cm^2	0.11 cm^2
Collagen-Dressing	1.84 cm^2	0.47 cm^2	0.43 cm^2	0.30 cm^2	0.15 cm^2
Autograft	1.80 cm^2	0.27 cm^2	0.26 cm^2	0.17 cm^2	0.00 cm^2

Assessment of scars was made using an adaptation of the Patient and Observer Scar Assessment Scale (POSAS - Table 16). Total score revealed that Autograft (6) and Fib/HA (8) presented better results than the other groups.

Table 16. POSAS results after 8 weeks.

Group of treatment	Vascularity[a]	Pigmentation[a]	Thickness[a]	Relief[a]	Pliability[a]	Surface Area[a]	Total Score[b]
Fib/HA	1	3	1	1	1	1	8
Control-Fib/HA	3	3	2	2	3	3	16
Fib/AG	2	2	2	3	2	2	13
Control-Fib/AG	3	2	3	3	4	2	17
Collagen-Dressing	4	2	3	2	3	3	17
Autograft	1	1	1	1	1	1	6

[a]All items are scored on a scale ranging from 1 ('like normal skin') to 10 ('worst scar imaginable').
[b]The lowest score, 6, reflects normal skin, whereas the highest score, 60, reflects the worst imaginable scar.

4.3. HOMEOSTASIS ANALYSIS

Temperature, pH, transepidermal water loss, elasticity and moisture were studied (**Fig. 42**). All treatment groups were compared with Healthy Mouse Skin group.

Temperature values (**Fig. 42A**, **42F**, **42K**, **42P**, **42U**, and **42Z**) were quite homogeneous and similar to Healthy Mouse Skin in all groups and weeks, without remarkable differences at the end of study. Interestingly, temperature of Autograft (**Fig. 42Z**) was practically the same as Healthy Mouse Skin through the study, in contrast with Collagen-Dressing group (**Fig. 42U**), where values were the lowest. Fib/HA results were slightly higher than Healthy Mouse Skin, but no significant differences existed. At the end of study (week 8), the average temperature of the three secondary wound healing approaches (Control-Fib/HA, Control-Fib/AG and Collagen-Dressing) was lower (31.35±0.51ºC) than bilayer HPSSs (33.09±0.07ºC for Fib/HA and 31.49±0.73ºC for Fib/AG).

In the case of pH (**Fig. 42B**, **42G**, **42L**, **42Q**, **42V** and **42AA**), values were homogeneous and similar to Healthy Mouse Skin results in all groups, and no significant differences were observed through the study. As well as in the temperature analysis, mean value at week 8 of the secondary wound healing approaches (4.77±0.30) was also lower than Fib/HA (5.56±0.26), Fib/AG (5.18±0.08) and Healthy Mouse Skin groups (5.24±0.13).

Transepidermal water loss study (**Fig. 42C**, **42H**, **42M**, **42R**, **42W** and **42AB**) revealed that values were consistent through the time with a decreasing trend after 8 weeks in all groups, except for Collagen-Dressing where values of TEWL increased (**Fig. 42W**). Interestingly at the end of the study, human TESS based on fibrin-hyaluronic acid biomaterial (Fib/HA) presented the same value (6.42±0.75 g/h/m^2) as Healthy Mouse Skin (6.40±0.43 g/h/m^2) (**Fig. 42C**).

Elasticity in Fib/HA, Control-Fib/HA, Fib/AG and Control-Fib/AG (**Fig. 42D**, **42I**, **42N** and **42S**, respectively) was higher than Healthy Mouse Skin, mainly in weeks 2 and 4 although without significant differences, except for Fib/HA in week 2 (*p-value<0.05*), but then decreased in a remarkable level (*p-value<0.01*). Collagen-Dressing group (**Fig. 42X**) presented similar values to Healthy Mouse Skin, in weeks 2 and 4, but increased significantly at week 6 (*p-value<0.001*). Autograft group (**Fig. 42AC**) presented similar values to Healthy Mouse Skin. Results after 8 weeks for secondary wound healing approaches were different to Healthy Mouse Skin (0.54±0.02 AU vs. 0.35±0.03 AU). In contrast, Fib/HA, Fib/AG and Autograft, presented similar values (0.42±0.08 AU, 0.49±0.09 AU and 0.40±0.08 AU, respectively).

In the case of moisture, there were also no differences with Healthy Mouse Skin (**Fig. 42E**, **42J**, **42O**, **42T**, **42Y** and **42AD**), only Fib/AG and Control-Fib/AG groups (**Fig. 42O** and **42T**), presented significantly lower values (*p-value<0.05*) at week 6.

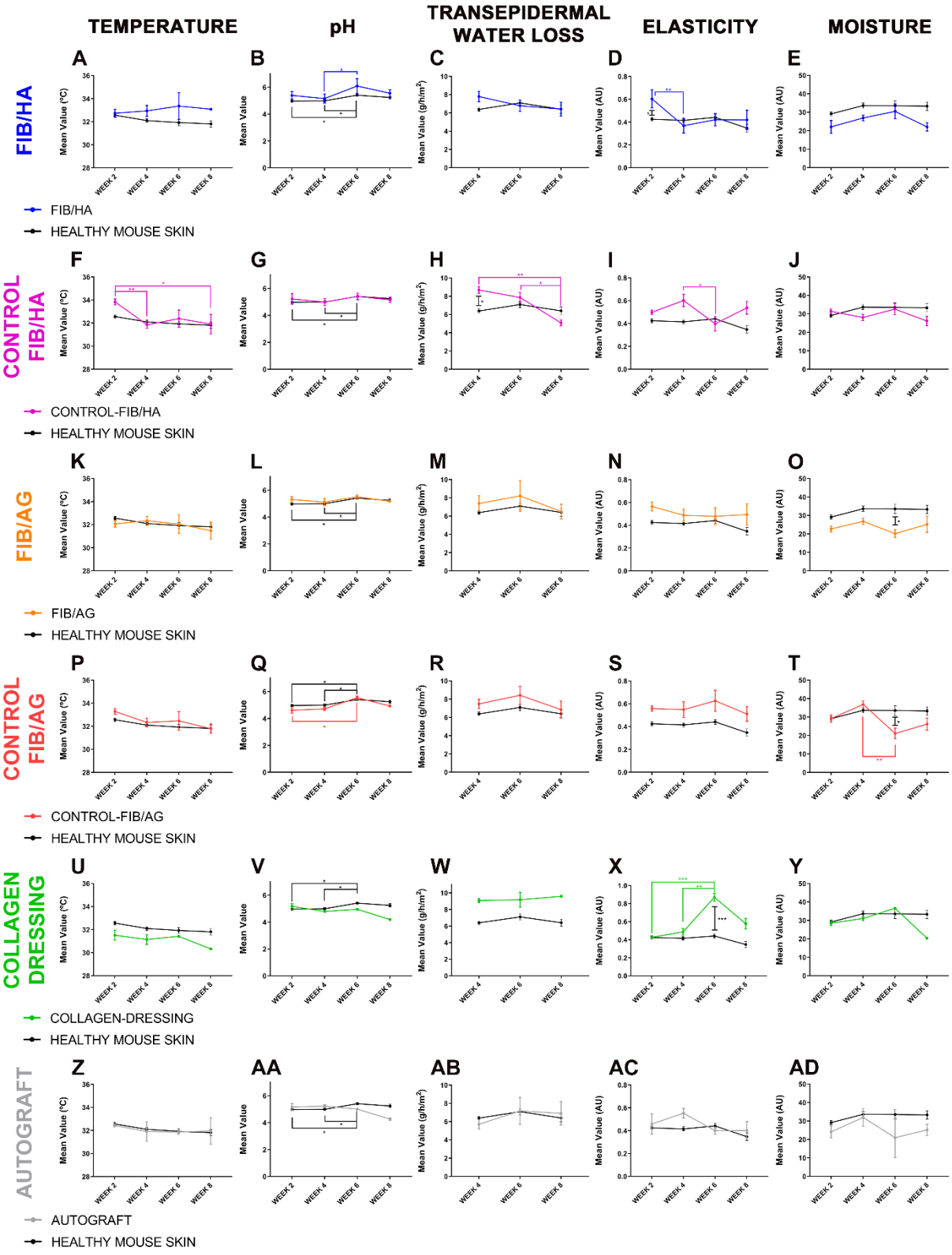

Fig. 42. ***Analysis of homeostasis parameters per week and compared with healthy mouse skin values for each group.*** *Graphs from left to right, for each group of treatment, represent temperature, pH, transepidermal water loss, elasticity and moisture.* ***Fib/HA*** *group (N week 2, 4, 6, 8 = 8, 8, 4, 4):* ***A***, ***B***, ***C***, ***D*** *and* ***E***; ***Control-Fib/HA*** *group (N week 2, 4, 6, 8 = 8, 8, 4, 4):* ***F***, ***G***, ***H***, ***I*** *and* ***J***; ***Fib/AG*** *group (N week 2, 4, 6, 8 = 8, 8, 4, 4):* ***K***, ***L***, ***M***, ***N*** *and* ***O***; ***Control-Fib/AG*** *group (N week 2, 4, 6, 8 = 8, 8, 4, 4):* ***P***, ***Q***, ***R***, ***S*** *and* ***T***; ***Collagen-Dressing*** *group (N week 2, 4, 6, 8 = 4, 4, 2, 2):* ***U***, ***V***, ***W***, ***X*** *and* ***Y***; ***Autograft*** *group (N week 2, 4, 6, 8 = 4, 4, 2, 2):* ***Z***, ***AA***, ***AB***, ***AC*** *and* ***AD***. ***Healthy Mouse Skin*** *(N week 2, 4, 6, 8 = 40, 40, 20, 20). 2 mice of Collagen-Dressing group and 2 mice of Autograft group died due to the surgery. Statistical significance: *p-value<0.05; **p-value<0.01, Two-way ANOVA and Tukey's multiple comparisons tests. Data is shown as mean value±SEM.*

4.4. ERYTHEMA AND PIGMENTATION ANALYSIS

Erythema analysis of all groups (**Fig. 43A**, **43C**, **43E**, **43G**, **43I** and **43K**) reported higher values than Healthy Mouse Skin. These results were quite significant except for Autograft group (**Fig. 43K**) where only values from week 4 were statistically significant (*p-value<0.01*). In general, results were homogenous through the time for the rest of groups and remarkable differences were observed compared with Healthy Mouse Skin (*p-value<0.001* and *p-value<0.0001*), mainly during the first weeks after engraftment. Interestingly, after 8 weeks, for Fib/HA and Autograft (**Fig. 43A** and **43K**), erythema levels decreased to similar values as Healthy Mouse Skin (365.04±35.78 AU, 291.53±16.44 AU and 286.98±7.01 AU, respectively).

In the case of melanin levels (**Fig. 43B**, **43D**, **43F**, **43H**, **43J** and **43L**), values were also higher than Healthy Mouse Skin, however, significant differences were only observed in Fib/HA and Fib/AG (*p-value<0.001* and *p-value<0.0001*) (**Fig. 43B** and **43F**).

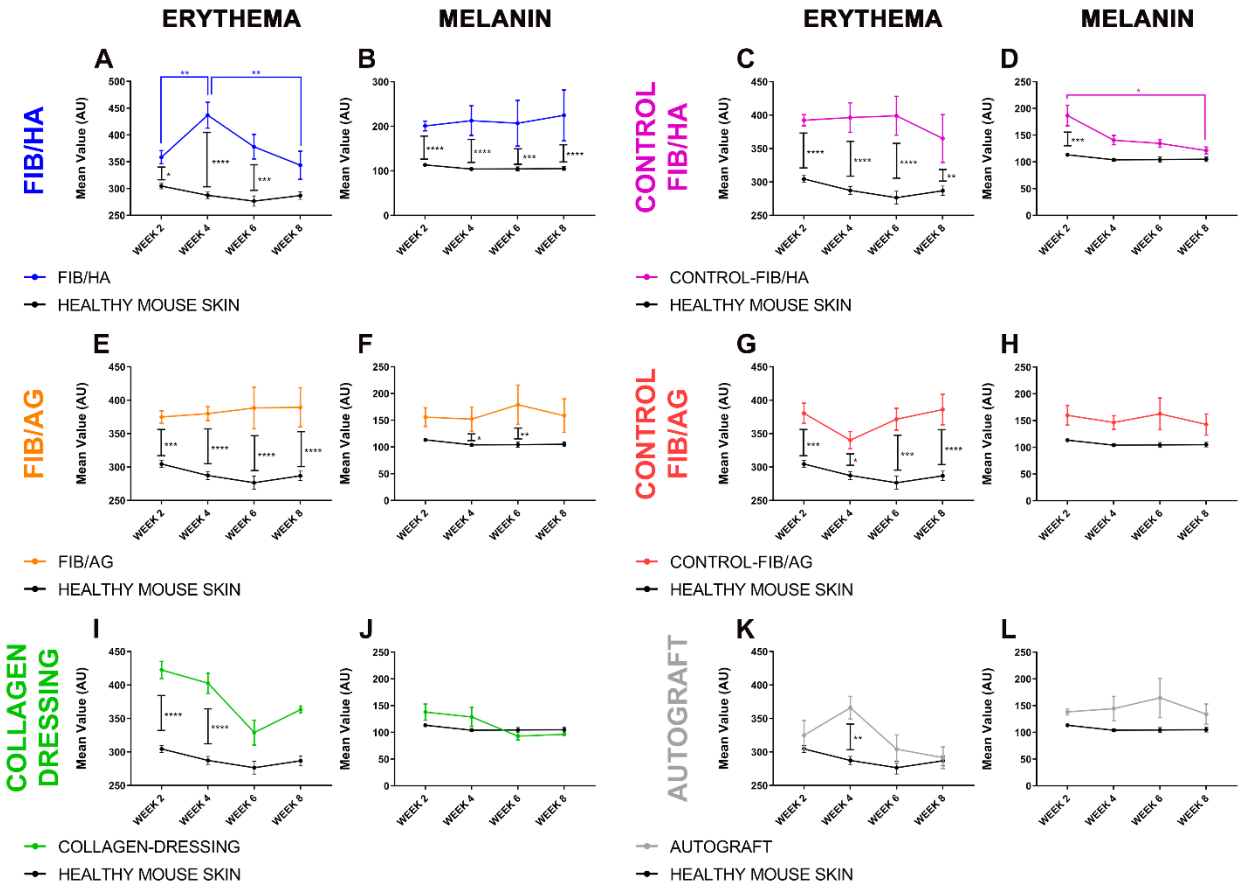

Fig. 43. ***Pigmentation and erythema analysis per week and compared with healthy mouse skin values for each group.*** *Graphs from left to right, for each group of treatment, represent erythema and melanin. **Fib/HA** group (N week 2, 4, 6, 8 = 8, 8, 4, 4): **A** and **B**; **Control-Fib/HA** group (N week 2, 4, 6, 8 = 8, 8, 4, 4): **C** and **D**; **Fib/AG** group (N week 2, 4, 6, 8 = 8, 8, 4, 4): **E** and **F**; **Control-Fib/AG** group (N week 2, 4, 6, 8 = 8, 8, 4, 4): **G** and **H**; **Collagen-Dressing** group (N week 2, 4, 6, 8 = 4, 4, 2, 2): **I** and **J**; **Autograft** group (N week 2, 4, 6, 8 = 4, 4, 2, 2): **K** and **L**. **Healthy Mouse Skin** (N week 2, 4, 6, 8 = 40, 40, 20, 20). 2 mice of Collagen-Dressing group and 2 mice of Autograft group died due to the surgery. Statistical significance: *p-value<0.05; **p-value<0.01; ***p-value<0.001; ****p-value<0.0001, Two-way ANOVA and Tukey's multiple comparisons tests. Data is shown as mean value ± SEM.*

4.5. HISTOLOGICAL AND IMMUNOHISTOCHEMICAL ANALYSIS

Hematoxylin / Eosin staining of engraftments (**Fig. 44**) revealed a correct regeneration of the epidermis and dermis after 4 weeks, however, Fib/HA, Fib/AG and Autograft groups (**Fig. 44A**, **44I** and **44U**) presented a more complex structure, composed of more cells in dermal matrix and more layers of epithelial cells than secondary wound healing approaches (Control-Fib/HA, Control-Fib/AG and Collagen-Dressing groups) (**Fig. 44E**, **44M** and **44Q**). After 8 weeks, structure was more complex and defined in all groups, but keratinization seemed to be higher in Fib/HA, Fib/AG and Autograft groups (**Fig. 44C**, **44K** and **44W**). These results were correlated with the expression of epithelial keratins (**Fig. 44**), which allowed to confirm the regeneration of epithelial layers after 4 weeks. Rete ridges and skin appendages were absent in all groups. Those mice treated with bilayer HPSSs and autografts (**Fig. 44B**, **44D**, **44J**, **44L**, **44V** and **44X**) presented better structure, keratinization and expression than the other groups, after 4 and 8 weeks.

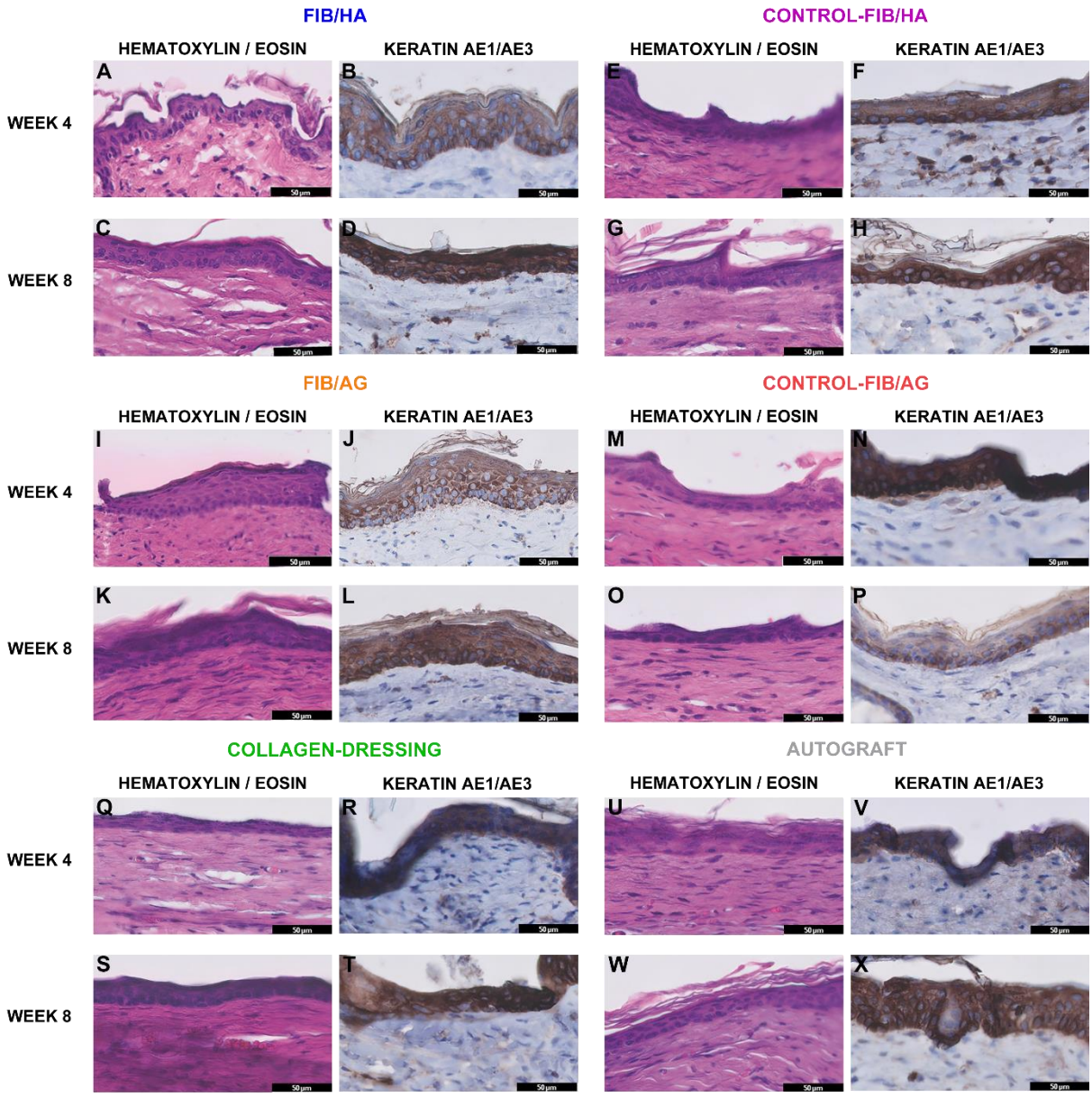

Fig. 44. ***Histological and immunohistochemical analysis of skin after 4 and 8 weeks post-engraftment.*** *Images from left to right and from the top to the bottom represent Hematoxylin / Eosin staining after 4 weeks, Keratin AE1/AE3 staining after 4 weeks, Hematoxylin / Eosin staining after 8 weeks and Keratin AE1/AE3 staining after 8 weeks.* ***Fib/HA*** *group:* ***A***, ***B***, ***C*** *and* ***D***; ***Control-Fib/HA*** *group:* ***E***, ***F***, ***G*** *and* ***H***; ***Fib/AG*** *group:* ***I***, ***J***, ***K*** *and* ***L***; ***Control-Fib/AG*** *group:* ***M***, ***N***, ***O*** *and* ***P***; ***Collagen-Dressing*** *group:* ***Q***, ***R***, ***S*** *and* ***T***; ***Autograft*** *group:* ***U***, ***V***, ***W*** *and* ***X***. *Scale bar: 50 µm.*

To determine the presence of human cells after 8 weeks of study, an immunohistochemical analysis of human HLA-E (**Fig. 45**) revealed that no expression in native mouse skin, Collagen-Dressing or Autograft groups (**Fig. 45A**, **45D** and **45E**) was observed. However, moderate expression in epithelial layers of Fib/HA and Fib/AG groups (**Fig. 45B** and **45C**) was confirmed.

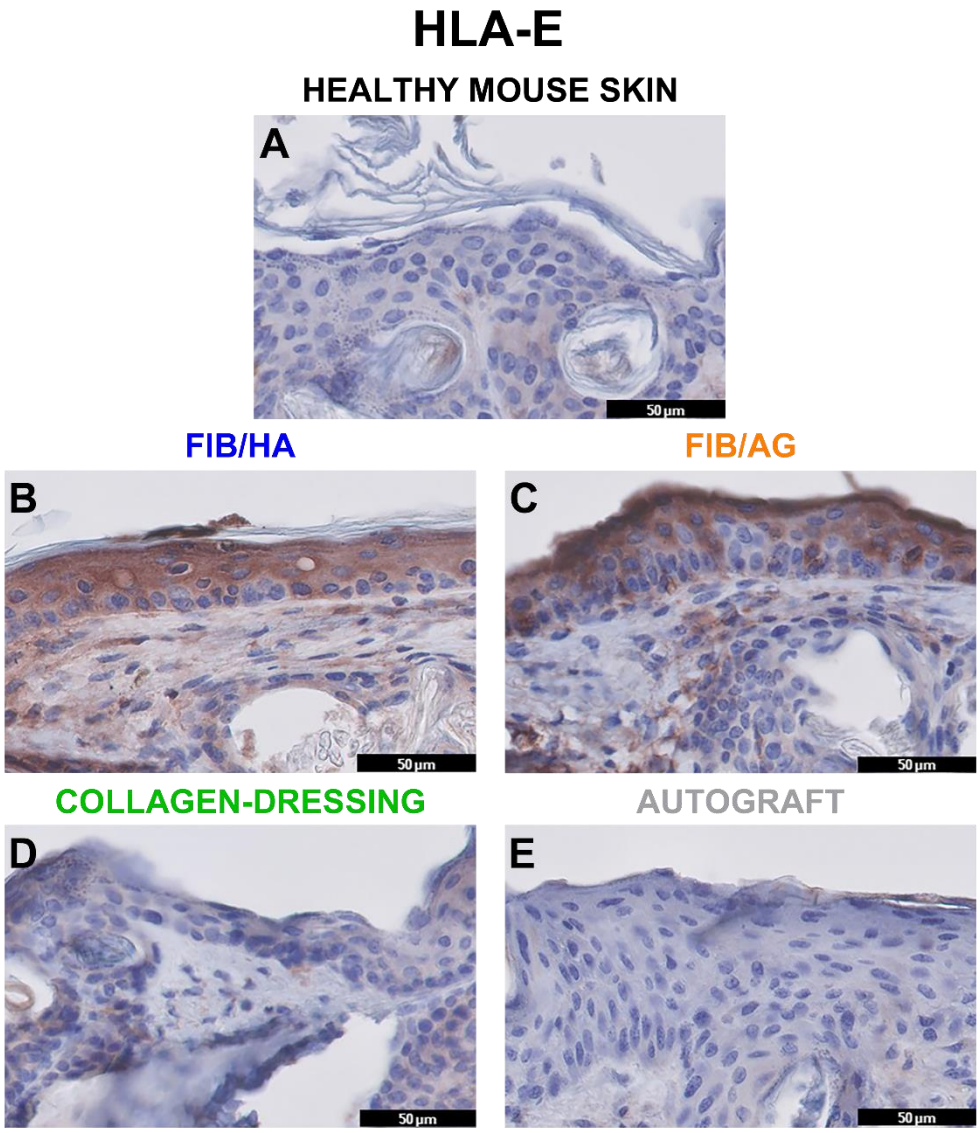

Fig. 45. ***Immunohistochemical analysis of HLA-E to corroborate the presence of human cells after 8 weeks post-engraftment.*** *A Healthy Mouse Skin control; B Fib/HA group; C Fib/AG group; D Collagen-Dressing group; E Autograft group. Scale bar: 50 µm.*

VI. DISCUSSION

DISCUSSION

The use of immortalized cell lines for the development of human tissue-engineered skin substitutes for research purposes is a useful strategy due to their homogeneous and well characterized properties through the time, avoiding inter-variability between samples and experiments[112]. However, they have been usually altered by different strategies in an artificial environment and therefore they are not representative of *in vivo* conditions or useful for clinical outcomes[112]. Therefore, the development of hTESSs as advanced therapy requires the extraction and expansion of human primary cells isolated from human skin biopsies, preserving the properties and characteristics of the different native human skin cell types as much as possible.

In **Chapter 1** of this Doctoral Thesis, the human skin cell isolation protocol used at UPCIT (Spain) for hbTESS manufacturing, was compared to the one independently developed at LOEX (Canada)[341,342] for the treatment of severely burned patients. The side-by-side comparison of the optimized protocols has shown that the number of epithelial cells obtained per surface area of the same skin biopsies and their viability were higher with the LOEX-Protocol. However, similar results were measured for the other evaluated parameters such as clonogenicity and the number of colonies. For the dermal cells, no difference was observed between cell viability and yield following isolation, and the subsequent cultures exhibited the same behavior.

The main difference between both protocols is the first step which is a mechanical preparation of the skin or an added digestion step. The protocols involving only one digestion step have been described, in which skin biopsies (epidermis-dermis) are incubated with a trypsin enzyme[90,120,356,357] to achieve epithelial cell isolation. However, the presence of the dermis results in the liberation of the fibroblasts that contaminate the epithelial cell population. To overcome this problem, other protocols, such as the UPCIT-Protocol, require mechanical isolation of the epidermis from the dermis with scissors to remove as much dermal tissue as possible or other tools, such as foot planers, to obtain epidermal sheets that are subsequently digested[358]. The remaining dermis can be used for fibroblast isolation.

Compared to one-step digestion protocols, the two-step digestion protocols are preferred mainly for epithelial cell isolation[359], and dispase[360–363] or thermolysin[341,342,364,365] are the two enzymes frequently used in this phase. In the case of the LOEX-Protocol, the added first digestion step with thermolysin allows the detachment of the epidermis from the dermis due to its specific effect between the bullous pemphigoid, located at the lamina lucida of the epithelial side[366], and the laminin of the dermal compartment, disrupting the hemidesmosomes more easily but preserving the desmosomes between keratinocytes[367]. This avoids the experience-based considerations of the researchers to decide when most of the dermis tissue is removed, as in the case of the UPCIT-Protocol.

For dermal cell isolation, the protocols are more similar and based on collagen digestion. Once the epidermis is digested or detached, the dermal tissue is incubated with a single[63,90,341,361,363] or a combination[362] of collagenases for various times, varying from 1[361] to 20[63] hours at 37ºC. In all cases, these matrix metalloproteinases cleave collagen molecules at a unique Gly-Leu/Ile bond, degrading their triple-helical main structure[368].

The higher epithelial cell yield after isolation with the LOEX-Protocol than the UPCIT-Protocol is consistent with previous studies where the application of the two-step digestion protocol allowed for isolating a higher number of epithelial cells/cm^2 of biopsy (1×10^6-2.6×10^6 cells/cm^2)[342,363,369] than when a mechanical detachment of the epidermis and subsequent digestion was applied (3.3×10^5-6.6×10^5 cells/cm^2)[358], which is similar to the UPCIT-Protocol's value. Interestingly, a higher number of epithelial cells was isolated (2×10^6-5×10^6 cells/cm^2) when skin biopsies are directly digested without trimming the dermis[90,342,356,357,369], although the risk of fibroblast contamination is higher, due to the unspecific separation, when using trypsin[342,367] and, therefore, an increased percentage of vimentin-positive cells (fibroblasts) has been reported after various times in culture[342]. Among the two-step digestion protocols, when thermolysin is applied for the first digestion, the epithelial cell yield has been higher than using other enzymes, such as dispase or trypsin[117,369], at the same step.

The colony-forming efficiency and total number of colonies were similar in both protocols, although slightly higher using the two-step digestion protocol (LOEX-Protocol) compared to the one-step protocol (UPCIT-Protocol) at P0. Similar results have been reported previously[342,370,371]. This is likely due to a better detachment of the dermis from the epidermis at the basement membrane level by thermolysin[371], which decreases the incubation time with trypsin and therefore, epithelial cell viability is less affected[357].

In addition, the total number of colonies was increased from P0 to P1 in both protocols, probably due to the keratinocytes' culture conditions (specific medium and *feeder* layer), which allow a good proliferation of keratinocytes, through maintaining Sp1 expression, and reduce the growth potential of the residual fibroblasts[342,346]. However, a lower proportion of holoclones was observed in P1 compared to P0 for both protocols. This is attributed to the fact that the cells grew faster in P1 and the culture was stopped earlier (at day 7-10 for P1 and day 10-14 for P0) because the colonies were close to each other. Therefore, these results have to be confirmed in future experiments by decreasing the number of keratinocytes seeded in P1.

Nevertheless, the percentage of K19$^+$ epithelial cells also decreased at the end of P1 for both protocols, which could be explained by the fact that culturing keratinocytes through passages can cause stress and reduce the number of epithelial-stem cells[372]. Therefore, these results suggest that the culture conditions, regardless of the cell isolation protocol, should be controlled since a decrease in stem cells could have a negative impact on human tissue-engineered skin substitute manufacturing.

On balance, although minor differences were observed in cell viability and yield of fresh epithelial cells, the skin cell isolation protocol applied at UPCIT has demonstrated its effectiveness for the procurement of human primary skin cells that will be useful for the development of the HPSS model that is applied for the treatment of patients.

Regarding hTESSs manufactured at UPCIT, the oldest is based on the use of human plasma as main biomaterial combined with agarose as secondary biomaterial. This dermal stroma has been combined with primary human keratinocytes and fibroblasts (hbTESSs) for the treatment of severely burned patients[94].

However, the use of agarose has certain drawbacks such as the necessity to be heated to 39ºC just before hbTESS manufacture, which supposes a challenge when working under GMP conditions and moreover, it is not naturally found in skin or human body. For this reason, the *in vitro* study of several secondary biomaterials (**Chapter 2**), such as serine (Fib/S), fibronectin (Fib/Fn), collagen (Fib/Col), laminin (Fib/Lam-1 and Fib/Lam-2) and hyaluronic acid (HA) which are components of human skin or body, and their comparison with the HPSS without a secondary biomaterial (Fib), has provided useful information to improve the model. Moreover, in search of a personalized medicine and a skin substitute that better resembles the native human skin the study of different human cell combinations to conform different cellular subtypes of this hTESS has allowed us to increase the knowledge of the model.

The combination of human plasma/fibrin with native biomaterials such as collagen[246,293,373,374], hyaluronic acid[247,327,375], fibronectin[247] and laminin[280] have been studied for different purposes. However, no comparative *in vitro* or *in vivo* studies exist, evaluating these different biomaterials' compositions.

The results of this Doctoral Thesis revealed, firstly, that no *in vitro* differences were observed regarding the secondary biomaterial added for any of the several conditions studied, in terms of cell viability, cell metabolic activity or protein secretion profile. Therefore, the major presence of human plasma into the scaffolds determines their biological *in vitro* properties. This conclusion was also achieved in a study where type I collagen was used as main component of bilayer TESSs and combined with several secondary biomaterials such as type III collagen, hyaluronic acid, elastin or dermatan sulfate, demonstrating that relative cell viability was similar at different time points regardless of the addition or not of these biomaterials, even at different concentrations[376]. However, the influence of the secondary biomaterials seems to be more interested *in vivo*, how it was demonstrated in previous studies where the incorporation of hyaluronic acid to fibrin matrices for the treatment of skin wounds in mice, reported faster microvessel formation than those constituted of fibronectin (14 vs. 28 days)[247].

In addition to the secondary biomaterial composition, the effect of the partial dehydration process applied for HPSS manufacture was studied in cell viability. The application of a partial dehydration process, also referred as plastic compression, has been described as a method to increase the mechanical properties of the hTESSs, for an improved clinical handling[361,377]. The effect of this process has been mainly evaluated in hydrogels composed of rat-tail type I collagen, demonstrating that the application of this methodology resulted in, approximately, 10% of reduction of viability[378] and that the viability of the embedded fibroblasts just after dehydration process was around 80%[379]. These results are in line with the ones reported in this Doctoral Thesis, where the effect of the partial dehydration process has been a reduction of ~10%, ~10% and ~6% in Trilayer, Bilayer and Monolayer groups, respectively. However, the viability of those substitutes with embedded fibroblasts and hAT-MSC was around 72%, which differs from the ~80% previously reported for rat-tail I collagen[379]. This could be explained by the higher stiffness of collagen, demonstrated by comparing its compressive modulus value (1.5±0.36 MPa)[378] with the one of human plasma/fibrin hydrogels (0.01 MPa)[242]. Therefore, collagen preserves cell viability much better when compression is applied.

Apart from these aspects, skin cell tissue source used for the manufacture of the different cellular HPSSs was evaluated. Most of the previous studies evaluating the use of different skin cell tissue sources have focused on the donor's age and their influence in cell proliferation and epidermal thickness, indicating that neonatal or young donors may be of advantage due to their regenerative nature[380–383]. However, other studies indicated that the influence of the donor in general is higher in terms of cell proliferation than a specific age or anatomical location of the skin samples[376].

Regarding those studies that directly studied the influence of the donor's tissue source, a higher CFE in keratinocyte cultures have been demonstrated when they were isolated from foreskin and compared with other anatomical regions[384]. In the case of the fibroblast culture, no differences were observed in terms of doubling population time when different skin tissue sources such as scalp, abdomen, breast or forearm were compared[385]. Therefore, the influence of the cell tissue source seems to be more determinant in keratinocyte proliferation and for *in vitro* culture rather than for hTESS manufacture, corroborated by histological appearance in this research. This explains that no differences were observed in terms of cell viability and metabolic activity, when the different HPSSs manufactured with abdominal skin or foreskin cells were directly compared.

Analysis of the protein secretion profile regarding the skin cell tissue source (bFGF, EGF, VEGF-A and CCL5) also demonstrated that no differences exist between them. In the case of bFGF and VEGF-A higher concentrations were reported for Trilayer and Bilayer substitutes, whereas, for EGF and CCL5, values were close to zero or negative (due to the subtraction of the control values) which means they are captured by the cells. Interestingly, in these last proteins, higher values were found for Monolayer HPSSs.

The analysis of these growth factors and cytokine is determined by the use of human plasma as a hydrogel or scaffold for the development of hTESSs, which contains many different useful proteins that facilitate cellular activities and enhance deposition of a new ECM[218,232]. Moreover, the addition of the different cell types also determines the protein profile, which could be useful for wound healing purposes:

Firstly, bFGF is a potent mitogen that stimulate the growth of fibroblasts in culture[386] and it is involved in several *in vivo* functions such as regulation of cell survival, division, differentiation and migration and also has angiogenic properties[387], playing a crucial role during remodeling phase in wound healing process[388,389]. The ELISA analysis revealed that Trilayer HPSSs secreted a slightly higher amount than Bilayer and much more than Monolayer groups, which could be explained because it is released by both fibroblasts (mainly) and keratinocytes[390,391] and also, although only in minimum amount, by hAT-MSCs[392].

In the case of EGF, it plays a pivotal role in enhancing epidermal and dermal regeneration by stimulating keratinocytes and fibroblasts' migration and proliferation *in vivo*[388]. It is known that EGF is synthetized and secreted by fibroblasts[393] but also by platelets, keratinocytes, and macrophages[394]. For this reason, the low concentration secreted by the HPSSs demonstrates that it is essential to be captured for both fibroblasts, predictably for stimulating the production of collagen mainly in young populations[395] (although not shown, ages of foreskin cell populations were younger and that could be the reason why more EGF is captured by them) and also, by keratinocytes for enhancing their proliferation and migration[396].

VEGF-A is a growth factor required in wound healing[397] due to its active role in angiogenesis, vasculogenesis and endothelial cell growth and promoting cell proliferation and migration[398]. A higher secretion was reported by Trilayer and Bilayer substitutes than Monolayer HPSSs which could be explained because of the cumulative secretion of this factor by keratinocytes[399], fibroblasts[400] and hAT-MSCs[392]. Moreover, the use of human plasma/fibrin as scaffold has a paracrine effect that increases the secretion of VEGF compared to other scaffolds[401] and especially in combination with hMSCs[402].

Regarding CCL5, also referred as RANTES, it is a chemoattractant for blood monocytes, memory T-helper cells and eosinophils[403] and secreted by T lymphocytes, macrophages, platelets, synovial fibroblasts[404], keratinocytes[405] but also by hAT-MSCs[406,407]. In addition, it also stimulates *in vitro* the mobilization of fibroblasts[408] and hAT-MSCs[409]. Therefore, the lower values of concentration obtained in this research demonstrates that CCL5 is *in vitro* captured by the mesenchymal stem cells and fibroblasts, but also by the keratinocytes. In accordance with this statement, the secretion was higher in Monolayer substitutes (where the total amount of cells was lower), which is corroborated by other

studies where similar results were observed when epidermal and bilayer substitutes' secretion was compared[410].

To conclude with the *in vitro* analysis of the HPSSs, a comparison between submerged (SUB) and air/liquid interface (ALI) culture methodologies revealed that cell viability after dehydration process was higher, although with slight differences, when air/liquid interface was applied for Trilayer and Bilayer groups. In the case of Monolayer substitutes, submerged culture reported higher viability, and in both cases, like in all viability studies here described, the value was significantly lower compared with their corresponding Trilayer and Bilayer HPSSs. In addition, these results were in line with the cell metabolic activity analysis, where lower values were reported for Monolayer groups, especially when ALI was applied. These results demonstrates that air/liquid interface affects monolayer substitutes or cultures in a higher degree, as previously observed in a study with the A549 epithelial cell line[411], and moreover, promotes early differentiation of epithelial cells instead of proliferation[412], corroborated by histological appearance in this Doctoral Thesis, something that maintain cell metabolic activity in contrast to when proliferation is promoted, where is increased[413].

Regarding protein secretion profile, the release patterns were similar in Trilayer, Bilayer and Monolayer HPSSs for bFGF and VEGF-A growth factors, although higher when ALI was applied, due probably to the longer culture time. In the case of EGF, lower values (negative) were reported in all groups for ALI methodology, mainly in Trilayer and Bilayer groups, which could be due to the suppression of this factor from the culture medium to promote epithelial differentiation. This means that the factor which is present in the own plasma and produced by the own cells[388,393,394] is captured by the fibroblasts to produce collagen[395], whereas, in the case of submerged methodology, EGF is already available into the culture medium. Finally, the secretion of CCL5 was the one that showed a different pattern compared to submerged culture, where a lower release was observed, especially in Trilayer and Bilayer HPSSs. This could be explained because, as previously described, CCL5 is secreted and captured by all types of cells here used[404–407], so Trilayer and Bilayer groups under ALI are able to release CCL5 but this is not captured by the keratinocytes, due to the lack of contact between them and culture medium, thereby increasing the amount of this factor released.

On balance, the *in vitro* analysis of several subtypes of the HPSS manufactured at UPCIT revealed that the human plasma/fibrin determines their *in vitro* properties more than the secondary biomaterial included. Moreover, the use of skin cell populations from different tissue sources neither has a highlighted impact. However, the manufacture of different cellular substitutes reported significant differences in terms of cell viability and metabolic activity, indicating that better clinical outcomes are expected with Trilayer and Bilayer substitutes. In terms of protein secretion profile, higher differences were observed when submerged and air/liquid interface methodologies were compared,

demonstrating that although significant differences exist and better histological structure is developed with ALI culture, both could be useful for clinical purposes.

To achieve a complete *in vitro* characterization of the new different versions of the UPCIT's hTESS model[94,334] a comparison with a clinical bilayer (fibroblasts and keratinocytes) self-assembled skin substitute (SASS)[2] developed in Canada was carried out (**Chapter 3**). To that purpose and based on the previous results where no significant differences were observed between secondary biomaterials, only two of them were chosen to this purpose due to their role in skin functions and structure: hyaluronic acid and collagen. In addition, bilayer HPSSs constituted of human plasma/fibrin without a secondary biomaterial were also studied.

Although the safety of these models has already been proven in a clinical setting, the direct comparison using the same cell populations has provided useful *in vitro* data on their respective mechanical and biological properties. Moreover, the addition of hyaluronic acid or collagen to the human plasma-based skin substitutes revealed only minor effects on hbTESSs properties, as in the previous section.

One main difference between both models is the culture time when air/liquid interface is applied. In this study, SASSs were generated in 46-55 days, which is similar to the delay previously reported before patients get their first grafts using SASSs[2], whereas HPSSs were manufactured in 32-39 days. This manufacturing time could be longer depending on the patient, for example, due to his/her age, a factor that could influence cell proliferation[384]. Moreover, some studies have reported that infections and septic complications are the main cause of death in severely burned patients[414,415]. Since the first protective barrier and several adnexal structures are damaged, the human body is highly exposed, therefore, a short hbTESS production time is a significant asset. Unfortunately, both manufacturing processes are still long and an immediate grafting of autologous tissue-engineered skin substitutes is not possible. However, the benefits of using autologous therapies when autografts can not be applied are higher and other clinical strategies, to diminish the risk of infection while waiting for a definitive treatment to replace the epidermis, should be developed. For example, Novosorb™ Biodegradable Temporizing Matrix was applied early on burn wounds until SASS was available for grafting with good results in 1 patient[416]. Nevertheless, other considerations apart from manufacturing time are equally important such as a high graft take, prevention of the development of hypertrophic scars, reduction in the number of additional surgeries (for SASSs engraftment[2]) and long-term persistence of the grafted hbTESSs.

In term of clinical use, human plasma-based skin substitutes need to be dehydrated to improve their biomechanical properties[242], but otherwise the grafting procedure is similar for both models; after surgical debridement, SASSs and HPSSs are applied to the wound bed and secured with staples or surgical glues (in SASSs[2]). For each model, the post-operative treatment is the same for autografts

and skin substitutes, but it differs in the two countries. Commercial gauzes were different; for SASSs, a conventional type of bolster is applied for 5-7 days[2], while for HPSSs, gauze changes and physiological saline solution and soap washes are applied every 2 days.

The study of both hbTESS models using the peel test methodology[349] revealed that the DEJ strength of SASSs was higher than in HPSSs. This lower force of adhesion is consistent with TEM results; where the basement membrane formation was not completed after 10 days of the culture at the air-liquid interface in contrast to SASSs where previous studies reported a continuous basement membrane using the same culture conditions[217,349,417]. Moreover, analysis of type IV collagen expression, the primary collagen found in basement membranes and a major component of the DEJ[418], demonstrated that it was overexpressed in the dermis of SASSs. The lower amount into the dermis of human plasma-based skin substitutes may be a matter of culture time or/and because of embedding the fibroblasts into the hydrogel[419]. The biomaterial could also diminish fibroblast interaction with type IV collagen, expressed by keratinocytes[420,421], resulting in a lack of hemidesmosomes and basement membrane formation. The importance of the presence of a basement membrane is likely to prevent the delamination of the epidermis from the dermis of the hbTESSs during manipulations at the time of grafting and thereafter. This is one of the factors that could explain the high SASS engraftment (98%) on severely burned patients[2]. However, the basement membrane could be formed after grafting *in vivo* as shown for biomaterial (collagen or human plasma)-based skin substitutes[90,316,422] and high engraftment has also been observed at discharge for this model (80-85%). Therefore, *in vivo* trials will be necessary to compare their regenerative potential.

Regarding tensile and elastic properties, the compression applied in human plasma-based hbTESSs creates a partial dehydration and aligns collagen[361] or fibrin fibers[242], generating stiffer and denser skin substitutes than fully hydrated models, improving their handling and rheological properties[242,361], although similar behavior has been observed regardless of biomaterial combination. However, SASSs are stiffer and more resistant to tensile forces which could be explained by the longer culture period of dermal layers and also, by the self-assembled nature of the ECM; more similar to native human dermis[355].

Concerning biological aspects, the lower amount of DNA per mg of tissue quantified in biomaterial-based skin substitutes compared with SASSs indicated that lower number of cells formed the HPSSs. This result was consistent with the slightly higher proportion of epidermal cells expressing Ki67 observed in SASSs, suggesting hyperproliferation. Despite the higher number of cells seeded (5.1×10^6 vs. 2.6×10^5 cells) and the longer epidermal culture time in HPSS protocol (17 vs. 14 days), the much longer culture time required for each of the three fibroblast-derived sheets manufactured in SASSs (18-20 vs. 1 day) resulted in more cells per mg of tissue. Moreover, although more physiologically similar in terms of structure than 2D cultures, the embedding of fibroblasts into a 3D

hydrogel for human plasma-based skin substitutes may constrain cell growth[419] and explain the lower amount of DNA. In contrast, cell metabolic activity was higher in HPSSs which could be explained by the presence of human plasma factors such as PDGF-BB or HGF, known to increase epidermal cell metabolic activity[215,423].

On balance, the comparison of both models revealed similar *in vitro* biological characteristics, however, SASSs present better *in vitro* mechanical properties. In contrast, its manufacturing process is more time-consuming than HPSSs, something that for the treatment of patients could be a key point.

Finally, considering these *in vitro* results, the last study of this Doctoral Thesis (**Chapter 4**) was focused on the *in vivo* analysis of one of the subtypes of the HPSSs previously evaluated and compare this with the oldest model manufactured at UPCIT, constituted of agarose as secondary biomaterial. Hyaluronic acid secondary biomaterial was chosen due to its *in vivo* properties previously reported[212–214] and bilayer substitutes (Fib/HA and Fib/AG) were manufactured because of their majority use for clinical purposes[116]. In this case, submerged methodology was applied to reduce manufacturing time and different parameters were evaluated for both types of cellular HPSSs but also for the gold standard treatment (Autograft) and secondary wound healing approaches. All results were compared with the healthy mouse skin.

The bilayer HPSSs based on human plasma and hyaluronic acid were grafted in mice after surgical excision, showing good clinical and histological integration, higher reduction of the wound/scar area and similar result in the POSAS than Autograft. Homeostasis parameters and epidermal barrier function showed similar values between Fib/HA, Autograft and Healthy Mouse Skin. Secondary wound healing approaches exhibited inferior results in all parameters studied, in accordance with previous investigations in which the incorporation of human cell sheets to 3D constructs improved the healing of full-thickness excisional wounds and the re-epithelialization process in mice[424].

Regarding homeostasis and epidermal barrier function, autograft demonstrated to be the best alternative because no significant differences with healthy mouse skin were observed for any parameter. Skin temperature plays a crucial role in thermoregulation and is involved in activating automatic responses such as vasoconstriction or vasodilation[425,426]. In humans, and according to the results of this study, also in mice, mean skin temperature in a neutral environment (24°C) ranges from 30 to 34°C[427], so the absence of significant differences with any of the groups indicates the correct integration and restoration of this function. Recently, the influence of temperature has been analyzed in epidermal morphogenesis *in vitro*[428].

Transepidermal water loss is highly used to determine skin barrier integrity *in vivo*, so when skin is damaged, its barrier function is impaired resulting in higher water loss[429] and, therefore, a reduction

in moisture[430]. Fib/HA and Autograft presented similar values as control skin at the end of study; however, in the case of the acellular substitutes, a fully restoring skin function was not achieved.

Elasticity presented higher values during the wound healing process in all groups except for Autograft. However, at the end of the study, Fib/HA and Fib/AG showed similar values to native mouse skin. Elasticity is a skin parameter directly associated to dermal layers, where fibroblasts are responsible of collagen and elastin fibers formation. Therefore, the use of hyaluronic acid and agarose as dermal matrix and their viscoelastic properties[242,431] may explain these results during the wound healing process. In a recent study, elasticity analysis showed similar values between autograft and artificial skin in a case series of 14 severely burned patients[2].

Erythema that shows the redness of skin caused by hyperemia in superficial capillaries, because of any skin injury, infection, inflammation or neovascularization, presented high levels in all groups. Fib/HA presented higher values during the first weeks of the study, which could be related with their angiogenic properties[214]. However, only in this group, erythema values were similar to Autograft and Healthy Mouse Skin groups after eight weeks, which confirms, in accordance with re-epithelialization and POSAS results, that the combination of human cells with hyaluronic acid properties enhances wound healing process and could be the best alternative to autografts.

Higher levels of melanin were found mainly in Fib/HA and Fib/AG, which was interesting because mice were albino. Melanin is a pigment produced by melanocytes but part of it could be transferred to keratinocytes[432], which explain the highest values of melanin obtained in both HPSSs that incorporated human cells. A previous study that analyzed melanin content (pigmentation) of autologous human skin substitutes (fibroblasts and keratinocytes) in patients showed no significant differences with healthy skin[2].

Histological and immunohistochemical staining of human TESSs and autografts revealed a morphology and structure similar to healthy mouse skin after eight weeks, showing a multilayer epithelium and a correct dermis with fibers and fibroblasts although rete ridges and skin appendages were absent. In the case of the application of acellular substitutes, histological results demonstrated an absence of total regeneration of the epithelium and dermis, due to the lack of the cell component[424]. These morphological results correlated with clinical, epidermal barrier function and homeostasis parameters.

Regarding the manufacturing process of HPSSs, although in previous studies substitutes were cultured for three or four weeks in air-liquid interface culture[316], the application of the submerged methodology reduced this period to one week. The result was cellular HPSSs constituted of a structure and histological architecture more similar to native immature skin, however, at the end of the *in vivo* analysis, they showed a well-differentiated epidermis and dermis. These outcomes

reinforce that reduce the culture period may facilitate faster clinical application with good morphological and functional results.

The presence of human cells eight weeks after grafting was studied with human HLA-E staining. This marker is expressed moderately in epithelial layers of skin, but it is not expressed in dermis[433], which was observed in both cellular HPSSs in contrast to healthy mouse skin, autografts and acellular substitutes. Higher levels of melanin expression in cellular substitutes in the albino mice also indicated the presence of human keratinocytes.

In summary, homeostasis parameters and epidermal barrier function restoration were better for Autograft and Fib/HA. Bilayer human plasma-based TESSs combined with hyaluronic acid and cells promote the formation of a structure and histological architecture very similar to normal skin, with similar expression of molecules such as keratins, involved in epidermis stability processes, migration and re-epithelization[434]. Moreover, advantages of hyaluronic acid for clinical use in human tissue-engineered skin substitutes are that it is easy to handle at GMP conditions, reduces scar formation[435] and it is naturally found in human skin[209,210].

In addition, biosafety of hyaluronic acid is corroborated by its widespread use as injectable dermal filler for cosmetic purposes[211], and even, an acellular synthetic tissue-based wound care product called Hyalomatrix®, which its main component is hyaluronic acid, is already commercialized. This device has been evaluated in humans as a cover dressing prior to skin graft[212,213,351,352], demonstrating an efficient skin restoration in terms of hydration and transepidermal water loss[212], mainly when the water regulation and neoangiogenic boost are relevant issues[213], which correlates with the results of this study.

On balance, the results of this Doctoral Thesis demonstrate that the design, development and manufacture of different subtypes of a HPSS model is a promising and useful strategy as advanced therapy. The possibility of using several secondary biomaterials, skin cell tissue sources, cellular compositions and culture methodologies and the homogeneity of their *in vitro* results, determine that this model is robust and successful, particularly when hyaluronic acid was *in vivo* studied as secondary biomaterial. Therefore, this research validates its translation into a clinical environment and recommends its use as an alternative to autografts for the treatment of several skin injuries and wounds.

VII. LIMITATIONS AND FUTURE PERSPECTIVES

LIMITATIONS

The methodology, protocols and guidelines followed for the development of this Doctoral Thesis are robust as it has been demonstrated after the analysis of the results. However, there are some limitations that could be improved for future research projects.

1) The number of molecular studies should be increased, both for the analysis of the skin cell isolation protocol used at the UPCIT and the different versions of the HPSS model manufactured.
2) Rheological and mechanical studies should be included to compare the different versions of the HPSS model manufactured. The use of several secondary biomaterials and the manufacture of skin substitutes with different cellular structures could report significant differences. Moreover, the measure of the thickness of the different HPSS subtypes will provide useful information to achieve a complete characterization of the model.
3) More comparative *in vivo* studies should be included, to analyze the wound healing potential of each secondary biomaterial and the role of the cellular structure.
4) To determine the regenerative and pro-angiogenic potential of the secondary biomaterials, the immunohistochemical analysis of protein markers such as VEGF or alpha Smooth Muscle Actin (α-SMA) should be included.

FUTURE PERSPECTIVES

The results of this Doctoral Thesis have provided useful information about the HPSS model manufactured at UPCIT. For this reason, the bilayer HPSS constituted of hyaluronic acid as secondary biomaterial is being studied in a comparative clinical trial (phases I and II) for the treatment of surgical wounds after the excision of basal cell carcinomas (PI17/02083).

Moreover, due to the nature of the hydrogels and their components, the UPCIT is involved in some preliminary preclinical projects where the final purpose is to combine this HPSS model and the use of 3D bioprinters, to automatize the process, increase its reproducibility and reduce the manufacturing time.

VIII. CONCLUSIONS

CONCLUSIONS

The following conclusions can be drawn from the results obtained in this Doctoral Thesis:

1) The one-step digestion protocol optimized and used at the UPCIT for human keratinocyte and fibroblast isolation has been proved to be useful for hTESS manufacture. Its comparison with the two-step digestion protocol applied at the LOEX laboratory (for clinical purposes) has demonstrated that no differences are observed for fibroblast viability and yield, just after isolation. Regarding epithelial cells, lower cell viability and yield has been reported when UPCIT protocol was applied, however, after isolation process no differences exist through the different passages cultured.

2) The comparison of several secondary biomaterials incorporated into the HPSS model manufactured at the UPCIT has revealed that no significant differences are noted. Therefore, the *in vitro* biological properties of the HPSSs are due to the human plasma used for their fabrication.

3) The effect of the partial dehydration process applied after submerged culturing process decreased cell viability of the HPSSs. However, this reduction was minimal and clinical handling was improved.

4) The use of different skin cell tissue sources for the manufacture of the HPSS and their *in vitro* evaluation has demonstrated that no significant differences exist. Therefore, any available skin source will be useful for the manufacture of the HPSS model.

5) The application of the air/liquid interface methodology for the manufacture of the HPSSs, generally increases the secretion of proteins that are useful in skin wound healing process. However, the manufacturing time is also increased, a key factor when patients are going to be treated. For this reason, and regarding the histological appearance, submerged methodology is also a useful strategy.

6) According to the cellular structure, Trilayer and Bilayer HPSSs have reported similar results, better than Monolayer substitutes. Among them, Bilayer TESS models are more clinically used.

7) The *in vitro* comparison of several bilayer HPSSs and another clinically used model of TESS (SASSs) has demonstrated that similar *in vitro* biological characteristics are observed. However, SASSs present better *in vitro* mechanical properties, although its manufacturing process is more time-consuming than HPSSs. The results of the different HPSS subtypes studied corroborate that their *in vitro* properties are more dependent on the human plasma used for their manufacture.

8) The *in vivo* analysis, in a surgical wound model in mice, of a bilayer HPSS composed of hyaluronic acid as secondary biomaterial and its comparison with the gold standard treatment (autografts), another bilayer HPSS composed of agarose and secondary wound healing approaches (commercial or not) has revealed that they are able to achieve a proper skin wound healing, in a similar way that autografts, and better than the rest of conditions studied. Therefore, it has been demonstrated that the bilayer HPSS composed of hyaluronic acid is a useful strategy for the treatment of patients.

IX. CONCLUSIONES

CONCLUSIONES

En base a los resultados de esta Tesis Doctoral, se pueden obtener las siguientes conclusiones:

1) El protocolo basado en una única digestión, optimizado y utilizado en la UPCIT para el aislamiento de queratinocitos y fibroblastos humanos ha demostrado ser útil para su uso en el proceso de producción de sustitutos de piel humana creados por ingeniería de tejidos. La comparación con el protocolo basado en dos digestiones aplicado en el laboratorio LOEX (para fines clínicos) ha determinado que no existen diferencias en la viabilidad y el rendimiento de los fibroblastos, justo después del aislamiento. En el caso de las células epiteliales, una menor viabilidad y rendimiento han sido obtenidos cuando se aplicó el protocolo de la UPCIT, sin embargo, una vez en cultivo no existen diferencias a lo largo de los pases celulares.

2) La comparación de diferentes biomateriales secundarios incorporados en el modelo de piel basado en el uso del plasma humano fabricado en la UPCIT ha demostrado que no se observan diferencias significativas. Por lo tanto, las propiedades biológicas *in vitro* de los sustitutos de piel producidos en la UPCIT se deben principalmente al plasma humano utilizado durante el proceso de fabricación.

3) El proceso de deshidratación por presión aplicado tras el cultivo sumergido de los sustitutos de piel basados en el uso del plasma humano de la UPCIT redujo su viabilidad celular. Sin embargo, este descenso de la viabilidad fue mínimo y la manipulación clínica de los sustitutos se vio mejorada.

4) El uso de diferentes regiones anatómicas para la obtención de los tipos celulares utilizados en la fabricación del modelo de piel basado en el uso del plasma humano fabricado en la UPCIT y su evaluación *in vitro* ha demostrado que no existen diferencias significativas entre ellas. Por lo tanto, cualquier región anatómica disponible podría ser de utilidad para la fabricación de este modelo.

5) La aplicación de la técnica de interfase aire/líquido para la fabricación del modelo de piel basado en el uso del plasma humano aumenta, de manera generalizada, la secreción de proteínas que son de utilidad durante el proceso de curación de heridas. Sin embargo, el tiempo de producción se incrementa, lo que es un factor importante cuando lo que se pretende es el tratamiento de pacientes. Por esta razón, y de acuerdo con los resultados de histología, el cultivo sumergido también es una estrategia útil.

6) Atendiendo a la composición celular, los sustitutos de piel trilaminares y bilaminares basados en el uso del plasma humano presentan resultados similares, mejores que los de los sustitutos monocapa. Entre ellos, los sustitutos bilaminares de piel humana creados por ingeniería de tejidos son los más extendidos en el ámbito clínico.

7) La comparativa *in vitro* de varios sustitutos de piel bilaminares fabricados según el modelo basado en el uso del plasma humano y otro modelo clínico de piel creada por ingeniería de tejidos mediante la denominada técnica de autoensamblaje (SASS en inglés), ha demostrado que las propiedades biológicas de ambos son similares. Sin embargo, el modelo de autoensamblaje presenta mejores propiedades mecánicas, aunque su proceso de fabricación es más largo. Además, los resultados de las diferentes variantes estudiadas para el modelo de piel basado en el uso del plasma humano corroboran que sus propiedades se deben principalmente al plasma humano utilizado durante su fabricación.

8) El estudio *in vivo,* en un modelo de herida quirúrgica en ratones, del sustituto de piel bilaminar basado en el uso del plasma humano y combinado con ácido hialurónico como biomaterial secundario, y su comparativa con el tratamiento de referencia (autoinjerto), otro sustituto de piel bilaminar constituido de plasma humano y agarosa y otras estrategias secundarias (comerciales o no), ha demostrado su potencial terapéutico en la curación de heridas, de manera similar al uso de autoinjertos y en un mayor grado que el resto de grupos de estudio. Por lo tanto, el uso del sustituto de piel bilaminar basado en el uso del plasma humano y combinado con ácido hialurónico es una estrategia terapéutica de utilidad.

X. REFERENCES

REFERENCES

1. Kolarsick, P. A. J., Kolarsick, M. A. & Goodwin, C. Anatomy and Physiology of the Skin. *J Dermatol Nurses Assoc* **3**, 203–213 (2011).
2. Germain, L. *et al.* Autologous bilayered self-assembled skin substitutes (SASSs) as permanent grafts: A case series of 14 severely burned patients indicating clinical effectiveness. *Eur Cell Mater* **36**, 128–141 (2018).
3. Naves, L. B., Dhand, C., Almeida, L., Rajamani, L. & Ramakrishna, S. In vitro skin models and tissue engineering protocols for skin graft applications. *Essays Biochem* **60**, 357–369 (2016).
4. Skin: The Histology Guide. https://www.histology.leeds.ac.uk/skin/skin_layers.php.
5. Lee, Y. & Hwang, K. Skin thickness of Korean adults. *Surg Radiol Anat* **24**, 183–189 (2002).
6. Wei, J. C. J. *et al.* Allometric scaling of skin thickness, elasticity, viscoelasticity to mass for micro-medical device translation: from mice, rats, rabbits, pigs to humans. *Scientific Reports 2017 7:1* **7**, 1–16 (2017).
7. Barker, J. N. W. N. *et al.* Keratinocytes as initiators of inflammation. *The Lancet* **337**, 211–214 (1991).
8. Tsatmali, M., Ancans, J. & Thody, A. J. Melanocyte function and its control by melanocortin peptides. *Journal of Histochemistry and Cytochemistry* **50**, 125–133 (2002).
9. Deckers, J., Hammad, H. & Hoste, E. Langerhans Cells: Sensing the Environment in Health and Disease. *Front Immunol* **9**, (2018).
10. Abraham, J. & Mathew, S. Merkel Cells: A Collective Review of Current Concepts. *Int J Appl Basic Med Res* **9**, 9 (2019).
11. Dehdashtian, A. *et al.* Anatomy and physiology of the skin. *Melanoma: A Modern Multidisciplinary Approach* 15–26 (2018) doi:10.1007/978-3-319-78310-9_2/COVER.
12. Sen, G. L. Remembering one's identity: the epigenetic basis of stem cell fate decisions. *The FASEB Journal* **25**, 2123–2128 (2011).
13. Michel, M. *et al.* Keratin 19 as a biochemical marker of skin stem cells in vivo and in vitro: keratin 19 expressing cells are differentially localized in function of anatomic sites, and their number varies with donor age and culture stage. *J Cell Sci* **109**, 1017–1028 (1996).
14. Anatomy, Skin (Integument), Epidermis - StatPearls - NCBI Bookshelf. https://www.ncbi.nlm.nih.gov/books/NBK470464/.
15. Brody, I. The ultrastructure of the tonofibrils in the keratinization process of normal human epidermis. *J Ultrastruct Res* **4**, 264–297 (1960).
16. Histology, Stratum Corneum - StatPearls - NCBI Bookshelf. https://www.ncbi.nlm.nih.gov/books/NBK513299/#!po=25.0000.
17. Histology, Dermis - StatPearls - NCBI Bookshelf. https://www.ncbi.nlm.nih.gov/books/NBK535346/.
18. Kanitakis, J. Anatomy, histology and immunohistochemistry of normal human skin. *Eur J Dermatol* **12**, 390–9; quiz 400 (2002).

19. Rippa, A. L., Kalabusheva, E. P. & Vorotelyak, E. A. Regeneration of Dermis: Scarring and Cells Involved. *Cells* **8**, 607 (2019).

20. Harper, R. A. & Grove, G. Human skin fibroblasts derived from papillary and reticular dermis: differences in growth potential in vitro. *Science* **204**, 526–527 (1979).

21. Roig-Rosello, E. & Rousselle, P. The Human Epidermal Basement Membrane: A Shaped and Cell Instructive Platform That Aging Slowly Alters. *Biomolecules 2020, Vol. 10, Page 1607* **10**, 1607 (2020).

22. Gantwerker, E. A. & Hom, D. B. Skin: histology and physiology of wound healing. *Facial Plast Surg Clin North Am* **19**, 441–453 (2011).

23. Shen, Z. *et al.* Rete ridges: Morphogenesis, function, regulation, and reconstruction. *Acta Biomater* **155**, 19–34 (2023).

24. Lawlor, K. T. & Kaur, P. Dermal Contributions to Human Interfollicular Epidermal Architecture and Self-Renewal. *Int J Mol Sci* **16**, 28098 (2015).

25. Briggaman, R. A. & Wheeler, C. E. The epidermal-dermal junction. *J Invest Dermatol* **65**, 71–84 (1975).

26. Woodley, D. T. Distinct Fibroblasts in the Papillary and Reticular Dermis: Implications for Wound Healing. *Dermatol Clin* **35**, 95–100 (2017).

27. Chen, M. *et al.* Restoration of type VII collagen expression and function in dystrophic epidermolysis bullosa. *Nat Genet* **32**, 670–675 (2002).

28. Sakai, L. Y., Keene, D. R., Morris, N. P. & Burgeson, R. E. Type VII collagen is a major structural component of anchoring fibrils. *J Cell Biol* **103**, 1577–1586 (1986).

29. Walko, G., Castañón, M. J. & Wiche, G. Molecular architecture and function of the hemidesmosome. *Cell Tissue Res* **360**, 363 (2015).

30. Zimoch, J. *et al.* Bio-engineering a prevascularized human tri-layered skin substitute containing a hypodermis. *Acta Biomater* **134**, 215–227 (2021).

31. Ferrero, R., Rainer, P. & Deplancke, B. Toward a Consensus View of Mammalian Adipocyte Stem and Progenitor Cell Heterogeneity. *Trends Cell Biol* **30**, 937–950 (2020).

32. Schmidt, B. A. & Horsley, V. Intradermal adipocytes mediate fibroblast recruitment during skin wound healing. *Development* **140**, 1517–1527 (2013).

33. Festa, E. *et al.* Adipocyte lineage cells contribute to the skin stem cell niche to drive hair cycling. *Cell* **146**, 761–771 (2011).

34. Reinke, J. M. & Sorg, H. Wound repair and regeneration. *Eur Surg Res* **49**, 35–43 (2012).

35. Rodrigues, M., Kosaric, N., Bonham, C. A. & Gurtner, G. C. Wound healing: A cellular perspective. *Physiol Rev* **99**, 665–706 (2019).

36. Berk, B. C., Wayne Alexander, R., Brock, T. A., Gimbrone, M. A. & Clinton Webb, R. Vasoconstriction: A new activity for platelet-derived growth factor. *Science (1979)* **232**, 87–90 (1986).

37. Pradhan, S., Khatlani, T., Nairn, A. C. & Vijayan, K. V. The heterotrimeric G protein G1 interacts with the catalytic subunit of protein phosphatase 1 and modulates G protein–coupled receptor signaling in platelets. *Journal of Biological Chemistry* **292**, 13133–13142 (2017).

38. Wagner, C. *et al.* Analysis of GPIIb/IIIa receptor number by quantification of 7E3 binding to human platelets. *Blood* **88**, 907–914 (1996).

39. Santoro, S. A. Identification of a 160,000 dalton platelet membrane protein that mediates the initial divalent cation-dependent adhesion of platelets to collagen. *Cell* **46**, 913–920 (1986).

40. Bielefeld, K. A., Amini-Nik, S. & Alman, B. A. Cutaneous wound healing: recruiting developmental pathways for regeneration. *Cell Mol Life Sci* **70**, 2059–81 (2013).

41. Van Der Vliet, A. & Janssen-Heininger, Y. M. W. Hydrogen peroxide as a damage signal in tissue injury and inflammation: Murderer, mediator, or messenger? *J Cell Biochem* **115**, 427–435 (2014).

42. Brazil, J. C., Quiros, M., Nusrat, A. & Parkos, C. A. Innate immune cell–epithelial crosstalk during wound repair. *Journal of Clinical Investigation* vol. 129 2983–2993 Preprint at https://doi.org/10.1172/JCI124618 (2019).

43. Ridiandries, A., Tan, J. T. M. & Bursill, C. A. The Role of Chemokines in Wound Healing. *Int J Mol Sci* **19**, (2018).

44. Dvorak, A. M. Mast cell-derived mediators of enhanced microvascular permeability, vascular permeability factor/vascular endothelial growth factor, histamine, and serotonin, cause leakage of macromolecules through a new endothelial cell permeability organelle, the vesiculo-vacuolar organelle. *Chem Immunol Allergy* **85**, 185–204 (2005).

45. Stone Ii, R. *et al.* Advancements in Regenerative Strategies Through the Continuum of Burn Care. *Front Pharmacol* **9**, 672 (2018).

46. Liu, Z.-J. *et al.* Regulation of Notch1 and Dll4 by Vascular Endothelial Growth Factor in Arterial Endothelial Cells: Implications for Modulating Arteriogenesis and Angiogenesis. *Mol Cell Biol* **23**, 14–25 (2003).

47. Hobbs, R. M., Silva-Vargas, V., Groves, R. & Watt, F. M. Expression of activated MEK1 in differentiating epidermal cells is sufficient to generate hyperproliferative and inflammatory skin lesions. *Journal of Investigative Dermatology* **123**, 503–515 (2004).

48. Pastar, I. *et al.* Epithelialization in Wound Healing: A Comprehensive Review. *Adv Wound Care (New Rochelle)* **3**, 445–464 (2014).

49. Watt, F. M., Celso, C. Lo & Silva-Vargas, V. Epidermal stem cells: an update. *Curr Opin Genet Dev* **16**, 518–524 (2006).

50. Fuchs, E. Skin stem cells: rising to the surface. *J Cell Biol* **180**, 273–284 (2008).

51. Ito, M. *et al.* Stem cells in the hair follicle bulge contribute to wound repair but not to homeostasis of the epidermis. *Nat Med* **11**, 1351–1354 (2005).

52. Gurtner, G. C., Werner, S., Barrandon, Y. & Longaker, M. T. Wound repair and regeneration. *Nature* **453**, 314–321 (2008).

53. Vig, K. *et al.* Advances in Skin Regeneration Using Tissue Engineering. *Int J Mol Sci* **18**, (2017).

54. Sierra-Sánchez, Á., Montero-Vilchez, T., Quiñones-Vico, M. I., Sanchez-Diaz, M. & Arias-Santiago, S. Current Advanced Therapies Based on Human Mesenchymal Stem Cells for Skin Diseases. *Front Cell Dev Biol* **9**, 643125 (2021).

55. Sharma, P., Kumar, P., Sharma, R., Bhatt, V. D. & Dhot, P. S. Tissue Engineering; Current Status & Futuristic Scope. *Journal of medicine and life* vol. 12 225–229 Preprint at https://doi.org/10.25122/jml-2019-0032 (2019).

56. Olson, J. L., Atala, A. & Yoo, J. J. Tissue Engineering: Current Strategies and Future Directions. *Chonnam Med J* **47**, 1 (2011).

57. Ikada, Y. Challenges in tissue engineering. *Journal of the Royal Society Interface* vol. 3 589–601 Preprint at https://doi.org/10.1098/rsif.2006.0124 (2006).

58. Sheridan, R. L. & Tompkins, R. G. Skin substitutes in burns. *Burns* **25**, 97–103 (1999).

59. Davison-Kotler, E., Sharma, V., Kang, N. V. & García-Gareta, E. A Universal Classification System of Skin Substitutes Inspired by Factorial Design. *Tissue Eng Part B Rev* **24**, 279–288 (2018).

60. Boyce, S. T. & Lalley, A. L. Tissue engineering of skin and regenerative medicine for wound care. *Burns Trauma* **6**, 4 (2018).

61. Leirós, G. J. *et al.* Dermal papilla cells improve the wound healing process and generate hair bud-like structures in grafted skin substitutes using hair follicle stem cells. *Stem Cells Transl Med* **3**, 1209–19 (2014).

62. Millán-Rivero, J. E. *et al.* Silk fibroin scaffolds seeded with Wharton's jelly mesenchymal stem cells enhance re-epithelialization and reduce formation of scar tissue after cutaneous wound healing. *Stem Cell Res Ther* **10**, (2019).

63. Sierra-Sánchez, Á. *et al.* Hyaluronic acid biomaterial for human tissue-engineered skin substitutes: Preclinical comparative *in vivo* study of wound healing. *Journal of the European Academy of Dermatology and Venereology* **34**, 2414–2427 (2020).

64. Garzón, I. *et al.* Wharton's Jelly Stem Cells: A Novel Cell Source for Oral Mucosa and Skin Epithelia Regeneration. *Stem Cells Transl Med* **2**, 625–632 (2013).

65. Mohd Hilmi, A. B., Halim, A. S., Jaafar, H., Asiah, A. B. & Hassan, A. Chitosan dermal substitute and Chitosan skin substitute contribute to accelerated full-thickness wound healing in irradiated rats. *Biomed Res Int* **2013**, (2013).

66. Salerno, S. *et al.* Dermal-epidermal membrane systems by using human keratinocytes and mesenchymal stem cells isolated from dermis. *Materials Science and Engineering C* **71**, 943–953 (2017).

67. Mohd Hilmi, A. B., Hassan, A. & Halim, A. S. A Bilayer Engineered Skin Substitute for Wound Repair in an Irradiation-Impeded Healing Model on Rat. *Adv Wound Care (New Rochelle)* **4**, 312–320 (2015).

68. Dong, C., Lv, Y., Dong, C. & Lv, Y. Application of Collagen Scaffold in Tissue Engineering: Recent Advances and New Perspectives. *Polymers (Basel)* **8**, 42 (2016).

69. Gardien, K. L. M. *et al.* Outcome of burns treated with autologous cultured proliferating epidermal cells: A prospective randomized multicenter intrapatient comparative trial. *Cell Transplant* **25**, 437–448 (2016).

70. Kashiwa, N. *et al.* Treatment of full-thickness skin defect with concomitant grafting of 6-fold extended mesh auto-skin and allogeneic cultured dermal substitute. *Artif Organs* **28**, 444–450 (2004).

71. Hasegawa, T. *et al.* An allogeneic cultured dermal substitute suitable for treating intractable skin ulcers and large skin defects prior to autologous skin grafting: Three case reports. *Journal of Dermatology* **32**, 715–720 (2005).

72. Yonezawa, M. *et al.* Clinical study with allogeneic cultured dermal substitutes for chronic leg ulcers. *Int J Dermatol* **46**, 36–42 (2007).

73. Yamada, N., Uchinuma, E., Matsumoto, Y. & Kuroyanagi, Y. Comparative evaluation of re-epithelialization promoted by fresh or cryopreserved cultured dermal substitute. *Journal of Artificial Organs* **11**, 221–224 (2008).

74. Yamada, N., Uchinuma, E. & Kuroyanagi, Y. Clinical trial of allogeneic cultured dermal substitutes for intractable skin ulcers. *Journal of Artificial Organs* **15**, 193–199 (2012).

75. Taniguchi, T., Amoh, Y., Tanabe, K., Katsuoka, K. & Kuroyanagi, Y. Treatment of intractable skin ulcers caused by vascular insufficiency with allogeneic cultured dermal substitute: A report of eight cases. *Journal of Artificial Organs* **15**, 77–82 (2012).

76. Hansbrough, J. F., Boyce, S. T., Cooper, M. L. & Foreman, T. J. Burn Wound Closure With Cultured Autologous Keratinocytes and Fibroblasts Attached to a Collagen-Glycosaminoglycan Substrate. *JAMA: The Journal of the American Medical Association* **262**, 2125–2130 (1989).

77. Kuroyanagi, Y. *et al.* A cultured skin substitute composed of fibroblasts and keratinocytes with a collagen matrix: Preliminary results of clinical trials. *Ann Plast Surg* **31**, 340–351 (1993).

78. Boyce, S. T. *et al.* Comparative assessment of cultured skin substitutes and native skin autograft for treatment of full-thickness burns. *Ann Surg* **222**, 743–752 (1995).

79. Dana Harriger, M., Warden, G. D., Greenhalgh, D. G., Kagan, R. J. & Boyce, S. T. Pigmentation and microanatomy of skin regenerated from composite grafts of cultured cells and biopolymers applied to full-thickness burn wounds. *Transplantation* **59**, 702–707 (1995).

80. Muhart, M., McFalls, S., Kirsner, R., Kerdel, F. & Eaglstein, W. H. Bioengineered skin [2]. *Lancet* **350**, 1142 (1997).

81. Boyce, S. T., Kagan, R. J., Meyer, N. A., Yakuboff, K. P. & Warden, G. D. Cultured skin substitutes combined with integra artificial skin to replace native skin autograft and allograft for the closure of excised full- thickness burns. in *Journal of Burn Care and Rehabilitation* vol. 20 453–461 (Mosby Inc., 1999).

82. Boyce, S. T. *et al.* Cultured skin substitutes reduce donor skin harvesting for closure of excised, full-thickness burns. *Ann Surg* **235**, 269–279 (2002).

83. Nanchahal, J., Dover, R. & Otto, W. R. Allogeneic skin substitutes applied to burns patients. *Burns* **28**, 254–257 (2002).

84. Boyce, S. T. *et al.* Cultured skin substitutes reduce requirements for harvesting of skin autograft for closure of excised, full-thickness burns. *Journal of Trauma - Injury, Infection and Critical Care* **60**, 821–829 (2006).

85. Golinski, P. *et al.* Development and characterization of an engraftable tissue-cultured skin autograft: Alternative treatment for severe electrical injuries? *Cells Tissues Organs* **200**, 227–239 (2015).

86. Boyce, S. T. *et al.* Randomized, Paired-Site Comparison of Autologous Engineered Skin Substitutes and Split-Thickness Skin Graft for Closure of Extensive, Full-Thickness Burns. in *Journal of Burn Care and Research* vol. 38 61–70 (Lippincott Williams and Wilkins, 2017).

87. Meuli, M. *et al.* A Cultured Autologous Dermo-epidermal Skin Substitute for Full-Thickness Skin Defects: A Phase I, Open, Prospective Clinical Trial in Children. *Plast Reconstr Surg* **144**, 188–198 (2019).

88. Pellegrini, G. *et al.* The control of epidermal stem cells (holoclones) in the treatment of massive full-thickness burns with autologous keratinocytes cultured on fibrin. *Transplantation* **68**, 868–879 (1999).

89. Ronfard, V., Rives, J. M., Neveux, Y., Carsin, H. & Barrandon, Y. Long-term regeneration of human epidermis on third degree burns transplanted with autologous cultured epithelium grown on a fibrin matrix. *Transplantation* **70**, 1588–98 (2000).

90. Llames, S. G. *et al.* Human plasma as a dermal scaffold for the generation of a completely autologous bioengineered skin. *Transplantation* **77**, 350–355 (2004).

91. Llames, S. *et al.* Clinical results of an autologous engineered skin. *Cell Tissue Bank* **7**, 47–53 (2006).

92. Gómez, C. *et al.* Use of an autologous bioengineered composite skin in extensive burns: Clinical and functional outcomes. A multicentric study. *Burns* **37**, 580–589 (2011).

93. Kljenak, A. *et al.* Fibrin gel as a scaffold for skin substitute – production and clinical experience. *Acta Clin Croat* **55**, 279–89 (2016).

94. Fernández-González, A. *et al.* Clinical, histological and homeostasis evaluation of an autologous tissue bio-engineered skin substitute in a patient with 70% of total body surface area (TBSA) burn. *Cytotherapy* **19**, S233 (2017).

95. Scuderi, N., Anniboletti, T., Carlesimo, B. & Onesti, M. G. Clinical application of autologous three-cellular cultured skin substitutes based on esterified hyaluronic acid scaffold: Our experience. *In Vivo (Brooklyn)* **23**, 991–1003 (2009).

96. Mineo, A., Suzuki, R. & Kuroyanagi, Y. Development of an artificial dermis composed of hyaluronic acid and collagen. *J Biomater Sci Polym Ed* **24**, 726–740 (2013).

97. Rodríguez-Cabello, J. C., González de Torre, I., Ibañez-Fonseca, A. & Alonso, M. Bioactive scaffolds based on elastin-like materials for wound healing. *Adv Drug Deliv Rev* **129**, 118–133 (2018).

98. Momeni, M. *et al.* A randomized, double-blind, phase I clinical trial of fetal cell-based skin substitutes on healing of donor sites in burn patients. *Burns* **45**, 914–922 (2019).

99. Hashemi, S. S. *et al.* The healing effect of Wharton's jelly stem cells seeded on biological scaffold in chronic skin ulcers: A randomized clinical trial. *J Cosmet Dermatol* **18**, 1961–1967 (2019).

100. Rennekampff, H. O., Kiessig, V., Griffey, S., Greenleaf, G. & Hansbrough, J. F. Acellular human dermis promotes cultured keratinocyte engraftment. *Journal of Burn Care and Rehabilitation* **18**, 535–544 (1997).

101. Boa, O. *et al.* Prospective study on the treatment of lower-extremity chronic venous and mixed ulcers using tissue-engineered skin substitute made by the self-assembly approach. *Adv Skin Wound Care* **26**, 400–409 (2013).

102. Takami, Y., Yamaguchi, R., Ono, S. & Hyakusoku, H. Clinical application and histological properties of autologous tissue-engineered skin equivalents using an acellular dermal matrix. *Journal of Nippon Medical School* **81**, 356–366 (2014).

103. Chaudhari, A. A. *et al.* Future prospects for scaffolding methods and biomaterials in skin tissue engineering: A review. *International Journal of Molecular Sciences* vol. 17 Preprint at https://doi.org/10.3390/ijms17121974 (2016).

104. Vojtassák, J. *et al.* Autologous biograft and mesenchymal stem cells in treatment of the diabetic foot. *Neuro Endocrinol Lett* **27 Suppl 2**, 134–7 (2006).

105. Yoshikawa, T. *et al.* Wound Therapy by Marrow Mesenchymal Cell Transplantation. *Plast Reconstr Surg* **121**, 860–877 (2008).

106. Arkoulis, N., Watson, S. & Weiler-Mithoff, E. Stem cell enriched dermal substitutes for the treatment of late burn contractures in patients with major burns. *Burns* vol. 44 724–726 Preprint at https://doi.org/10.1016/j.burns.2017.09.026 (2018).

107. Pajardi, G. *et al.* Skin substitutes based on allogenic fibroblasts or keratinocytes for chronic wounds not responding to conventional therapy: A retrospective observational study. *Int Wound J* **13**, 44–52 (2016).

108. Stessuk, T. *et al.* A topical cell therapy approach for diabetic chronic ulcers: Effects of mesenchymal stromal cells associated with platelet-rich plasma. *J Cosmet Dermatol* (2020) doi:10.1111/jocd.13321.

109. Sheridan, R. L. *et al.* Initial experience with a composite autologous skin substitute. *Burns* **27**, 421–424 (2001).

110. Morimoto, N. *et al.* An exploratory clinical study on the safety and efficacy of an autologous fibroblast-seeded artificial skin cultured with animal product-free medium in patients with diabetic foot ulcers. *Int Wound J* **11**, 183–189 (2014).

111. Xu, Y., Huang, S. & Fu, X. Autologous transplantation of bone marrow-derived mesenchymal stem cells: a promising therapeutic strategy for prevention of skin-graft contraction. *Clin Exp Dermatol* **37**, 497–500 (2012).

112. Phelan, K. & May, K. M. Mammalian Cell Tissue Culture Techniques. *Curr Protoc Mol Biol* **117**, (2017).

113. Combes, R. D. The use of human cells in biomedical research and testing. *Altern Lab Anim* **32 Suppl 1A**, 43–49 (2004).

114. Advanced therapy medicinal products: Overview | European Medicines Agency. https://www.ema.europa.eu/en/human-regulatory/overview/advanced-therapy-medicinal-products-overview.

115. Philippeos, C., Hughes, R. D., Dhawan, A. & Mitry, R. R. Introduction to cell culture. *Methods Mol Biol* **806**, 1–13 (2012).

116. Sierra-Sánchez, Á., Kim, K. H., Blasco-Morente, G. & Arias-Santiago, S. Cellular human tissue-engineered skin substitutes investigated for deep and difficult to heal injuries. *NPJ Regen Med* **6**, (2021).

117. Ścieżyńska, A. *et al.* Isolation and culture of human primary keratinocytes—a methods review. *Exp Dermatol* **28**, 107–112 (2019).

118. Kino-oka, M. & Taya, M. Recent developments in processing systems for cell and tissue cultures toward therapeutic application. *J Biosci Bioeng* **108**, 267–276 (2009).

119. Kino-oka, M., Mizutani, M. & Medcalf, N. Cell manufacturability. *Cell Gene Ther Insights* **5**, 1347–1359 (2019).

120. Rheinwald, J. G. & Green, H. Serial cultivation of strains of human epidermal keratinocytes: the formation of keratinizing colonies from single cells. *Cell* **6**, 331–343 (1975).

121. Chocarro-Wrona, C., López-Ruiz, E., Perán, M., Gálvez-Martín, P. & Marchal, J. A. Therapeutic strategies for skin regeneration based on biomedical substitutes. *Journal of the European Academy of Dermatology and Venereology* **33**, 484–496 (2019).

122. Dill, V. & Mörgelin, M. Biological dermal templates with native collagen scaffolds provide guiding ridges for invading cells and may promote structured dermal wound healing. *Int Wound J* iwj.13314 (2020) doi:10.1111/iwj.13314.

123. O'Connor, N. E., Mulliken, J. B., Banks-Schlegel, S., Kehinde, O. & Green, H. Grafting of burns with cultured epithelium prepared from autologous epidermal cells. *The Lancet* **317**, 75–78 (1981).

124. Teepe, R. G. C. *et al.* The use of cultured autologous epidermis in the treatment of extensive burn wounds. *Journal of Trauma - Injury, Infection and Critical Care* **30**, 269–275 (1990).

125. Blight, A., Mountford, E. M., Cheshire, I. M., Clancy, J. M. P. & Levick, P. L. Treatment of full skin thickness burn injury using cultured epithelial grafts. *Burns* **17**, 495–498 (1991).

126. Donati, L., Magliacani, G., Bormioli, M., Signorini, M. & Baruffaldi Preis, F. W. Clinical experiences with keratinocyte grafts. *Burns* **18**, S19–S26 (1992).

127. Rue, L. W., Cioffi, W. G., McManus, W. F. & Pruitt, B. A. Wound closure and outcome in extensively burned patients treated with cultured autologous keratinocytes. *Journal of Trauma - Injury, Infection and Critical Care* **34**, 662–668 (1993).

128. Hickerson, W. L., Compton, C., Fletchall, S. & Smith, L. R. Cultured epidermal autografts and allodermis combination for permanent burn wound coverage. *Burns* **20 Suppl 1**, S52-5; discussion S55-6 (1994).

129. Williamson, J. S., Snelling, C. F., Clugston, P., Macdonald, I. B. & Germann, E. Cultured epithelial autograft: five years of clinical experience with twenty-eight patients. *J Trauma* **39**, 309–19 (1995).

130. Paddle-Ledinek, J. E., Cruickshank, D. G. & Masterton, J. P. Skin replacement by cultured keratinocyte grafts: An Australian experience. *Burns* **23**, 204–211 (1997).

131. Barret, J. P., Wolf, S. E., Desai, M. H. & Herndon, D. N. Cost-efficacy of cultured epidermal autografts in massive pediatric burns. *Ann Surg* **231**, 869–876 (2000).

132. Yamaguchi, Y. *et al.* Epithelial-mesenchymal interactions in wounds: treatment of palmoplantar wounds by nonpalmoplantar pure epidermal sheet grafts. *Arch Dermatol* **137**, 621–8 (2001).

133. Elliott, M. & Vandervord, J. Initial experience with cultured epithelial autografts in massively burnt patients. *ANZ J Surg* **72**, 893–895 (2002).

134. You, H. J., Han, S. K. & Rhie, J. W. Randomised controlled clinical trial for autologous fibroblast-hyaluronic acid complex in treating diabetic foot ulcers. *J Wound Care* **23**, 521–530 (2014).

135. Galipeau, J. & Sensébé, L. Mesenchymal Stromal Cells: Clinical Challenges and Therapeutic Opportunities. *Cell Stem Cell* **22**, 824–833 (2018).

136. Sun, B. K., Siprashvili, Z. & Khavari, P. A. Advances in skin grafting and treatment of cutaneous wounds. *Science* **346**, 941–5 (2014).

137. Bell, E., Ehrlich, H. P., Buttle, D. J. & Nakatsuji, T. Living tissue formed in vitro and accepted as skin-equivalent tissue of full thickness. *Science* **211**, 1052–4 (1981).

138. Liu, Y. *et al.* Reconstruction of a tissue-engineered skin containing melanocytes. *Cell Biol Int* **31**, 985–990 (2007).

139. Biedermann, T. *et al.* Tissue-engineered dermo-epidermal skin analogs exhibit de novo formation of a near natural neurovascular link 10 weeks after transplantation. *Pediatr Surg Int* **30**, 165–172 (2014).

140. Biedermann, T., Klar, A. S., Böttcher-Haberzeth, S., Reichmann, E. & Meuli, M. Myelinated and unmyelinated nerve fibers reinnervate tissue-engineered dermo-epidermal human skin analogs in an in vivo model. *Pediatr Surg Int* **32**, 1183–1191 (2016).

141. Klar, A. S. *et al.* Differential expression of granulocyte, macrophage, and hypoxia markers during early and late wound healing stages following transplantation of tissue-engineered skin substitutes of human origin. *Pediatr Surg Int* **30**, 1257–64 (2014).

142. Boyce, S. T. *et al.* Restoration of cutaneous pigmentation by transplantation to mice of isogeneic human melanocytes in dermal-epidermal engineered skin substitutes. *Pigment Cell Melanoma Res* **30**, 531–540 (2017).

143. Supp, D. M. *et al.* Light or Dark Pigmentation of Engineered Skin Substitutes Containing Melanocytes Protects Against Ultraviolet Light-Induced DNA Damage In Vivo. *Journal of Burn Care & Research* **41**, 751–760 (2020).

144. Goyer, B. *et al.* Impact of ultraviolet radiation on dermal and epidermal DNA damage in a human pigmented bilayered skin substitute. *J Tissue Eng Regen Med* **13**, 2300–2311 (2019).

145. Bechetoille, N. *et al.* Effects of solar ultraviolet radiation on engineered human skin equivalent containing both langerhans cells and dermal dendritic cells. *Tissue Eng* **13**, 2667–2679 (2007).

146. Laubach, V. *et al.* Integration of Langerhans-like cells into a human skin equivalent. *Arch Dermatol Res* **303**, 135–139 (2011).

147. Fransson, J., Heffler, L. C., Linder, M. T. & Scheynius, A. Culture of human epidermal Langerhans cells in a skin equivalent. *British Journal of Dermatology* **139**, 598–604 (1998).

148. Régnier, M., Patwardhan, A., Scheynius, A. & Schmidt, R. Reconstructed human epidermis composed of keratinocytes, melanocytes and Langerhans cells. *Med Biol Eng Comput* **36**, 821–4 (1998).

149. Hafemann, B. *et al.* Use of a collagen/elastin-membrane for the tissue engineering of dermis. *Burns* **25**, 373–384 (1999).

150. Centanni, J. M. *et al.* Stratagraft skin substitute is well-tolerated and is not acutely immunogenic in patients with traumatic wounds: Results from a prospective, randomized, controlled dose escalation trial. *Ann Surg* **253**, 672–683 (2011).

151. Hahn, J. M. *et al.* Identification of Merkel cells associated with neurons in engineered skin substitutes after grafting to full thickness wounds. *PLoS One* **14**, e0213325 (2019).

152. Ojeh, N., Pastar, I., Tomic-Canic, M. & Stojadinovic, O. Stem Cells in Skin Regeneration, Wound Healing, and Their Clinical Applications. *OPEN ACCESS Int. J. Mol. Sci* **16**, 16 (2015).

153. Shi, C., Zhu, Y., Su, Y. & Cheng, T. Stem cells and their applications in skin-cell therapy. *Trends Biotechnol* **24**, 48–52 (2006).

154. Martin, M. T., Vulin, A. & Hendry, J. H. Human epidermal stem cells: Role in adverse skin reactions and carcinogenesis from radiation. *Mutat Res Rev Mutat Res* **770**, 349–368 (2016).

155. Potten, C. S. & Booth, C. Keratinocyte Stem Cells: a Commentary. *Journal of Investigative Dermatology* **119**, 888–899 (2002).

156. Sellheyer, K. & Krahl, D. Skin mesenchymal stem cells: Prospects for clinical dermatology. *J Am Acad Dermatol* **63**, 859–865 (2010).

157. Higgins, C. A. *et al.* Multifaceted role of hair follicle dermal cells in bioengineered skins. *British Journal of Dermatology* **176**, 1259–1269 (2017).

158. Michalak-Micka, K. *et al.* Impact of human mesenchymal cells of different body site origins on the maturation of dermo-epidermal skin substitutes. *Pediatr Surg Int* **35**, 121–127 (2019).

159. Zomer, H. D., Jeremias, T. da S., Ratner, B. & Trentin, A. G. Mesenchymal stromal cells from dermal and adipose tissues induce macrophage polarization to a pro-repair phenotype and improve skin wound healing. *Cytotherapy* **22**, 247–260 (2020).

160. Takahashi, K. *et al.* Induction of pluripotent stem cells from adult human fibroblasts by defined factors. *Cell* **131**, 861–72 (2007).

161. Itoh, M. *et al.* Generation of 3D Skin Equivalents Fully Reconstituted from Human Induced Pluripotent Stem Cells (iPSCs). *PLoS One* **8**, e77673 (2013).

162. Gledhill, K. *et al.* Melanin Transfer in Human 3D Skin Equivalents Generated Exclusively from Induced Pluripotent Stem Cells. *PLoS One* **10**, e0136713 (2015).

163. Petrova, A. *et al.* 3D In Vitro Model of a Functional Epidermal Permeability Barrier from Human Embryonic Stem Cells and Induced Pluripotent Stem Cells. *Stem Cell Reports* **2**, 675–689 (2014).

164. Kim, Y. *et al.* Establishment of a complex skin structure via layered co-culture of keratinocytes and fibroblasts derived from induced pluripotent stem cells. *Stem Cell Res Ther* **9**, 217 (2018).

165. Muller, Q. *et al.* Development of an innervated tissue-engineered skin with human sensory neurons and Schwann cells differentiated from iPS cells. *Acta Biomater* **82**, 93–101 (2018).

166. Mushahary, D., Spittler, A., Kasper, C., Weber, V. & Charwat, V. Isolation, cultivation, and characterization of human mesenchymal stem cells. *Cytometry A* **93**, 19–31 (2018).

167. Lin, Y. & Hogan, W. J. Clinical Application of Mesenchymal Stem Cells in the Treatment and Prevention of Graft-versus-Host Disease. *Adv Hematol* **2011**, 1–17 (2011).

168. Liang, J. *et al.* Allogenic mesenchymal stem cells transplantation in refractory systemic lupus erythematosus: a pilot clinical study. *Ann Rheum Dis* **69**, 1423–1429 (2010).

169. Koppula, P. R., Chelluri, L. K., Polisetti, N. & Vemuganti, G. K. Histocompatibility testing of cultivated human bone marrow stromal cells – A promising step towards pre-clinical screening for allogeneic stem cell therapy. *Cell Immunol* **259**, 61–65 (2009).

170. Squillaro, T., Peluso, G. & Galderisi, U. Clinical Trials with Mesenchymal Stem Cells: An Update. *Cell Transplant* **25**, 829–848 (2016).

171. Ankrum, J. A., Ong, J. F. & Karp, J. M. Mesenchymal stem cells: Immune evasive, not immune privileged. *Nat Biotechnol* **32**, 252–260 (2014).

172. Lohan, P., Treacy, O., Griffin, M. D., Ritter, T. & Ryan, A. E. Anti-donor immune responses elicited by allogeneic mesenchymal stem cells and their extracellular vesicles: Are we still learning? *Front Immunol* **8**, (2017).

173. Zangi, L. *et al.* Direct imaging of immune rejection and memory induction by allogeneic mesenchymal stromal cells. *Stem Cells* **27**, 2865–2874 (2009).

174. Dixit, S. *et al.* Immunological challenges associated with artificial skin grafts: Available solutions and stem cells in future design of synthetic skin. *Journal of Biological Engineering* vol. 11 (2017).

175. Di Nicola, M. *et al.* Human bone marrow stromal cells suppress T-lymphocyte proliferation induced by cellular or nonspecific mitogenic stimuli. *Blood* **99**, 3838–43 (2002).

176. Seo, B. F., Kim, K. J., Kim, M. K. & Rhie, J. W. The effects of human keratinocyte coculture on human adipose-derived stem cells. *Int Wound J* **13**, 630–635 (2016).

177. He, L. J. *et al.* Full-thickness tissue engineered skin constructed with autogenic bone marrow mesenchymal stem cells. *Sci China C Life Sci* **50**, 429–437 (2007).

178. Zuk, P. A. *et al.* Human adipose tissue is a source of multipotent stem cells. *Mol Biol Cell* **13**, 4279–95 (2002).

179. Martin-Piedra, M. *et al.* Effective use of mesenchymal stem cells in human skin substitutes generated by tissue engineering. *Eur Cell Mater* **37**, 233–249 (2019).

180. Ojeh, N. O. & Navsaria, H. A. An in vitro skin model to study the effect of mesenchymal stem cells in wound healing and epidermal regeneration. *J Biomed Mater Res A* **102**, 2785–2792 (2014).

181. Kalaszczynska, I. & Ferdyn, K. Wharton's jelly derived mesenchymal stem cells: future of regenerative medicine? Recent findings and clinical significance. *Biomed Res Int* **2015**, 430847 (2015).

182. Ertl, J. *et al.* Comparative study of regenerative effects of mesenchymal stem cells derived from placental amnion, chorion and umbilical cord on dermal wounds. *Placenta* **65**, 37–46 (2018).

183. Shi, S., Jia, S., Liu, J. & Chen, G. Accelerated Regeneration of Skin Injury by Co-transplantation of Mesenchymal Stem Cells from Wharton's Jelly of the Human Umbilical Cord Mixed with Microparticles. *Cell Biochem Biophys* **71**, 951–956 (2015).

184. Chavez-Munoz, C. *et al.* Transdifferentiation of adipose-derived stem cells into keratinocyte-like cells: engineering a stratified epidermis. *PLoS One* **8**, e80587 (2013).

185. Ebrahimian, T. G. *et al.* Cell Therapy Based on Adipose Tissue-Derived Stromal Cells Promotes Physiological and Pathological Wound Healing. *Arterioscler Thromb Vasc Biol* **29**, 503–510 (2009).

186. Paganelli, A. *et al.* In vitro Engineering of a Skin Substitute Based on Adipose-Derived Stem Cells. *Cells Tissues Organs* **207**, 46–57 (2019).

187. Moriyama, M. *et al.* Adipose-derived stromal/stem cells improve epidermal homeostasis. *Sci Rep* **9**, 18371 (2019).

188. Motamed, S. *et al.* Cell-based skin substitutes accelerate regeneration of extensive burn wounds in rats. *Am J Surg* **214**, 762–769 (2017).

189. Zhang, A.-J., Jiang, T., Li, Q., Jin, P.-S. & Tan, Q. Experimental research on ADSCs-NCSS in wound repair. *Exp Ther Med* **16**, 4429–4436 (2018).

190. Mendez, J. J. *et al.* Mesenchymal stromal cells form vascular tubes when placed in fibrin sealant and accelerate wound healing in vivo. *Biomaterials* **40**, 61–71 (2015).

191. Huang, S.-P. *et al.* Adipose-Derived Stem Cells Seeded on Acellular Dermal Matrix Grafts Enhance Wound Healing in a Murine Model of a Full-Thickness Defect. *Ann Plast Surg* **69**, 656–662 (2012).

192. Sánchez-Muñoz, I. *et al.* The use of adipose mesenchymal stem cells and human umbilical vascular endothelial cells on a fibrin matrix for endothelialized skin substitute. *Tissue Eng Part A* **21**, 214–223 (2015).

193. Klar, A. S. *et al.* Human Adipose Mesenchymal Cells Inhibit Melanocyte Differentiation and the Pigmentation of Human Skin via Increased Expression of TGF-β1. *J Invest Dermatol* **137**, 2560–2569 (2017).

194. Moon, K. C. *et al.* Potential of allogeneic adipose-derived stem cell–hydrogel complex for treating diabetic foot ulcers. *Diabetes* **68**, 837–846 (2019).

195. Ratner, B. D. & Bryant, S. J. Biomaterials: Where We Have Been and Where We Are Going. *Annu Rev Biomed Eng* **6**, 41–75 (2004).

196. Kulinets, I. Biomaterials and their applications in medicine. in *Regulatory Affairs for Biomaterials and Medical Devices* 1–10 (Elsevier Inc., 2015). doi:10.1533/9780857099204.1.

197. Williams, D. F. & European Society for Biomaterials. *Definitions in biomaterials: proceedings of a consensus conference of the European Society for Biomaterials, Chester, England, March 3-5, 1986*. (Elsevier, 1987).

198. Ratner, B. D., Hoffman, A. S., Schoen, F. J. & Lemons, J. E. *Biomaterials Science: An Introduction to Materials: Third Edition*. *Biomaterials Science: An Introduction to Materials: Third Edition* (Elsevier Inc., 2013). doi:10.1016/B978-0-08-087780-8.00148-0.

199. Sheikholeslam, M., Wright, M. E. E., Jeschke, M. G. & Amini-Nik, S. Biomaterials for Skin Substitutes. *Adv Healthc Mater* **7**, 1700897 (2018).

200. Lu, G. & Huang, S. Bioengineered skin substitutes: Key elements and novel design for biomedical applications. *International Wound Journal* vol. 10 365–371 Preprint at https://doi.org/10.1111/j.1742-481X.2012.01105.x (2013).

201. Goodarzi, P. *et al.* Tissue engineered skin substitutes. in *Advances in Experimental Medicine and Biology* vol. 1107 143–188 (Springer New York LLC, 2018).

202. Place, E. S., Evans, N. D. & Stevens, M. M. Complexity in biomaterials for tissue engineering. *Nat Mater* **8**, 457–470 (2009).

203. Bakhshandeh, B. *et al.* Tissue engineering; strategies, tissues, and biomaterials. *Biotechnol Genet Eng Rev* **33**, 144–172 (2017).

204. Shin, H., Jo, S. & Mikos, A. G. Biomimetic materials for tissue engineering. *Biomaterials* **24**, 4353–4364 (2003).

205. Yu, J. R. *et al.* Current and Future Perspectives on Skin Tissue Engineering: Key Features of Biomedical Research, Translational Assessment, and Clinical Application. *Adv Healthc Mater* **8**, 1801471 (2019).

206. Chattopadhyay, S. & Raines, R. T. Review collagen-based biomaterials for wound healing. *Biopolymers* vol. 101 821–833 Preprint at https://doi.org/10.1002/bip.22486 (2014).

207. Bi, Y., Patra, P. & Faezipour, M. Structure of collagen-glycosaminoglycan matrix and the influence to its integrity and stability. in *2014 36th Annual International Conference of the IEEE Engineering in Medicine and Biology Society, EMBC 2014* vol. 2014 3949–3952 (Institute of Electrical and Electronics Engineers Inc., 2014).

208. Lee, D. H., Oh, J. H. & Chung, J. H. Glycosaminoglycan and proteoglycan in skin aging. *Journal of Dermatological Science* vol. 83 174–181 Preprint at https://doi.org/10.1016/j.jdermsci.2016.05.016 (2016).

209. Fallacara, A., Manfredini, S., Durini, E. & Vertuani, S. Hyaluronic Acid Fillers in Soft Tissue Regeneration. *Facial Plastic Surgery* **33**, 087–096 (2017).

210. Yang, J.-A. *et al.* Transdermal delivery of hyaluronic acid – Human growth hormone conjugate. *Biomaterials* **33**, 5947–5954 (2012).

211. Greene, J. J. & Sidle, D. M. The Hyaluronic Acid Fillers. *Facial Plast Surg Clin North Am* **23**, 423–432 (2015).

212. Nicoletti, G. *et al.* Long-term *in vivo* assessment of bioengineered skin substitutes: a clinical study. *J Tissue Eng Regen Med* **9**, 460–468 (2015).

213. Nicoletti, G. *et al.* Versatile use of dermal substitutes: A retrospective survey of 127 consecutive cases. *Indian Journal of Plastic Surgery* vol. 51 46–53 Preprint at https://doi.org/10.4103/ijps.IJPS_217_17 (2018).

214. Chen, W. Y. & Abatangelo, G. Functions of hyaluronan in wound repair. *Wound repair and regeneration* **7**, 79–89 (1999).

215. Alexaline, M. M. *et al.* Influence of fibrin matrices and their released factors on epidermal substitute phenotype and engraftment. *J Tissue Eng Regen Med* **13**, 1362–1374 (2019).

216. Lo, V. & Pope, E. Amniotic membrane use in dermatology. *International Journal of Dermatology* vol. 48 935–940 Preprint at https://doi.org/10.1111/j.1365-4632.2009.04173.x (2009).

217. Larouche, D. *et al.* Improved Methods to Produce Tissue-Engineered Skin Substitutes Suitable for the Permanent Closure of Full-Thickness Skin Injuries. *Biores Open Access* **5**, 320–329 (2016).

218. Anderson, N. L. *et al.* The human plasma proteome: a nonredundant list developed by combination of four separate sources. *Mol Cell Proteomics* **3**, 311–26 (2004).

219. Viode, A. *et al.* A simple, time- and cost-effective, high-throughput depletion strategy for deep plasma proteomics. *Sci Adv* **9**, eadf9717 (2023).

220. Barreda, L. *et al.* Human plasma gels: Their preparation and rheological characterization for cell culture applications in tissue engineering. *J Mech Behav Biomed Mater* **89**, 107–113 (2019).

221. Murphy, K. C. & Leach, J. K. A reproducible, high throughput method for fabricating fibrin gels. *BMC Res Notes* **5**, 423 (2012).

222. Siebenlist, K. R. & Mosesson, M. W. Progressive cross-linking of fibrin gamma chains increases resistance to fibrinolysis. *Journal of Biological Chemistry* **269**, 28414–28419 (1994).

223. Cornwell, K. G. & Pins, G. D. Discrete crosslinked fibrin microthread scaffolds for tissue regeneration. *J Biomed Mater Res A* **82**, 104–112 (2007).

224. Carr, M. E., Gabriel, D. A. & McDonagh, J. Influence of Ca2+ on the structure of reptilase-derived and thrombin-derived fibrin gels. *Biochemical Journal* **239**, 513 (1986).

225. Okada, M. & Blombäck, B. Calcium and fibrin gel structure. *Thromb Res* **29**, 269–280 (1983).

226. Green, D. Coagulation cascade. *Hemodial Int* **10 Suppl 2**, (2006).

227. Weisel, J. W. Fibrinogen and fibrin. *Adv Protein Chem* **70**, 247–299 (2005).

228. Ahmed, T. A. E., Dare, E. V. & Hincke, M. Fibrin: a versatile scaffold for tissue engineering applications. *Tissue Eng Part B Rev* **14**, 199–215 (2008).

229. Brown, A. C. & Barker, T. H. Fibrin-based biomaterials: modulation of macroscopic properties through rational design at the molecular level. *Acta Biomater* **10**, 1502–1514 (2014).

230. Weisel, J. W. & Litvinov, R. I. Fibrin Formation, Structure and Properties. *Subcell Biochem* **82**, 405 (2017).

231. Chernysh, I. N. & Weisel, J. W. Dynamic imaging of fibrin network formation correlated with other measures of polymerization. *Blood* **111**, 4854 (2008).

232. Noori, A., Ashrafi, S. J., Vaez-Ghaemi, R., Hatamian-Zaremi, A. & Webster, T. J. A review of fibrin and fibrin composites for bone tissue engineering. *Int J Nanomedicine* **12**, 4937–4961 (2017).

233. Weisel, J. W. Structure of fibrin: impact on clot stability. *J Thromb Haemost* **5 Suppl 1**, 116–124 (2007).

234. Kim, O. V., Litvinov, R. I., Weisel, J. W. & Alber, M. S. Structural basis for the nonlinear mechanics of fibrin networks under compression. *Biomaterials* **35**, 6739–6749 (2014).

235. Kim, O. V. *et al.* Foam-like compression behavior of fibrin networks. *Biomech Model Mechanobiol* **15**, 213 (2016).

236. Janmey, P. A., Amis, E. J. & Ferry, J. D. Rheology of Fibrin Clots. VI. Stress Relaxation, Creep, and Differential Dynamic Modulus of Fine Clots in Large Shearing Deformations. *J Rheol (N Y N Y)* **27**, 135–153 (1983).

237. Duong, H., Wu, B. & Tawil, B. Modulation of 3D Fibrin Matrix Stiffness by Intrinsic Fibrinogen–Thrombin Compositions and by Extrinsic Cellular Activity. *Tissue Eng Part A* **15**, 1865 (2009).

238. Sander, E. A., Barocas, V. H. & Tranquillo, R. T. Initial Fiber Alignment Pattern Alters Extracellular Matrix Synthesis in Fibroblast Populated Fibrin Gel Cruciforms and Correlates with Predicted Tension. *Ann Biomed Eng* **39**, 714 (2011).

239. Namani, R., Wood, M. D., Sakiyama-Elbert, S. E. & Bayly, P. V. Anisotropic mechanical properties of magnetically aligned fibrin gels measured by magnetic resonance elastography. *J Biomech* **42**, 2047–2053 (2009).

240. Gersh, K. C., Edmondson, K. E. & Weisel, J. W. Flow rate and fibrin fiber alignment. *J Thromb Haemost* **8**, 2826–2828 (2010).

241. Carlisle, C. R. *et al.* The mechanical properties of individual, electrospun fibrinogen fibers. *Biomaterials* **30**, 1205 (2009).

242. Scionti, G. *et al.* Effect of the hydration on the biomechanical properties in a fibrin-agarose tissue-like model. *J Biomed Mater Res A* **102**, 2573–2582 (2014).

243. Ahmann, K. A., Weinbaum, J. S., Johnson, S. L. & Tranquillo, R. T. Fibrin Degradation Enhances Vascular Smooth Muscle Cell Proliferation and Matrix Deposition in Fibrin-Based Tissue Constructs Fabricated In Vitro. *Tissue Eng Part A* **16**, 3261 (2010).

244. Currie, L. J., Sharpe, J. R. & Martin, R. The use of fibrin glue in skin grafts and tissue-engineered skin replacements: a review. *Plast Reconstr Surg* **108**, 1713–1726 (2001).

245. Gorodetsky, R. *et al.* Fibrin microbeads (FMB) as biodegradable carriers for culturing cells and for accelerating wound healing. *J Invest Dermatol* **112**, 866–872 (1999).

246. DeBlois, C., Côté, M. F. & Doillon, C. J. Heparin-fibroblast growth factor-fibrin complex: in vitro and in vivo applications to collagen-based materials. *Biomaterials* **15**, 665–672 (1994).

247. Fournier, N. & Doillon, C. J. Biological molecule-impregnated polyester: An in vivo angiogenesis study. *Biomaterials* **17**, 1659–1665 (1996).

248. Nien, Y. D. *et al.* Fibrinogen inhibits fibroblast-mediated contraction of collagen. *Wound Repair and Regeneration* **11**, 380–385 (2003).

249. Elvin, C. M. *et al.* Evaluation of photo-crosslinked fibrinogen as a rapid and strong tissue adhesive. *J Biomed Mater Res A* **93**, 687–695 (2010).

250. Kesselman, D., Kossover, O., Mironi-Harpaz, I. & Seliktar, D. Time-dependent cellular morphogenesis and matrix stiffening in proteolytically responsive hydrogels. *Acta Biomater* **9**, 7630–7639 (2013).

251. Marino, D., Luginbühl, J., Scola, S., Meuli, M. & Reichmann, E. Bioengineering dermo-epidermal skin grafts with blood and lymphatic capillaries. *Sci Transl Med* **6**, (2014).

252. Klar, A. S. *et al.* Tissue-engineered dermo-epidermal skin grafts prevascularized with adipose-derived cells. *Biomaterials* **35**, 5065–5078 (2014).

253. Gainza, G. *et al.* Development and in vitro evaluation of lipid nanoparticle-based dressings for topical treatment of chronic wounds. *Int J Pharm* **490**, 404–411 (2015).

254. Sharma, V. *et al.* Viscoelastic, physical, and bio-degradable properties of dermal scaffolds and related cell behaviour. *Biomed Mater* **11**, (2016).

255. Sharma, V. *et al.* Design of a Novel Two-Component Hybrid Dermal Scaffold for the Treatment of Pressure Sores. *Macromol Biosci* **17**, 1700185 (2017).

256. Lim, X., Potter, M., Cui, Z. & Dye, J. F. Manufacture and characterisation of EmDerm-novel hierarchically structured bio-active scaffolds for tissue regeneration. *J Mater Sci Mater Med* **29**, (2018).

257. Cheng, R. Y. *et al.* Handheld instrument for wound-conformal delivery of skin precursor sheets improves healing in full-thickness burns. *Biofabrication* **12**, (2020).

258. Jorgensen, A. M. *et al.* Decellularized Skin Extracellular Matrix (dsECM) Improves the Physical and Biological Properties of Fibrinogen Hydrogel for Skin Bioprinting Applications. *Nanomaterials (Basel)* **10**, 1–10 (2020).

259. Gsib, O., Eggermont, L. J., Egles, C. & Bencherif, S. A. Engineering a macroporous fibrin-based sequential interpenetrating polymer network for dermal tissue engineering. *Biomater Sci* **8**, 7106–7116 (2020).

260. Tan, J. *et al.* Biofunctionalized fibrin gel co-embedded with BMSCs and VEGF for accelerating skin injury repair. *Mater Sci Eng C Mater Biol Appl* **121**, (2021).

261. Chen, H., Ma, X., Zhang, M. & Liu, Z. Injectable and biofunctionalized fibrin hydrogels co-embedded with stem cells induce hair follicle genesis. *Regen Biomater* **10**, (2022).

262. Kotlarz, M., Ferreira, A. M., Gentile, P., Russell, S. J. & Dalgarno, K. Droplet-based bioprinting enables the fabrication of cell–hydrogel–microfibre composite tissue precursors. *Biodes Manuf* **5**, 512–528 (2022).

263. Zhou, G. *et al.* Fabrication of Fibrin/Polyvinyl Alcohol Scaffolds for Skin Tissue Engineering via Emulsion Templating. *Polymers (Basel)* **15**, (2023).

264. De La Puente, P. *et al.* Autologous fibrin scaffolds cultured dermal fibroblasts and enriched with encapsulated bFGF for tissue engineering. *J Biomed Mater Res A* **99**, 648–654 (2011).

265. Burmeister, D. M., Roy, D. C., Becerra, S. C., Natesan, S. & Christy, R. J. In Situ Delivery of Fibrin-Based Hydrogels Prevents Contraction and Reduces Inflammation. *J Burn Care Res* **39**, 40–53 (2018).

266. Idrus, R. B. H. *et al.* Allogeneic bilayered tissue-engineered skin promotes full-thickness wound healing in ovine model. *Biomedical Research* **25**, 192–198 (2014).

267. Idrus, R. B. H. *et al.* Full-thickness skin wound healing using autologous keratinocytes and dermal fibroblasts with fibrin: bilayered versus single-layered substitute. *Adv Skin Wound Care* **27**, 171–180 (2014).

268. Hermeto, L. C., de Rossi, R., de Pádua, S. B., Pontes, E. R. J. & Santana, A. E. Comparative study between fibrin glue and platelet rich plasma in dogs skin grafts. *Acta Cir Bras* **27**, 789–794 (2012).

269. Soares, C. S., Dias, I. R., Pires, M. A. & Carvalho, P. P. Canine-Origin Platelet-Rich Fibrin as an Effective Biomaterial for Wound Healing in Domestic Cats: A Preliminary Study. *Vet Sci* **8**, (2021).

270. Nica, O., George Popa, D., Florian Grecu, A., LastNameLastNameMihai Ciucă, E. & Eugen Ciurea, M. Histological aspects of full-thickness skin grafts augmented with platelet-rich fibrin in rat model. *Rom J Morphol Embryol* **60**, 581–588 (2019).

271. Bastidas, J. G., Maurmann, N., Da Silveira, M. R., Ferreira, C. A. & Pranke, P. Development of fibrous PLGA/fibrin scaffolds as a potential skin substitute. *Biomed Mater* **15**, (2020).

272. Kouketsu, A. *et al.* Wound healing effect of autologous fibrin glue and polyglycolic acid sheets in a rat back skin defect model. *Transfus Apher Sci* **60**, (2021).

273. Zhao, M. *et al.* Functionalizing multi-component bioink with platelet-rich plasma for customized in-situ bilayer bioprinting for wound healing. *Mater Today Bio* **16**, (2022).

274. Tian, K. *et al.* Autologous i-PRF promotes healing of radiation-induced skin injury. *Wound Repair Regen* (2023) doi:10.1111/WRR.13083.

275. Bastidas, J. G. *et al.* Bilayer scaffold from PLGA/fibrin electrospun membrane and fibrin hydrogel layer supports wound healing in vivo. *Biomed Mater* **18**, (2023).

276. Scardino, M. S. *et al.* Evaluation of fibrin sealants in cutaneous wound closure. *J Biomed Mater Res* **48**, 315–321 (1999).

277. Romanos, G. E. & Strub, J. R. Effect of Tissucol on connective tissue matrix during wound healing: an immunohistochemical study in rat skin. *J Biomed Mater Res* **39**, 462–468 (1998).

278. Gugerell, A. *et al.* Thrombin as important factor for cutaneous wound healing: comparison of fibrin biomatrices in vitro and in a rat excisional wound healing model. *Wound Repair Regen* **22**, 740–748 (2014).

279. Rahman, M. M. *et al.* A platelet-derived hydrogel improves neovascularisation in full thickness wounds. *Acta Biomater* **136**, 199–209 (2021).

280. Ishihara, J. *et al.* Laminin heparin-binding peptides bind to several growth factors and enhance diabetic wound healing. *Nat Commun* **9**, (2018).

281. Lei, X., Yang, Y., Shan, G., Pan, Y. & Cheng, B. Preparation of ADM/PRP freeze-dried dressing and effect of mice full-thickness skin defect model. *Biomed Mater* **14**, (2019).

282. Hu, L. *et al.* In Situ-Formed Fibrin Hydrogel Scaffold Loaded With Human Umbilical Cord Mesenchymal Stem Cells Promotes Skin Wound Healing. *Cell Transplant* **32**, (2023).

283. Reinertsen, E., Skinner, M., Wu, B. & Tawil, B. Concentration of fibrin and presence of plasminogen affect proliferation, fibrinolytic activity, and morphology of human fibroblasts and keratinocytes in 3D fibrin constructs. *Tissue Eng Part A* **20**, 2860–2869 (2014).

284. Sörgel, C. A., Schmid, R., Kengelbach-Weigand, A., Promny, T. & Horch, R. E. Air-Pressure-Supported Application of Cultured Human Keratinocytes in a Fibrin Sealant Suspension as a Potential Clinical Tool for Large-Scale Wounds. *Journal of Clinical Medicine 2022, Vol. 11, Page 5032* **11**, 5032 (2022).

285. Yanaga, H. *et al.* Take percentage and conditions of cultured epithelium were improved when basement membrane of the graft was maintained and anchoring mesh was added. *Plast Reconstr Surg* **107**, 105–115 (2001).

286. Peura, M. *et al.* Paracrine factors from fibroblast aggregates in a fibrin-matrix carrier enhance keratinocyte viability and migration. *J Biomed Mater Res A* **95**, 658–664 (2010).

287. Mis, B., Rolland, E. & Ronfard, V. Combined use of a collagen-based dermal substitute and a fibrin-based cultured epithelium: A step toward a total skin replacement for acute wounds. *Burns* **30**, 713–719 (2004).

288. Solovieva, E. V., Fedotov, A. Y., Mamonov, V. E., Komlev, V. S. & Panteleyev, A. A. Fibrinogen-modified sodium alginate as a scaffold material for skin tissue engineering. *Biomed Mater* **13**, (2018).

289. Zhou, Y., Fan, Y., Chen, Z., Yue, Z. & Wallace, G. Catechol functionalized ink system and thrombin-free fibrin gel for fabricating cellular constructs with mechanical support and inner micro channels. *Biofabrication* **14**, (2021).

290. Kouhbananinejad, S. M. *et al.* A fibrinous and allogeneic fibroblast-enriched membrane as a biocompatible material can improve diabetic wound healing. *Biomater Sci* **7**, 1949–1961 (2019).

291. Natesan, S. *et al.* PEGylated Platelet-Free Blood Plasma-Based Hydrogels for Full-Thickness Wound Regeneration. *https://home.liebertpub.com/wound* **8**, 323–340 (2019).

292. Formigli, L. *et al.* Dermal matrix scaffold engineered with adult mesenchymal stem cells and platelet-rich plasma as a potential tool for tissue repair and regeneration. *J Tissue Eng Regen Med* **6**, 125–134 (2012).

293. Natesan, S., Zamora, D. O., Wrice, N. L., Baer, D. G. & Christy, R. J. Bilayer hydrogel with autologous stem cells derived from debrided human burn skin for improved skin regeneration. *J Burn Care Res* **34**, 18–30 (2013).

294. Wahl, E. A. *et al.* In Vitro Evaluation of Scaffolds for the Delivery of Mesenchymal Stem Cells to Wounds. *Biomed Res Int* **2015**, (2015).

295. Samberg, M. *et al.* Platelet rich plasma hydrogels promote in vitro and in vivo angiogenic potential of adipose-derived stem cells. *Acta Biomater* **87**, 76–87 (2019).

296. Huynh, T. D. *et al.* Soft tissue regeneration in animal models using grafts from adipose mesenchymal stem cells and peripheral blood fibrin gel. *Eur Rev Med Pharmacol Sci* **27**, 3670–3680 (2023).

297. Zebardast, N., Lickorish, D. & Davies, J. E. Human umbilical cord perivascular cells (HUCPVC): A mesenchymal cell source for dermal wound healing. *Organogenesis* **6**, 197–203 (2010).

298. Grieb, G. *et al.* Improved in vitro cultivation of endothelial progenitor cells as basis for dermal substitutes with enhanced angiogenic capabilities. *Langenbecks Arch Surg* **396**, 1255–1262 (2011).

299. Jarrell, D. K. *et al.* Increasing salinity of fibrinogen solvent generates stable fibrin hydrogels for cell delivery or tissue engineering. *PLoS One* **16**, e0239242 (2021).

300. El Ghalbzouri, A., Lamme, E. N., Van Blitterswijk, C., Koopman, J. & Ponec, M. The use of PEGT/PBT as a dermal scaffold for skin tissue engineering. *Biomaterials* **25**, 2987–2996 (2004).

301. Kamolz, L. P. *et al.* The Viennese culture method: cultured human epithelium obtained on a dermal matrix based on fibroblast containing fibrin glue gels. *Burns* **31**, 25–29 (2005).

302. Panacchia, L. *et al.* Nonirradiated human fibroblasts and irradiated 3T3-J2 murine fibroblasts as a feeder layer for keratinocyte growth and differentiation in vitro on a fibrin substrate. *Cells Tissues Organs* **191**, 21–35 (2010).

303. Seet, W. T. *et al.* Shelf-life evaluation of bilayered human skin equivalent, MyDerm™. *PLoS One* **7**, (2012).

304. Guzmán-Uribe, D. *et al.* Oral mucosa: an alternative epidermic cell source to develop autologous dermal-epidermal substitutes from diabetic subjects. *J Appl Oral Sci* **25**, 186–195 (2017).

305. Blasco-Morente, G. *et al.* Comparative Study of Shrinkage in Human Skin, Artificial Human Skin, and Mouse Skin. *Am J Dermatopathol* **40**, 240–246 (2018).

306. do Amaral, R. J. F. C. *et al.* Functionalising Collagen-Based Scaffolds With Platelet-Rich Plasma for Enhanced Skin Wound Healing Potential. *Front Bioeng Biotechnol* **7**, (2019).

307. Ionescu, A. M. *et al.* Evaluation of the optical and biomechanical properties of bioengineered human skin generated with fibrin-agarose biomaterials. *J Biomed Opt* **25**, 1 (2020).

308. Montero, A., Atienza, C., Elvira, C., Jorcano, J. L. & Velasco, D. Hyaluronic acid-fibrin hydrogels show improved mechanical stability in dermo-epidermal skin substitutes. *Mater Sci Eng C Mater Biol Appl* **128**, (2021).

309. Montero, A. *et al.* Effect of Fibrin Concentration on the In Vitro Production of Dermo-Epidermal Equivalents. *Int J Mol Sci* **22**, (2021).

310. Montero, A. *et al.* Contraction of fibrin-derived matrices and its implications for in vitro human skin bioengineering. *J Biomed Mater Res A* **109**, 500–514 (2021).

311. Stojic, M. *et al.* Elastin-Plasma Hybrid Hydrogels for Skin Tissue Engineering. *Polymers (Basel)* **13**, (2021).

312. Malheiro, A. *et al.* A Humanized In Vitro Model of Innervated Skin for Transdermal Analgesic Testing. *Macromol Biosci* **23**, 2200387 (2023).

313. Meana, A. *et al.* Large surface of cultured human epithelium obtained on a dermal matrix based on live fibroblast-containing fibrin gels. *Burns* **24**, 621–630 (1998).

314. Gache, Y. *et al.* Construction of skin equivalents for gene therapy of recessive dystrophic epidermolysis bullosa. *Hum Gene Ther* **15**, 921–933 (2004).

315. Escámez, M. J. *et al.* An in vivo model of wound healing in genetically modified skin-humanized mice. *J Invest Dermatol* **123**, 1182–1191 (2004).

316. Carriel, V. *et al.* Epithelial and stromal developmental patterns in a novel substitute of the human skin generated with fibrin-agarose biomaterials. *Cells Tissues Organs* **196**, 1–12 (2012).

317. Cubo, N., Garcia, M., Del Cañizo, J. F., Velasco, D. & Jorcano, J. L. 3D bioprinting of functional human skin: production and in vivo analysis. *Biofabrication* **9**, (2016).

318. Persinal-Medina, M. *et al.* Polymerizable Skin Hydrogel for Full Thickness Wound Healing. *Int J Mol Sci* **23**, (2022).

319. Carriel, V. *et al.* Epithelial and Stromal Developmental Patterns in a Novel Substitute of the Human Skin Generated with Fibrin-Agarose Biomaterials. *Cells Tissues Organs* **196**, 1–12 (2011).

320. Monfort, A., Soriano-Navarro, M., García-Verdugo, J. M. & Izeta, A. Production of human tissue-engineered skin trilayer on a plasma-based hypodermis. *J Tissue Eng Regen Med* **7**, 479–490 (2013).

321. Kober, J., Gugerell, A., Schmid, M., Kamolz, L. P. & Keck, M. Generation of a Fibrin Based Three-Layered Skin Substitute. *Biomed Res Int* **2015**, (2015).

322. Kreimendahl, F. *et al.* Macrophages significantly enhance wound healing in a vascularized skin model. *J Biomed Mater Res A* **107**, 1340–1350 (2019).

323. Chan, R. K. *et al.* Development of a vascularized skin construct using adipose-derived stem cells from debrided burned skin. *Stem Cells Int* **2012**, (2012).

324. Mooney, R. G. *et al.* Indentation micromechanics of three-dimensional fibrin/collagen biomaterial scaffolds. *J Mater Res* **21**, 2023–2034 (2006).

325. Houdek, M. T. *et al.* Collagen and Fractionated Platelet-Rich Plasma Scaffold for Dermal Regeneration. *Plast Reconstr Surg* **137**, 1498–1506 (2016).

326. Stone, R., Wall, J. T., Natesan, S. & Christy, R. J. PEG-Plasma Hydrogels Increase Epithelialization Using a Human Ex Vivo Skin Model. *Int J Mol Sci* **19**, (2018).

327. Monteiro, I. P. *et al.* A two-component pre-seeded dermal-epidermal scaffold. *Acta Biomater* **10**, 4928–4938 (2014).

328. Zhou, J. *et al.* Hyaluronic acid-based dual network hydrogel with sustained release of platelet-rich plasma as a diabetic wound dressing. *Carbohydr Polym* **314**, (2023).

329. Tapasztó, I. & Kerényi, G. Skin replacement with Bioplast fibrin in Ophthalmology. *J Biomed Mater Res* **11**, 799–809 (1977).

330. Jeschke, M. G. *et al.* Development of new reconstructive techniques: use of Integra in combination with fibrin glue and negative-pressure therapy for reconstruction of acute and chronic wounds. *Plast Reconstr Surg* **113**, 525–530 (2004).

331. Valbonesi, M., Giannini, G., Migliori, F., Dalla Costa, R. & Dejana, A. M. Cord blood (CB) stem cells for wound repair. Preliminary report of 2 cases. *Transfus Apher Sci* **30**, 153–156 (2004).

332. Taghiabadi, E. *et al.* Treatment of Hypertrophic Scar in Human with Autologous Transplantation of Cultured Keratinocytes and Fibroblasts along with Fibrin Glue. *Cell J* **17**, 49–58 (2015).

333. Carducci, M., Bozzetti, M., Spezia, M., Ripamonti, G. & Saglietti, G. Treatment of a Refractory Skin Ulcer Using Punch Graft and Autologous Platelet-Rich Plasma. *Case Rep Dermatol Med* **2016**, 1–4 (2016).

334. Egea-Guerrero, J. J. *et al.* Transplant of Tissue-Engineered Artificial Autologous Human Skin in Andalusia: An Example of Coordination and Institutional Collaboration. *Transplant Proc* **51**, 3047–3050 (2019).

335. Klama-Baryła, A. *et al.* The use of biostatic human amnion and platelet-rich plasma in topical treatment of toxic epidermal necrolysis—A case report. *J Cosmet Dermatol* **20**, 2887–2893 (2021).

336. Shashank, B. & Bhushan, M. Injectable Platelet-Rich Fibrin (PRF): The newest biomaterial and its use in various dermatological conditions in our practice: A case series. *J Cosmet Dermatol* **20**, 1421–1426 (2021).

337. Saha, S. Minimalistic reconstruction of exposed skull in a complex craniovertebral polytrauma. *Surg Neurol Int* **12**, 1–5 (2021).

338. Morimoto, N. *et al.* Exploratory clinical trial of combination wound therapy with a gelatin sheet and platelet-rich plasma in patients with chronic skin ulcers: study protocol. *BMJ Open* **5**, (2015).

339. Allogeneic ADSCs and Platelet-Poor Plasma Fibrin Hydrogel to Treat the Patients With Burn Wounds (ADSCs-BWs) - Full Text View - ClinicalTrials.gov. https://clinicaltrials.gov/ct2/show/study/NCT03113747?term=%28%28skin+AND+substitute+OR+%28artificial+AND+skin%29+OR+%28tissue+AND+engineered+AND+skin+AND+substitute%29+OR+%28tissue+AND+engineered+AND+skin%29+OR+%28tissue+AND+engineering%29%29+AND+human+AND+plasma+OR+fibrin%29+AND+%28hydrogel+OR+biomaterial%29+AND+skin&draw=2&rank=1 (2017).

340. Nilforoushzadeh, M. A. *et al.* Engineered skin graft with stromal vascular fraction cells encapsulated in fibrin-collagen hydrogel: A clinical study for diabetic wound healing. *J Tissue Eng Regen Med* **14**, 424–440 (2020).

341. Larouche, D. *et al.* Regeneration of skin and cornea by tissue engineering. *Methods in Molecular Biology* **482**, 233–256 (2009).

342. Germain, L. *et al.* Improvement of human keratinocyte isolation and culture using thermolysin. *Burns* **19**, 99–104 (1993).

343. Barrandon, Y. & Green, H. Three clonal types of keratinocyte with different capacities for multiplication. *Proc Natl Acad Sci U S A* **84**, 2302 (1987).

344. Ghio, S. C. *et al.* A Newly Developed Chemically Defined Serum-Free Medium Suitable for Human Primary Keratinocyte Culture and Tissue Engineering Applications. *Int J Mol Sci* **24**, 1821 (2023).

345. Trujillo-Rodríguez, M. *et al.* Mesenchymal stromal cells in human immunodeficiency virus-infected patients with discordant immune response: Early results of a phase I/II clinical trial. *Stem Cells Transl Med* **10**, 534–541 (2021).

346. Bisson, F. *et al.* Irradiated human dermal fibroblasts are as efficient as mouse fibroblasts as a feeder layer to improve human epidermal cell culture lifespan. *Int J Mol Sci* **14**, 4684–4704 (2013).

347. Lavoie, A. *et al.* Human epithelial stem cells persist within tissue-engineered skin produced by the self-assembly approach. *Tissue Eng Part A* **19**, 1023–1038 (2013).

348. Gauvin, R. *et al.* Minimal contraction for tissue-engineered skin substitutes when matured at the air-liquid interface. *J Tissue Eng Regen Med* **7**, 452–460 (2013).

349. Larose, A. E. *et al.* Peel Test to Assess the Adhesion Strength of the Dermal-Epidermal Junction in Tissue-Engineered Skin. *Tissue Eng Part C Methods* **26**, 180–189 (2020).

350. Cantin-Warren, L. *et al.* Specialized living wound dressing based on the self-assembly approach of tissue engineering. *J Funct Biomater* **9**, (2018).

351. Faga, A. *et al.* Hyaluronic acid three-dimensional scaffold for surgical revision of retracting scars: A human experimental study. *Int Wound J* **10**, 329–335 (2013).

352. Simman, R., Mari, W., Younes, S. & Wilson, M. Use of Hyaluronic Acid-Based Biological Bilaminar Matrix in Wound Bed Preparation: A Case Series. *Eplasty* **18**, e10 (2018).

353. Draaijers, L. J. *et al.* The patient and observer scar assessment scale: a reliable and feasible tool for scar evaluation. *Plast Reconstr Surg* **113**, 1960–5; discussion 1966-7 (2004).

354. van de Kar, A. L. *et al.* Reliable and Feasible Evaluation of Linear Scars by the Patient and Observer Scar Assessment Scale. *Plast Reconstr Surg* **116**, 514–522 (2005).

355. Michel, M. *et al.* Characterization of a new tissue-engineered human skin equivalent with hair. *In Vitro Cell Dev Biol Anim* **35**, 318–326 (1999).

356. Xue, M., Dervish, S. & Jackson, C. J. Isolation of Human Skin Epidermal Stem Cells Based on the Expression of Endothelial Protein C Receptor. *Methods Mol Biol* **1879**, 165–174 (2019).

357. Vaughan, F. L. & Bernstam, L. I. Isolation, purification, and cultivation of murine and human keratinocytes. *Methods Mol Biol* **290**, 187–206 (2005).

358. Johansen, C. Generation and Culturing of Primary Human Keratinocytes from Adult Skin. *J Vis Exp* **2017**, (2017).

359. Daniels, J. T., Kearney, J. N. & Ingham, E. Human keratinocyte isolation and cell culture: a survey of current practices in the UK. *Burns* **22**, 35–39 (1996).

360. Aasen, T. & Belmonte, J. C. I. Isolation and cultivation of human keratinocytes from skin or plucked hair for the generation of induced pluripotent stem cells. *Nat Protoc* **5**, 371–382 (2010).

361. Braziulis, E. *et al.* Modified plastic compression of collagen hydrogels provides an ideal matrix for clinically applicable skin substitutes. *Tissue Eng Part C Methods* **18**, 464–474 (2012).

362. Korosec, A., Frech, S. & Lichtenberger, B. M. Isolation of Papillary and Reticular Fibroblasts from Human Skin by Fluorescence-activated Cell Sorting. *J Vis Exp* **2019**, (2019).

363. Supp, D. M., Hahn, J. M., Combs, K. A., McFarland, K. L. & Powell, H. M. Isolation and feeder-free primary culture of four cell types from a single human skin sample. *STAR Protoc* **3**, (2022).

364. Park, H. S. *et al.* Application of physical force is essential to enrich for epidermal stem cells in primary human keratinocyte isolation. *Tissue Eng* **10**, 343–351 (2004).

365. Rakhorst, H. A. *et al.* Mucosal keratinocyte isolation: a short comparative study on thermolysin and dispase. *Int J Oral Maxillofac Surg* **35**, 935–940 (2006).

366. Prost, C., Dubertret, L., Fosse, M., Wechsler, J. & Touraine, R. A routine immuno-electron microscopic technique for localizing an auto-antibody on epidermal basement membrane. *Br J Dermatol* **110**, 1–7 (1984).

367. Walzer, C., Benathan, M. & Frenk, E. Thermolysin Treatment: A New Method for Dermo-epidermal Separation. *Journal of Investigative Dermatology* **92**, 78–81 (1989).

368. Yu, Z., Visse, R., Inouye, M., Nagase, H. & Brodsky, B. Defining Requirements for Collagenase Cleavage in Collagen Type III Using a Bacterial Collagen System. *J Biol Chem* **287**, 22988 (2012).

369. Hybbinette, S., Boström, M. & Lindberg, K. Enzymatic dissociation of keratinocytes from human skin biopsies for in vitro cell propagation. *Exp Dermatol* **8**, 30–38 (1999).

370. Raxworthy, M. J., Cunlife, W. J. & Wood, E. J. The influence of proteases on the colony-forming efficiency of human keratinocytes in culture. *Biochem Soc Trans* **15**, 519–520 (1987).

371. Gragnani, A., Sobral, C. S. & Ferreira, L. M. Thermolysin in human cultured keratinocyte isolation. *Brazilian Journal of Biology* **67**, 105–109 (2007).

372. Barrandon, Y. *et al.* Capturing epidermal stemness for regenerative medicine. *Semin Cell Dev Biol* **23**, 937–944 (2012).

373. Natesan, S. *et al.* A bilayer construct controls adipose-derived stem cell differentiation into endothelial cells and pericytes without growth factor stimulation. *Tissue Eng Part A* **17**, 941–953 (2011).

374. Braziulis, E. *et al.* Skingineering I: engineering porcine dermo-epidermal skin analogues for autologous transplantation in a large animal model. *Pediatr Surg Int* **27**, 241–247 (2011).

375. Ramakrishnan, R. *et al.* Silk Fibroin-Based Bioengineered Scaffold for Enabling Hemostasis and Skin Regeneration of Critical-Size Full-Thickness Heat-Induced Burn Wounds. *ACS Biomater Sci Eng* **8**, 3856–3870 (2022).

376. Motter Catarino, C. *et al.* Evaluation of native and non-native biomaterials for engineering human skin tissue. *Bioeng Transl Med* **7**, e10297 (2022).

377. Pensalfini, M. *et al.* Factors affecting the mechanical behavior of collagen hydrogels for skin tissue engineering. *J Mech Behav Biomed Mater* **69**, 85–97 (2017).

378. Brown, R. A., Wiseman, M., Chuo, C.-B., Cheema, U. & Nazhat, S. N. Ultrarapid Engineering of Biomimetic Materials and Tissues: Fabrication of Nano- and Microstructures by Plastic Compression. *Adv Funct Mater* **15**, 1762–1770 (2005).

379. Levis, H. J., Brown, R. A. & Daniels, J. T. Plastic compressed collagen as a biomimetic substrate for human limbal epithelial cell culture. *Biomaterials* **31**, 7726–7737 (2010).

380. Kaji, K. *et al.* Donor age reflects the replicative lifespan of human fibroblasts in culture. *Hum Cell* **22**, 38–42 (2009).

381. Ng, M. H. *et al.* Correlation of donor age and telomerase activity with in vitro cell growth and replicative potential for dermal fibroblasts and keratinocytes. *J Tissue Viability* **18**, 109–116 (2009).

382. De Corte, P. *et al.* Feeder layer- and animal product-free culture of neonatal foreskin keratinocytes: improved performance, usability, quality and safety. *Cell Tissue Bank* **13**, 175–189 (2012).

383. Lange, J. *et al.* Interactions of donor sources and media influence the histo-morphological quality of full-thickness skin models. *Biotechnol J* **11**, 1352–1361 (2016).

384. Mountford, E. M., Blight, A. & Cheshire, I. M. Implications for would healing of patient age and time elapsed since burn injury. *J Wound Care* **4**, (1995).

385. Moulin, V., Mayrand, D., Laforce-Lavoie, A., Larochelle, S. & Genest, H. In Vitro Culture Methods of Skin Cells for Optimal Skin Reconstruction by Tissue Engineering. in *Regenerative Medicine and Tissue Engineering - Cells and Biomaterials* (InTech, 2011). doi:10.5772/20341.

386. Shipley, G. D., Keeble, W. W., Hendrickson, J. E., Coffey, R. J. & Pittelkow, M. R. Growth of normal human keratinocytes and fibroblasts in serum-free medium is stimulated by acidic and basic fibroblast growth factor. *J Cell Physiol* **138**, 511–518 (1989).

387. FGF2 - Fibroblast growth factor 2 - Homo sapiens (Human) | UniProtKB | UniProt. https://www.uniprot.org/uniprotkb/P09038/entry.

388. Hosseini, M. & Shafiee, A. Engineering Bioactive Scaffolds for Skin Regeneration. *Small* **17**, 2101384 (2021).

389. Koike, Y., Yozaki, M., Utani, A. & Murota, H. Fibroblast growth factor 2 accelerates the epithelial–mesenchymal transition in keratinocytes during wound healing process. *Scientific Reports 2020 10:1* **10**, 1–13 (2020).

390. Nayak, S., Dey, S. & Kundu, S. C. Skin Equivalent Tissue-Engineered Construct: Co-Cultured Fibroblasts/ Keratinocytes on 3D Matrices of Sericin Hope Cocoons. *PLoS One* **8**, e74779 (2013).

391. Demidova-Rice, T. N., Hamblin, M. R. & Herman, I. M. Acute and Impaired Wound Healing: Pathophysiology and Current Methods for Drug Delivery, Part 2: Role of Growth Factors in Normal and Pathological Wound Healing: Therapeutic Potential and Methods of Delivery. *Adv Skin Wound Care* **25**, 349 (2012).

392. Rehman, J. *et al.* Secretion of angiogenic and antiapoptotic factors by human adipose stromal cells. *Circulation* **109**, 1292–1298 (2004).

393. Kurobe, M., Furukawa, S. & Hayashi, K. Synthesis and secretion of an epidermal growth factor (EGF) by human fibroblast cells in culture. *Biochem Biophys Res Commun* **131**, 1080–1085 (1985).

394. Choi, S. Y. *et al.* Epidermal Growth Factor Relieves Inflammatory Signals in Staphylococcus aureus-Treated Human Epidermal Keratinocytes and Atopic Dermatitis-Like Skin Lesions in Nc/Nga Mice. *Biomed Res Int* **2018**, (2018).

395. Kim, D., Kim, S. Y., Mun, S. K., Rhee, S. & Kim, B. J. Epidermal growth factor improves the migration and contractility of aged fibroblasts cultured on 3D collagen matrices. *Int J Mol Med* **35**, 1017–1025 (2015).

396. Gibbs, S. *et al.* Epidermal growth factor and keratinocyte growth factor differentially regulate epidermal migration, growth, and differentiation. *Wound Repair and Regeneration* **8**, 192–203 (2000).

397. Brown, L. F. *et al.* Expression of vascular permeability factor (vascular endothelial growth factor) by epidermal keratinocytes during wound healing. *J Exp Med* **176**, 1375–1379 (1992).

398. VEGFA - Vascular endothelial growth factor A, long form - Homo sapiens (Human) | UniProtKB | UniProt. https://www.uniprot.org/uniprotkb/P15692/entry.

399. Ballaun, C., Weninger, W., Uthman, A., Weich, H. & Tschachler, E. Human keratinocytes express the three major splice forms of vascular endothelial growth factor. *J Invest Dermatol* **104**, 7–10 (1995).

400. Ito, T. K., Ishii, G., Chiba, H. & Ochiai, A. The VEGF angiogenic switch of fibroblasts is regulated by MMP-7 from cancer cells. *Oncogene* **26**, 7194–7203 (2007).

401. Hojo, M. *et al.* Induction of vascular endothelial growth factor by fibrin as a dermal substrate for cultured skin substitute. *Plast Reconstr Surg* **111**, 1638–1645 (2003).

402. Myung, H. *et al.* Platelet-rich plasma improves the therapeutic efficacy of mesenchymal stem cells by enhancing their secretion of angiogenic factors in a combined radiation and wound injury model. *Exp Dermatol* **29**, 158–167 (2020).

403. CCL5 - C-C motif chemokine 5 - Homo sapiens (Human) | UniProtKB | UniProt. https://www.uniprot.org/uniprotkb/P13501/entry.

404. Soria, G. & Ben-Baruch, A. The inflammatory chemokines CCL2 and CCL5 in breast cancer. *Cancer Lett* **267**, 271–285 (2008).

405. Szabo, I., Wetzel, M. A. & Rogers, T. J. Cell-density-regulated chemotactic responsiveness of keratinocytes in vitro. *J Invest Dermatol* **117**, 1083–1090 (2001).

406. Kimura, K. *et al.* The role of CCL5 in the ability of adipose tissue-derived mesenchymal stem cells to support repair of ischemic regions. *Stem Cells Dev* **23**, 488–501 (2014).

407. Amable, P. R., Teixeira, M. V. T., Carias, R. B. V., Granjeiro, J. M. & Borojevic, R. Protein synthesis and secretion in human mesenchymal cells derived from bone marrow, adipose tissue and Wharton's jelly. *Stem Cell Res Ther* **5**, (2014).

408. Monsuur, H. N. *et al.* Methods to study differences in cell mobility during skin wound healing in vitro. *J Biomech* **49**, 1381–1387 (2016).

409. Kroeze, K. L. *et al.* Chemokine-mediated migration of skin-derived stem cells: predominant role for CCL5/RANTES. *J Invest Dermatol* **129**, 1569–1581 (2009).

410. Spiekstra, S. W., Breetveld, M., Rustemeyer, T., Scheper, R. J. & Gibbs, S. Wound-healing factors secreted by epidermal keratinocytes and dermal fibroblasts in skin substitutes. *Wound Repair and Regeneration* **15**, 708–717 (2007).

411. Barosova, H. *et al.* Inter-laboratory variability of A549 epithelial cells grown under submerged and air-liquid interface conditions. *Toxicol In Vitro* **75**, (2021).

412. Fatimah, S. S. *et al.* Organotypic culture of human amnion cells in air-liquid interface as a potential substitute for skin regeneration. *Cytotherapy* **15**, 1030–1041 (2013).

413. Martinez Villegas, K., Rasouli, R. & Tabrizian, M. Enhancing metabolic activity and differentiation potential in adipose mesenchymal stem cells via high-resolution surface-

acoustic-wave contactless patterning. *Microsystems & Nanoengineering 2022 8:1* **8**, 1–14 (2022).

414. Finnerty, C. C. *et al.* Determination of burn patient outcome by large-scale quantitative discovery proteomics. *Crit Care Med* **41**, 1421–1434 (2013).

415. Pavoni, V., Gianesello, L., Paparella, L., Buoninsegni, L. T. & Barboni, E. Outcome predictors and quality of life of severe burn patients admitted to intensive care unit. *Scand J Trauma Resusc Emerg Med* **18**, (2010).

416. Kelly, C. *et al.* Surviving an Extensive Burn Injury Using Advanced Skin Replacement Technologies. *J Burn Care Res* **42**, 1288–1291 (2021).

417. Beaudoin Cloutier, C. *et al.* Production of a Bilayered Self-Assembled Skin Substitute Using a Tissue-Engineered Acellular Dermal Matrix. *Tissue Eng Part C Methods* **21**, 1297–1305 (2015).

418. Velez, A. M. A. & Howard, M. S. Collagen IV in Normal Skin and in Pathological Processes. *N Am J Med Sci* **4**, 1 (2012).

419. Caliari, S. R. & Burdick, J. A. A practical guide to hydrogels for cell culture. *Nat Methods* **13**, 405–414 (2016).

420. Tang, L., Sierra, J. O., Kelly, R., Kirsner, R. S. & Li, J. Wool-derived keratin stimulates human keratinocyte migration and types IV and VII collagen expression. *Exp Dermatol* **21**, 458–460 (2012).

421. Li, Y. *et al.* Positive Promoting Effects of Smilax China Flower Absolute on the Wound Healing/Skin Barrier Repair-Related Responses of HaCaT Human Skin Keratinocytes. *Chem Biodivers* **18**, (2021).

422. Liu, T. *et al.* A novel recombinant human collagen hydrogel as minced split-thickness skin graft overlay to promote full-thickness skin defect reconstruction. *Burns* (2022) doi:10.1016/J.BURNS.2022.02.015.

423. Alexaline, M. M. *et al.* Bioengineering a Human Plasma-Based Epidermal Substitute With Efficient Grafting Capacity and High Content in Clonogenic Cells. *Stem Cells Transl Med* **4**, 643–654 (2015).

424. Cerqueira, M. T. *et al.* Cell sheet technology-driven re-epithelialization and neovascularization of skin wounds. *Acta Biomater* **10**, 3145–3155 (2014).

425. Romanovsky, A. A. Skin temperature: its role in thermoregulation. *Acta Physiol (Oxf)* **210**, 498–507 (2014).

426. Filingeri, D. Neurophysiology of Skin Thermal Sensations. in *Comprehensive Physiology* vol. 6 1429–1491 (John Wiley & Sons, Inc., 2016).

427. Gagge, A. & Gonzalez, R. Mechanisms of heat exchange: biophysics and physiology. in *Handbook of Physiology, Environmental Physiology* 45–84 (1996).

428. Mieremet, A. *et al.* Characterization of human skin equivalents developed at body's core and surface temperatures. *J Tissue Eng Regen Med* **13**, term.2858 (2019).

429. Pinnagoda, J., Tupkek, R. A., Agner, T. & Serup, J. Guidelines for transepidermal water loss (TEWL) measurement. *Contact Dermatitis* **22**, 164–178 (1990).

430. Busch, K.-H., Aliu, A., Walezko, N. & Aust, M. Medical Needling: Effect on Moisture and Transepidermal Water Loss of Mature Hypertrophic Burn Scars. *Cureus* **10**, e2365 (2018).

431. Lee, B., Litt, M. & Buchsbaum, G. Rheology of the vitreous body: part 3. Concentration of electrolytes, collagen and hyaluronic acid. *Biorheology* 339–51 (1994).

432. Delevoye, C. Melanin Transfer: The Keratinocytes Are More than Gluttons. *Journal of Investigative Dermatology* **134**, 877–879 (2014).

433. Tissue expression of HLA-E - Staining in skin - The Human Protein Atlas. https://www.proteinatlas.org/ENSG00000204592-HLA-E/tissue/skin.

434. Moll, R., Divo, M. & Langbein, L. The human keratins: biology and pathology. *Histochem Cell Biol* **129**, 705–33 (2008).

435. Moore, A. L. *et al.* Scarless wound healing: Transitioning from fetal research to regenerative healing. *Wiley Interdiscip Rev Dev Biol* **7**, (2018).